From the Institute of Research Center Borstel Leibniz Lung Center

of the University of Lübeck

Director: Prof. Dr. Ulrich Schaible

Adaptation of *Mycobacterium tuberculosis* complex strains to antibiotics

Dissertation

for Fulfillment of

Requirements

for the Doctoral Degree

of the University of Lübeck

from the Department of Natural Sciences

Submitted by

Lindsay Ruth Sonnenkalb M.Sc.

from Pittsburgh, Pennsylvania

Lübeck 2021

First referee: Prof. Dr. Stefan Niemann

Second referee: Prof. Dr. Jan Rupp

Date of oral examination: 07.06.2022

Approved for printing. Lübeck, 09.06.2022

Declaration

Ich erkläre mich damit einverstanden, dass die Zentrale Hochschulbibliothek Lübeck die elektronische Dissertation und die dazugehörigen Daten in Datennetzen zur öffentlichen Nutzung bereitstellt. Die Zentrale Hochschulbibliothek ist berechtigt, die elektronische Dissertation und dazugehörigen Daten an die Deutsche Nationalbibliothek weiterzugeben.
Falls persönliche Daten (Lebenslauf) in meiner Dissertation enthalten sind, bin ich damit einverstanden, dass diese von der Zentrale Hochschulbibliothek Lübeck und der Deutschen Nationalbibliothek maschinell gespeichert und zur öffentlichen Nutzung bereitgestellt werden.

I agree that the Central University Library Lübeck makes the electronic dissertation and the associated data available in data networks for public use. The Central University Library is authorized to forward the electronic dissertation and associated data to the German National Library.
If personal data (curriculum vitae) are included in my dissertation, I agree that they may be stored by machine by the Central University Library Lübeck and the German National Library and made available for public use.

Sincerely,

Lindsay Ruth Sonnenkalb

Am Schmiedeholz 19

23845, Borstel

Table of Contents

1. Abstract 1
1. Zusammenfassung 3
2. Introduction 7
2.1 Tuberculosis Epidemiology 7
2.2 Tuberculosis treatment 10
2.3 Drug resistance in *Mycobacterium tuberculosis* complex strains 11
2.4 Tuberculosis diagnostics 13
2.5 Pathology of tuberculosis infection 15
2.6 Mechanisms of antibiotic resistance evolution 17
2.7 Applying evolutionary medicine principles and precision medicine to fight tuberculosis 20
Study objectives 22
3.1 Materials 23
3.1.1 Consumables 23
3.1.2 Reagents & Buffers 24
3.1.3 Antibiotics 25
3.1.4 *Mycobacterium tuberculosis* strains 25
3.1.5 Kits 26
3.1.6 Laboratory equipment 26
3.1.7 Computer Software 27
3.1.8 Solution and media preparation 28
3.2 Methods 30
3.2.1 Basic laboratory procedures 30
3.2.1.1 Colony forming unit plating and counting 30
3.2.1.2 Colony forming unit plating on selective media plates (antibiotic supplemented) 30
3.2.1.3 Optical density measurements 31
3.2.1.4 Ziehl-Neeson Staining - Acid fast staining 31

3.2.1.5 Contamination exclusion by blood agar plating 31

3.2.1.6 Brain-heart-infusion and lysogeny broth culturing 32

3.2.1.7 Isolation of genomic DNA from patient isolates 32

3.2.1.8 Deactivation of *Mycobacterium tuberculosis* strains from liquid and solid media 32

3.2.1.9 CTAB DNA isolation 33

3.2.2 Evolutionary experimental model 33

3.2.2.1 Sub-minimum inhibitory concentration evolution model 33

3.2.2.2 Re-plating of experimental cultures 35

3.2.2.3 Mutant isolation from selective media plates 35

3.2.3 Phenotypic assays 36

3.2.3.1 Resazurin emission microtiter assay – minimum inhibitory concentration testing 36

3.2.3.3 Mycobacterium growth indicator tube assay – drug susceptibility testing 37

3.2.3.4 Mycobacterium growth indicator tube – mutant selection window 37

3.2.3.5 Fitness experiments – allele competition 38

3.2.4 Genotypic and Computational Analysis 39

3.2.4.1 Next generation sequencing 39

3.2.4.2 Genomic analysis 39

3.2.4.3 PacBio® sequencing 40

3.2.3.2 Minimum inhibitory concentration testing of patient strains 40

3.2.4.4 Core genome multi locus sequence typing 40

3.2.4.5 Mutation catalogue literature search 41

4. Results 42

4.1 Multi-drug and extensively drug resistant intra-patient resistance evolution of a single *Mycobacterium tuberculosis* complex strain 42

4.1.1 Patient History 42

4.1.2 Intra-patient microevolution towards extensively drug resistant tuberculosis 44

4.1.3 Evolutionary arms race of individual subpopulations 46

4.1.4 Compensatory and tolerance associated mutations selected during treatment 47

4.2 An experimental model of antibiotic resistance evolution in bacteria of the *Mycobacterium tuberculosis* complex 48

4.2.1 Developing an evolution model for *Mycobacterium tuberculosis* adaptation to antibiotics..... 49

4.2.2 Sub-inhibitory antibiotic exposure selects and enriches drug resistant *Mycobacterium tuberculosis* complex bacterial populations 53

4.2.3 Cross-resistance selection of bedaquiline mutants after clofazimine exposure..... 60

4.2.4 Sub-inhibitory drug exposure selects a diversity of mutations in resistance-associated genes 62

4.2.5 Bedaquiline and clofazimine resistance-associated mutations described in patient cohorts ... 73

4.3 Defining evolutionary processes of a weak selection pressure on bacteria of the *Mycobacterium tuberculosis* complex – a quantitative analysis 78

4.3.1 Secondary mutations arise and are selected with resistant variants 78

4.3.2 The mutation selection window of fluoroquinolone and bedaquiline resistance conferring mutations 79

4.3.3 Bacterial fitness of resistance mediating mutations 82

4.3.4 Non-canonical mutations potentially implicated in bedaquiline/clofazimine resistance..... 84

5. Discussion 89

5.1 Elucidating factors of intra-patient resistance evolution of a *Mycobacterium tuberculosis* complex bacterial infection 89

5.1.1 Failing treatment regimens foster resistance selection 90

5.1.2 The adaptive landscape and heterogeneous populations 91

5.2.3 Off-target mutations implementing putative compensatory and tolerance mechanisms 93

5.2 The impact of sub-inhibitory drug exposure on *Mycobacterium tuberculosis* bacteria 95

5.2.1 Sub-inhibitory drug exposure selects resistance conferring clones..... 95

5.2.2 Sub-minimum inhibitory concentration evolution model captures a wide diversity of resistance associated mutations 96

5.2.3 Developing a mutational catalogue for bedaquiline and clofazimine..... 99

5.2.4 Hypersusceptible phenotypes in patient strains with *Rv0678* mutations may be linked to epistasis 100

5.3 Deciphering resistance mechanisms and their implications 102

5.3.1 The mutant selection window of resistance-associated mutations in bacteria of the *Mycobacterium tuberculosis* complex 102

5.3.2 The fitness impact of resistance-associated variants 103

5.3.3 Co-selection of off-target mutations 104

5.3.4 Cross-resistance between bedaquiline and clofazimine 106

5.3.5 Large scale gene rearrangement as a novel bedaquiline/clofazimine resistance mechanism 107

5.5 Conclusion 109

6. References 110

7. List of Figures 135

8. List of Tables 137

9. Abbreviations 139

Appendix A 142

Introduction supplementary materials and extended data 142

Appendix B 143

Supplementary Material and extended tables of Results 4.1 143

Appendix C 153

Supplementary Material and extended tables of Results 4.2 153

Appendix D 190

Supplementary Material and extended tables of Results 4.3 190

Appendix E 196

Statistics 196

Acknowledgments 198

Curriculum vitae ..... **Error! Bookmark not defined.**

List of Publications 201

List of Presentations 202

1. Abstract

The causative agents of tuberculosis (TB), bacteria of the *Mycobacterium tuberculosis* complex (Mtbc), continue to be among the deadliest pathogens worldwide killing about 1.4 million people per year. Infections with Mtbc strains mainly affect the lungs and require a minimum of six months antibiotic treatment consisting of four drugs, even increasing to over 20 months treatment in some patients with multidrug resistant (MDR, resistance against isoniazid and rifampicin) strains. Such treatment durations cause a long-term selection pressure on the bacteria that can rapidly develop resistance if antibiotic regimens are not effective. Recent pharmacodynamic studies also demonstrated that not all drugs in combination therapy reach target sites of infection, e.g. lung granulomas, at a therapeutic level. Thus, even with a fully functional antibiotic regimen, Mtbc bacteria may survive and evolve in evolutionary niches with sub-inhibitory drug concentrations. How these microenvironments contribute to the evolution of antibiotic resistance in a patient, and if sub-inhibitory concentrations can select for resistant bacterial subpopulation with low fitness costs is currently not well understood in Mtbc bacterial infections.

To address these questions, this study investigated resistance evolution in serial isolates from a patient under MDR-TB treatment by whole genome sequencing (WGS), and developed an *in vitro* evolution model to study the selection of resistant subpopulation at low drug doses, i.e. below the minimum inhibitory concentrations (MICs) of major MDR-TB antibiotics. The resistant clones obtained were investigated for resistance mechanisms by WGS, and for selected clones the mutant selection window (MSW) was defined in which resistant strains outcompete their susceptible counterparts. These experiments were carried out with moxifloxacin (MFX), the new anti-TB drug bedaquiline (BDQ), and the repurposed drug clofazimine (CFZ). All mutations selected *in vitro* were combined with mutations found in clinical strains, including a large-scale strain collection (CRyPTIC cohort) to eventually build up an improved mutation catalogue for WGS-based molecular resistance prediction.

First, this study examined the intra-patient resistance evolution of a single infectious strain throughout a complex 13-year treatment period. Thirteen bacterial isolates were analyzed by WGS, and compared to phenotypic drug susceptibility testing (DST) and the clinical treatment history. Several phases of mono-therapy or with no active drugs were detected, correlating with the emergence of heteroresistant subpopulations. Indeed, the rise and fixation of 7 resistance-associated mutations over treatment was observed, in a strain which harbored 8 pre-existing resistance mutations.

To further define the impact of sub-inhibitory drug exposure on resistance development and to quantify the mutant selection window, an *in vitro* evolution model based on long-term exposure of the Mtbc

reference strain H37Rv to drug concentrations below the MIC was established. After exposure to MFX, BDQ, or CFZ, resistant subpopulations increased over time, already at concentrations as low as 1:16 the MIC. In fact, all sub-inhibitory concentrations tested, selected for numerous clonal subpopulations with a diverse set of resistance associated variants defined by population WGS and selection of single colony clones. Mutation diversity was large for all drugs, and a mutant strain collection was established including 356 selected and characterized clones, harboring one of 79 unique resistance-associated variants. To develop a resistance mutation catalogue for BDQ and CFZ, *in vitro* data was combined with an extensive literature search and data from a large patient cohort (consisting of over 14,000 strains) resulting in an interpretation database with more than 150 variants. Interestingly, thirteen clones with a BDQ and/or CFZ resistant phenotype were found to have a 2.5 Mb inversion, which cut through the gene *Rv0678*, and was categorized as a novel resistance mechanism. Finally, competition experiments showed that the most commonly selected MFX and BDQ clones harboring a mutation in either *gyrA, gyrB, atpE*, or *Rv0678*, had little to no fitness loss in direct growth completion experiments with the wild-type ancestor clone. Further, growth of these clones was measured in the automated MGIT system at various sub-inhibitory concentrations, which showed that resistance mutations have a selective advantage to the wild-type under a weak selection pressure far below the MIC, pointing to a wide mutant selection window.

In conclusion, the analyses performed in this thesis confirmed that the microevolution of Mtbc strains in TB patients under therapy is a highly dynamic process of competing heteroresistant populations that is driven by poor treatment regimens. The developed *in vitro* evolution model under sub-inhibitory drug concentrations has a high potential to study resistance evolution and define resistance mechanisms as they generate clones with a wide spectrum of mutations, including clinically relevant mutations. Similar models could be used to investigate new drug compounds before coming to market; but also, to explore the effect of alternative treatment models such as synergy and antagonistic drug combinations, or drug-cycling on resistance development. The mutation catalogue established far extends current knowledge on BDQ/CFZ genomics for resistance prediction, to be used for personalized medicine of MDR-TB patients. It became also clear that the majority of mutations in *Rv0678* confer cross-resistance to BDQ and CFZ, and that CFZ exposure selects for mutant populations resistant to BDQ. The *in vitro* models employed demonstrated for the first time that resistant Mtbc subpopulations can be selected in an environment with a weak selection pressure far below the MIC. This has important implications for personalized MDR-TB therapies suggesting that therapeutic drug monitoring, MIC determination, and bacterial mutation profiles can improve therapy outcomes in the most difficult to treat MDR-TB patients.

1. Zusammenfassung

Mit jährlich etwa 1,4 Millionen Todesfällen gehören die Erreger der Tuberkulose (TB), Bakterien des *Mycobacterium tuberculosis*-Komplex (Mtbk), nach wie vor zu den tödlichsten Krankheitserregern weltweit. Die TB wird mindestens sechs Monate mit vier Medikamenten behandelt; bei multiresistenten (MDR, Resistenz gegen Isoniazid und Rifampicin) Fällen kann die Behandlungsdauer sogar 20 Monate und mehr betragen. Diese langwierige Behandlung führt zu einem hohen Selektionsdruck auf die Tuberkulosebakterien, was z.B. im Falle von ineffektiven Therapieregimen schnell zur Selektion von Resistenzen führen kann. Pharmakodynamische Studien haben zudem gezeigt, dass nicht alle Medikamente in der Kombinationstherapie die Infektionsherde, z. B. die Lungengranulome, in ausreichender Konzentration erreichen. Somit können Mtbk-Stämme selbst bei einer generell wirksamen Antibiotikatherapie in diesen „evolutionären Nischen" mit sub-inhibitorischen Antibiotikakonzentrationen überleben und neue Resistenzen entwickeln. Welchen Einfluss das auf die Entwicklung von Antibiotikaresistenzen unter Therapiebedingungen hat und ob sub-inhibitorische Konzentrationen eine Selektion von resistenten Stämmen mit geringen Fitnesskosten bewirken können ist bei TB nicht ausreichend geklärt.

Um diese Fragen zu beantworten, wurde in dieser Arbeit die Resistenzentwicklung von seriellen Isolaten eines MDR-TB Patienten mittels Gesamtgenomsequenzierung („whole genome sequencing", WGS) untersucht. Des Weiteren wurde ein *in vitro* Evolutionsmodell zur Analyse der Selektion von resistenten Klonen bei sub-inhibitorischen Antibiotikakonzentrationen, d. h. unterhalb der minimalen Hemmkonzentrationen (MHK), entwickelt. Die resistenten Klone wurden mittels WGS auf Resistenzmechanismen untersucht und für ausgewählte Klone wurde das so genannte „mutant selection window" (MSW) definiert, in dem resistente Stämme einen Selektionsvorteil gegenüber sensiblen Wildtyp-Stämmen haben. Die Selektions-Experimente wurden mit drei MDR-TB Medikamenten, Moxifloxacin (MFX), dem neuen anti-TB Antibiotikum Bedaquilin (BDQ) und dem Antibiotikum Clofazimin (CFZ) durchgeführt. Zur Erstellung eines verbesserten Mutationskatalog für die WGS-basierte molekulare Resistenzvorhersage wurden die *in vitro* selektionierten Mutationen mit Resistenz-vermittelnden Mutationen von Mtbk-Stämmen aus der großen CRyPTIC Stammsammlung und mit Daten aus einer umfassenden Literatursuche kombiniert.

In dieser Arbeit wurde zunächst die Resistenzentwicklung eines einzelnen MDR-Mtbk-Stammes (Dreizehn klinische Isolate) im Verlauf von 13 Jahren MDR-TB Therapie untersucht. Mehrere Phasen mit Monotherapie oder sogar ohne effektive Antibiotika korrelierten mit dem Auftreten von heteroresistenter Bakterien Subpopulationen und späterer Fixierung der Mutationen. So erwarb der initial achtfach resistente Stamm im Verlauf der Behandlung sieben neue Antibiotikaresistenzen.

Um die Auswirkungen von niedrigen Antibiotikakonzentrationen auf die Resistenzentwicklung genauer zu untersuchen wurde ein *in vitro* Evolutionsmodell etabliert, in dem der Mtbk-Referenzstamm (H37Rv) bei sub-inhibitorischen Antibiotika Konzentrationen (unterhalb der MHK) passagiert („evolviert“) wurde. Bei allen verwendeten Antibiotika (MFX, BDQ und CFZ) wurden resistente Subpopulationen bereits bei Konzentrationen von 1:16 der MHK selektioniert. Die WGS Analyse von Selektionsklonen und Bakterienpopulationen (alle Zellen von einer Platte) zeigte, dass bereits bei geringen Antibiotikakonzentrationen eine Vielzahl von Klonen mit unterschiedlichen Resistenz-vermittelnden Mutationen selektioniert wird. Insgesamt wurden 356 Selektionsklone untersucht und Klone mit 79 unterschiedliche Resistenz-vermittelnde Mutationen phänotypisch charakterisiert. Weiter Untersuchungen des „mutant selection window“ (MSW) ergaben das ausgewählter Klone mit Mutationen in *gyrA, gyrB, atpE* und *Rv0678* selbst bei schwachem Selektionsdruck weit unterhalb der MHK einen Selektionsvorteil gegenüber dem Wildtyp haben, was auf eine breite MSW hindeutet.

Diese Mutationsdaten aus den *in vitro* Experimenten wurden dann mit Daten aus einer großen Patientenkohorte (mehr als 14.000 Stämmen) und mit publizierten BDQ und CFZ Resistenz-vermittelnden Mutationen kombiniert. Die etablierte Interpretationsdatenbank umfasst mehr als 150 Mutationen. Bei 13 resistenten Selektionsmutanten wurde eine 2,5 Mb-Inversion im Genom detektiert, die das Gen *Rv0678* betrifft und als neuartiger Resistenzmechanismus eingestuft wurde. Kompetitions-Experimente zeigten, dass die am häufigsten selektionierten MFX und BDQ-resistenten Klone im Vergleich mit dem Wildtyp Stamm nur geringe bis gar keine Fitnessverluste hatten.

Zusammenfassend bestätigen die durchgeführten Analysen, dass die Mikroevolution von Mtbk-Stämmen bei ineffektiven Antibiotikatherapien ein hochdynamischer Prozess mit konkurrierender heteroresistenter Subpopulationen ist. Das entwickelte *in vitro* Evolutionsmodell ist hervorragenden für die Untersuchung von Resistenzmechanismen geeignet und könnte in Zukunft zur Analyse Resistenz-vermittelnde Mutationen für neue Antibiotika vor der Markteinführung genutzt werden. In ähnlichen Modellen sollen in Zukunft auch alternative Kombinationstherapien untersucht werden, die Synergien und Antagonismen zwischen verschiedenen Antibiotika berücksichtigen. Der entwickelte Mutationskatalog verbessert die Möglichkeiten für die Pathogenom basierte Resistenzdiagnostik und besonders durch das verbesserte Verständnis von BDQ und CFZ Resistenzmechanismen. So wurden die hier generierten Daten bereits bei der personalisierten Behandlung von MDR-TB Patienten eingesetzt. Die erhobenen Daten bestätigten, dass Mutationen in *Rv0678* eine Kreuzresistenz zwischen BDQ und CFZ vermitteln. Die durchgeführten Experimente zeigten zum ersten Mal, dass resistente Subpopulationen unter schwachem Selektionsdruck weit unterhalb der MHK selektiert werden können. Dies hat wichtige Auswirkungen auf die personalisierte MDR-TB-Therapie und legt nahe, dass therapeutische Arzneimittelüberwachung, MHK-Bestimmung und

die Analyse bakterieller Mutationsprofile die Therapieergebnisse bei MDR-TB-Patienten verbessern können.

"But I would like to sound one note of warning. Penicillin is to all intents and purposes non-poisonous so there is no need to worry about giving an overdose and poisoning the patient. There may be a danger, though, in underdosage. It is not difficult to make microbes resistant to penicillin in the laboratory by exposing them to concentrations not sufficient to kill them, and the same thing has occasionally happened in the body."

- Alexander Fleming, Nobel Lecture, December 11, 1945

2. Introduction

2.1 Tuberculosis Epidemiology

It is conservatively estimated that bacteria of the *Mycobacterium tuberculosis* complex (Mtbc) have been causing tuberculosis (TB) in humans for over 40,000 to 75,000 years [1], [2]. TB mainly manifests as a disease of the lungs, but can also affect almost any other tissue in the body. In 1882, Robert Koch first discovered that “tubercle bacilli” were responsible for TB diseases, which later earned him the Nobel Prize in medicine in 1905 [3]. At this turn of the century the leading cause of death in humans were communicable infections, such as wound infections, diphtheria, cholera, or TB. Over 120 years later, the leading cause of death today has shifted to ailments such as heart disease and cancer, yet TB still remains the deadliest disease caused by a single pathogen, only surpassed by major pandemics like the 1918 Flu and SARS-CoV-2 outbreak in 2020 [4]–[6].

According to the World Health Organization (WHO), in 2020 alone, bacteria of the Mtbc were responsible for 1.5 million deaths worldwide, with over 10 million newly reported cases [4]. The areas with the highest TB incidence include Southern and Eastern Asia (especially India, Indonesia, and the Philippines) as well as Sub-Saharan Africa (with exceptionally high incidence rates in South Africa and the Central African Republic) (Figure 2.1A) [7]. Fortunately, there has been a steady decrease in human immunodeficiency virus (HIV)-positive TB-cases, yet infection control efforts have failed every milestone target (Figure 2.1B).

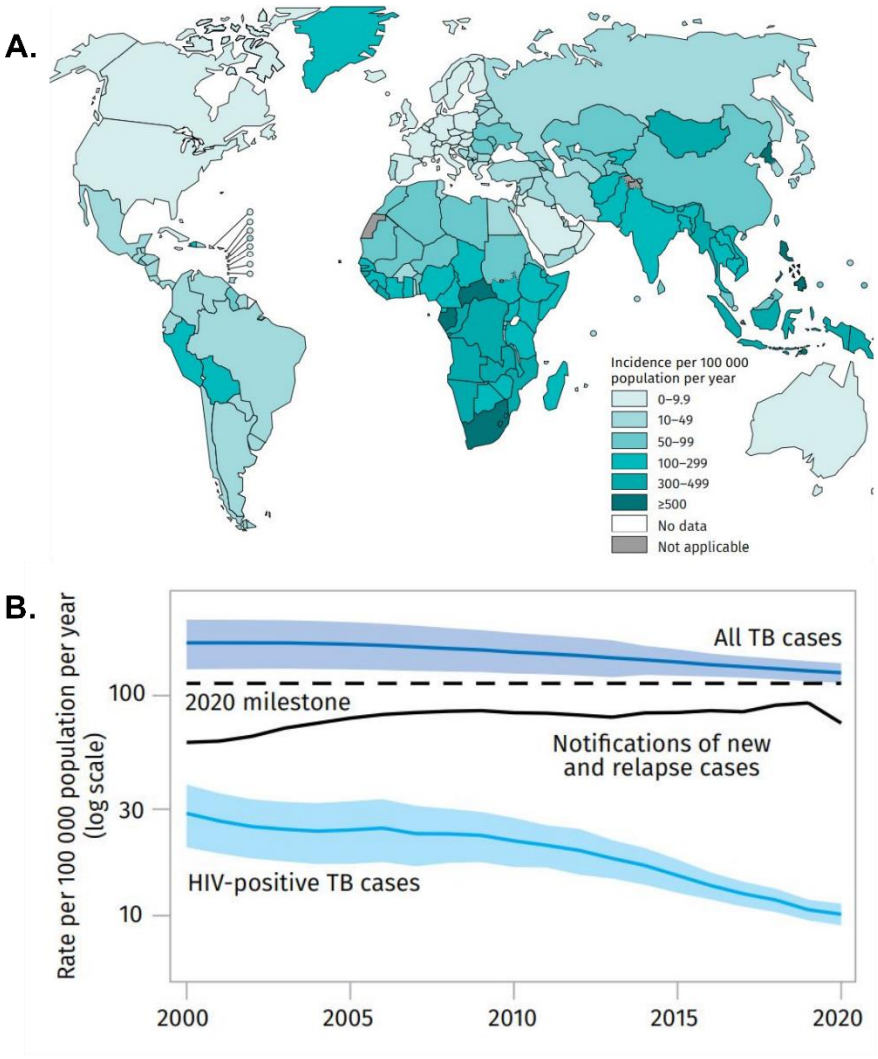

Figure 2.1: Estimated tuberculosis incidence rates per 100,000 in 2020. (A) Global incidence rate colored by country; higher incidence indicated by darker coloration. (B) Global trends of all tuberculosis cases (dark blue), notified new cases (black), and HIV-positive TB cases (light blue); 95% confidence intervals indicated as shaded areas. Images obtained from World Health Organization - Global tuberculosis report 2021 [4].

Nearly one third of the total world population is estimated to be infected with an Mtbc strain, yet only 5-10% of those enter a symptomatic state, known as active-TB [8]. Active infection, defined as the presentation of clinical symptoms such as cough, weight loss, and night sweats; is required for the bacteria to be transmitted. It is not fully clear why a low rate of those infected progress to active disease, although there are several risk factors such as a weak immune system due to immunocompromising pathogens like HIV, or comorbidities including (but not limited to): malnourishment (poverty), diabetes, cancer, or substance (tobacco/drug/alcohol) abuse [4], [9]. Nevertheless, TB disease in most high incidence settings is linked to malnutrition and poverty [4].

For those who develop active TB, it can take months, years, even decades after initial infection for symptoms to arise [10]. It is also possible to be re-infected after successful treatment [11]–[13]. When treatment is not successful, patients can suffer a “relapse” or “recurrent” infection, which usually occurs within the 12 months following treatment conclusion [14], [15]. It is unclear why some patients suffer from recurrent infection, although it is likely linked to high bacterial load or poor diagnosis [16].

It has been confirmed that resistant Mtbc strains have been transmitted throughout human populations for decades [17], [18]. Resistance acquisition in Mtbc strains is at the forefront of the antibiotic resistance crisis, in which TB accounts for one-third of all resistant bacterial deaths worldwide [7]. Although the highest number of TB cases consolidates in Africa and East Asia (Figure 2.1), most rifampicin resistant (RR) and MDR cases occur in Eastern Europe, especially countries of the former Soviet Union (Figure 2.2). MDR-TB is defined as being resistant to RIF and INH, the two most effective anti-TB drugs [7].

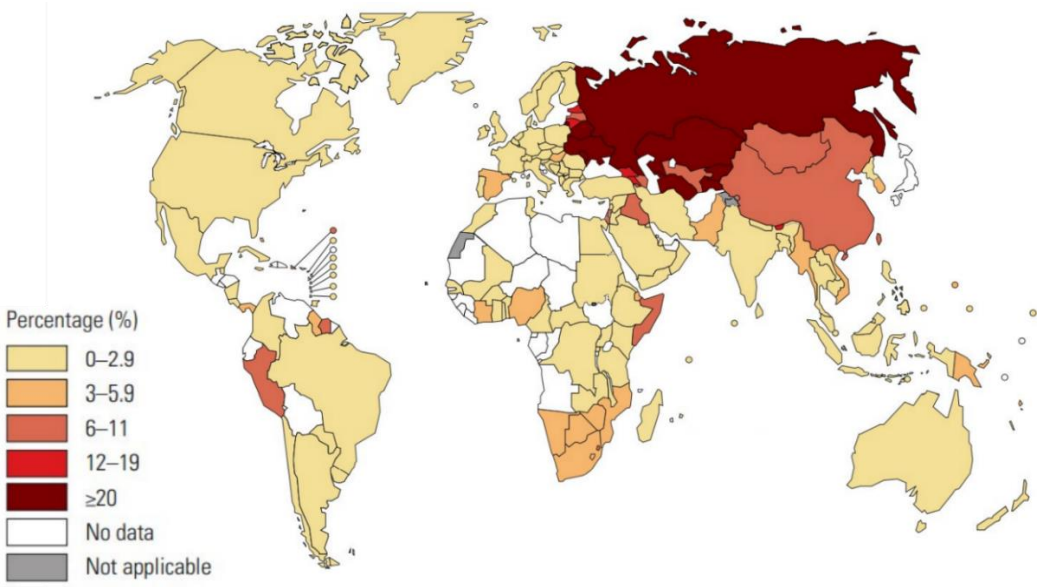

Figure 2.2: Percentage of rifampicin or multi-drug resistant tuberculosis among newly-reported tuberculosis cases worldwide. Percentage of resistant tuberculosis cases colored by country; higher incidence indicated by darker coloration. Images obtained from World Health Organization - Global tuberculosis report 2020 [7].

Large-scale global strategies which enhance supportive systems and research initiatives are needed in order to stop the spread of TB. As outlined by the WHO End TB Strategy, the aid needed for TB eradication is to: “Achieve universal health coverage, including financial risk protection, access to quality essential health-care services and access to safe, effective, quality and affordable essential medicines and vaccines” [7].

2.2 Tuberculosis treatment

The current, worldwide treatment success rate for susceptible TB infections is around 85%; in low income, high incidence countries treatment success ranges between 50 and 90% [7]. While there are many potential causes of treatment failure, non-compliance to treatment and poor drug regimens are foremost important [19], [20]. Patient non-compliance is a pitfall for treating any bacterial infection, and implies that the patient arbitrarily stopped taking their medication before treatment conclusion, or were taking their medication inappropriately (skipping doses for example). Due to the fact that even a susceptible TB infection takes at least 4 to 6 months to treat, it is not uncommon for patients to discontinue therapy once symptoms subside. A recent study in India determined that up to 25% of patients discontinue therapy before reaching 5 months of treatment [21]. Inappropriate drug regimens are often prescribed due to unknown drug resistance, or dwindling treatment options in highly resistant cases. Other factors associated with treatment failure include: relapse, over-active patient metabolism, and pathological factors which impede drug delivery as highlighted in recent pharmacokinetics and pharmacodynamic studies [22]–[24].

Several strategies have been implemented to defeat these treatment limitations such as extensive and rapid drug susceptibility testing (DST), centralized treatment methods, and precision medicine [25], [26]. One strategy developed by the WHO to combat this problem was “DOTS”, or Directly Observed Treatment, Short-course (short course referring to a six- to eight-month therapy). The DOTS program was shown effective in high burden countries, not only because it included consistent anti-TB drug administration by trained personnel, but also patient education, standardized treatment protocols, and treatment follow-up [27].

Although there have been major technological advances in medicine in the past decade, a protective and effective pulmonary TB vaccine has yet to be established. It has been 80 years since the only TB vaccine, *M. bovis* bacillus Calmette-Guérin (BCG) vaccine, has been employed, and still it is only conclusively protective against the exceptionally lethal TB meningitis, in young children and infants [28]. Currently, there are two promising vaccines in phase III clinical trials. VPM1002, a recombinant BCG whole-cell vaccine, for preventative and therapeutic application; and the MIP vaccine, a BCG vaccine booster composed of heat inactivated *Mycobacterium indicus pranii* [29]–[32]. Until an effective vaccine is authorized and administered, the main (and most effective) strategy to fight Mtbc bacteria is through robust antibiotic treatment.

2.3 Drug resistance in *Mycobacterium tuberculosis* complex strains

In 1943, just a few years after the implementation of the first antibiotic penicillin, the first anti-TB drug was discovered by A. Schatz, E. Bugle, and S. Waksman [33]. Streptomycin (SM), a protein synthesis inhibitor, was administered on a wide-scale after proving efficacious in a Guinea pig model, in which 70% of the control group succumbed to infection compared to only 8% of the treated group [34]–[37]. Concurrently, para-aminosalicylic acid (PAS) was being developed and came to market as drug resistance was already being described in patients who received SM mono-therapy [38], [39]. Early experiments and trials proved that giving these drugs in combination was most effective, and from that time on, it was advised never to treat TB with a single compound [40]–[42].

Combination therapy is a hallmark and obligatory aspect in the treatment of TB. Since the golden era of antibiotic discovery/development and today, some 25+ TB antibiotics have been included in treatment regimen combinations, based on efficacy and safety (Table 2.1). As set by the WHO, the standard treatment regimen of a susceptible TB infection requires six months of antibiotics; four months of INH, RIF, ethambutol (EMB), and pyrazinamide (PZA) plus two months of continued INH and RIF [43]. As resistance to the most effective drugs arise, the drug regimen is modified to include more toxic drugs and can increase treatment duration from nine months to two or more years.

Table 2.1 Overview of the most important anti-tuberculosis drugs

Antibiotics	Abbreviation	Resistance-associated genes	Mode of action
Rifampicin[†]	RIF	*rpoB* [44], *ponA* [45]	Blocks bacterial transcription by binding RNA polymeraseβ subunit
Isoniazid[†]	INH	*katG* [46], *inhA* [47], *fabG1 promotor* [48]	Inhibits mycolic acid synthesis (cell-wall component)
Ethambutol[†]	EMB	embC [49], embA, embB [50], [51]	Inhibits arabinoglycan synthesis (cell-wall component)
Pyrazinamide[†]	PZA	*pncA* [52], *rpsA* [53]	Inhibits membrane transport and fatty acid synthesis
Streptomycin	SM	*rrs* [54], *rpsL* [55], *gidB* [56]	Inhibits protein synthesis by binding 16S rRNA subunit
Fluoroquinolones[α]	FQ	*gyrA, gyrB* [57], [58]	Inhibits DNA gyrase through binding of type II topoisomerase.
Amikacin	AMK	*rrs* [59]	Disrupts protein synthesis by binding 30S ribosomal subunit
Kanamycin	KAN	*rrs* [60], *eis* [61], *whiB7* [62]	Disrupts protein synthesis by binding 30S ribosomal subunit
Capreomycin	CPR	*rrs* [59], *tlyA* [63]	Disrupts protein synthesis by binding to the 70S ribosomal subunit
Ethionamide/ prothionamide	ETH/ PTH	*ethA* [64], *ethR* [65], *fabG1* promotor [48], *inhA* [47]	Inhibits mycolic acid synthesis (cell-wall component)
Para-Aminosalicylic Acid	PAS	*ribD* promotor [66], *thyA* [67], *folC* [66]	Inhibits folic acid synthesis
Linezolid	LZD	*rplC* [68], *rrl* [69]	Inhibits protein synthesis
Cycloserine/ Terizidone	CS/ TRD	*alr* [70], *ddl* [71], *ald* [72]	Inhibits peptidoglycan synthesis (cell-wall component)
Clofazimine	CFZ	*Rv0678* [73], *pepQ* [74]	Inhibits cell growth, binds bacterial DNA (may also bind bacterial potassium transporter)
Bedaquiline	BDQ	*atpE* [75], *Rv0678* [76], *pepQ* [77]	ATP synthase inhibitor
Delamanid/ Pretomanid	DLM/ PRT	*fbiA/fbiB/fbiC* [78], *ddn* [79], *fgd1* [79]	Inhibits mycolic acid biosynthesis (cell-wall component)

[†]First-line antibiotics, multi-drug resistance (MDR) defined as resistance to both INH and RIF

[α]class of antibiotics which includes ofloxacin (OFX), moxifloxacin (MFX), gatifloxacin (GFX), and levofloxacin[β] (LFX)

Still, the emergence and spread of resistant Mtbc strains continued over the last years. There were about half a million estimated RR cases in 2019, approximately 78% of which were MDR. Even with amended WHO guidelines to treat these critical patients, treatment success is reduced to 57% in RR/MDR cases [7]. Further resistant cases are classified as extensively-drug resistant (XDR), defined as an MDR-Mtbc strain with resistance to a fluoroquinolone (FQ) such as levofloxacin (LFX) or moxifloxacin (MFX), plus one other group A drug such as bedaquiline (BDQ) or linezolid (LZD) (Table 2.2) [80].

Table 2.2 World Health Organization drug grouping and treatment recommendation for multi-drug resistant tuberculosis regimens

Groups	Compound/drug
Group A: Include all three	Levofloxacin or moxifloxacin Bedaquiline Linezolid
Group B: Add one of both to treatment	Clofazimine Cycloserine or terizidone
Group C: Add when drugs from Group A and B are not applicable	Ethambutol Delamanid Pyrazinamide Imipenem-cilastatin or meropenem Amikacin or Streptomycin Ethionamide or prothionamide *P*-aminosalicylic Acid

It is clear that resistance can arise within a patient under treatment, but recent studies using DNA-sequencing technologies to evaluate clinical isolates derived from a single patient, showed that this is a dynamic process [81], [82]. This process often includes heterogeneous populations consisting of multiple variants which arise spontaneously and compete until one is ultimately selected, and then becomes fixed in the population [81], [83]–[87].

2.4 Tuberculosis diagnostics

Fast and accurate diagnosis of a bacterial infection with an Mtbc strain is critical for prompt and successful treatment, as well as for tracking and reducing transmission. Current diagnostic tests fall into four main categories: diagnosis of disease, DST, detection of exposure, and monitoring treatment progress. Although

there have been major advances in diagnostics by immunological and molecular assays, confirmation of active infection still relies on older methods such as microscopy, primary isolation, and culturing [88].

The WHO recommends molecular assays as initial testing for TB infection, which will likely become the new gold standard in TB diagnostics [89]. The most widely used tests employed in diagnostic laboratories are polymerase-chain reaction (PCR) based assays such GeneXpert® Ultra (Cepheid, USA) and Truenat™ MTB (Molbio Diagnostics, India), which include detection of TB and screening for RIF resistance. Line-probe assays such as the Hain GenoType MTBDRplus (Hain Lifescience, Germany) and Nipro NTM+MDRTB Detection Kit (Nipro, Japan) are also used in initial diagnosis, but can detect further resistances to the most important drugs (RIF, INH, and FQs). However, line-probe assays are more difficult to perform than the nearly, fully automated PCR based assays.

Currently, the gold standard for diagnosing antibiotic resistance is phenotypic DST. These diagnostics can be performed using microtiter broth assays by observing growth inhibition though color changing and fluorescence dyes such as alamarBlue™ or resazurin (resazurin emission microtiter assay, REMA), and growth inhibition on sold agar plates supplemented with high concentrations of the drug [89]. For diagnostic laboratories with more infrastructure, the mycobacterium growth indicator tube (MGIT) BD BACTECH™ (USA) automated system is used, which measures growth through oxygen consumption. While these assays are more sensitive and can detect a wide range of resistance, they are incredibly time consuming taking 10 days for liquid culture systems, and from 3-6 weeks on solid media [90].

With advancements in next generation sequencing (NGS) technology, plus a major reduction in their cost, whole genome sequencing (WGS) may become the new gold-standard for genomic DST. Genomic DST is accomplished by comparing the NGS data of a particular clinical Mtbc strain to a reference genome, and identifying genomic variants of known drug resistance-associated variations. In a landmark paper in the New England Journal of Medicine, the authors concluded that “WGS can now characterize profiles of susceptibility to first-line anti-tuberculosis drugs with a degree of accuracy sufficient for clinical use” [91]. NGS gives the option to not only evaluate all possible resistances through analyzing variants in all resistance-associated genes, but also to detect heterogeneous populations (clonal subpopulations and mixed infections) [92], [93]. Unfortunately, NGS is currently not yet in widespread use due to high infrastructure cost and required training for data interpretation (which will be overcome by web-based tools for data interpretation such as PhyResSE) [94], [95]. An additional pitfall of genomic DST is the difficulty in predicting level of resistance, due to the wide range of mutations and the phenotypic variability of Mtbc strains [96].

A major effort is also being made to improve treatment progress monitoring which can enhance short-term therapy strategies and overall cure rates. In most settings, treatment progress is monitored by observation of clinical symptoms, but does not always predict the treatment success/failure. To better predict early treatment failures and overall outcomes, efforts are being made to identify biological markers. These markers are biological measurements of the host or microbe, performed as immunological and molecular assays, which might be less biased and more sensitive [97]–[99].

Taken together, TB diagnostics has advanced significantly over the last years, as a large-scale effort by private and publicly funded entities are being made to develop and distribute diagnostic tools to bolster treatment and reduce resistance development in populations which need them most [100].

2.5 Pathology of tuberculosis infection

TB disease mainly manifests as a pulmonary infection, but Mtbc bacteria have the capacity to infect nearly any cell, and thus, can spread to other regions of the body [101]. When the bacilli are inhaled into the lungs of a new host, a complex interplay of innate and adaptive immune responses is triggered, which defines the pathology of the disease [102].

The primary cellular hosts of Mtbc bacteria are alveolar macrophages. When the bacteria are phagocytosed, the macrophage must quickly kill them through autophagy, or the bacteria may be able to prevent phagosome maturation, and eventually escape into the cellular cytosol [103], [104]. After infection, the macrophage will begin recruiting other immune cells such as neutrophils, dendritic cells, T-cells, B-cells, and other types of macrophages, in an attempt to clear the pathogen [105]. In the case that the bacteria are not eliminated, these different cell types work together to form a granuloma, a structure which can contain the viable bacteria and prevent further dissemination throughout the body [106].

The granuloma is a hallmark feature of TB disease which varies in composition and size. The formation of these dynamic structures requires an adaptive immune response, in which T-cells produce an abundance of cytokines (most importantly tumor necrosis factor alpha and interferon gamma) that aid in the recruitment of other immune cells, activate macrophage killing, and stimulate the production of collagen [105], [107]. The collagen produced by fibroblasts not only helps in tissue repair, but creates the fibrous cuff lining the granuloma, which walls off and contains the bacteria [105], [108]. Although granulomas are important for bacterial containment, they can also allow the bacilli to persist in their necrotic center, also called the caseum [109], [110]. Not only does the granuloma prevent contract with immune cells, but also decreases the capacity of several antibiotics to reach the bacteria at therapeutic concentrations [111]–

[114]. Many anti-TB drugs accumulate in the fibrous-cuff and host-cellular regions of the granuloma, with a few that are capable of reaching and diffusing across the caseum (Figure 2.3; Appendix A, Table A.1). The antibiotics which can reach the caseum, can exhibit a major reduction in concentration level. When the cellular granuloma matures and expands it can reach the lumen, or airway, causing an abscess and the formation of a cavity (Figure 2.3) [115].

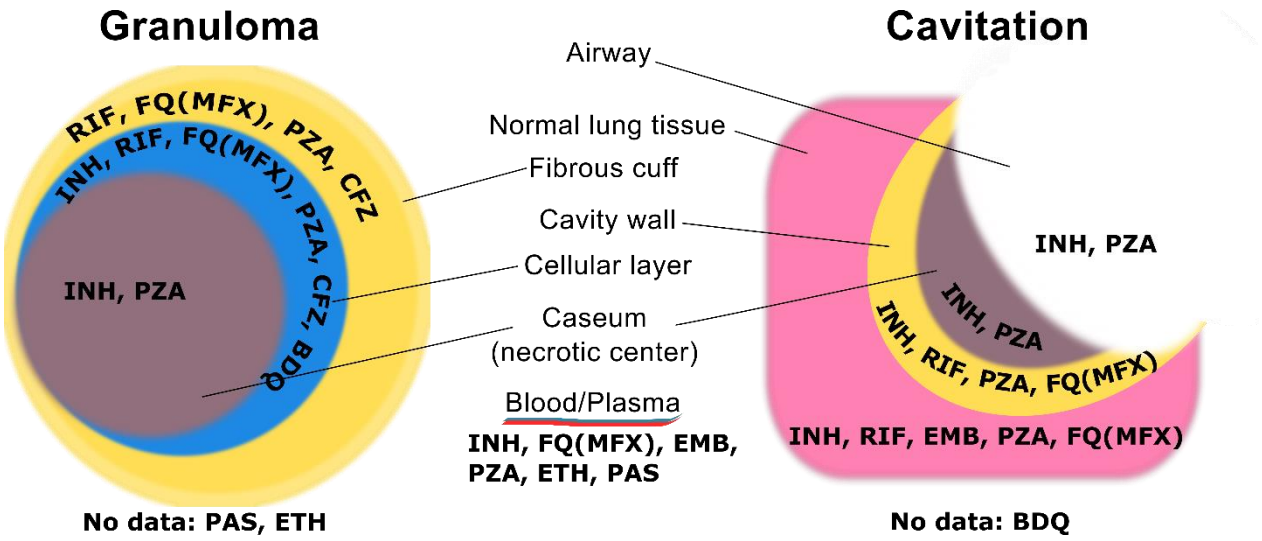

Figure 2.3: Capacity of anti-tuberculosis drugs to accumulate throughout the granuloma and lung cavitation. A number of pharmacokinetic and pharmacodynamic studies investigating human and rabbit material, have found that not all antibiotics are capable of penetrating the granuloma and/or cavitation. Here are the highlighted areas where the different drugs have been found to accumulate at a therapeutic level (at or above the critical concentration needed for Mtbc bacterial killing). CS/TRD, CPR, AMK, LZD, KAN, DLM anti-TB drugs not included. Extended data table of high, medium, and low drug accumulation throughout granuloma and cavatation zones in Appendix A, Table A.1. Data from [111]–[114], [116]–[118].

AMK: amikacin, BDQ: bedaquiline, CFZ: clofazimine, CPR: capreomycin, CS: cycloserine, EMB: ethambutol, ETH: ethionamide, FQ: fluroquinolone, INH: isoniazid, MFX: moxifloxacin, PAS: para-aminosalicylic acid, PZA: pyrazinamide, RIF: rifampicin.

Lung cavitation is another important pathological feature of TB disease, and one of the leading risk factors linked to recurrent infection [16], [119]. Lung cavitations are especially beneficial to the bacteria, as they allow for an oxygen rich environment with a direct path to the airway for transmission. These structures further protect the bacteria from most anti-TB drugs due to poor vascularization and low pharmacokinetic potential [116]–[118]. Sub-inhibitory drug concentrations have been measured throughout the lung cavity for most drugs, as they must diffuse from the blood vessel into normal lung tissue, past activated immune

cells, through the fibrous cuff of the cavity, into the necrotic center full of cell debris and to the cavity surface where the Mtbc bacilli also form a biofilm of replicating and non-replicating bacteria (Figure 2.3) [115].

All-in-all, there are four patterns of drug distribution throughout these pathological lesions, rapid and homogenous (INH, PZA, and LZD), rapid and heterogeneous with high accumulation in the cellular layer versus the caseum (FQs), slow distribution including gradual accumulation in the caseum (RIF), and rapid distribution mainly accumulating in the cellular layer with poor caseum diffusion (BDQ or clofazimine; CFZ) (Figure 2.3) [120]. It is likely that these pockets of low, below MIC, drug distribution could play a role in intra-patient antibiotic resistance evolution, although a clear connection has yet to be established.

2.6 Mechanisms of antibiotic resistance evolution

Understanding the mode and conditions under which drug resistances arise, is paramount in the fight to cure the world of TB. As described by Alexander Fleming in his Nobel Prize Lecture, it was observed for the first discovered antibiotic - penicillin, that microbes can develop resistance when exposed to sub-inhibitory drug concentrations [121]. While he was correct in this statement, it was not yet known, that resistance alleles arise stochastically in bacteria, and that a selection pressure is required for those alleles to proliferate (high or low concentrations of antibiotics, interspecies and allele competition, etc.).

Evolutionary theory describes the rise of resistant variants in bacteria via horizontal gene transfer (by plasmids or transposons), the recombination of external DNA into the chromosome, or by other changes of the chromosome by gene rearrangements, single nucleotide polymorphisms (SNPs), insertions/deletions (indels), or by full gene deletion/duplication [122]. Selection pressures, such as antibiotic/antiviral exposure, lack of nutrients, competition with other species, or DNA damage (such as host induced oxidative stress), influence the mutation rates of bacteria [123]–[126]. Mutation rate can be defined as the probability of a mutation to arise in a bacterial clone [127]–[129]. Antibiotic resistance rates can be measured *in vitro* through experimentation such as the Luria-Delbrück fluctuation assay, which measures the rise/appearance of an alternative allele over time, in the presence or absence of a selection pressure [127]. One caveat to such methods, is that the number of mutant cells is being counted and not the number of mutational events i.e. mutation frequency. Hence, quantification of mutation frequency is not easily accomplished, and with this method in particular you would not detect all mutation events.

Antibiotics can increase mutation rates through triggering stress activated pathways such as the “SOS pathway”, leading to an error prone-alternative polymerase activation (e.g. increased expression in the

nucleotide excision repair proteins like *recA*) [126]. Other stress pathways include regulatory changes in gene expression mediated by induced genes like the alternative sigma factor *RpoS* [130], or by enhancing the production of DNA damaging reactive oxygen species (particularly affected by quinolones, aminoglycosides, and beta-lactams) [131]. Furthermore, different antibiotics can lead to different mutation rates, aka mutability, based on their target's function (translation, transcription, or protein synthesis for example) or number of independent targets. In other words, mutability is the probability a mutation will give rise to a resistant phenotype which is dependent on structure and number of genes which can produce a resistant phenotype (Figure 2.4). For example, if the bacteria can become resistant from a single mutation in gene A, and the mutability of gene A is 10^{-7}, the mutation rate for the drug is 10^{-7}. If the bacteria required a mutation in gene A or gene B to become resistant, and the mutability of gene A is 10^{-7} and gene B is also 10^{-7}, then the mutation rate for the drug is 2×10^{-7}. This is seen in prodrugs, where a mutation in the drug activating enzyme gene or the direct target gene, results in resistance. On the other hand, if the drug has two direct targets, then a mutation in both gene A and gene B is required for resistance and the mutation rate is 10^{-14}. Therefore, the most effective drugs have a very low mutability rate, enhanced by having multiple modes of action (or direct targets).

Mutability of gene A = $\mathbf{10^{-7}}$ Mutability of gene B = $\mathbf{10^{-7}}$

Mutation rates:

- Only to gene A = $\mathbf{10^{-7}}$
- Either gene A or gene B = $10^{-7} + 10^{-7} = \mathbf{2 \times 10^{-7}}$
- Both gene A and gene B = $10^{-7} * 10^{-7} = \mathbf{10^{-14}}$

Figure 2.4 Mutation rate calculations based on mutability of resistance-associated genes. Calculation of mutation rates based on gene mutability in a clonal population, when gene A and gene B both have a hypothetical mutation rate of 10-7.

When exploring and understanding antibiotic resistance evolution to particular anti-TB drugs, an important concept to consider is the mutant selection window (MSW). The MSW is defined as the drug concentration range in which a resistance allele is selected and outperforms the genetically wild-type (gWT) population (Figure 2.5A). The minimum selection concentration is defined as the lowest drug concentration required in order for the resistant mutation to be selected, i.e. the weakest selection pressure needed. This is especially important as mutations generally compromise bacterial fitness; therefore, some amount of antibiotic is required in order to give resistant subpopulations an advantage

over the wild-type population. Both mutant and gWT populations can only tolerate an antibiotic to a certain concentration, known as the MIC.

It has been hypothesized that by exposing a heteroresistant bacterial population to a weak selection pressure, drug concentrations between the minimum selection concentration and the wild-type MIC, the competition with the surviving wild-type population would facilitate the selection of more fit resistant variants (Figure 2.5B). Due to the heterogeneous phenotype of variants in different genes/loci, the size of MSW can fluctuate between variants, to the same antibiotic.

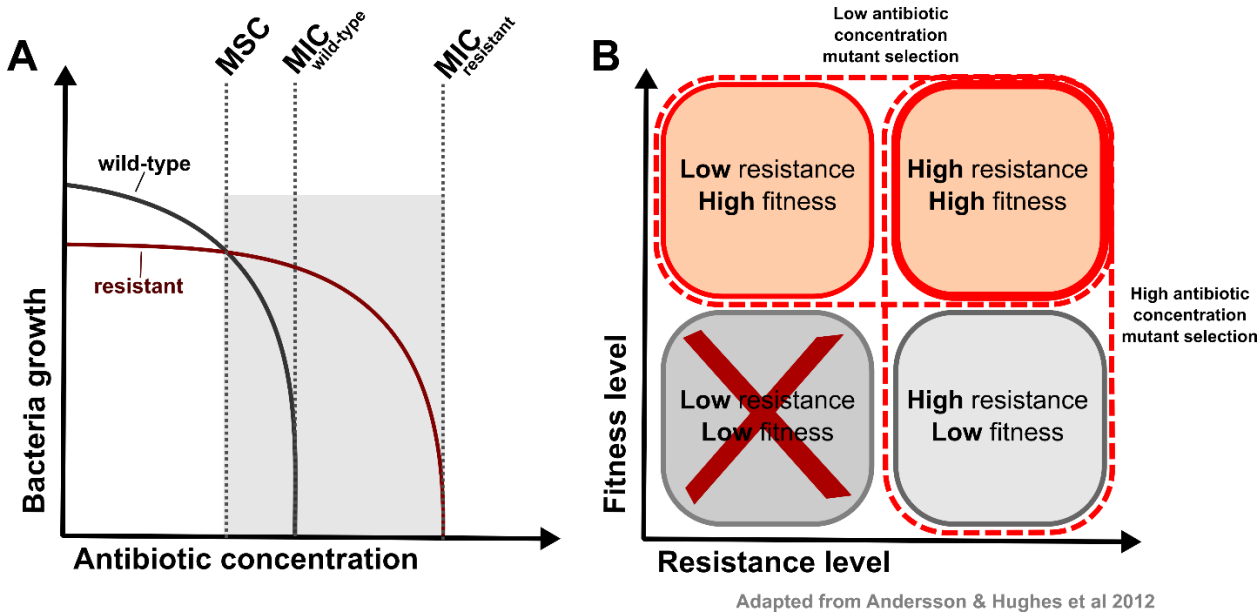

Figure 2.5 The mutant selection window and fitness/resistance level selection. (A) The mutant selection window (MSW) is defined as the drug concentration range in which resistance conferring mutations are selected and enriched, for any given mutation this is between the minimum selection concentration (MSC) and the minimum inhibitory concentration (MIC) of the resistant mutant (gray colored zone). Within the MSW is the MIC of the wild-type (or susceptible ancestor), generally (but not always) the concentration in which the resistant mutant begins to outgrow the wild-type. (B) Fitness level and resistance level are important indicators of the potential survival of certain mutations. Mutations which lower the fitness of the resistant clone are less likely to be selected due to competition with a heterogenous population (including the susceptible ancestor). Adapted from Andersson and Hughes *et al.* 2012 [132].

Within the last 15 years, studies pioneered by Gullberg *et al.* 2011 and Liu *et al.* 2011, found that low concentration drug exposure, in some cases as low as 100-fold below the MIC, selected and enriched antibiotic resistant bacterial populations [133], [134]. These studies included bacterial species such as

Escherichia coli and *Salmonella enterica*, which have highly diverse genomes and dynamic mobile gene mechanisms. So far, similar evolutionary experiments have not been conducted with strains of the Mtbc, where previous studies applied a high-selection pressure environment, i.e. drug concentrations at or above the MIC, or oxidative stress like H_2O_2 [135]–[137]. However, as outlined in the previous section, due to the complex pathology of TB disease, there are a number of intra-patient niches where the bacteria could be exposed to sub-inhibitory drug concentrations, thus potentially fostering the emergence of resistant subpopulations even in virtually effective combination therapy. Understanding the MSW in relation to pharmacokinetics and the spatial distribution of drugs used in combination therapy is crucial to design the most effective treatment regimens especially for RR-, MDR-, and XDR-TB cases.

2.7 Applying evolutionary medicine principles and precision medicine to fight tuberculosis

In bacteria of the Mtbc, resistance principally arises due to variations in the chromosome, observed as SNPs and either large or small insertions or deletions (indels). There have also been reports of large-scale gene rearrangement events, but these are rare [138]–[140]. This microevolution, or clonal nature, of Mtbc strains is further evident by their highly stable genome. The largest difference between any two Mtbc strains is about 2,000 SNPs (out of 4.4 million base pairs), therefore over 99% of the genetic material between all strains in the complex is conserved [2]. This genome stability of Mtbc bacteria makes them perfect organisms for WGS analysis, and a prime candidate for genomic DST.

An up and coming field which aims to integrate evolutionary principles to better understand, prevent, and treat disease is evolutionary medicine. In the case of treating infectious diseases, evolutionary medicine aims to understand and use pathogen evolution to better treat and mitigate pathogen adaptation to therapeutics [141]. In this scope, when developing treatment guidelines, one should consider: pathogen virulence, the role and management of the microbiome, immune system evasion & suppression by the pathogen, their rapid adaptation to antibiotics and how alternative therapies could reduce resistance evolution.

Precision medicine then takes evolutionary medicine to the next level by considering the patient and strain data in order to optimize a treatment strategy tailored to the individual patient [26]. WGS is integral in this method as it allows for detailed epidemiological analysis for outbreak tracing, as well as rapid resistance diagnostics by predicting drug resistance profiles based on a mutation catalogue. These catalogues are developed from extensive datasets including patient and *in vitro* derived isolate genome sequences

coupled with phenotypic DST results (i.e. MIC) [140], [142]. From these catalogues, one can determine drug regimens by predicting the likelihood in which a genomic point mutation can lead to high-level resistance (discontinue drug), low-level resistance (adjust drug dosage), or whether the mutation is benign (continue normal treatment) [26], [143]. Such efforts have unparalleled clinical value, as they accelerate diagnosis and reduce treatment failure through improved, better informed treatment designs.

Overall knowledge of TB infection, transmission, and pathology has greatly increased over the last 40 years, but evolutionary mechanisms of intra-patient resistance acquisition are not well understood. Still, there are important gaps in current knowledge on resistance development in relation to patient characteristics; e.g. granuloma structures, the MSW for different drugs/variants, and further factors that may boost mutation frequencies of Mtbc strains in the patient. There is still virtually no experimental data available which focuses on the consequences of long-term antibiotic exposure, a situation which is required for successful tuberculosis treatment.

Study objectives

As outlined above, several aspects of resistance evolution in clinical Mtbc strains are currently not well defined. To address these gaps, the main aim of this thesis is to elucidate mechanisms of resistance acquisition in clinical Mtbc strains.

Main goals were:

- Elucidate factors which enhance intra-patient resistance evolution in a failing MDR treatment
- Develop and explore the drug resistance evolution of Mtbc bacteria in a long-term evolutionary model - using a prolonged weak selection pressure.
- Define the MSW for important group A & B drugs used for treatment of MDR-TB patients
- Validate the genomic variants found in the weak selection pressure evolution model by using data from a large patient strain collection
- Provide an extended mutation catalogue for BDQ and CFZ

3.1 Materials

3.1.1 Consumables

Product	Order number	Company
8-Lid chain, flat	65.989.002	Sarstedt
96-well plate, flat bottom, sterile	833.924	Sarstedt
96-well plate, U-shape bottom, sterile	833.925	Sarstedt
Adhesive film for microplates	60941-062	VWR
AMPure® PB Beads	100-265-900	PacBio
BD MGIT™ Tubes (100 tubes)	245113	Becton Dickinson
Biosphere Filter Tips 10µL	70.1114.210	Sarstedt
Biosphere Filter Tips 100µL	70.760.212	Sarstedt
Biosphere Filter Tips 1250µL	70.1186.210	Sarstedt
Biosphere Filter Tips 200µL	70.760.211	Sarstedt
Cannula 0.4 x 23mm (26G)	59507	M+W Select
Cannula 1.2 x 40mm (18G)	4038088-01	Brau - Sterican®
Cuvettes 10x4x45 mm	67.742	Sarstedt
Cuvette single-use lids	XK25.1	Roth
Dispenser tips (for multi-stepper pipette)	613-1012	VWR
Inoculation loops (sterile)	612-2495	VWR
Latex gloves (Medium & Small)	MAG 08029	Dahlhausen
Löwenstein-Jensen with glycerol	TV5114C	Artelt-Enclit
MagSi – Magnetic beads for clean-up	MDKT00010075	Steinbrenner
Microscope slides	03-0060	R. Langenbrinck
Nitrile gloves (Small)	MAG 08047	VWR
Nonstick, RNase-free Tubes, 1.5 mL	AM12450	Thermo Fisher
Parafilm®	P7793-1EA	Pechiney
Petri dishes 92 x 16 mm	82.1472	Sarstedt
Reagent reservoir (55mL, sterile)	E831.2	Roth
Roller bottle (490cm^2)	430195	Corning
Screw Cap Tube 1.5mL with lid	72.692	Sarstedt
SealMat for 96 well plates	710889	Biozym
Sequel SMRT Cell Oil	100-621-300	Pac-Bio
SMRT Cell 8M Tray	101-389-001	Pac-Bio
Square media bottle, sterile, PETG, 30 mL	2019-0030	Nalgene™
Square media bottle, sterile, PETG, 60 mL	2019-0060	Nalgene™
Stripette® serological pipette 10mL	4488	Corning Inc.
Stripette® serological pipette 25mL	4489	Corning Inc.
Stripette® serological pipette 5mL	4487	Corning Inc.

Syringe 1mL	303172	Becton Dickinson
Syringe 20mL	300629	Becton Dickinson
Syringe 50mL	300865	Becton Dickinson
Syringe filtration unit Filtropur 0.2µm	83.1826.001	Sarstedt
Syringe filtration unit PTFE membrane 0.2µm	SLLG013SL	Millex
Trypticase Soy Agar 5% sheep blood 120 plates	254087	Becton Dickinson
Tube 1.5mL safety cap	S 72690001	Sarstedt
Tube 15mL, polypropylene screw caps	62.554.502	Sarstedt
Tube 50mL, polypropylene screw caps	62.547.254	Sarstedt
Tubes 0.5 ml (Qubit)	732-0675	Axygen
UKMYC5 plate	*	Thermo Fisher
UKMYC6 plate	*	Thermo Fisher

*prepared special order for CRyPTIC partners

3.1.2 Reagents & Buffers

Product	Order number	Company
2-Propanol (Isopropanol)	AE73.1	Roth
BBL^{tm} Brain Heart Infusion Broth, Modified	299070	Becton Dickinson
Buffer AE (5nM 10mM Tris/HCl, pH8.5)	740917.1	Macherey -Nagel
Carbolic fuchsine solution	A130.1	Roth
CTAB (N-Cetyl-N,N,N- trimethylammonium-bromide)	1023421000	Merck
DEPC water	T143.3	Roth
Difco^{TM} Middlebrook 7H10 Agar 500g	262710	Becton Dickinson
Difco^{TM} Middlebrook 7H11 Agar 500g	212203	Becton Dickinson
Difco^{TM} Middlebrook 7H9 Broth 500g	271310	Becton Dickinson
Dimethyl Sulfoxide, sterile filtered (DMSO)	A7248,0010	PanReac AppliChem
Elution Buffer (for PacBio sample prep)	101-633-500	Pac-Bio
Elution Buffer AE (5mM Tris/HCL, pH 8,5)	12716563	Fisher Scientific
Ethanol 100%	2005786	Roth
Glycerol (Glycerin)	A2926,1000	PanReac AppliChem
HCl 0.1 mol/L	2315957	Roth
HCl-ethanol 3% for histology	6477.3	Roth
Isoamyl alcohol	T870.1	Roth
LB-Broth 1 kg	L3022	Sigma-Aldrich
Lysozyme	8259.2	Roth
MagSi-NGS Prep Plus	SL-MDKT01075	Steinbrenner

Methylene blue solution	AE64.3	Roth
Multiply-µStripe 0,2ml chain	72.985.002	Sarstedt
NaCl	9265.2	Roth
NaOH	20765.03	Serva
OADC Middlebrook Enrichment 500mL	212351	Becton Dickinson
Proteinase K	19133	Qiagen
Pursept® A Xpress	230131	Schülke & Mayr
Resazurin sodium salt	R7017-1G	Sigma-Aldrich
Rotistock 100 X TE	1052.1	Roth
SDS	2326.2	Roth
Sodium Acetate	1539.5	Merck
Sodium Chloride	131659.1211	PanReac AppliChem
Trichlormethane/Chloroform	6340.1	Roth
Tris-Hydrochloride	9090.2	Roth
Tween 20	1.09280.0100	Merck
Tween 80	P8074	Sigma-Aldrich
Water	0082479E	Braun

3.1.3 Antibiotics

Drug	Form	Reconstituted in	Order number	Company
Bedaquiline	powder	DMSO	-	Janssen-Cilag GmbH
Clofazimine	powder	DMSO	C8895-1G	Sigma-Aldrich (Merck)
Moxifloxacin	powder	0.1N NaOH	SML1581-50MG	Sigma-Aldrich (Merck)

3.1.4 *Mycobacterium tuberculosis* strains

Strain	Distributor	Lot/ID number	Accession number
H37Rv	ATCC	27294	U06259
Mtbc patient isolate	FZB	1060-97	ERS4932039
Mtbc patient isolate	FZB	4177-97	ERS4932040
Mtbc patient isolate	FZB	2698-00	ERS4932041
Mtbc patient isolate	FZB	1633-02	ERS4932042
Mtbc patient isolate	FZB	9512-03	ERS4932043
Mtbc patient isolate	FZB	31-04	ERS4932044
Mtbc patient isolate	FZB	10202-04	ERS4932045
Mtbc patient isolate	FZB	3444-05	ERS4932046
Mtbc patient isolate	FZB	1126-07	ERS4932047

Mtbc patient isolate	FZB	5257-07	ERS4932048
Mtbc patient isolate	FZB	3082-08	ERS4932049
Mtbc patient isolate	FZB	6974-09	ERS4932050
Mtbc patient isolate	FZB	7686-10	ERS4932051

Information on CRyPTIC strains included in Appendix C. Table C.10

3.1.5 Kits

Product	Order number	Company
BACTEC™ MGIT™ 960 SIRE Kit	245123	Becton Dickinson
Barcoded Overhang Adapter Kit- 8A	101-628-400	Pac-Bio
DNF-473 Standard Sensitivity NGS Fragment Analysis Kit, (1bp – 6000 bp)	DNF-473-1000	Advanced Analytical
NextSeq 500/550 High Output Kit v2.5 (300 cycles)	20024908	Illumina
NextSeq 500/550 Mid Output Kit v2.5 (300 cycles)	20024905	Illumina
Nextera XT DNA Sample Preparation Kit (96 samples)	FC-131-1096	Illumina
Nextera XT Index Kit v2 Set A (96 indices, 384 samples)	FC-131-2001	Illumina
Nextera XT Index Kit v2 Set B (96 indices, 384 samples)	FC-131-2002	Illumina
Nextera XT Index Kit v2 Set C (96 indices, 384 samples)	FC-131-2003	Illumina
Nextera XT Index Kit v2 Set D (96 indices, 384 samples)	FC-131-2004	Illumina
Qubit dsDNA HS assay kit (500)	Q32854	Life Technologies
Sequel II Binding Kit 2.0	101-789-500	Pac-Bio
Sequencing Primer v2	101-847-900	Pac-Bio
SMRTbell Enzyme Clean Up Kit	101-746-400	Pac-Bio
SMRTbell Express Template Prep Kit 2.0	100-938-900	Pac-Bio

3.1.6 Laboratory equipment

Product	Company
Analytical Balance EMB 2000-2	KERN
Autoclave	Systec
BD BACTEC™ MGIT™ 320	Becton Dickinson
Synergy 2 plate reader	BioTek (Agilent)
Cell Density Meter model 40	Fisher Scientific
Centrifuge 5430	Eppendorf
Centrifuge 5430	Eppendorf
DynaMag™-PCR Magnet	Thermo Fisher Scientific
Fragment Analyzer™	Advanced Analytical
Heating Block	Biozym Scientific GmbH
Hera Safe - Safety bench	Thermo, Germany
Multi-channel pipettes (100µl, 300µl)	Eppendorf

NextSeq500	Illumina
Öko Refrigerator	Privileg
Pipet boy	Integra Biosciences
Pipettes (10µl, 100µl, 200µl, 1000µl)	Eppendorf
Premium No Frost Freezer	Liebherr
Qubit 3.0	Life technologies
Roller apparatus	Wheaton
Sequel II System	PacBio
Spectrophotometer DS-11 FX	DeNovix
Thermocycler	Analytik Jena
Thermocycler C1000 Touch	Biorad
Vortex Genie2	Scientific Industries
Vortex Genius 3	IKA Vortex
Water bath	Köttermann
Water bath 14 L	Gesellschaft für Labortechnik®

3.1.7 Computer Software

Software	Developer	Free Software Source
AMyGDA	P. Fowler *et al.* [144]	https://github.com/philipwfowler/amygda
BD EpiCenter™ Data Management	Becton Dickinson, USA	
binoSNP	V. Dreyer *et al.* [92]	https://github.com/ngs-fzb/binoSNP
Clockwork	M. Hunt *et al.*	https://github.com/iqbal-lab-org/clockwork
Gen5™	BioTek	
Microsoft® Office (Word & Excel)	Microsoft	
Minos	Hunt *et al.* [145]	https://github.com/iqbal-lab-org/minos
MTBseq	FZB [146]	https://github.com/ngs-fzb/MTBseq_source
RStudio	Rstudio, PBC	https://cran.r-project.org/
SeqSphere v5.9	Ridom, Münster, Germany	https://www.ridom.de/seqsphere/
SMRT® Link software version 9	PacBio	http://www.pacb.com/support/software-downloads

3.1.8 Solution and media preparation

Solution/Media	Procedure
0.83% Saline Solution	Dissolve 8.3 g NaCl in 1000 mL distilled H_2O, autoclave, store in fridge
1:10 Methylene Blue Solution	Dilute 5 mL methylene blue in 45 mL distilled H_2O, store at room temperature
10% sodium dodecyl sulfate (SDS)	Add 100 g SDS to 1000 mL distilled H_2O, store room temperature
10mg/mL Lysozyme	Dissolve 100 mg lysozyme in 10 mL DEPC water, store at -20°
10mM Tris-HCl Buffer pH 8.5	Dissolve 1,576 g Tris HCl in 1000 mL distilled H_2O, set to pH 8.5, store room temperature
20% Tween^{80}	Combine 20 mL Tween^{80} with 80 mL distilled H_2O, stir with metal rod until completely dissolved, pass through 0.2 µm syringe filter, store at room temperature - protect from direct light
5M NaCl	Dissolve 146.1 g NaCl in 500 mL distilled H_2O, store at room temperature
70% ethanol	Combine 70 mL 100% ethanol with 30 mL distilled H_2O, store at room temperature
7H10 agar plates	Dissolve 19 g 7H10 powder and 5 mL glycerol in 900 mL distilled H_2O, autoclave, add 100 mL bovine serum, transfer 20-25 mL to petri dishes, allow time to solidify, store in refrigerator
7H11 agar plates	Dissolve 19 g 7H11 powder and 5 mL glycerol in 900 mL distilled H_2O, autoclave, add 100 mL OADC, transfer 20-25 mL to petri dishes, allow time to solidify, store in refrigerator
7H9 medium (broth)	Dissolve 4.7 g 7H9 powder and 2 mL glycerol in 900mL distilled H_2O, autoclave, add 2.5 mL 20% Tween^{80}; add 10% OADC shortly before use, store at fridge
BDQ selective media	1 liter 7H11, cool to ~56°C, add 50 µL or 25 µl bedaquiline stock (5mg/mL BDQ concentrated), transfer 20-25 mL to petri dishes, allow time to solidify, store in refrigerator no more than 2 days
CFZ selective media	1 liter 7H11, cool to ~56°C, add 100 µL clofazimine stock (5mg/mL CFZ concentrated), transfer 20-25 mL to petri dishes, allow time to solidify, store in refrigerator no more than 2 days
Chloroform/Isoamyl alcohol (24:1)	Combine 48 mL chloroform with 2mL isoamyl alcohol, store at room temperature

CTAB/NaCl	Dissolve 4.1 g NaCl in 80 mL distilled H_2O, while stirring add 10 g N-Cetyl-N,N,N- trimethylammonium-bromide (CTAB), heat solution to 65°C to dissolve, store at room temperature
MFX selective media	1 liter 7H10 agar, cool to ~56°C, add 100µl moxifloxacin stock (5mg/mL MFX concentrated), transfer 20-25 mL to petri dishes, allow time to solidify, store in refrigerator no more than 7 days
Resazurin	Weigh resazurin salt and transfer to a tube. for every 1 mg of resazurin salt add 10 mL water, mix well by vortex, let dissolve for 5 minutes, pass through 0.5 µm syringe filter, protect from light, use immediately.
Water + 0.05% Tween80	Autoclave 1000 mL distilled H_2O, add 2.5 mL 20% Tween80, store in fridge

3.2 Methods

3.2.1 Basic laboratory procedures

3.2.1.1 Colony forming unit plating and counting

Colony forming units (CFU) refers to the number of bacterial colonies which grow on solid agar, and are an indication of bacterial quantity at time of plating, 1 CFU = 1 bacterial cell. CFU plating was performed on 7H10 agar plates. Bacteria grown in liquid culture were first passed through an 18 G cannula four times. The culture was then diluted up to $1{:}10^7$. This was achieved by conducting 1:10 dilutions in a 96-well plate, starting by transferring 25 µL of bacterial culture into 225 µL water with 0.05% Tween[80]. All subsequent dilutions were conducted by transferring 25 µL into 225 µL, pipette tips were changed between each dilution. Next, 100 µL from each dilution was transferred to half of a 7H10 agar plate, and spread until dry with a sterile loop. Dilutions were performed in technical triplicates; each triplicate was plated one time. Once plates were dried, they were inverted (agar on top) and sealed in plastic bags (20 plates per bag). All plates were incubated at 37°C for at least 21 days. After incubation colonies were counted and bacterial numbers were calculated.

$$n\ colonies * dilution\ factor * 10 = \frac{CFU}{mL}$$

3.2.1.2 Colony forming unit plating on selective media plates (antibiotic supplemented)

In order to quantify the number of mutants which arose in a population over time, CFU plating was also conducted on 7H10 (for MFX) or 7H11 (for BDQ and CFZ) agar plates. CFU dilutions were performed like normal CFU plating (Methods 3.2.1.2), except 100-200 µL of diluted culture was spread across the entire agar plate. Additionally, a five times concentrated dilution was plated of each culture. This was achieved by transferring 10 mL of culture to a screw cap tube, then centrifuged for 10 minutes at 4,000 g at room temperature. The supernatant was then discarded, and the bacterial pellet was resuspended in 2 mL water + 0.05% Tween[80]. After plates were sealed and incubated at 37°C for 21.28 days, mutant colonies were counted and quantified as a ratio - mutant per million CFU:

$$\frac{Mutant\ {}^{CFU}/_{mL}}{Total\ {}^{CFU}/_{mL}} * 10^6 = Mutant\ per\ million\ CFU$$

3.2.1.3 Optical density measurements

Turbidity of bacterial cultures was measured by optical density at 600 nm in cell density meter (spectrophotometer). Spectrophotometer was calibrated with culturing media (7H9), 1 mL was added to a cuvette, covered with a single-use lid, and read as the blank. Bacterial cultures were then measured in 1 mL aliquots in cuvette tubes, covered with single-use lids.

3.2.1.4 Ziehl-Neeson Staining - Acid fast staining

Acid fast staining was performed to check for fungal or bacterial combinations throughout experiments. First, 10 µl of bacterial culture was transferred to a microscopic slide and spread around in a small area using a pipette. Once the slide was fully dried, it was passed through a Bunsen burner flame 5 times (bottom side, opposite bacteria). Slide was left to cool for some seconds and passed through the flame another 5 times, then passed through the flame one additional time on the bacteria side of the slide. Slides were then taken out of the biosafety level 3 lab and taken to the biosafety level 2 chemical hood.

Slides were stained by first covering the slide completely with carbolic fuchsine solution and heated over a flame until it started to steam (do not boil). Slides were allowed to cool slightly, then heated again by flame until steaming. This was done a total of three times. After heating the slide was left to cool for ten minutes. Carbolic fuchsine solution was then rinsed off by dipping the slide in distilled water. The slide was then dipped in HCl-ethanol 3% for histology. The slide was again washed in distilled water. Next, the slide was immersed in 1:10 diluted methylene blue solution for 1 minute. Finally, the slide was washed by dipping in distilled water. After the slide dried, observation was conducted by oil immersion microscopy. If only pink rods were observed no contamination was determined. If blue forms are observed (bacilli or cocci) culture was likely contaminated.

3.2.1.5 Contamination exclusion by blood agar plating

Blood agar plating was performed to check if cultures were contaminated with fungi or other bacterial species. About 50-100µl of experimental culture was dropped on blood agar plates. Plates were incubated at 37°C for at least one week. If growth was observed, culture was likely contaminated.

3.2.1.6 Brain-heart-infusion and lysogeny broth culturing

Additional checks for exogenous bacterial/fungal species in experimental cultures were performed by culturing in additional broths. Ten mL brain-heart-infusion and 10 mL lysogeny broth were added to separate tubes. Depending on bacterial density, 50µl-100µL of experimental culture was transferred to each tube. Tubes were sealed and incubated at 37°C for up to two weeks, and checked for growth after 7 and 14 days. If cloudy cultures were observed, experimental culture was considered contaminated, and checked again by acid fast staining.

3.2.1.7 Isolation of genomic DNA from patient isolates

Bacterial samples which were originally recovered from sputum samples were removed from -80°C freezer and grown on Löwenstein-Jensen medium at 37°C until growth became viable. Next, bacterial colonies were scraped and transferred to 1.5 mL screw cap tubes containing 400 µl distilled water. Bacteria was then deactivated (killed) by incubation in an 80°C water bath, for 20 minutes. DNA isolation was conducted by CTAB procedure.

3.2.1.8 Deactivation of *Mycobacterium tuberculosis* strains from liquid and solid media

Mtbc bacteria was grown in 7H9 media, and 5-10 mL was transferred to a 15 mL screw-cap tube. The sample was then centrifuged for 10 minutes at 4,000 g, at room temperature. The supernatant was discarded by pouring, then pellet was resuspended in 400 µL distilled water and transferred to 1.5 mL screw cap tube. Screw cap tubes were closed, and incubated in an 80°C water bath for 20 minutes for deactivation (killing) of bacteria. Samples were then safe to remove from biosafety level 3 lab.

From solid agar, bacteria were scraped from plates with sterile loops and transferred to a 1.5 mL screw cap tube containing 400 µL distilled water. Screw cap tubes were closed, and incubated in an 80°C water bath for 20 minutes for deactivation (killing) of bacteria. Samples were then safe to remove from biosafety level 3 lab.

3.2.1.9 CTAB DNA isolation

First, tubes containing deactivated (killed) bacteria were centrifuged for 3 minutes at 12,000 relative centrifugal force (rcf), the supernatant was discarded and the pellet was resuspended in 400 µL 5nM Tris/HCl, pH 8.5. Next, 50 µL of 10 mg/mL lysozyme was added, the sample was vortexed for 5 seconds, and incubated at least 1 hour (or overnight) in a 37°C water bath.

Next, 75 µL of 10% SDS/proteinase K mix (5µL Proteinase K (10 mg/mL) + 70 µL 10% SDS) was added to sample, vortexed shortly, and incubated for 10 minutes at 65°C. Then, 100 µL 5M NaCl and 100 µL CTAB/NaCl mix (prewarmed at 65°C) was added. Sample was vortexed until the liquid contents became white, and was then incubated for 10 minutes in a 65°C water bath. After, about 750 µL chloroform/isoamyl alcohol (24:1) mix was added and the sample was vortexed 10 seconds, then centrifuge 15 minutes at 12,000 rcf at room temperature. The aqueous supernatant was then transferred to a new tube and 0.6 volume (450 µL) isopropanol was added. The sample was carefully mixed (by inverting tube several times) and incubated for 30 minutes at -20°C.

Samples were then centrifuged for 15 minutes at 12,000 rcf, the supernatant was discarded and remaining liquid was dabbed on a paper towel. Next, 500 µL of cold 70% ethanol was added, samples were centrifuged again at 12,000 rcf for 5 minutes. The ethanol was discarded and the remaining liquid was dabbed on a paper towel. Samples were again centrifuged for 5 minutes at 12,000 rcf, and remaining liquid was carefully removed with pipette (careful not to disturb the DNA pellet). The DNA pellet was then dried in a heating block for 20 minutes at 60°C. Finally, the DNA pellet was resuspended in 40-80 µL water or 5nM Tris/HCl, pH8.5 buffer. Samples were again incubated in a heating block for 20 minutes at 60°C to help dissolve the DNA pellet. Tubes were then vortexed, liquid was spun down by short (3 seconds) centrifugation, then concentration and purity were measured in Spectrophotometer DS-11 FX.

3.2.2 Evolutionary experimental model

3.2.2.1 Sub-minimum inhibitory concentration evolution model

Mycobacterium tuberculosis complex (Mtbc) strain H37Rv frozen stock was taken from -80°C freezer and thawed to room temperature. Bacterial stock was passed through 18 G cannula 10 times, and 0.5 – 1.0 mL was transferred to 60 mL Nalgene® culture bottle containing 2 mL 7H9 medium. Culture was incubated at 37°C standing. After 1 – 2 days incubation, an additional 10 - 20mL 7H9 medium was added. Optical density was measured at 600nm (OD) daily, and additional 7H9 media was added after an OD of 0.2 was reached,

which increased the culture volume to at least 40 mL. Once bacteria reached an OD of 0.4 – 0.6, bacteria were passaged to experimental culture bottles containing sub-MIC antibiotics (Table 3.1). The final bacterial concentration was calculated to an OD of 0.05 in 50 mL 7H9 medium (supplemented with antibiotic or no antibiotic for control culture). Experimental culture bottles were then incubated at 37° standing. At the start of each experiment the sub-culture was also analyzed by CFU plating on 7H10 agar plates and selective media plates. Some of the original culture was saved for DNA isolation.

Table 3.1: Antibiotic concentrations examined in evolutionary experiments. Final concentrations in mg/L in 50 mL 7H9 medium.

Antibiotic	MIC	1:2 MIC	1:4 MIC	1:8 MIC	1:16 MIC	1:32 MIC	Control
Moxifloxacin	0.12 mg/L	0.06 mg/L	0.03 mg/L	0.015 mg/L	0.008 mg/L	NA	0.0 mg/L
Bedaquiline	NA	0.06 mg/L	0.03 mg/L	0.015 mg/L	0.008 mg/L	0.004 mg/L	0.0 mg/L
Clofazimine	NA	0.25 mg/L	0.12 mg/L	0.06 mg/L	0.03 mg/L	NA	0.0 mg/L

MIC – minimum inhibitory concentration, NA – not applicable

The OD of the experimental cultures was measured daily. On day two, the experimental cultures were transferred to a shake plate set to a speed of 50 rcf. On day four, all experimental cultures were passaged to new culture bottles, with the bacterial culture concentration again adjusted to OD 0.05 in 50 mL 7H9 medium, and antibiotic was added (Table 3.1). A total of five bacterial passages were conducted for each experiment, passage 1 - day 4, passage 2 - day 8, passage 3 - day 12, passage 4 - day 16, and passage 5 - day 20.

After passages 1, 3, and 5, experimental cultures were:

- Quantified by CFU plating
- Drug resistant mutant population was quantified by CFU plating on antibiotic supplemented plates
- Samples were taken for DNA analysis
- Backup stocks were made – 1 mL aliquot of culture, plus two 1 mL aliquots of 5x condensed culture
- Blood agar sterility checks were performed on all experimental cultures

After passaged 2 and 4:

- Samples were taken for DNA analysis
- Backup stocks were made – 1 mL aliquot of culture, plus two 1 mL aliquots of 5x condensed culture
- Blood agar sterility checks were performed on all experimental cultures

3.2.2.2 Re-plating of experimental cultures

It was necessary to repeat CFU plating on selective media plates due to:

- Plate contamination (when plates were made, during storage, or incubation)
- Over growth of colonies (mutant plating was not always diluted enough)
- Further investigation (e.g. experiments conducted with CFZ were later decided to be plated on BDQ plates; Results 4.2.3)

Backup culture stocks (which were frozen after each passage) were taken from -80°C freezer and thawed to room temperature. Bacteria was then passed through an 18 G cannula four times, and diluted or further plated on selective media plates. Blood agar sterility checks were performed. Leftover stocks were marked each time they were thawed and again stored in -80°C freezer.

3.2.2.3 Mutant isolation from selective media plates

After 21 – 35 days of growth on selective agar plates, mutant colonies were isolated as either single colonies (for single mutation selection), or multiple colonies (for total population deep sequencing).

First, a single colony was removed from the agar plate with a sterile loop (noted size and morphology of colonies), and transferred to a 1.5 mL tube with 1 mL culture medium. It was then passed through an 18 G cannula ten times to break up clumps. The sample was then split between two Nalgene® culture bottles (0.5 mL each), or all was transferred to one Nalgene® bottle (only done with CFZ experiments) containing 2 mL 7H9 medium. Cultures were incubated standing, at 37°C, for 1-2 weeks. Once the culture bottle appeared cloudy (OD of 0.2-0.6), 15 mL 7H9 was added. OD was measured daily, once OD reached 0.4 to 0.8, two 1 mL aliquots were made and stored in -80°C freezer. A sample was also taken for DNA isolation and WGS analysis. Sterility of culture was checked by spot plating on blood agar plates.

Mutant isolation for total population deep sequencing was conducted by scraping all remaining colonies from selective agar plates and transferring them to 1.5 mL screw cap tubes, containing 400 µL water. Each experimental condition was grouped separately (by experiment, passage, and drug concentration exposure). No sub-culturing was done. These bacteria were directly heat killed as previously described and DNA isolated by CTAB method.

3.2.3 Phenotypic assays

3.2.3.1 Resazurin emission microtiter assay – minimum inhibitory concentration testing

MIC testing of mutants isolated from evolutionary experiments were tested using REMA. A sub-culture was starting from frozen stocks (100 µl) or from the Nalgene® bottle in which mutants were first grown. Bacteria were cultured in 7H9, and when an OD of 0.2-0.8 was achieved, a MIC test was started. One day prior to starting the test, cultures were checked for contamination by plating on blood agar.

Plates were prepared by diluting antibiotics in 7H9 media and transferring 100 µl to a flat bottom 96-well plate. All plates included a positive control (well containing no antibiotic) and a negative control (7H9 media only) (Figure 3.1).

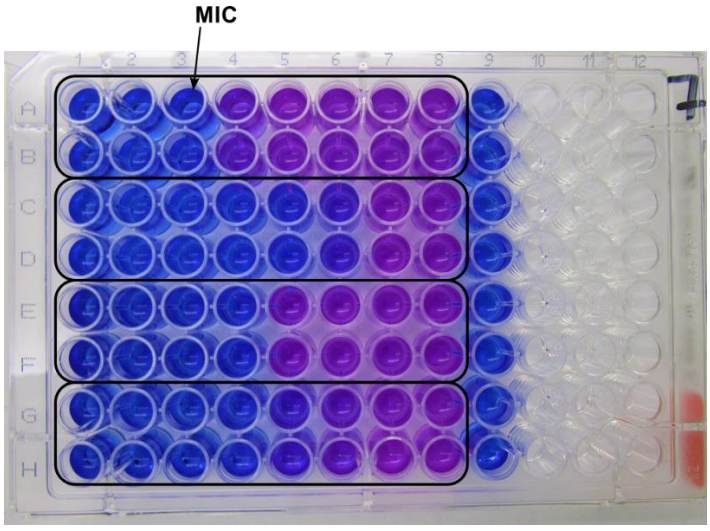

Figure 3.1 Resazurin emission microtiter assay set-up. Four bacteria strains were seeded in duplicates per plate. Each column contained a different drug concentration Positive control wells were exposed to no antibiotic (0.0 mg/L) and negative controls were the blanks (only 7H9; column 9). Fluorescence was measured in a Synergy 2 plate reader and interpreted visually, as positive growth (purple/pink) or inhibited growth (blue). The lowest concentration which inhibited growth (blue well) was considered the minimum inhibitory concentration (MIC).

Next, bacterial sub-cultures were diluted to an OD of 0.3 ±0.02, and 0.5 mL was transferred to a new tube containing 9.5 mL 7H9 to achieve a 1:20 dilution. Bacteria were mixed evenly by inverting the tube or vortexing. Next, 100 µL of bacterial suspension was added to appropriate wells of 96-well plate containing 100 µL of 7H9 with or without antibiotics, using a multi-stepper pipette (Figure 3.1). All drug concentrations were tested in duplicates. The gWT ancestor strain was included in every test.

Plates were then sealed with adhesive film for microtiter plates, and stored in sealed boxes. Wet paper towels were also placed in boxes to reduce evaporation. Plates were incubated at 37° standing for 6-9 days. After incubation 30 µL resazurin was added to each well. Plates incubated at 37°, overnight. Finally, the plates were measured in Synergy 2 plate reader, absorbance was measured at 570 nm, and fluorescence was measured at 544/590 nm. Photographs were taken of plates before they were discarded.

3.2.3.3 Mycobacterium growth indicator tube assay – drug susceptibility testing

MGIT MIC testing was performed by personnel at the National Reference Center for Mycobacterium Borstel. First, frozen bacterial stocks were thawed and 100 µL was transferred to Löwenstein-Jensen solid agar, and incubated for three weeks at 37°. MGIT tubes were prepared using BACTEC™ MGIT™ 960 SIRE Kit. Colonies were removed from agar plates using sterile loops and transferred to 2 mL 0.83% saline solution. Colonies were homogenized using sterile glass sticks and allowed to settle for 10 min. Bacterial suspension was adjusted to a McFarland standard of 0.5 using 0.83% saline solution. From this suspension, a 1:5 dilution in 0.83% saline solution was performed. Then 0.5 mL was added to MGIT tubes which were supplemented with 0.8 mL SIRE supplement and 100 µL antibiotic. A bacterial growth control was included by diluting to a McFarland standard of 0.5 by 1:500. Drug concentrations tested were 0.5, 1.0, and 2.0 mg/L for BDQ; 0.5, 1.0, and 2.0 mg/L for CFZ; 0.03, 0.06, and 0.12 mg/L for delamanid (DLM); and 0.5, 1.0, and 2.0 mg/L for LZD. Bacteria was considered resistant if a growth unit of 400 was reached before the growth control. An H37Rv gWT strain was not included in this test.

3.2.3.4 Mycobacterium growth indicator tube – mutant selection window

Sub-cultures were first started from frozen bacterial stocks. After stocks were thawed, 1 mL was added to the Nalgene® bottle with 10 mL 7H9. Cultures were incubated at 37°C standing. After two days, 5-10 mL

7H9 was added and cultures were incubated at 37°C on a shake plate at 50 rcf. Once cultures reached an OD >0.5, cultures were diluted to a McFarland standard of 1.0 (OD of 0.08-0.1). A second 1:5 dilution was done, and 0.5 mL was added to MGIT tubes supplemented with 0.8 mL OADC, and 100 µL antibiotics (or no antibiotic). A growth control was included by diluting to a McFarland standard by 1:500, and 0.5 mL was added to MGIT tubes supplemented with 0.8 mL OADC only. Experiments were carried out as biological duplicates or triplicates for all conditions (including growth control). MGIT tubes were loaded into BD Bactec™ MGIT and hourly measurements were taken for 15 days. Time to positivity was measured as hours or days until the tube fluorescence signal reached 400 units.

3.2.3.5 Fitness experiments – allele competition

Sub-cultures of the gWT ancestor and mutant clones were started from frozen bacterial stocks. After stocks were thawed, 1 mL was added to a Nalgene® bottle with 10 mL 7H9. Cultures were incubated at 37°C standing. After two days, 10-30 mL 7H9 was added and cultures were incubated at 37°C on a shake plate at 50 rcf. Once cultures reach an OD >0.5 culture was transferred to a roller bottle containing 100 mL 7H9. A 50:50 mixture of the gWT ancestor strain and one mutant clone was achieved by transferring culture to a roller bottle adjusted to a final concentration of 0.01 OD of each (OD 0.02 total). Biological triplicates were made of each, and CFU plating of sub-cultures were performed. Bottles were incubated at 37°C on a roller-bottle system, rolling at a motor voltage of 15 volts.

After seven days of incubation, 1 mL of culture was transferred to a new roller bottle containing 100 mL fresh 7H9. Roller bottles were again incubated for 7 days, then the experiment was concluded. Back-up culture stocks were made, transferring 1 mL culture to 1.5 mL screw cap tubes, and stored at -80°C. A 10mL culture sample was taken for DNA analysis.

Results were represented as changes in allele frequency. The starting allele frequency (Fi) was calculated from the initial CFU (i) of the starting inoculum (sub-culture inoculums from mutant stocks with the variant at 100% frequency). The final frequency of the mutant (M) allele and gWT allele were defined by WGS, M_{Ff} and gWT_{Ff} respectively. Fitness was indicated by change in allele frequency.

CFU inoculum calculation:

$$\frac{M_{\frac{CFU}{mL}} * mL}{100} = M_{CFUi} \qquad \frac{gWT_{\frac{CFU}{mL}} * mL}{100} = gWT_{CFUi}$$

Starting frequency of gWT and mutant alleles:

$$\frac{M_{CFUi}}{(M_{CFUi})(WT_{CFUi})} = M_{Fi}(\%) \qquad 100\% - M_{Fi} = gWT_{Fi}$$

$$Allele\ Frequency\ change\ of\ Mutant = M_{Ff} - M_{Fi}$$

$$Allele\ Frequency\ change\ of\ \mathrm{g}WT = gWT_{Ff} - gWT_{Fi}$$

Statistics calculated as non-parametric Kruskal-Wallis chi-squared test using R studio software (Appendix E).

3.2.4 Genotypic and Computational Analysis

3.2.4.1 Next generation sequencing

All DNA samples collected from *in vitro* experiments and MDR-TB case study (Results 4.1), were sequenced at Research Center Borstel. CTAB method was used to isolate DNA and libraries were prepared using Nextera-XT kits, performed according to manufacturer instructions. Quality of DNA and NGS libraries were verified on Fragment Analyzer using Standard Sensitivity NGS Fragment Analysis kits, according to manufacturer instructions. Samples were sequenced on NextSeq 500. Normal samples were loaded once onto the flow cell, deep sequenced samples were loaded three times.

NGS conducted on CRyPTIC samples was carried out by 14 independent laboratories, and data was collected for analysis by the group of Prof. Philip W. Fowler, Oxford University; and shared as excel files.

3.2.4.2 Genomic analysis

Analysis was performed using the bioinformatics pipeline MTBseq [146]. The pipeline was customized to run at “Low-Frequency Mode”, which excluded variant call thresholds of the standard pipeline output, and included all alternative allele calls. Variant tables were then manually filtered dependent on experiment using Microsoft® Excel. Low-frequency variants included in the MDR-TB patient case report (Results 4.1) were verified using binoSNP software [92].

Clinical strain sequences which were shared by CRyPTIC were analyzed using the Clockwork pipeline (https://github.com/iqbal-lab-org/clockwork), and the graph-based adjudication tool Minos (Minos, https://github.com/iqbal-lab-org/minos) to create a final variant output file.

3.2.4.3 PacBio® sequencing

Genomic DNA was isolated using the CTAB method from bacteria in 7H9 culture. Libraries were prepared using SMRTbell® Express Template prep Kit 2.0 and SMRTbell® Enzyme Clean Up Kit according to manufacturer's "Procedure & Checklist - Preparing Multiplexed Microbial Libraries Using SMRTbell® Express Template Prep Kit 2.0". Primers were then added to libraries using Sequel II Primer v4 and Sequel II Binding Kit 2.0 according to "Loading and Pre-extension Recommendations for Sequel® System - Quick Reference Card". Samples were analyzed using SMRT® Link software according to "SMRT Link User Guide - Sequel® Systems" version 10. Dr. Christian Utpatel processed these samples and aided in computation analysis.

3.2.3.2 Minimum inhibitory concentration testing of patient strains

MIC testing of Mtbc isolates collected by Comprehensive Resistance Prediction for Tuberculosis: an International Consortium (CRyPTIC) partners, were performed in UKMYC5 or UKMYC6 plates. Testing was carried out in 14 national and international laboratories. This method was validated by Rancoita *et al,* and performed as described [147]. Results were manually read and images were taken for additional automated assessment and quality control by AMyGDA software [144]. When results between laboratory visual assessment and AMyGDA did not correlate, plates were flagged as low quality and a third, independent assessment was performed by Citizen Science Project (BashTheBug.org). When two or three assessments did not correlate the Mtbc isolate was removed from this dataset.

3.2.4.4 Core genome multi locus sequence typing

A core genome multi locus sequence typing was used to calculate the minimum spanning tree of serial patient isolates (Results 4.1). This was accomplished using SeqSphere v5.9 (Ridom, Münster, Germany) software, as described in Kohl *et al.* [148].

3.2.4.5 Mutation catalogue literature search

A thorough literature search was performed to summarize all BDQ/CFZ resistance-associated mutations in genes *Rv0678*, *atpE*, *pepQ*, and *Rv1979c*. Search engines used were: Google, Googles Scholar, and PubMed, and included literature published from 2014 to June 2021. Key words used in literature search included: “Tuberculosis”, “TB”, “MTB”, “Mycobacterium tuberculosis”, “bedaquiline”, “BDQ”, “clofazimine”, “CFZ”, “treatment”, “drug resistance”, “patient”, “clinical report”, “MDR-TB”, “diarylquinolone”.

4. Results

4.1 Multi-drug and extensively drug resistant intra-patient resistance evolution of a single *Mycobacterium tuberculosis* complex strain

MDR/XDR-TB infections are especially hard to treat and require long-lasting, combination therapies (nine months or longer) [96]. Therefore, elucidating long-term microbial adaptations in the course of the therapy is particularly important. Through analysis of MDR-TB patient-derived sequential isolates, we can better understand how resistant populations emerge and trace successful/failed treatment interventions.

In this section, serial Mtbc isolates were investigated from a patient who suffered from five distinct treatment episodes, and underwent a total of 27 years of anti-TB treatment. Thirteen isolates were recovered from the final TB episode and analyzed by WGS to determine newly emerging mutations under the therapy. The molecular data was coupled with results from phenotypic DST and the analysis of an extensive patient treatment history. This study described the emergence of seven additional drug resistances while under therapy, observed several heteroresistant populations, and correlated treatment failures with treatment regimens at a given time point.

4.1.1 Patient History

A native-born German patient was first diagnosed with pulmonary TB in Western Germany at the age of four, and treated over four months with isoniazid (INH), para-aminosalicylic acid (PAS), and a streptomycin (SM) derivative (dihydrothenat). Although the treatment was classified as successful, the patient suffered an additional four relapse or reinfection events, which included 4 months, 41 months, 88 months and finally 216 months of treatment (Appendix B, Table B.1). In the patient records, an instance of treatment non-compliance was noted, as was immunosuppressive behavior such as smoking cigarettes and alcohol abuse. It was not mentioned that the patient suffered from immunocompromising disorders/diseases (such as human immunodeficiency virus). Although previous therapy interventions were successful, the patient succumbed to infection in the final treatment period.

The treatment regimen of this patient was frequently changed, especially throughout the final infectious episode. Drug regimens were not always consistent with phenotypic DST, resulting in regimens consisting of only two, one, or even no effective drugs in the final 18 years of treatment (Figure 4.1.1).

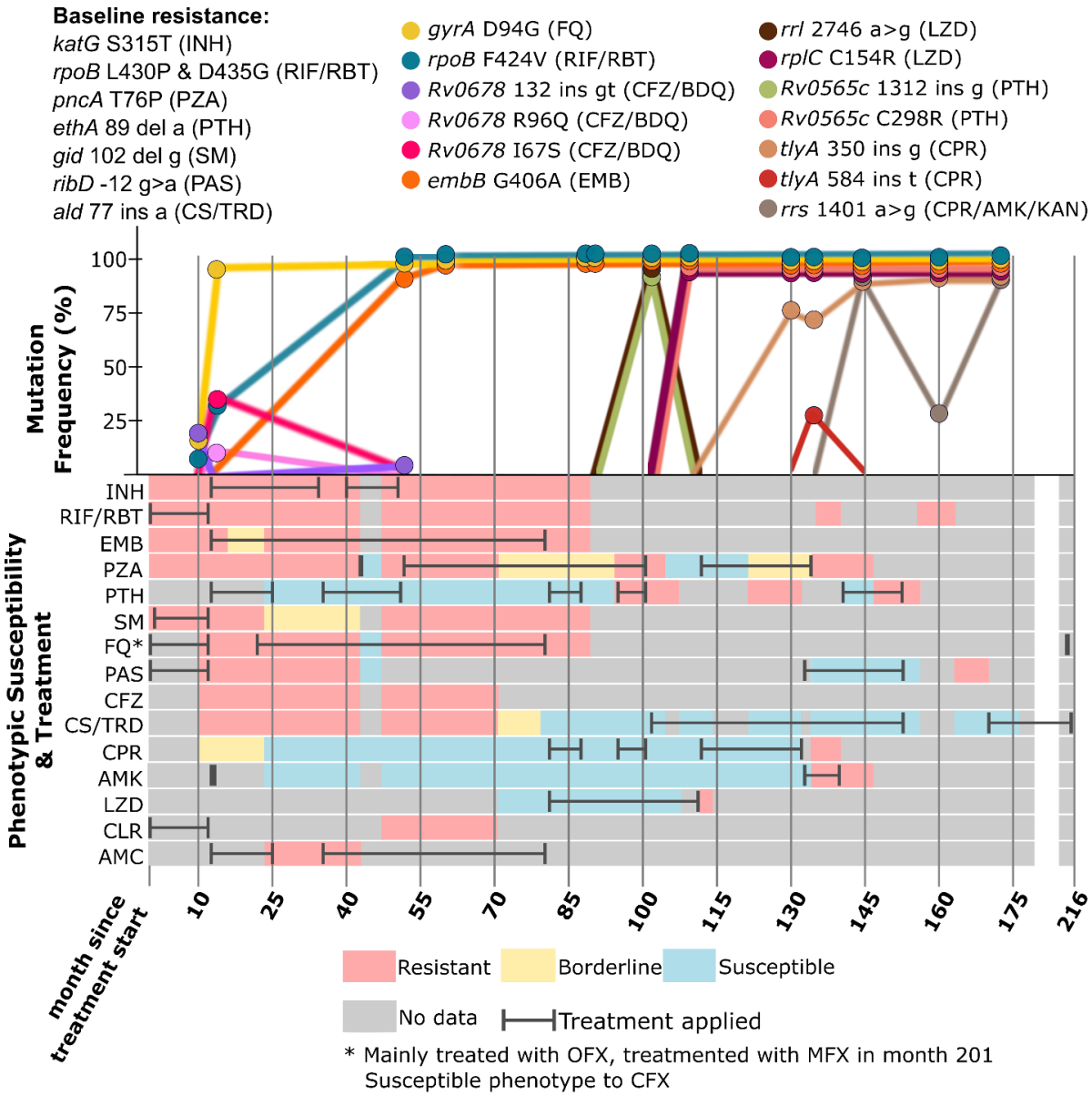

Figure 4.1.1: Final treatment episode: treatment history, phenotypic drug susceptibility results, and genetic diversity of resistance-associated mutations. Whole genome sequencing data is presented in the upper panel, and describes mutation frequency (y-axis) of emerging resistance mutations. Circles in the upper panel indicate when bacterial isolates were acquired from the patient. The lower panel shows results from phenotypic drug susceptibility testing as either resistant (red), borderline (yellow), susceptible (blue), or no data (gray). Dark gray bars which overlap phenotypic susceptibility testing, indicate when each drug was included in treatment. Adapted from Sonnenkalb *et al*. 2021 [87]

AMK: amikacin, AMC: amoxicillin+clavulanic acid, BDQ: bedaquiline, CFX: ciprofloxacin, CFZ: clofazimine, CLR: clarithromycin, CPR: capreomycin, CS: cycloserine, EMB: ethambutol, FQ: fluoroquinolone, INH: isoniazid, KAN: kanamycin, LZD: linezolid, MFX: moxifloxacin, OFX: ofloxacin, PAS: para-aminosalicylic acid, PTH: prothionamide, PZA: pyrazinamide, RIF: rifampicin, RBT: rifabutin, SM: streptomycin, TRD: terizidone

4.1.2 Intra-patient microevolution towards extensively drug resistant tuberculosis

Thirteen serial isolates which were collected throughout the final infectious episode (over 13 years), were analyzed via WGS, to predict drug resistance/susceptibility based on Research Center Borstel's mutation catalogue [146], [149]. Core genome multilocus sequence typing on these isolates confirmed clonal evolution of a single strain with a maximum distance of four or less alleles between sequential isolates, excluding a re-infection event (Figure 4.1.2).

Ten months after treatment began, the first bacterial isolate was obtainable for WGS. This isolate revealed baseline resistance to seven different antibiotics due to the following mutations: *katG* S315T for INH, *rpoB* L430P and D435G for rifampicin/rifabutin (RIF/RBT), *pncA* T76P for pyrazinamide (PZA), *ribD* at -12 g>a for PAS, *ethA* 89 del a for prothionamide (PTH), *gidB* 102 del g for SM, *ald* 77 ins a for cycloserine/terizidone (CS/TRD) which confirmed phenotypic DST results (Figure 4.1.1). INH, RIF, PZA, SM, PAS, PTH, TRD, ethambutol (EMB), capreomycin (CPR), and clarithromycin (CLR) were all included in previous treatment regimens for at least three consecutive months, but most were prescribed for ten or more months (Appendix B, Table B.1).

In month 13, phenotypic resistance was found to FQ drugs, mediated by the mutation *gyrA* D94G (Figure 4.1.1). This resistance arose after one year of ofloxacin (OFX) treatment (Appendix B, Table B.1). The subsequent isolate was collected nearly three years later (month 47), and revealed genotypic resistance to EMB mediated by *embB* G406A. Phenotypic resistance had already been detected in month 22, yet EMB was included in the treatment regimen from month 13 to 81. A third RIF/RBT associated mutation (*rpoB* F424V) was co-selected with *embB* G406A, and likely arose during the first 12 months of treatment (when RBT was prescribed) (Figure 4.1.1).

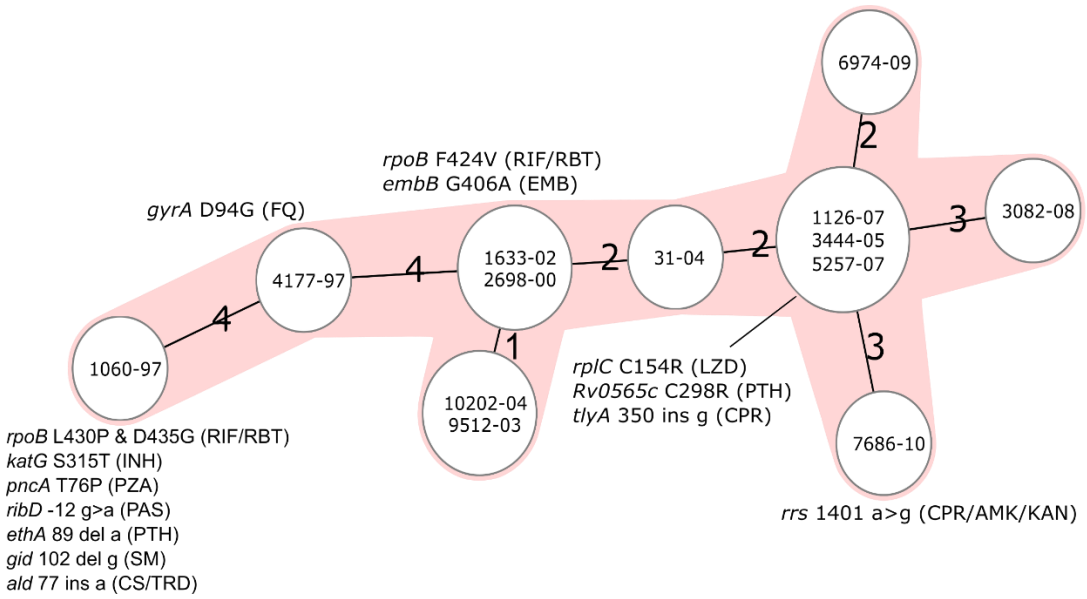

Figure 4.1.2: Minimum spanning tree based on a core genome multi locus sequence type analysis of thirteen serial isolates. Thirteen patient-derived serial isolates were whole genome sequenced and analyzed by core genome multi locus sequence typing. Number on connecting lines between nodes designates allele differences between isolates. Resistance-associated mutations (and linked drug) indicated next to isolate in which it was first fixed in the genome. Adapted from Sonnenkalb *et al. 2021* [87].

AMK: amikacin, AMC: amoxicillin+clavulanic acid, BDQ: bedaquiline, CFZ: clofazimine, CLR: clarithromycin, CPR: capreomycin, CS: cycloserine, EMB: ethambutol, FQ: fluoroquinolone, INH: isoniazid, KAN: kanamycin, LZD: linezolid, MFX: moxifloxacin, PAS: para-aminosalicylic acid, PTH: prothionamide, RIF: rifampicin, RBT: rifabutin, SM: streptomycin, TRD: terizidone, PZA: pyrazinamide

The isolate taken in month 108, following 26 months of LZD therapy, harboured the mutation *rplC* C154R at 100% frequency mediating LZD resistance. The mutation *Rv0565c* C298R, was co-selected with the LZD-linked mutation, and was likely responsible for the PTH resistance phenotype detected. These mutations emerged incredibly fast, in the four months since the previous isolate was collected. Next, CPR resistance was genotypically predicted in month 130, by the mutation *tlyA* 350 ins g (at a frequency over 75%). Finally, phenotypic and genotypic resistance to all second line injectables (CPR plus AMK and KAN) was attributed to the mutation *rrs* 1401 a>g detected in month 145. In total, resistance arose to seven anti-TB drugs mediated by five high-confidence resistance-associated mutations, over 13 years of MDR/XDR-TB treatment.

4.1.3 Evolutionary arms race of individual subpopulations

To understand resistance development more precisely, the presence of hetero-resistance (gWT and mutant alleles or several mutant alleles in a single population) populations was investigated, plus the emergence and extinction of resistant subpopulations over the course of the therapy. This was accomplished by analyzing mutations in genes implicated in resistance and compensatory evolution at a population frequency of >1% (Appendix B, Table B.2). All variants detected at a frequency below 75%, were statistically validated using binoSNP (Appendix B, Table B.3), a software developed for calling and verifying low-frequency SNPs from short-read Illumina® sequencing data [92]. In total, ten low-frequency resistance mediating mutations were observed, which fluctuated in the bacterial population before they reached fixation and/or disappeared in subsequent isolates (Appendix B, Table B.2; Figure 4.1.1).

As mentioned in the previous section, FQ resistance was attributed to *gyrA* D94G and became fixed at month 13. This mutation was already identified in the preceding isolate, three months prior, at a frequency of 21%. At month 10, a third RIF/RBT associated mutation, *rpoB* F424V, was detected at a frequency of 5%, then 30% in the subsequent isolate, followed by 96% then 100% in the two following isolates (Appendix B, Table B.2). Both of these mutations arose while under OFX (FQ) and RBT treatment.

Early isolates collected in months 10 and 13, but also month 47, harboured fluctuating BDQ/CFZ associated *Rv0678* mutations (Figure 4.1.1, Appendix B, Table B.2). First, the mutation *Rv0678* 132 ins gt was identified at 22% in the month 10 isolate, but was not observed in the subsequent isolate, then again appeared at only 3.6% in month 47 before it disappeared from the population. Similarly, in month 13, a heterogeneous population of *Rv0678* I67S (37%) and R96Q (10%) was detected, however, these two mutations were not found in any other isolate. Interestingly, these mutations arose and fluctuated without exposure to BDQ or CFZ, their resistance-associated drugs. However, phenotypic CFZ DST was conducted at that time and indicated resistance, likely attributed to these mutations.

Another heteroresistance event was observed, relating to CPR (Figure 4.1.1; Appendix B, Table B.2). In month 130, *tlyA* 350 ins g was first detected at a frequency of 79%. In the subsequent isolate (month 135), this mutation decreased to 71% coinciding with the appearance of *tlyA* 584 ins t at 28%. The next isolate, collected in month 144, revealed the fixation of tlyA 350 ins g and the loss of 584 ins t.

Finally, in later isolates, the resistance mutation *rrs* 1401 a>g was found fixed in the population at 100%. This mutation is responsible for second-line injectable drug (CPR, AMK, and KAN) cross-resistance, and

arose following 20 months of CPR then 7 months AMK treatment (Figure 4.1.1, Appendix B, Table B.2). Surprisingly, this mutation decreased to a 30% frequency in the preceding isolate. About one year later, *rrs* 1401 a>g was again fixed in the population at 99% frequency, absent treatment with any associated drugs.

4.1.4 Compensatory and tolerance associated mutations selected during treatment

Finally, three mutations linked to bacterial fitness and drug tolerance were selected in the last available isolates. The mutation F334L in the gene *prpR* (*Rv1129c*) linked to drug tolerance [150], was first found in month 92, was not observed in month 104 isolate, but was then fixed in the population at month 108 (Appendix B, Table B.2).

Another two mutations arose in the monooxygenase *Rv0565c*, a gene with a possible compensatory mechanism which is discussed to overcome fitness defects brought on by mutations in the monooxygenase *ethA* gene (activating the drugs ethionamide (ETH) and PTH) (Appendix B, Table B.2)[151]. These mutations in *Rv0565c* developed in isolates after the mutation *ethA* 89 del a. First, the mutation *Rv0565c* 1312 ins g arose to 97% frequency in month 104, but was lost in all proceeding isolates. In the subsequent isolate, a second mutation *Rv0565c* C298R was detected at 99% and remained fixed in the population.

4.2 An experimental model of antibiotic resistance evolution in bacteria of the *Mycobacterium tuberculosis* complex

As seen in the previously described treatment case, drug selection pressure especially in sub-optimal treatment regimens is shaping the evolutionary trajectories of bacterial populations. Still, conditions for selection of resistant subpopulations have not been fully explored for Mtbc strains, and the MSW, meaning the drug concentration range in which resistant subpopulations can be selected, has not been well defined. As several studies have shown that a variety of pathological niches within patients exist in which not all drugs can penetrate at a therapeutic level [111]–[114], [152]–[155], it is crucial to understand the evolutionary impact of low-concentration drug exposure on resistance development of Mtbc bacterium.

To address this question, a work-flow was designed for a sub-MIC evolution model performed *in vitro*, which included long- and short-term antibiotic exposure of the Mtbc reference strain H37Rv (ATCC 27294) (Figure 4.2.1). Each evolutionary experiment was conducted over five bacterial culture passages, allowing for analysis of over 17 bacterial generations (Appendix C, Table C.1). Throughout the passaging process, bacterial quantification was performed by CFU plating and OD measurements. In addition to normal CFU plating, bacteria were plated on solid media supplemented with antibiotics at concentrations 1- to 5-fold higher than the MIC to the given drug. The proportion of mutants which arose in the total population over time was quantified (mutants/million CFU). Finally, single colonies were picked and re-cultured from selection plates to characterize the genotype and phenotype of single mutants and performed deep sequencing of total colony populations from a particular plate to investigate the overall diversity of resistance-associated variants (Figure 4.2.1). These experiments were carried out with important MDR-TB treatment drugs: MFX, BDQ, and CFZ.

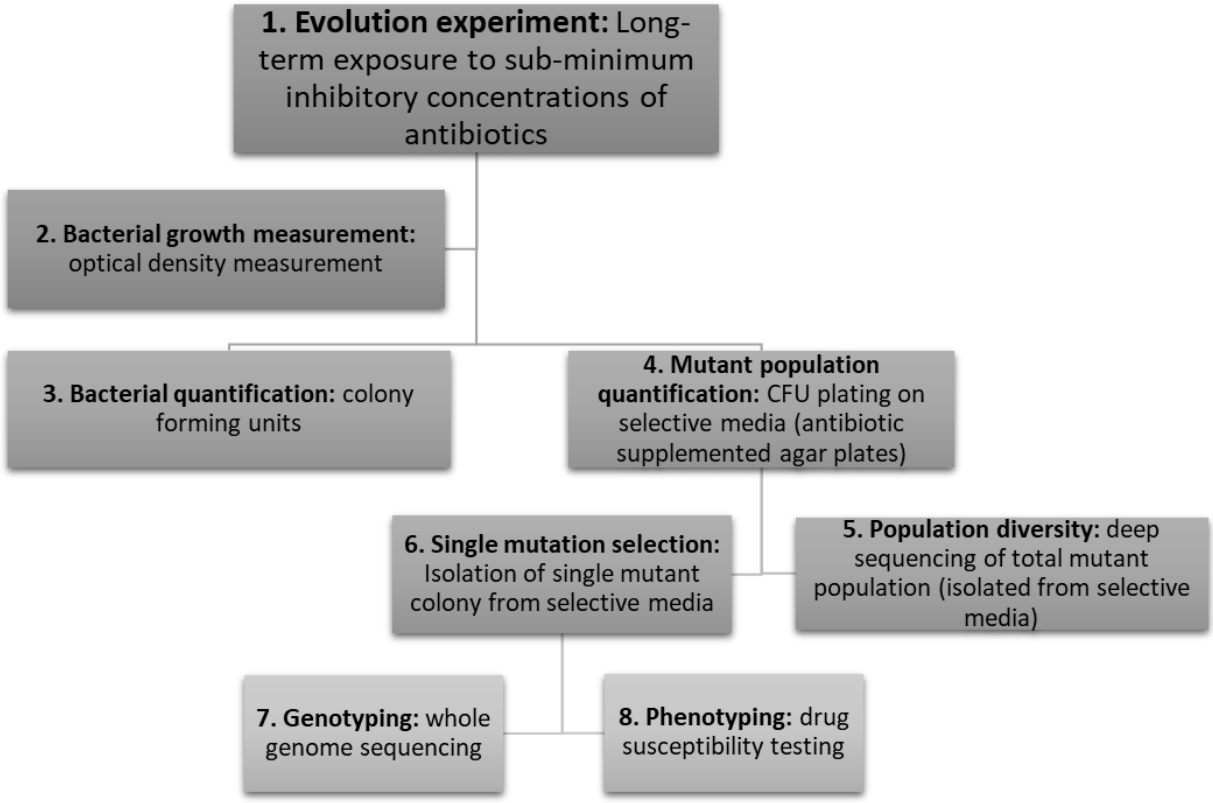

Figure 4.2.1: Experimental flow chart. (1) Evolutionary experiments were conducted by exposing H37Rv to sub-minimum inhibitory concentrations (MIC) of antibiotics over 20 days, i.e. five culture passages. (2) Growth was measured at each culture passage as optical density (OD) and (3) quantified by colony forming unit (CFU) plating. (4) Mutant population was also quantified through CFU plating on solid agar plates supplemented with antibiotics at the strain MIC or higher. (5) Bacterial colonies which grew on antibiotic supplemented media were collected and whole genome sequencing was conducted for mutant population diversity evaluation. (6) Further, single colonies were isolated from selective agar plates and were (7) genotyped by whole genome sequencing and (8) phenotyped by drug susceptibility testing in resazurin microtiter plate assays, to evaluate the MIC.

4.2.1 Developing an evolution model for *Mycobacterium tuberculosis* adaptation to antibiotics

The initial parameters to be established for the sub-MIC evolution model were the appropriate drug concentrations to be included. First, the MIC of the H37Rv reference strain was ascertained by REMA. The MIC here for MFX was 0.12 mg/L, 0.25 mg/L for BDQ, and 0.5 mg/L for CFZ. Since the bacterial inoculum was higher in these evolutionary experiments (1×10^7 CFU/mL) than in REMA (1×10^5 CFU/mL), the MIC, 1:2, 1:4, 1:8, and 1:16 the MIC of each drug was determined for the higher inoculum. Two bacterial passages were carried out, and the four highest concentrations which had a final growth measurement of OD >0.1 were selected for the evolutionary experiments (Figure 4.2.2).

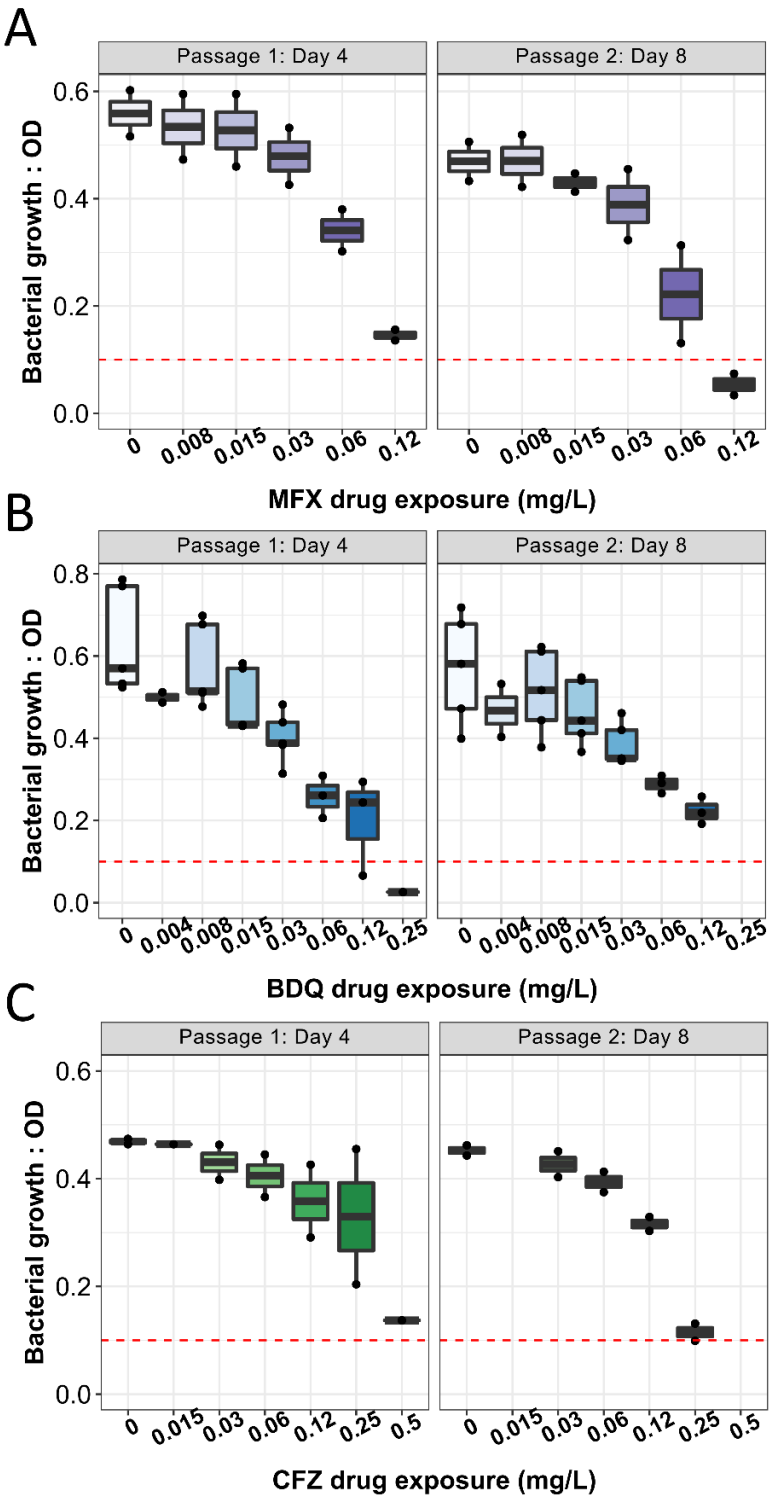

Figure 4.2.2: Sub-minimum inhibitory drug exposure of moxifloxacin, bedaquiline, and clofazimine over two culture passages. *Mycobacterium tuberculosis* complex strain H37Rv was cultured in 50 mL 7H9 medium and exposed to a range of antibiotic concentrations, starting at 0.12 mg/L for MFX, 0.25 mg/L for BDQ, and 0.5 mg/L for CFZ, and decreasing by 1:2 dilutions. Optical density of 600nm (OD) was measured at the end of each passage as an indication of bacterial growth. An OD below 0.1 (red line) was determined as insufficient growth.

Each experiment was conducted two times, and drug concentrations were tested in 1-fold dilutions (MIC, 1:2 MIC, 1:4 MIC, etc.). Of the MFX concentrations tested, 0.06, 0.03, 0.015, and 0.008 mg/L of MFX exposure did not inhibit the Mtbc growth below an OD of 0.1 (Figure 4.2.2A). After two passages of 0.12 mg/L MFX exposure, the OD was 0.05, and therefore excluded from future experiments. For BDQ, all concentrations tested did not inhibit growth of the H37Rv strain below an OD of 0.1 (Figure 4.2.2B). Final evolutionary experiments with BDQ included 0.12, 0.06, 0.03, 0.015, and 0.008 mg/L. Finally, experiments with CFZ indicated a concentration of 0.5 mg/L CFZ inhibited growth with an OD <0.2, and all lower concentrations tested (0.25, 0.12, 0.06, 0.03, and 0.015 CFZ) grew to an OD >0.1 after two passages (Figure 4.2.2C). The concentrations included in the final CFZ experiment were 0.03, 0.06, 0.12, and 0.25 mg/L CFZ.

These experiments were carried out over five culture passages, with samples taken at the beginning (passage 1: day 4), middle (passage 3: day 12) and end (passage 5: day 20) of the experiment (Figure 4.2.3). On average, there were 3.4 ±0.8 bacterial generations per passage, with a total of 17 generations per experiment (Appendix C, Table C.1). Evaluation of resistant populations and mutation characterization was accomplished by WGS and REMA MIC testing.

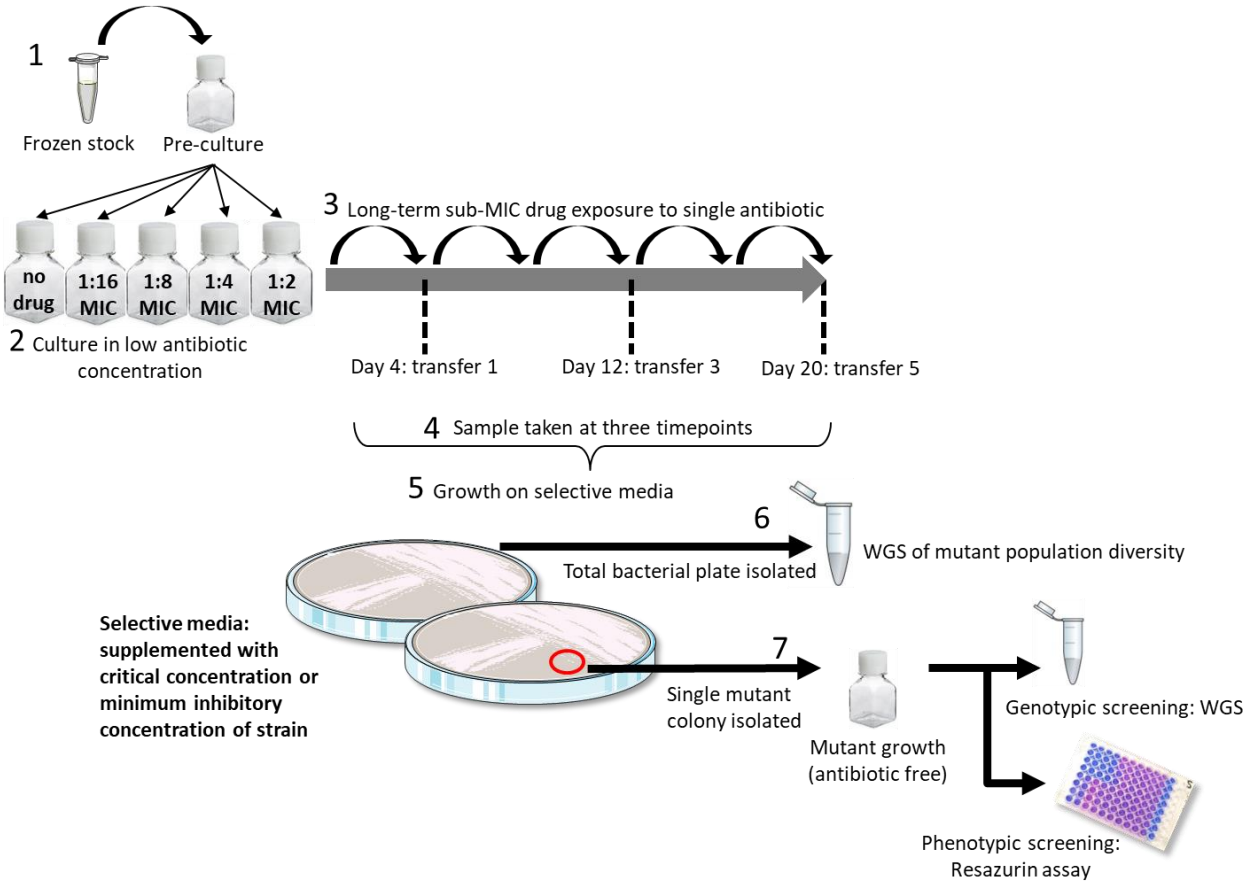

Figure 4.2.3: Sub-minimum inhibitory concentration evolution model experimental design for resistant variant selection, detection and analysis. (1) A pre-culture was started from frozen stocks of *Mycobacterium tuberculosis* complex strain H37Rv, (2) after recovery (5-7 days) some bacterial culture was transferred into new culture bottles and exposed to sub-minimum inhibitory concentrations (MIC) of antibiotics. (3) Bacteria were culture for 20 days including five bacterial passages, (4) cultures were sampled at passages 1, 3, and 5, (5) and grown on selective media plates, supplemented with the antibiotic. (6) After growth on selective media plates all colonies were pooled and deep sequencing was performed. (7) Single mutant colonies were isolated from selective media plates, characterized by whole genome sequencing and MIC tested by resazurin emission microtiter assays.

4.2.2 Sub-inhibitory antibiotic exposure selects and enriches drug resistant *Mycobacterium tuberculosis* complex bacterial populations

Three independent evolutionary experiments were conducted with MFX (Figure 4.2.4). Growth was initially evaluated by OD, which demonstrated a dose dependent growth inhibition as drug concentration exposure increased (Figure 4.2.4A). CFU analysis of the total bacterial population revealed that MFX exposure of 1:2 the MIC, or 0.06 mg/L MFX, reduced bacterial growth by an average of 9×10^7 CFU/mL, as compared to the growth of the unexposed (antibiotic free control) bacteria ($p=2.87 \times 10^{-4}_{passage1,}$ $0.024_{passage3,}$ $2.7 \times 10^{-6}_{passage5}$) (Figure 4.2.4B; Appendix C, Table C.2). Exposure to 1:4 the MIC, or 0.03 mg/L MFX, significantly inhibited bacterial growth only after 5 passages ($p=2.9 \times 10^{-4}$), with a 2×10^7 CFU reduction. When exposed to MFX, 1:8 and 1:16 below the MIC, or 0.015 mg/L and 0.008mg/L MFX respectively, significant bacterial growth inhibition was not observed as compared to the unexposed (antibiotic free) culture.

Then, the number of mutants recovered overtime at the different experimental conditions was quantified by plating on selective plates (mutant per million CFU; Methods 3.2.1.2) (Figure 4.2.4C). Throughout the entire experiment, in the unexposed bacterial culture (antibiotic free control), an average of 0.03 mutants/million CFU was observed. After 4 days of antibiotic exposure (passage 1), the highest exposure concentration, 0.06 mg/L MFX, exhibited ten times more mutants (0.3 mutants/million CFU, $p=1.57 \times 10^{-9}$), as compared to the antibiotic-free control. Twelve days of antibiotic exposure (passage 3), resulted in a significant increase in recovered mutants at the two highest exposure concentrations, 0.03 and 0.06 mg/L MFX, with an average of 0.3 ($p=7.9 \times 10^{-5}$) and 67 mutants ($p=9.5 \times 10^{-7}$) per million CFU selected, respectively. Significantly more mutants were also selected after long-term (20 days) antibiotic exposure at concentration: 0.015 mg/L MFX as 0.1 mutants/million CFU selected ($p=2.4 \times 10^{-4}$), 0.03 mg/L MFX as 2 mutants/million CFU ($p=1.7 \times 10^{-7}$), and 0.06 mg/L MFX as 5.3×10^3 mutants/million ($p=9.5 \times 10^{-8}$). The lowest drug concentration, 1:16 below the MIC (0.008 mg/L MFX), displayed no significant increase in mutants compared to the unexposed bacteria throughout the experiment, with only 0.03 mutants/million CFU recovered (Figure 4.2.4C, Appendix C, Table C.2).

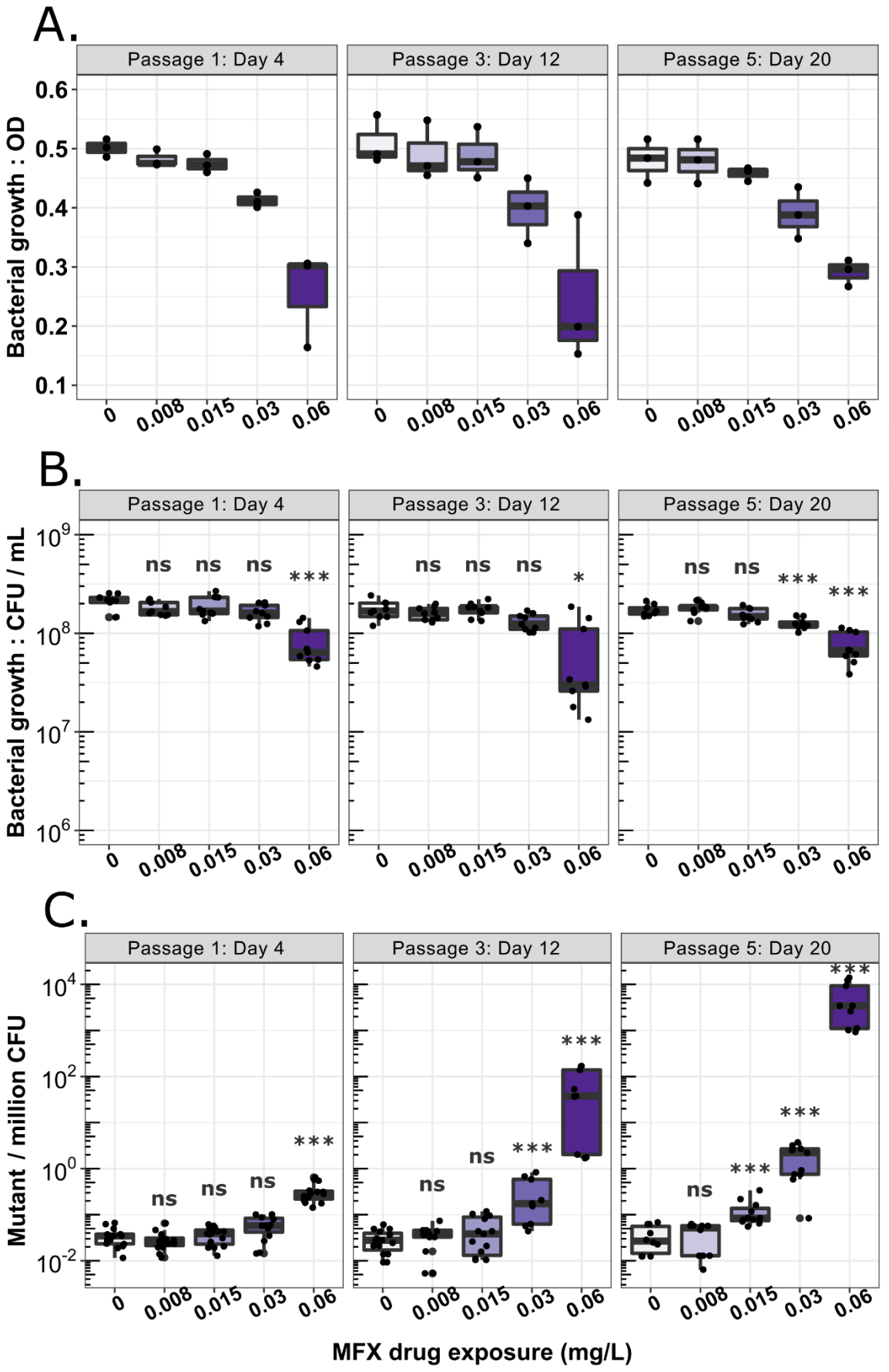
A.
Passage 1: Day 4
Passage 3: Day 12
Passage 5: Day 20
Bacterial growth : OD
0.6
0.5
0.4
0.3
0.2
0.1
0
0.008
0.015
0.03
0.06
B.
Bacterial growth : CFU / mL
10^9
10^8
10^7
10^6
ns
ns
ns
***
ns
ns
ns
*
ns
ns
***
***
C.
Mutant / million CFU
10^4
10^2
10^0
10^{-2}
ns
ns
ns
***
ns
ns
***
***
ns
***
***
***
MFX drug exposure (mg/L)

Figure 4.2.4: Sub-inhibitory exposure of moxifloxacin affects bacterial growth and mutant enrichment in a dose-dependent manner. The Mtbc lab strain H37Rv was exposed to four concentrations of moxifloxacin (MFX), 0.06, 0.03, 0.015, and 0.008 mg/L plus an antibiotic free control (0 mg/L MFX), with the highest concentration at 1:2 the minimum inhibitory concentration (MIC), MIC= 0.12 mg/L MFX. The bacteria were exposed to the antibiotic for 20 days, consisting of 5 culture passages. Bacterial samples were evaluated at three time points during the experiment, after day 4 or "passage: 1", day 12 "passage: 3", and day 20 "passage: 5". (A) Optical density (OD) was measured at each time point and indicated bacterial growth. (B) As a second measure of bacterial growth and further quantification, colony forming units (CFU) were measured by plating each culture on 7H10 agar plates and after 14-21 days of growth, CFU were counted. (C) The cultures were also plated on 7H10 agar plates supplemented with the critical concentration of MFX (0.25 mg/L), and after 14 – 21 days of growth, CFU were counted. The number of counted mutant CFU was divided by the total CFU to get the mutant enrichment ratio, then multiplied by 10^6 to get mutants/million CFU.

Statistics: Three independent experiments were conducted, OD standard deviation was calculated from 3 independent experiments with one biological replicate each, too few values for statistical analysis. Bacterial growth: CFU and mutants/million CFU, were calculated from 3 independent experiments, one biological replicate each, and 3 to 5 technical replicates per biological replicate (9 to 15 values). Statistics was calculated as nonparametric multiple contrast test (Kruskal) with a confidence interval of 95%, p-values between drug exposed and the antibiotic free control (0 mg/L MFX): *p<0.05, **p<0.01, ***p<0.001

The effect of sub-MIC drug exposure was similarly explored for BDQ (Figure 4.2.5). Bacterial growth as measured by OD, indicated a dose dependent decrease in growth as drug exposure concentration increased (Figure 4.2.5A). This dose-dependent decrease in growth was similarly observed by CFU analysis. The antibiotic free bacteria grew to 1.5 x 10^8 CFU/mL at each passage. The highest exposure concentration, 1:2 the MIC or 0.06 mg/L BDQ, reduced the bacterial growth by 2-5 x 10^7 CFU/mL , significantly more than the antibiotic free control at all passages ($p=3.4 \times 10^{-5}_{passage1,}$ $4.9 \times 10^{-3}_{passage3,}$ $2.4 \times 10^{-7}_{passage5}$) (Figure 4.2.5B, Appendix C, Table C.2). Exposure to 1:4 the MIC, or 0.03 mg/L BDQ, significantly reduced growth after passages 3 (p=0.029) and passage 5 ($p=2.8 \times 10^{-4}$) compared to the antibiotic free control, with a CFU reduction at 5 - 20 x 10^6 CFU/mL respectively. The concentration 0.015 mg/L BDQ, or 1:8 the MIC, inhibited growth from 8-32 x 10^6 CFU/mL compared to the control, which was significant after the 1st (p=0.046) and 5th ($p=9.8 \times 10^{-3}$) passages. The lowest concentration examined, 0.008 mg/L BDQ, 1:16 the MIC, did not show any significant growth defect as compared to the antibiotic free control, after all time points (p>0.05).

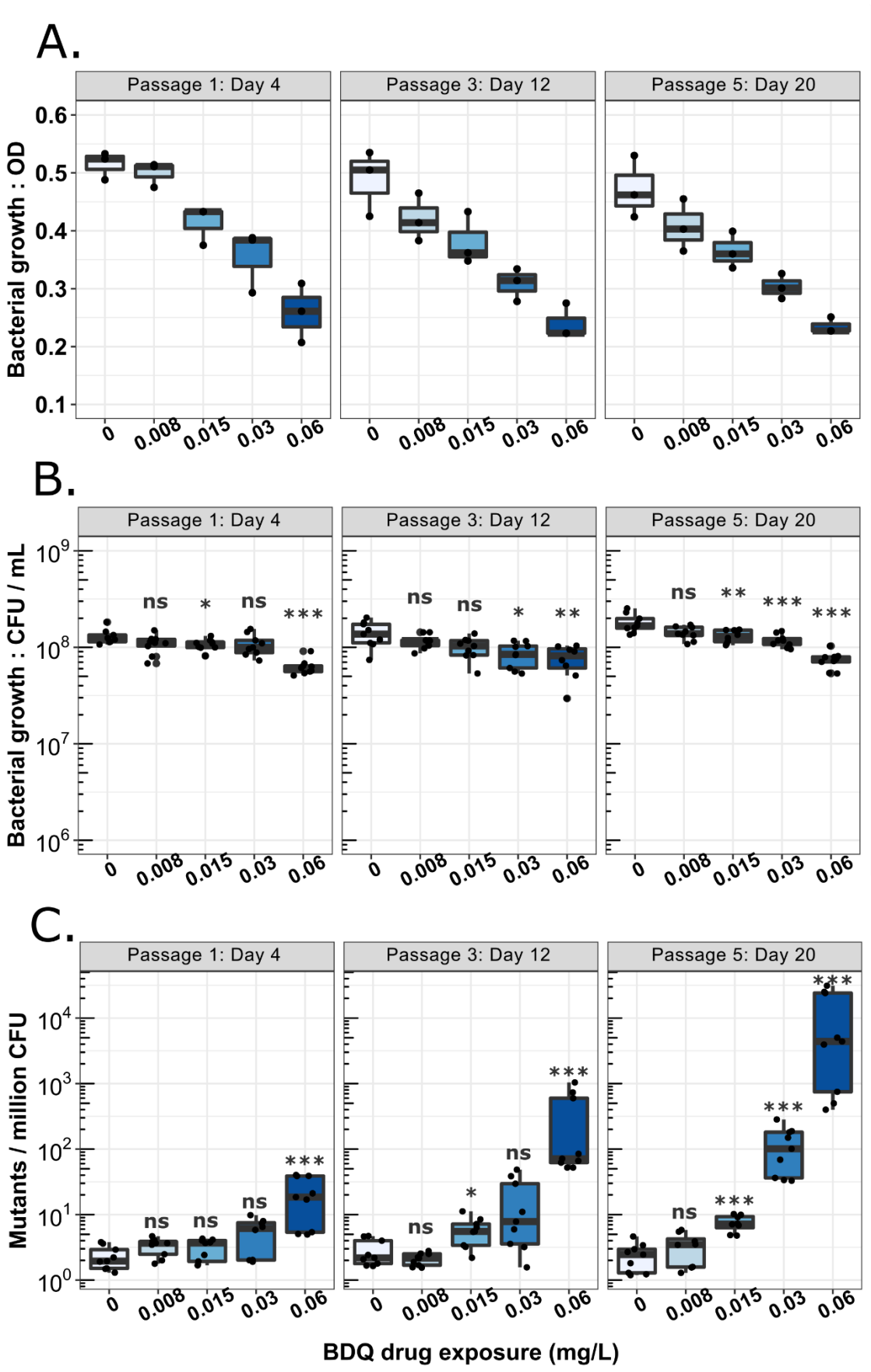
A.
Passage 1: Day 4
Passage 3: Day 12
Passage 5: Day 20
Bacterial growth : OD
0.6
0.5
0.4
0.3
0.2
0.1
0
0.008
0.015
0.03
0.06
B.
Bacterial growth : CFU / mL
10^9
10^8
10^7
10^6
ns
*
**
***
C.
Mutants / million CFU
10^4
10^3
10^2
10^1
10^0
BDQ drug exposure (mg/L)

Figure 4.2.5: Sub-inhibitory exposure of bedaquiline affects bacterial growth and mutant enrichment in a dose-dependent manner. The *Mycobacterium tuberculosis* complex lab strain H37Rv was exposed to four concentrations of bedaquiline (BDQ) (0.06, 0.03, 0.015, and 0.008 mg/L) plus an antibiotic free control (0 mg/L BDQ), with the highest concentration at 1:2 the minimum inhibitory concentration (MIC), MIC= 0.12 mg/L BDQ. The bacteria were exposed to the antibiotic for 20 days, consisting of 5 culture passages. Bacterial samples were evaluated at three time points during the experiment, after day 4 or "passage: 1", day 12 "passage: 3", and day 20 "passage: 5". (A) Optical density (OD) was measured at each time point and indicated bacterial growth. (B) As a second measure of bacterial growth and further quantification, colony forming units (CFU) were measured by plating each culture on 7H11 agar plates and after 14-21 days of growth, CFU were counted. (C) The cultures were also plated on 7H11 agar plates supplemented with the MIC of BDQ (0.12 mg/L BDQ), and after 14 – 21 days of growth, CFUs were counted. The number of counted mutant CFU was divided by the total CFU to get the mutant enrichment ratio, then multiplied by 10^6 for mutants/million CFU.

Statistics: Three independent experiments were conducted, OD standard deviation was calculated from 3 independent experiments with one biological replicate each, too few values for statistical analysis. Bacterial growth: CFU and mutants/million CFU, were calculated from three independent experiments, with one biological replicate each, and three to five technical replicates per biological replicate (9 to 15 values). Statistics was calculated as nonparametric multiple contrast test (Kruskal) with a confidence interval of 95%, p-values between drug exposed and the antibiotic free control (0 mg/L BDQ): *p<0.05, **p<0.01, ***p<0.001

The mutants recovered after each passage, increased over time with the most mutants observed at higher exposure concentrations (Figure 4.2.5C). The number of mutants recovered in the antibiotic-free control culture was 2.5 mutants/million CFU throughout the experiment. The highest exposure concentration, 1:2 the MIC or 0.06 mg/L BDQ, showed the uppermost mutant recovery as 21 mutants/million CFU after passage 1, 306 mutants/million CFU after passage 3, and 1 x 10^4 after passage 5, significantly more than the antibiotic free control ($p=7.3 \times 10^{-5}_{\text{passage 1}}$, $p=1.04 \times 10^{-6}_{\text{passage 3}}$, p= $p=1.4 \times 10^{-13}_{\text{passage 5}}$) (Appendix C, Table C.2). The second highest exposure concentration, 1:4 the MIC or 0.03 mg/L BDQ, presented a significant mutant increase as compared to the antibiotic free control after passage 5 with an average of 119 mutants/million recovered ($p=6.4 \times 10^{-14}$). Nevertheless, at a concentration exposure of 1:8 the MIC, 0.015 mg/L BDQ, a small but steady increase overtime was observed, from 6 mutants/million CFU after passage 3, to 8 mutants after passage 5, a significant increase as compared to the antibiotic free control at p=0.018 and $p=2.8 \times 10^{-10}$ respectively. There was no significant or observable increase in mutant population after exposure to 1:16 the MIC, 0.008 mg/L BDQ, as compared to the antibiotic free control.

These evolutionary experiments were the performed with CFZ (Figure 4.2.6). OD measurements indicated a reduction in growth, as CFZ exposure concentration increased (Figure 4.2.6A). After passage three (12 days), the highest exposure concentration 0.25 mg/L CFZ was no longer passaged due to high growth inhibition.

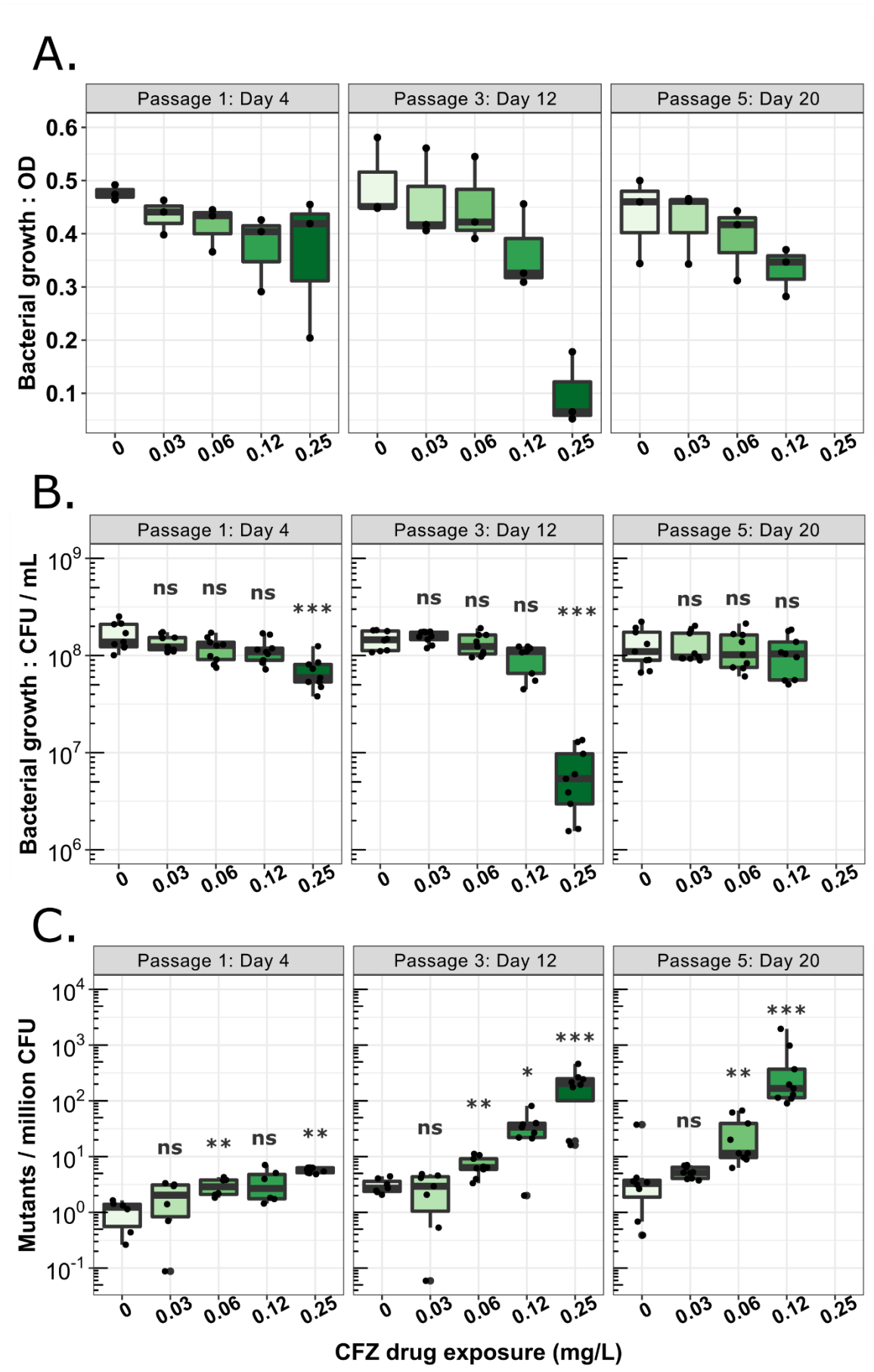
A.
Passage 1: Day 4
Passage 3: Day 12
Passage 5: Day 20
Bacterial growth : OD
0.6
0.5
0.4
0.3
0.2
0.1
0
0.03
0.06
0.12
0.25
B.
Bacterial growth : CFU / mL
10^9
10^8
10^7
10^6
ns
***
C.
Mutants / million CFU
10^4
10^3
10^2
10^1
10^0
10^{-1}
ns
**
*
***
CFZ drug exposure (mg/L)

Figure 4.2.6: Sub-inhibitory exposure of clofazimine affects bacterial growth and mutant enrichment in a dose-dependent manner. The *Mycobacterium tuberculosis* complex lab strain H37Rv was exposed to four concentrations of clofazimine (CFZ) (0.25, 012, 0.06, and 0.03 mg/L) plus an antibiotic free control (0 mg/L CFZ), with the highest concentration at 1:2 the minimum inhibitory concentration (MIC), MIC= 0.5 mg/L CFZ. The bacteria were exposed to the antibiotic for 20 days, consisting of 5 culture passages. Bacterial samples were evaluated at three time points during the experiment, after day 4 or "passage: 1", day 12 "passage: 3", and day 20 "passage: 5". (A) Optical density (OD) was measured at each time point and indicated bacterial growth. (B) As a second measure of bacterial growth and further quantification, colony forming units (CFU) were measured by plating each culture on 7H10 agar plates and after 14-21 days of growth, CFU were counted. (C) The cultures were also plated on 7H11 agar plates supplemented with the MIC of CFZ (0.5 mg/L CFZ), and after 14 – 21 days of growth, CFU were counted. The number of counted mutant CFU was divided by the total CFU to get the mutant enrichment ratio, then multiplied by 10^6 to get mutants/million CFU.

Statistics: Three independent experiments were conducted, OD standard deviation was calculated from 3 independent experiments with one biological replicate each, too few values for statistical analysis. Bacterial growth: CFU and mutants/million CFU, were calculated from three independent experiments, with one biological replicate each, and three to five technical replicates per biological replicate (9 to 15 values). Statistics was calculated as nonparametric multiple contrast test (Kruskal) with a confidence interval of 95%, p-values between drug exposed and the antibiotic free control (0 mg/L CFZ): *p<0.05, **p<0.01, ***p<0.001

Although there was a slight downward trend in growth as drug exposure concentration increased, CFU analysis indicated no growth defect, except at the highest drug exposure concentration. Exposure to 0.25 mg/L CFZ or 1:2 the MIC, reduced bacterial growth as compared to the antibiotic free control by 9.4×10^7 CFU/mL after passage 1 ($p=7.5 \times 10^{-4}$), and 1.4×10^8 CFU/mL after passage 3 ($p=4.9 \times 10^{-4}$) (Figure 4.2.6B, Appendix C, Table C.2).

Even though the changes in drug concentration had little effect on growth, an overall dose dependent increase in mutant enrichment was observed (Figure 4.2.6C, Appendix C, Table C.2). The lowest exposure concentration, 1:16 the MIC or 0.03 mg/L CFZ, did not inhibit bacterial growth as compared to the antibiotic free control. After passage 1, all other exposure concentrations appeared to have a slightly higher mutant enrichment than the unexposed bacteria, which was significant at concentrations 1:2 the MIC (0.25 mg/L CFZ, $p=1.1 \times 10^{-3}$) and 1:8 the MIC (0.06 mg/L CFZ, $p=5.5 \times 10^{-3}$). After passage 3, the mutant population increased compared to the antibiotic free control at 3 mutants/million CFU to 7 mutants/million CFU after 0.06 mg/L CFZ exposure ($p=1.9 \times 10^{-3}$), 34 after 0.12 mg/L CFZ exposure ($p=0.016$), and 199 after 0.25 mg/L CFZ ($p=2.2 \times 10^{-5}$). Finally, 20 days of antibiotic exposure (passage 5) an increase at 26 mutants/ million CFU after 0.06 mg/L CFZ exposure ($p=2.4 \times 10^{-3}$) and 458 mutants/ million after 0.12 mg/L CFZ exposure ($p=3.5 \times 10^{-5}$) was realized.

4.2.3 Cross-resistance selection of bedaquiline mutants after clofazimine exposure

Cross-resistance has been observed between CFZ and BDQ, when off-target mutations arise in the *Rv0678* gene, which regulates the expression of the *mmpS5-mmpL5* efflux system [76]. Therefore, it was questioned at what rate CFZ exposure selected for mutants which are also resistant to BDQ. To answer this question, evolutionary experiments were again performed by sub-inhibitory drug exposure with CFZ or BDQ, then the bacteria was plated on selective agar supplemented with BDQ (Figure 4.2.7). CFZ exposed cultures were plated from frozen back-up stocks.

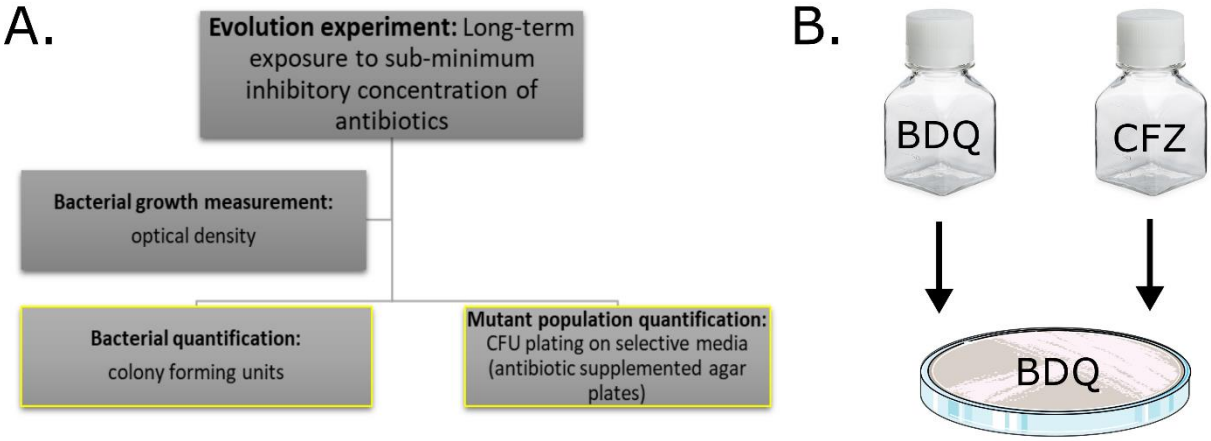

Figure 4.2.7: Experimental flow chart: bedaquiline/clofazimine cross-resistance. (A) Evolutionary experiments were conducted by exposing the *Mycobacterium tuberculosis* complex strain H37Rv to low levels of antibiotics over a long period of time. (B) First the bacteria were exposed to sub-inhibitory concentrations of bedaquiline (BDQ) or clofazimine (CFZ). The cultures were then plated on BDQ selective media, and mutant enrichment was then compared between CFZ and BDQ, at correlating reductions in minimum inhibitory concentration values.

At passage 1, it was observed that the mutant enrichment following BDQ exposure was significantly higher compared to that of CFZ exposure at most concentrations: 1:16 MIC ($p=0.002$), 1:8 MIC ($p=0.01$), and 1:2 MIC ($p=8.85 \times 10^{-2}$) (Figure 4.2.8; Appendix C, Table C.3). However, in all subsequent passages, this effect decreased. After the 3rd passage, mutant enrichment was similar between both drugs, except at 1:8 below the MIC, in which 6 mutants over 2 mutants/million CFU were recovered after BDQ exposure than CFZ exposure ($p=0.042$). There was not a difference in mutant enrichment between BDQ and CFZ exposure after passage 5. The 1:2 MIC exposure concentration of CFZ was excluded at passage 5, since passaging was discontinued after the 3rd passage.

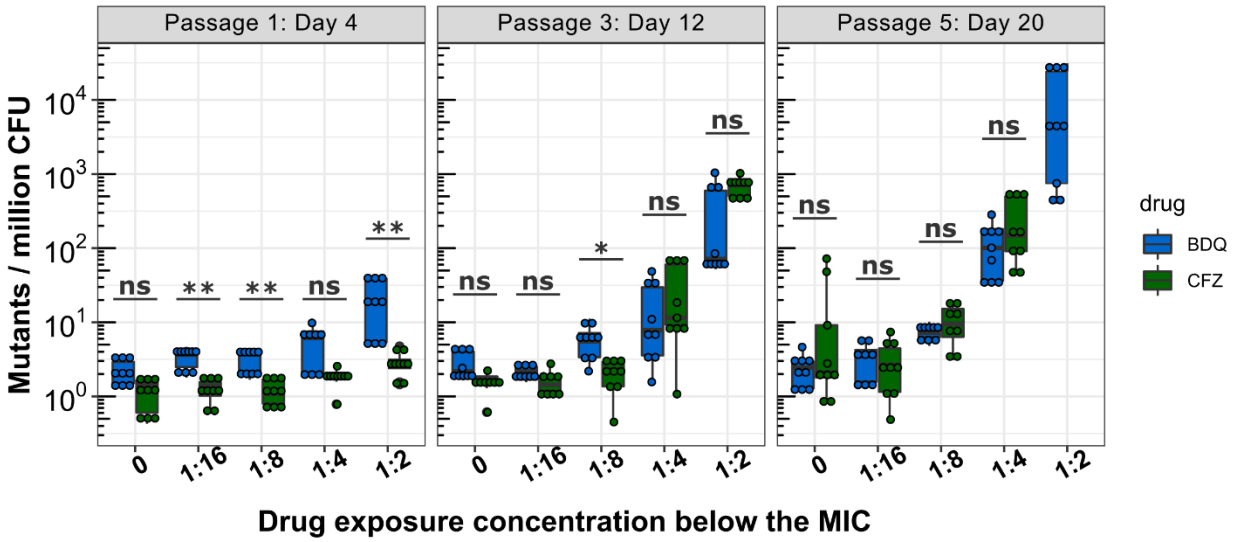

Figure 4.2.8: Cross-resistance comparison of bedaquiline and clofazimine exposure. The *Mycobacterium tuberculosis* complex lab strain H37Rv was exposed to four concentrations below the minimum inhibitory concentration (MIC) of bedaquiline (BDQ; blue) or clofazimine (CFZ; green). BDQ exposure concentrations were 0.06 mg/L (1:2 MIC), 0.03 mg/L (1:4 MIC), 0.015 mg/L (1:8 MIC), 0.008 mg/L (1:16 MIC), or no antibiotic (0). CFZ concentrations used were 0.25 mg/L (1:2 MIC), 0.12 mg/L (1:4 MIC), 0.06 mg/L (1:8 MIC), 0.03 mg/L (1:16 MIC), no antibiotic (0). The bacteria were exposed to the antibiotic for 5 culture passages. Bacterial samples were evaluated after passage 1 (4 days), passage 3 (12 days), and passage 5 (20 days). At each time point, the cultures were plated on 7H11 agar plates containing the critical concentration of BDQ (0.12 mg/L), and after 14 – 21 days of growth on plates, colony forming units (CFU) were counted. The number of counted mutant CFU was divided by total CFU for the mutant enrichment ratio, then multiplied by 10^6 to get mutants/million CFU.

Statistics: Three independent experiments were conducted, mutants/million CFU were calculated with one biological replicate per experiment, and three to five technical replicates per biological replicate (9 to 15 values). Statistics were calculated as a pairwise comparison of CFZ and BDQ by nonparametric multiple contrast test (Kruskal) with a confidence interval of 95%. *p<0.05, **p<0.01, ***p<0.001.

Overall, it was observed that after short term drug exposure, BDQ has a higher capacity to enrich BDQ resistant mutants than does CFZ. However, after long-term exposure, BDQ and CFZ have nearly equal capacities to enrich BDQ mutant populations.

4.2.4 Sub-inhibitory drug exposure selects a diversity of mutations in resistance-associated genes

The experiments performed so far with sub-MIC *in vitro* evolution under MFX, BDQ, and CFZ exposure revealed that sub-inhibitory drug exposure (up to 1:8 below the MIC) selected and enriched drug resistant populations (Results 4.2.2). It was then questioned whether these mutant populations were composed of a diversity of variants, or whether only few, or just one variant was selected. Therefore, WGS was conducted on the total mutant population of a given selection plate, grouped by drug exposure concentration and isolation time point (passage) (Figure 4.2.1). Further, single mutant colonies were isolated, which were then sub-cultured for characterization of resistance phenotype (MIC by REMA) and genotype (WGS) (Figure 4.2.1).

Moxifloxacin

Three independent experiments were conducted with MFX, as previously described (Figure 4.2.3). A total of 45 bacterial populations were evaluated, grouped by experiment, exposure concentration, and time point (passage). Of DNA isolated from 45 bacterial populations, 41 were successfully sequenced and analyzed (four were excluded due to low quality DNA isolation or sequencing). WGS deep sequencing of DNA was performed on the Illumina® platform, with a base coverage depth ranging from 277-1087x and an average of 595x (Appendix C, Table C.4).

It is known that resistance to MFX and other FQ drugs arise due to SNPs mainly in the quinolone resistance determining region (QRDR) of the *gyrA* (codon 74 to 113) and *gyrB* (codon 461 and 504) genes [156], [157]. Here, all high and low-frequency variants detected throughout the *gyrA* and *gyrB* genes were determined, and variant positions were excluded which did not have at least one read in both forward and reverse orientation, and a frequency >1%. Through population sequencing, 14 different SNPs were detected, seven in *gyrA* and seven in *gyrB* (Table 4.2.1). The most common mutations detected in different populations were *gyrA* A90V, *gyrA* D94G, and *gyrB* N499D; which appeared in 38, 25, and 23 different populations respectively. The least common variants detected were *gyrA* D94H, *gyrB* N499I, and *gyrB* N499T, each of which only appeared in one population.

Table 4.2.1: Summary of variant diversity in *gyrA* and *gyrB* genes of mutant population after moxifloxacin evolutionary experiments. DNA from mutant populations was individually collected and pooled by experiment, time point, and drug exposure concentration. "Appearance in n-populations" indicates the number of independent populations in which the variant was detected.

Gene	Gene name	Variant position	Variant	Type	Reference allele	Alternative allele	Appearance in n-populations
Rv0005	*gyrB*	6101	E288_	SNP	g	t	2
Rv0005	*gyrB*	6117	W293S	SNP	g	c	5
Rv0005	*gyrB*	6734	N499D	SNP	a	g	23
Rv0005	*gyrB*	6735	N499I	SNP	a	t	1
Rv0005	*gyrB*	6735	N499T	SNP	a	c	1
Rv0005	*gyrB*	6736	N499K	SNP	c	a	10
Rv0005	*gyrB*	6742	E501D	SNP	a	c	10
Rv0006	*gyrA*	7566	D89N	SNP	g	a	10
Rv0006	*gyrA*	7570	A90V	SNP	c	t	38
Rv0006	*gyrA*	7572	S91P	SNP	t	c	8
Rv0006	*gyrA*	7581	D94H	SNP	g	c	1
Rv0006	*gyrA*	7581	D94N	SNP	g	a	9
Rv0006	*gyrA*	7581	D94Y	SNP	g	t	3
Rv0006	*gyrA*	7582	D94G	SNP	a	g	25

N - number, SNP - single nucleotide polymorphism

Next, single mutant colonies were selected at random and sub-cultured for further phenotypic and genotypic analysis of the resistance-associated mutation (Figure 4.2.3). From two independent experiments, a total of 140/150 mutants were successfully characterized (10 were excluded due to low quality DNA isolation or sequencing) (Table 4.2.2).

Each mutant harbored one non-synonymous SNP in a resistance-associated gene, including three *gyrB* mutations and seven *gyrA* mutations (Table 4.2.2). The most abundant mutations were *gyrA* A90V and *gyrB* N499D which were independently selected 68 and 26 times respectively. The two least commonly selected mutations, each only selected one time, were *gyrB* N499K and E501D. All mutations presented an 8- to 33-fold MIC increase as compared to the gWT susceptible ancestor (Figure 4.2.9A). The lowest MIC observed was 0.5 mg/L MFX (8- to 16-fold higher than the gWT MIC) and the maximum MIC increase observed was at 2 mg/L MFX (16- to 33-fold higher than the gWT MIC) (Table 4.2.2).

Table 4.2.2: Genotypic and phenotypic characterization of resistant variants isolated after moxifloxacin exposure. Whole genome sequencing was conducted to detect the resistant variant under selection, minimum inhibitory concentration (MIC) was measured by resazurin emission microtiter assay and compared to the genetically wild-type (gWT) susceptible ancestor.

Gene name	Variant position	Variant	Ref. allele	Alt. allele	Number of isolates	Selection conc. (mg/L MFX)	MFX MIC (mg/L)	Fold MIC increase
Susceptible ancestor (gWT)						4	-	0.06-0.12
gyrB	6734	N499D	a	g	26	0.5	0.5-1	8-16
gyrB	6736	N499K	c	a	1	0.5	1	8-16
gyrB	6742	E501D	a	t	1	0.5	1	8-16
gyrA	7566	D89N	g	a	4	0.5	1	8-16
gyrA	7570	A90V	c	t	68	0.5	0.5-2	8-33
gyrA	7572	S91P	t	c	2	0.5	1	8-16
gyrA	7581	D94H	g	c	4	0.5	1	8-16
gyrA	7581	D94N	g	a	8	0.5	1	16-33
gyrA	7581	D94Y	g	t	2	0.5	1-2	8-33
gyrA	7582	D94G	a	g	24	0.5	1-2	8-33

Alt. - alternative, Ref. - reference, MFX - moxifloxacin

Next, all thirteen MFX (FQ) resistance-associated variants observed after population sequencing (Table 4.2.1) and single mutant selection (Table 4.2.2) were mapped on the sequences of the *gyrA* and *gyrB* genes (Figure 4.2.9B). Here, it was observed that over 87% of the variants appeared within the QRDR. Two of the thirteen detected variants were not observed in the QRDR (*gyrB* E288_ and W293S). Since these mutations were not independently selected and characterized, the phenotypic effect could not be determined (i.e. resistant or benign).

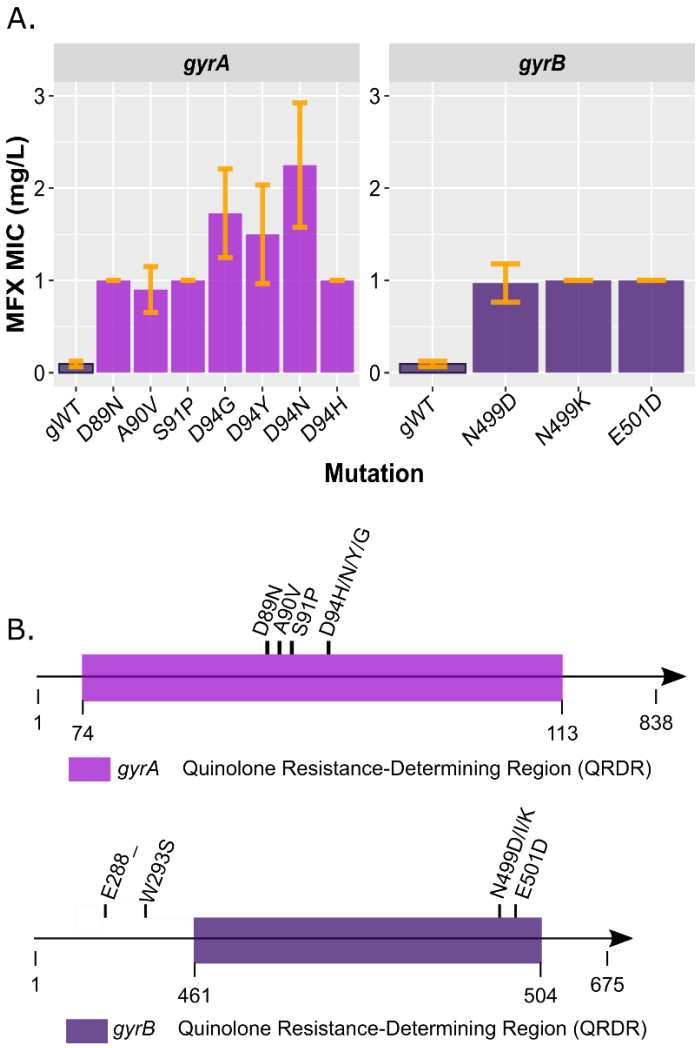

Figure 4.2.9: Characterization of mutations throughout *gyrA* and *gyrB* genes. (A) Single variants were isolated, minimum inhibitory concentration was determined and compared to the genetically wild-type (gWT) susceptible ancestor. (B) All mutations detected in population sequencing (Table 4.2.1.) and selected as single colonies (Table 4.2.2) were mapped along gyrA and gyrB genes, with an enhanced view of the quinolone resistance determining regions (QRDR).

Bedaquiline

As described above, exposure to sub-inhibitory concentrations of BDQ led to the selection of BDQ resistant clones on BDQ supplemented media (Figure 4.2.6). To determine the nature and diversity of mutations resulting in BDQ resistance, WGS was performed focusing on previously described BDQ resistance associated genes (Figure 4.2.3). Several mutations occurred in the genes *Rv0678* and *atpE*, which have been previously described as conferring low- and high-level BDQ resistance [76], [158]–[160]. No mutations were detected in other BDQ resistance related genes (i.e. *pepQ* and *Rv1979c*).

From three independent experiments, DNA from a total of 45 bacterial populations was isolated, 43 of which were successfully sequenced (two were excluded due to low quality DNA isolation). Each DNA sample was deep sequenced with a coverage depth from 205-383x, and an average of 284x (Appendix C, Table C.5). The threshold for calling a mutation was at least 1 forward and 1 reverse read, and a frequency >1%.

WGS of mutant populations revealed 39 unique SNPs possibly conferring BDQ resistance (Table 4.2.3). Of these resistances associated variants, 37 were located throughout the *Rv0678* gene including 11 indels and 28 non-synonymous SNPs (Appendix C, Table C.6). The most common *Rv0678* mutations were 193 del g, L43P, and A99V; which appeared in 34, 33, and 32 different populations respectively (Table 4.2.3). Also, two variants were detected in the *atpE* gene, A63P in three different populations, and D28G in one population (Table 4.2.3).

Table 4.2.3: Summary of variant diversity in *Rv0678* and *atpE* genes of mutant population after bedaquiline evolutionary experiment. DNA from mutant populations was individually collected and pooled by experiment, time point, and drug exposure concentration. "Appearance in n-population" indicates the number of independent populations in which the variant was detected. Extended table in Appendix C, Table C.6.

Mutations in *Rv0678*	37 / 39
Mutations in *atpE*	2 / 39

Gene name	Variant position	Variant	Type	Reference allele	Alternative allele	Appearance in n-populations
Rv0678	779117	L43P	SNP	T	c	33
Rv0678	779137	R50W	SNP	C	t	30
Rv0678	779181	192 ins g	Ins	C	g	28
Rv0678	779182	193 del g	Del	G	-	34
Rv0678	779191	S68G	SNP	a	g	30
Rv0678	779210	L74P	SNP	t	c	20
Rv0678	779225	F79C	SNP	t	g	20
Rv0678	779281	292 del a	Del	a	-	19
Rv0678	779285	A99V	SNP	c	t	32
Rv0678	779330	L114P	SNP	t	c	22
Rv0678	779349	360 del g	Del	g	-	19
Rv1305	1461127	D28G	SNP	a	g	1
Rv1305	1461231	A63P	SNP	g	c	3

Del - deletion, Ins - insertion, SNP - single nucleotide polymorphism

The mutations found in clones derived from single colonies after BDQ exposure are described along with mutant clones recovered after CFZ exposure in the following section.

Clofazimine

Finally, the mutant population diversity of CFZ exposed bacteria was examined. In total, DNA from 45 populations was collected for analysis, of which 38 were successfully sequenced (7 were excluded due to low quality DNA isolation or sequencing). Deep sequencing of DNA was achieved with an average depth of 336x, ranging from 257-422x (Appendix C, Table C.7). In this dataset, mutations were detected in the CFZ resistance-associated genes *Rv0678* and *pepQ* (*Rv2535*c) but not in *Rv1979c*.

WGS revealed 73 possible resistance conferring mutations, with 60 variants throughout *Rv0678* and 13 in *pepQ* (Table 4.2.4). In *Rv0678*, there were 31 indels, 38 non-synonymous SNPs, and one synonymous SNP (Appendix C, Table C.8). Within the *pepQ* gene, there were 8 non-synonymous and 5 synonymous SNPs observed. The most frequently observed *Rv0678* variants were A99V, G121E, or R50W which were observed in 33, 25, and 22 different experimental populations (Table 4.2.4). Interestingly, A99V was also one of the most commonly selected variants after BDQ exposure (Table 4.2.3). Finally, the three variants which appeared most often in *pepQ* were A87G, L114R, and A90G and were detected 9, 4, and 2 times respectively.

Taken together, the diversity of mutations detected by deep sequencing, which possibly conferred BDQ and/or CFZ resistance, was quite extensive with 96 unique mutations throughout three genes, and 14 substitutions which arose after both BDQ and CFZ exposure (Appendix C, Tables C.6 & C.8).

Table 4.2.4: Summary of variant diversity in *Rv0678* and *pepQ* (Rv2535c) genes of mutant population after clofazimine evolutionary experiment. DNA from mutant populations was individually collected and pooled by experiment, time point, and drug exposure concentration. "Appearance in n-population" indicates the number of independent populations in which the variant was detected.
Extended table in Appendix C, Table C.8.

Mutations in *Rv0678*	60 / 73
Mutations in *pepQ* (Rv2535c)	13 / 73

Gene	Gene name	Variant position	Variant	Type	Reference allele	Alternative allele	Appearance in n-populations
Rv0678	-	779120	L44P	SNP	t	c	15
Rv0678	-	779126	C46Y	SNP	g	a	15
Rv0678	-	779137	R50W	SNP	c	t	22
Rv0678	-	779181	192 ins g	Ins	c	g	15
Rv0678	-	779182	193 del g	Del	g	-	21
Rv0678	-	779191	S68G	SNP	a	g	15
Rv0678	-	779285	A99V	SNP	c	t	33
Rv0678	-	779351	G121E	SNP	g	a	25
Rv0678	-	779355	366 del g	Del	g	-	15
Rv2535c	*pepQ*	2860078	L114R	SNP	a	c	4
Rv2535c	*pepQ*	2860150	A90G	SNP	g	c	2
Rv2535c	*pepQ*	2860159	A87G	SNP	g	c	9

Del - deletion, Ins - insertion, SNP - single nucleotide polymorphism

Bedaquiline & Clofazimine selected mutants

Single bacterial colonies were isolated from selective agar plates supplemented with 0.12 mg/L BDQ, 0.25 mg/L BDQ, or 0.5 mg/L CFZ. A total of 150 mutant colonies were isolated from two independent BDQ experiments, with a total of 128 colonies successfully genotyped (WGS) and 117 phenotypically characterized (i.e. MIC). From the CFZ exposure experiments, 97 colonies out of 120 were successfully sequenced and 102 phenotypically characterized.

Of the 215 mutant colonies analyzed, 68 different nucleotide substitutions were detected, including 45 amino acid changes (Appendix C, Table C.9). The mutants selected harbored resistance-associated variants in two genes, five in *atpE* (*Rv1305*) and 63 in *Rv0678*, interestingly thirteen isolated clones did not harbor a mutation in any resistance-associated genes (further described in Results 4.3). Nine identical mutations were independently selected after both BDQ and CFZ experiments (Table 4.2.5). The two most common mutations selected were 192 ins g and A99V, which were independently selected in 18 and 17 clones respectively.

Table 4.2.5: Genotypic and phenotypic characterization of resistant variants isolated after bedaquiline or clofazimine evolutionary experiments. Whole genome sequencing was conducted to detect the resistant variant under selection, minimum inhibitory concentration (MIC) was measured by resazurin emission microtiter assay and compared to the genetically wild-type (gWT) ancestor. Table includes variants which were selected at least three times. Extended table in Appendix C, Table C.9.

Gene	Variant position	Variant	Type	BDQ MIC (mg/L)	CFZ MIC (mg/L)	Number of isolates	BDQ or CFZ isolate	Selection conc. (mg/L)
Susceptible ancestor (gWT)				0.25-0.5	0.5-1.0			
Rv0678	779060	G24V	SNP	2	2	3	CFZ	0.25
Rv0678	779101	R38_	SNP	2	2	4	CFZ	0.25
Rv0678	779117	L43P	SNP	1-2	2	5	BDQ/CFZ	0.12 / 0.25
Rv0678	779120	L44P	SNP	1	2	4	CFZ	0.25
Rv0678	779137	R50W	SNP	1-2	2	16	CFZ	0.25
Rv0678	779176	S63G	SNP	2	2	3	CFZ	0.25
Rv0678	779181	192 ins g	Ins	1-4	2-4	18	BDQ/CFZ	0.12 / 0.25
Rv0678	779182	193 del g	Del	1-2	2-4	13	BDQ/CFZ	0.12 & 0.25 / 0.25
Rv0678	779191	S68G	SNP	1-2	2	9	BDQ/CFZ	0.12 / 0.25
Rv0678	779204	R72L	SNP	2-4	2-6	3	BDQ	0.12
Rv0678	779210	L74P	SNP	1-2	2-4	8	BDQ/CFZ	0.12 / 0.25
Rv0678	779263	274 ins a	Ins	1	2	3	CFZ	0.25
Rv0678	779285	A99V	SNP	1-2	1-2	17	BDQ/CFZ	0.12 / 0.25
Rv0678	779293	A102T	SNP	1-4	2-4	4	BDQ	0.12
Rv0678	779349	360 del g	Del	1-4	2-4	8	BDQ/CFZ	0.12 / 0.25
Rv0678	779351	G121E	SNP	2	2-4	3	CFZ	0.25
Rv0678	779406	417 ins 20bp	Ins	1-2	2	3	BDQ	0.12
Rv0678	779424	Y145_	SNP	1-2	NA	5	BDQ	0.12 & 0.25
Rv0678	779455	R156_	SNP	2	NA	3	BDQ/CFZ	0.12 & 0.25 / 0.25
Rv1305	1461127	D28V	SNP	≥4	NA	3	BDQ	0.25
Rv1305	1461227	E61D	SNP	2-≥10	2	3	BDQ	0.25
Rv1305	1461227	E61D	SNP	≥4	1	4	BDQ	0.12 & 0.25
Rv1305	1461231	A63P	SNP	≥8	1-2	7	BDQ	0.25
NA	NA	NA	-	2	1-2	13	BDQ/CFZ	0.12

Alt. - alternative, BDQ - bedaquiline, bp – base pairs, CFZ - clofazimine, conc. - concentration, Del - deletion, Ins - insertion, NA - not available, Ref. - reference, _ - stop codon insertion

When compared to the gWT susceptible ancestor, mutations in *Rv0678* resulted in a 2- to 16-fold MIC increase to BDQ, and either no increase or up to a 12-fold MIC increase to CFZ (Appendix C, Table C.9). Most clones which harbored an *atpE* mutation did not present an increase in MIC to CFZ, with exception to some clones which harbored an E61D or A63P mutation, and demonstrated a 4-fold MIC increase as compared to the gWT to CFZ. All *atpE* mutants demonstrated a substantial MIC increase to BDQ, from 4- to ≥20-fold more than the gWT MIC (Table 4.2.5).

Several clones which were isolated after the first passage (from two independent experiments) underwent MIC verification through a second phenotypic testing method: MGIT (Table 4.2.6). Here, *Rv0678* mutations exhibited an increased BDQ MIC from the gWT of 0.25-0.5 mg/L to ≥2 mg/L, and CFZ MIC from 0.25 mg/L to 2 mg/L. Further, *atpE* mutations increased BDQ MICs above the highest tested concentration (MIC >2 mg/L BDQ) and presented mild or no increase in CFZ MIC, as compared to the gWT.

Additional MIC testing conducted for DLM and LZD demonstrated no cross-resistance as the MIC was the same as the gWT for all mutant clones at ≤0.03 mg/L and ≤0.5 mg/L respectively. Although the gWT was not tested with LZD, the strains tested indicated an MIC below the WHO defined critical concentration of 1.0 mg/L.

To describe the diversity of mutations observed in all experiments performed, all resistance-associated mutations were mapped on the sequences of the *atpE*, *Rv0678*, and *pepQ* genes (Figure 4.2.10). This analysis allows for a visual representation of the mutational distribution throughout these resistance-associated genes, and the identification of potential hot-spot regions. In *atpE*, there were two areas where variants were clustered, around codon 28, and from codon 61 to 63. Mutations in the *Rv0678* gene were spread throughout the gene with no clear clustering regions. In the *pepQ* gene, there was one clustering region from codon 87 to 114. However, no mutants harboring a variant in *pepQ* were independently selected, so it is not clear these mutations lead to elevated BDQ or CFZ MICs.

Table 4.2.6: Mycobacterium growth indicator tube testing of *Rv0678* and *atpE* mutants. Drug resistant clones selected on bedaquiline agar plates (after passage one from two independent experiments) underwent minimum inhibitory concentration (MIC) testing by mycobacterium growth indicator tubes, performed by colleagues at the Super-National Reference Center for Mycobacteria, Borstel. Previous testing of the genetically wild-type (gWT) strain showed an MIC of 0.25-0.5 mg/L bedaquiline, 0.25 mg/L clofazimine, 0.015-0.03 mg/L for delamanid, and 1.0 mg/L for linezolid [96].

			Bedaquiline			Clofazimine			Delamanid			Linezolid		
Strain ID	**gene**	**loci**	**0.5 mg/L**	**1.0 mg/L**	**2.0 mg/L**	**0.5 mg/L**	**1.0 mg/L**	**2.0 mg/L**	**0.03 mg/L**	**0.06 mg/L**	**0.12 mg/L**	**0.5 mg/L**	**1.0 mg/L**	**2.0 mg/L**
gWT	-	-	S	S	S	S	S	S	S	S	S	NA	NA	NA
LS011001	*atpE*	A63P	R	R	R	S	S	S	S	S	S	R	S	S
LS011002	*atpE*	A63P	R	R	R	R	S	S	S	S	S	R	S	S
LS011003	*Rv0678*	193 del g	R	R	S	R	R	S	S	S	S	R	S	S
LS011004	*Rv0678*	R156_	R	R	S	R	R	S	S	S	S	S	S	S
LS011005	*Rv0678*	Y145_	R	R	S	R	R	S	S	S	S	S	S	S
LS011041	*atpE*	E61D	R	R	R	S	S	S	S	S	S	R	S	S
LS011081	*Rv0678*	G25S	R	R	S	R	R	S	S	S	S	S	S	S
LS011061	*Rv0678*	Y145_	R	R	S	R	R	S	S	S	S	S	S	S
LS011062	*Rv0678*	Y145_	R	R	R	R	R	S	S	S	S	R	S	S
LS011063	*Rv0678*	Y145_	R	R	S	R	R	S	S	S	S	S	S	S
LS0210151	*atpE*	D28V	R	R	R	S	S	S	S	S	S	R	S	S
LS0210154	*atpE*	E61D	R	R	R	R	S	S	S	S	S	R	S	S

NA - not available, R - resistant, S - susceptible, _ - stop codon insertion

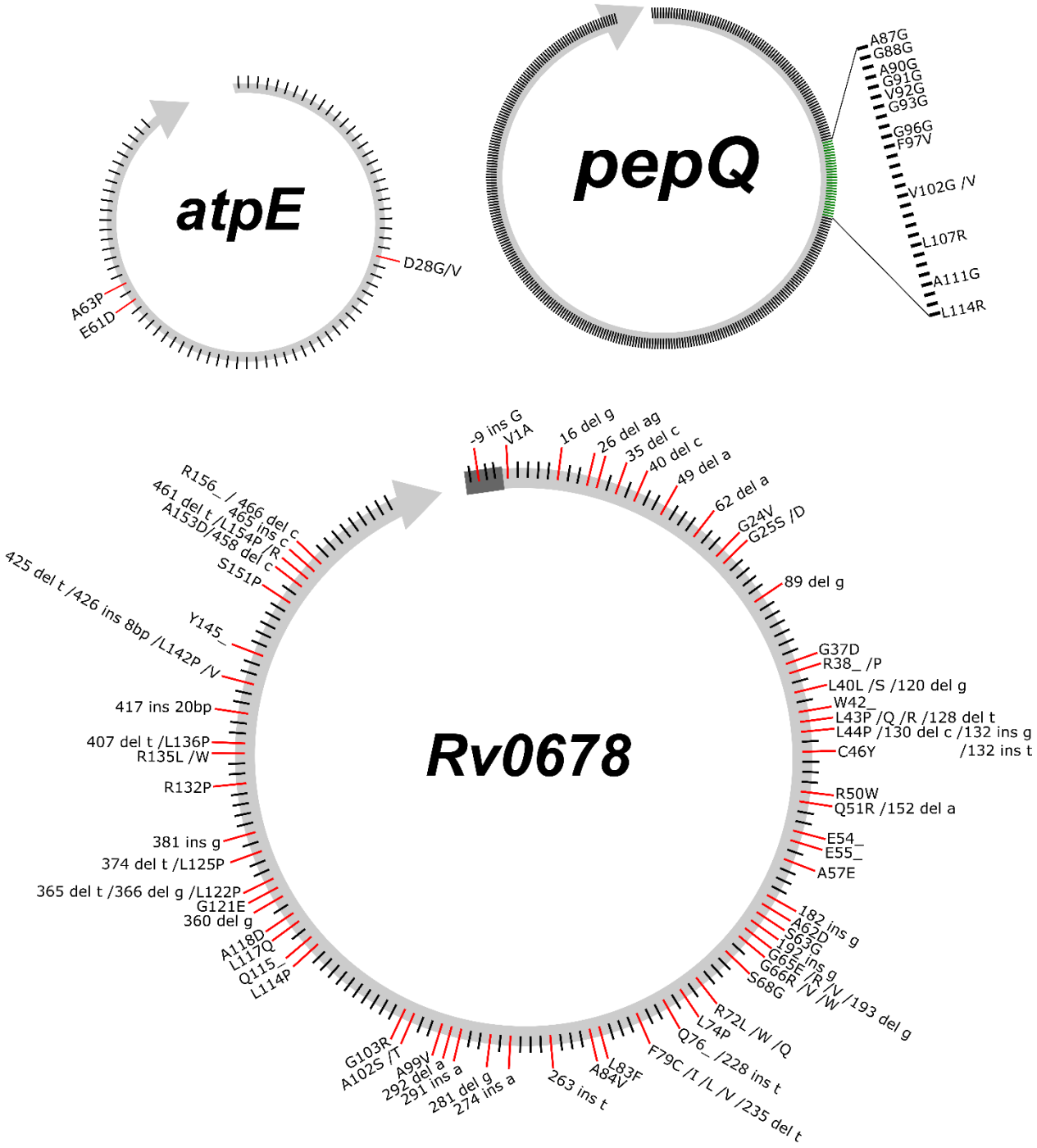

Figure 4.2.10: Mutations detected after *in vitro* experiments, mapped to *atpE*, *Rv0678*, and *pepQ* genes. Resistance-associated mutations detected after *in vitro* selection experiments in single isolated mutants and total mutant populations were designated along *Rv0678*, *atpE*, and *pepQ* genes at corresponding coding positions by non-synonymous single nucleotide polymorphisms, and by a protein disrupting mutation such as a stop codon insertion (_) or frameshift mutations - nucleotide insertion (ins) or deletions (del). Resistance-associated variants included from Appendix C, Tables C.6, C.8, and C.9.

4.2.5 Bedaquiline and clofazimine resistance-associated mutations described in patient cohorts

In the previous section, it was demonstrated that sub-MIC, long-term antibiotic exposure selected a diversity of resistance conferring mutations to BDQ and CFZ through mutations in *Rv0678*. Next, *in vitro* selected mutations were compared with mutations determined in a large patient-derived strain collection. This contributed to the development of a large variant catalogue, allowing genomic resistance prediction for BDQ/CFZ, and also gave a better view to the extent at which the sub-MIC evolution model reflects resistance evolution in Mtbc strains obtained from patients.

In cooperation with the CRyPTIC consortium, a 14,151 clinical strain collection which included WGS and MIC data based on UKMYC5/6 microtiter broth plates was analyzed (Appendix C, Table C.10) [140], [147]. The whole dataset was filtered for strains with single mutations in *Rv0678*, *atpE*, *Rv1979c* or *pepQ*. Since *Rv1979c* and *pepQ* mediated resistance is not well described in patients, isolates with susceptible phenotypes were not included [161]–[163]. Altogether, 235 strains were found with a mutation in one of these four genes (Appendix C, Table C.10). Overall, 178 strains had mutations in *Rv0678*, three in *atpE*, 35 in *Rv1979c*, and 19 in *pepQ* (Table 4.2.7). Resistance profiles were determined on UKMYC5/6 plates and interpreted as >0.12 mg/L BDQ/CFZ as resistant, =0.12 mg/L BDQ/CFZ borderline, and <0.12 mg/L BDQ/CFZ susceptible.

Table 4.2.7 Patient cohort dataset summary. Of the 14,151 clinical isolates collected and characterized by Comprehensive Resistance Prediction for Tuberculosis: An International Consortium partners, 235 strains harbored a mutation in one of four bedaquiline (BDQ) / clofazimine (CFZ) resistance-associated genes; *Rv0678*, *atpE*, *Rv1979c*, or *pepQ*.

Implicated resistance-associated gene	Number of isolates	BDQ/CFZ resistant phenotype (>0.12 mg/L)	BDQ/CFZ borderline resistance (=0.12 mg/L)	BDQ/CFZ susceptible phenotype (<0.12 mg/L)	Strains with no CFZ MIC data
Rv0678	178	52 / 36	32 / 38	94 / 75	0 / 32
atpE (Rv1305)	3	3 / 1	0 / 1	0 / 1	0 / 0
Rv1979c	35	35 / 16	0 / 4	0 / 1	0 / 14
pepQ (Rv2535c)	19	19 / 2	0 / 3	0 / 3	0 / 11

In addition to this large CRyPTIC dataset, an in-depth literature search was included, in order to further define the genotypic landscape of BDQ (and CFZ) resistance conferring mutations (Appendix C, Table C.11). This study summarized all phenotypically resistant (based on study definition or WHO accepted critical concentration) patient-derived and *in vitro* isolates described in 28 studies. In total, 159 resistance conferring variants, 30 borderline, 26 benign/susceptible, and 15 with variable resistance profiles to BDQ were defined. For CFZ, these same strains presented 117 resistance-associated variants, 25 borderline, 23 benign/susceptible, and 15 with variable resistance/susceptibility (Appendix C, Table C.11).

To allow for an overview of the mutation diversity identified, all borderline and resistance-associated mutations found in strains obtained from patients throughout were mapped on the sequences of *Rv0678* (101), *atpE* (5), *pepQ* (5), and *Rv1979c* (5). Interestingly, an overlap of 13 mutations in the *in vitro* selected mutants and the patient-derived isolates was identified (Figure 4.2.11). Through gene mapping, it was possible to visually identify potential hotpot regions or "resistance determining regions" throughout the different genes. Mutations in *atpE* appeared to affect two regions at codons 28 and 61-63. Mutations in *Rv1979c* and *pepQ* are not so clearly clustered, therefore more variants are needed to determine potential hotspot regions. Finally, variants in *Rv0678* were diverse and appeared throughout the entire gene affecting 77 of 165 coding positions (Figure 4.2.11)

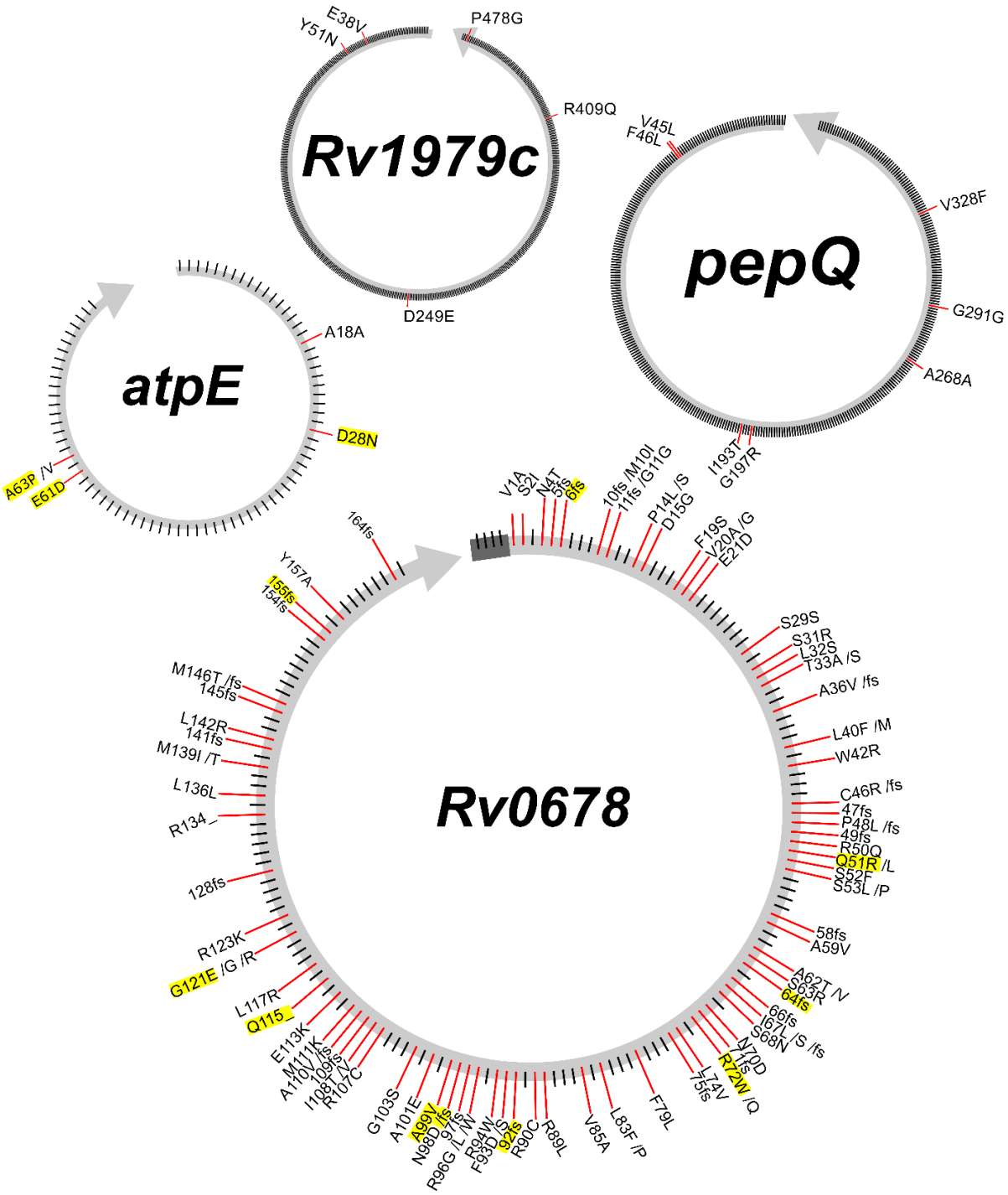

Figure 4.2.11: Patient-derived resistance-associated variant mapping throughout *Rv0678*, *atpE*, *Rv1979c*, and *pepQ*. Variants which were detected in patient isolates (CRyPTIC dataset and previously published strains) and were characterized as resistant or borderline resistant were mapped along resistance-associated genes, by codon position. All variants which were detected in *in vitro* single mutant selection, were highlighted in yellow. Based on variant catalogue in Appendix C, Table C.11. Adapted from Sonnenkalb *et al.* 2021 [140].

CRyPTIC - Comprehensive Resistance Prediction for Tuberculosis: An International Consortium, fs - frameshift, _- stop codon insertion

Since BDQ/CFZ resistance-conferring mutations appear throughout the *Rv0678* gene, it was attempted to locate hot-spot regions by evaluating the abundance of resistance conferring mutations by codon (Figure 4.2.14). This comparison included variants found in patient isolates including the CRyPTIC dataset and published literature, single selected *in vitro* clones from the sub-MIC evolution experiments, and *in vitro* population sequencing. In all three datasets, there were 10 codons which harbored a resistant conferring mutation, with six codons affected in patient-derived isolates and at least one of the *in vitro* datasets (Figure 4.2.12). When looking at the number of mutations over codon positions, it can be observed that the most highly affected codons are between codons 38 to 51, but also 61 and 68 (Figure 4.2.12).

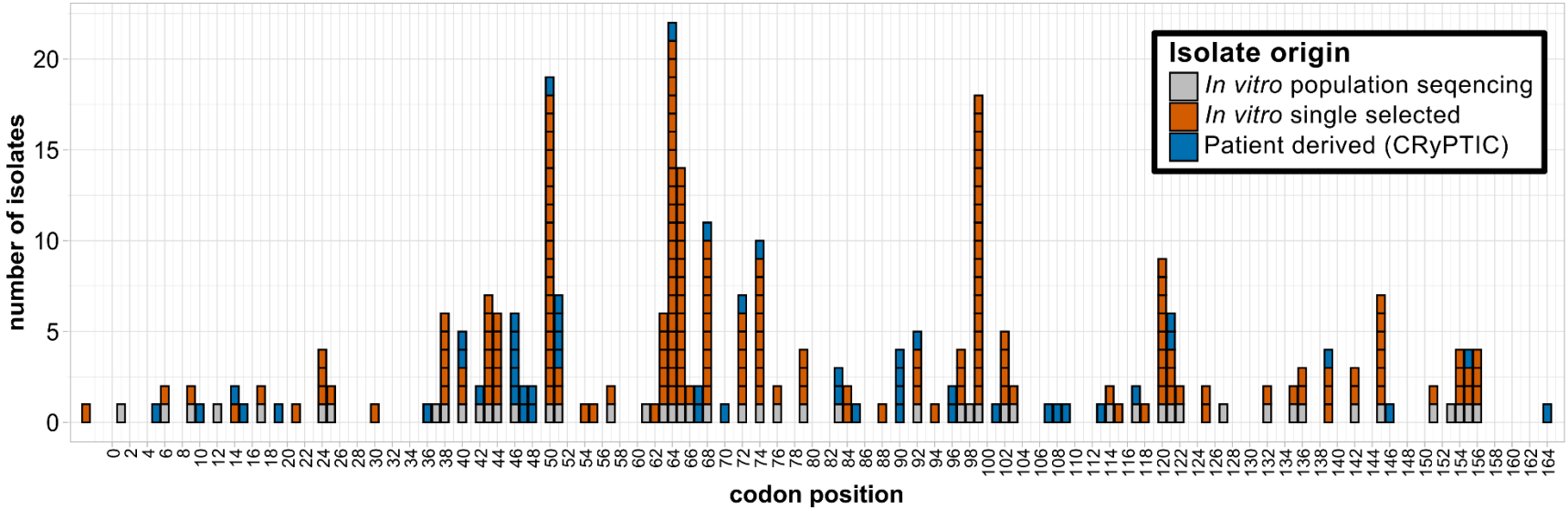

Figure 4.2.12: Resistance association by codon position in *Rv0678* gene. Overlapping mutations were compared between three datasets; *in vitro* population sequencing (Appendix C, Table C.6 & C.8), *in vitro* single selected mutants (Appendix C, Table C.9), and patient-derived isolates (Appendix C, Table C.11). Number of independent isolates detected throughout the datasets in each coding position; *in vitro* population sequencing noted as a single isolate. Adapted from Sonnenkalb *et al.* 2021 [140].

CRyPTIC - Comprehensive Resistance Prediction for Tuberculosis: An International Consortium

4.3 Defining evolutionary processes of a weak selection pressure on bacteria of the *Mycobacterium tuberculosis* complex – a quantitative analysis

In order to better understand the selection and enrichment of clonal subpopulations with particular mutations, especially in clonal competition in a heterogeneous population, several aspects related to the phenotype of the mutant harboring clones were addressed. First, the selection of off-target mutations, which were co-selected with a resistant variant was explored. Next, the MSW was determined and relative fitness of clones with different resistance mutations was investigated. Finally, a non-canonical resistance mechanism was uncovered using alternative WGS techniques.

4.3.1 Secondary mutations arise and are selected with resistant variants

As described in the previous sections, a set of clones with diverse resistance-associated variants were selected after the Mtbc H37Rv strain was exposed to sub-MICs of MFX, BDQ, or CFZ. All mutant clones harbored only one variant in a resistance-associated gene, accompanied with an elevated MIC as compared to the gWT ancestor. Previous studies have shown that additional mutations can arise after (and in some cases before) a resistance-associated variant [150], [164]–[166]. These off-target, or secondary, mutations have been linked to compensatory and drug tolerance effects which can either reduce the fitness defects caused by the resistant variants, or allow the bacteria to handle stressful environmental conditions (e.g. a high drug concentration) better than the gWT. It was hypothesized that additional variants may have been co-selected with the resistance-associated mutation in at least some of the *in vitro* selected clones, which also may induce a phenotypic effect.

In order to determine such off-target variants, the whole genome of each mutant clone was compared to the gWT ancestor genome. Then, the dataset was filtered to include only variants with a >98% frequency in the genome, excluded all synonymous SNPs and repetitive genes, and included strains with only one additional variant aside from the resistance conferring mutation. With these filtering criteria, 20 different off-target variants were detected, co-selected with a resistance-associated mutation in 84 different mutant clones (Appendix D, Table D.1).

These mutations were selected after MFX exposure (with *gyrA* and *gyrB* variants), BDQ exposure (with *atpE* and *Rv0678* variants), and CFZ exposure (with *Rv0678*). The genes affected were associated with cell wall and cell processes (affecting 5 different genes), intermediate metabolism and respiration (4 genes),

information pathways (3 genes), lipid metabolism (1 gene), and protein regulation (1 gene). Interesting, off-target mutations were detected in six different conserved hypothetical proteins, which may be of particular interest as their functions are not well described (Appendix D, Table D.1). All information on genes and function was extracted from Mycobrowser (mycobrowser.epfl.ch).

It is not obvious whether these off-target mutations may influence fitness compensation, drug toleration, or other important cellular mechanisms as they have not yet been well characterized. In the following sections two mutant clones, with an off-target mutation, were characterized further and compared with the gWT ancestor, and resistant clone with a gWT off-target gene.

4.3.2 The mutation selection window of fluoroquinolone and bedaquiline resistance conferring mutations

The MSW is the defined drug range in which a mutation is selected and enriched; which is flanked by the lowest concentration the "minimum selection concentration" and the highest concentration, the MIC. The relative fitness is defined as the bacterial strain's ability to reproduce and cause disease, this can be described in the lab by comparing the growth rate of the mutant clone with the gWT ancestor strain.

To define the MSW for clones with different mutations, several mutant clones and the gWT ancestor strain were exposed to different concentrations of antibiotics (MFX-related resistance with MFX, and BDQ with BDQ), and measured their growth every hour for 15 days (360 hours), in the automated BD Bactec™ MGIT system. In these experiments the growth capacity was measured as time until MGIT was positive (cut-off value of 400 units by internal MGIT system algorithm). The rate of growth was determined by hours until a positive culture was measured.

Experiments were first carried out with mutant clones which were selected after MFX exposure (Figure 4.3.1). Clones which harbored the most common mutations *gyrB* N499D, *gyrA* A90V and D94G, as well as *gyrB* E501D which was selected one time, were investigated. Additionally, to evaluate the effect of a secondary (off-target) mutation on relative fitness and the MSW, a clone with the mutation *gyrA* A90V with an additional variant, *ppgK* _266S, was evaluated (Appendix D, Table D.1). The mutant clones examined were genetically identical to the gWT ancestor, except for the defined variant(s). The drug concentration range tested was between 4 mg/L to 0.03 mg/L MFX, with all 2-fold dilutions evaluated in between (4, 2, 1, 0.5, 0.25, 0.12, 0.06, 0.03, and 0 mg/L MFX). After 82-84 hours incubation, positive cultures were first detected for all clones including the gWT ancestor, in tubes without antibiotics. At the

lowest drug concentration evaluated (0.03 mg/L MFX) all mutant clones began to outgrow the gWT ancestor (p≤0.0053) (Appendix D, Table D.2).

Interestingly, the experiments performed revealed that the growth rate of clones with different resistance-associated mutations began to diverge at MFX concentrations at or above 0.25 mg/L (Figure 4.3.1). The clones harboring mutations *gyrA* A90V or *gyrB* N499D exhibited an MIC of 1 mg/L MFX, although it appeared that the *gyrB* N499D clone reached positive growth more quickly than *gyrA* A90V mutant clone at 0.5 mg/L MFX exposure (86 hours faster on average), this was not significant (p=0.988, Appendix D, Table D.2). Clones with *gyrA* D94G or *gyrB* E501D mutations had an MIC of 2 mg/L, with *gyrB* E501D mutant growing more quickly on average than *gyrA* D94G, but this was not significant (p=0.999).

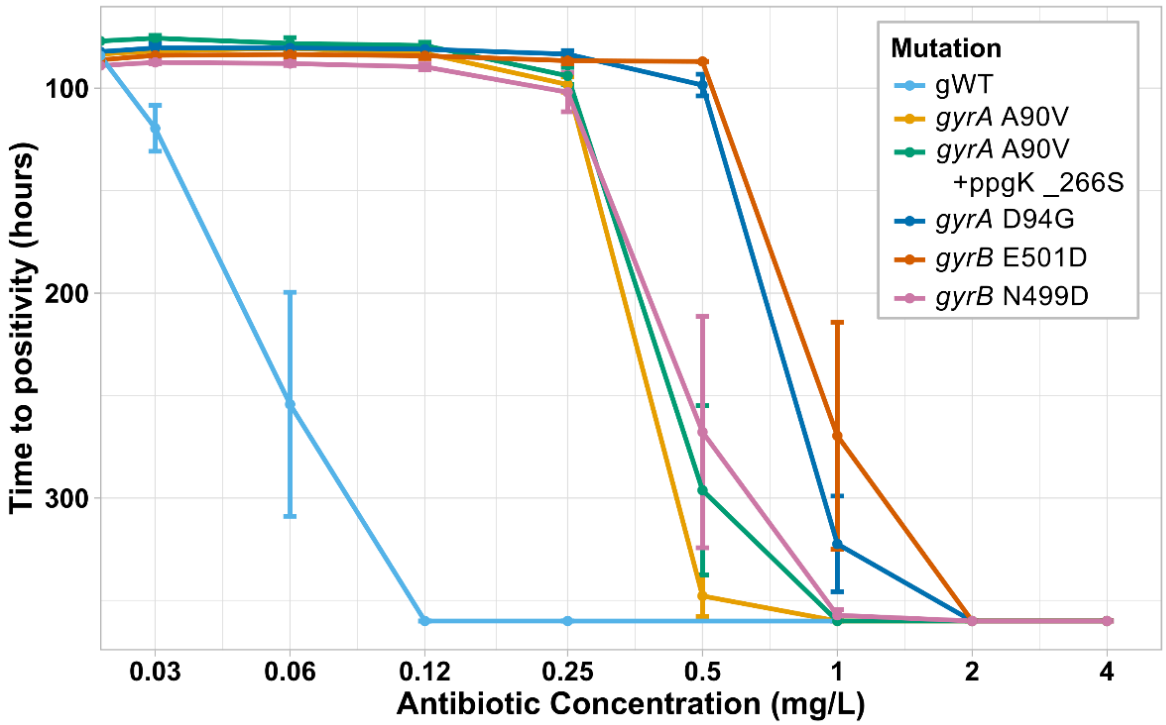

Figure 4.3.1: Mutant selection window of moxifloxacin resistant clones. H37Rv clones with resistance-associated mutations *gyrA* A90V, *gyrA* D94G, *gyrB* E501D, and *gyrB* N499D were selected from MFX evolutionary experiments. Each mutant clone was separately cultured in mycobacterium growth indicator tubes and growth was measured hourly, until time to positivity (fluorescence signal measured greater than or equal to 400 units) was achieved. Data is representative of two independent experiments, with a total of five biological replicates, including the genetically wild-type (gWT) ancestor clone.

Statistics: Two independent experiments were conducted including 2 or 3 biological replicates (5 values). Statistics were calculated as a nonparametric multiple contrast test (Kruskal) with a confidence interval of 95%. P-values in Appendix D, Table D.2.

Finally, when comparing growth characteristics of clones with a single *gyrA* A90V mutation with a clone with *gyrA* A90V in combination with the off-target mutation *ppgK*_266S, a slight difference in average growth rate at concentration 0.5 mg/L MFX (by 52 hours on average) was observed, and an MIC for both mutants at 1.0 mg/L (Figure 4.3.1). Although it appeared, on average, that the off-target mutation may give a growth advantage at higher concentrations, this was not significant ($p>0.5$, Appendix D, Table D.2).

Next, several clones with BDQ resistance mutations were evaluated. Three clones with *Rv0678* mutations were evaluated, one with gene disrupting mutation R153_, one with the missense mutation S68G, and one with the *Rv0678* S68G plus an additional mutation in the downstream efflux pump gene as *mmpL5* A423D. Two clones with missense mutations in *atpE* were included: A63P and D28V. All clones were genetically identical to the gWT ancestor except for the indicated mutations. The drug concentration range tested for the *Rv0678* mutant harboring clones and gWT was between 8 mg/L to 0.12 mg/L BDQ with 2-fold dilutions evaluated in between (8, 4, 2, 1, 0.5, 0.25, 0.12, and 0 mg/L BDQ). Previous MIC testing indicated that *atpE* mutations highly enhanced the clone's BDQ MIC, therefore two higher testing concentrations were included, 30 and 15 mg/L BDQ.

Bacterial growth time to positivity was first detected, after 75-82 hours in the antibiotic free tubes. In the absence of antibiotics, the gWT outgrew all mutant clones, except *Rv0678* R156_ (Figure 4.3.2). The lowest drug concentration tested (0.12 mg/L BDQ) already suppressed the growth of the gWT and the *Rv0678* clones, increasing the time to detected growth to 100-150 hours. The MIC of the gWT ancestor was 1 mg/L BDQ, and both *Rv0678* mutant clones presented a 4-fold MIC increase, at 4 mg/L BDQ. It appeared that the clone with the S68G mutation, had a higher growth rate in most drug concentrations as compared to the gene disrupting mutation R156_. The *atpE* mutant harboring clones displayed virtually no reduction of growth, even at the highest tested concentration (Figure 4.3.2, Appendix D, Figure D.1). When comparing the *Rv0678* S68G mutant harboring clone to the clone with the same resistance mutation plus the *mmpL* A423D mutation, no difference in MIC and little difference in growth was observed. Although it appeared that the *mmpL* A423D mutation may have given a slight growth advantage on average, the standard deviation was large and overlapped between the clones. More experiments must be conducted in order to perform statistics (data represent one experiment with three biological replicates).

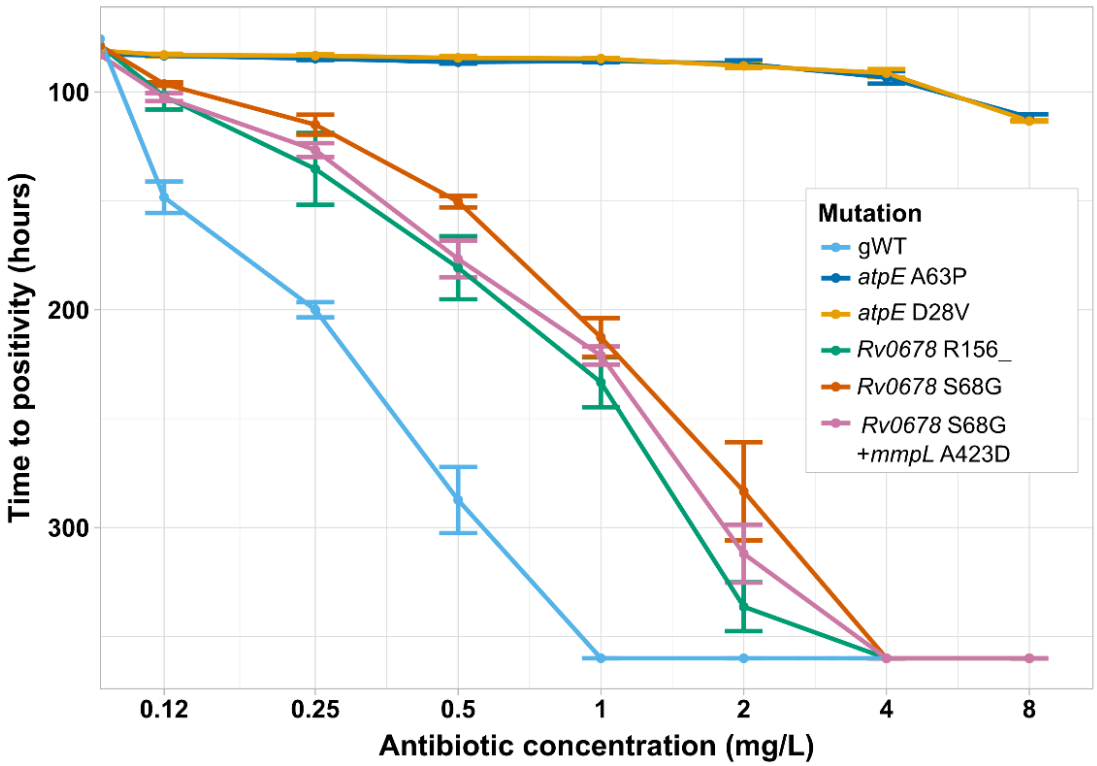

Figure 4.3.2: Mutant selection window of bedaquiline resistant clones. Resistance-associated mutations *atpE* A63P and D28V, *Rv0678* R156_ and S68G were isolated from BDQ evolutionary experiments. Each mutant clone was separately cultured in mycobacterium growth indicator tubes and growth was measured hourly, until time to positivity (fluorescence signal measured greater than or equal to 400 units) was achieved. Data is representative of one independent experiment, with a total of three biological replicates.

4.3.3 Bacterial fitness of resistance mediating mutations

In the following section, this study aimed to show the effect different resistance conferring mutations have on the relative bacterial fitness through direct growth competition experiments, between a mutation harboring clone and gWT ancestor. The same H37Rv MFX and BDQ resistant clones evaluated in the previous section were investigated, except *gyrB* N499D which was excluded due to culturing issues. The experiment was carried out by inoculating a culture with about 50% of the gWT ancestor and 50% the resistant clone, after 14 days of growth (including one culture passage) the final frequency of the resistant allele was determined by WGS.

After the competition experiments, the frequency of *gyrA* mutations D94G increased by an average of 4.2% (p=0.15) over the gWT allele (Figure 4.3.3, Appendix D, Table D.3). The A90V mutation frequency increased on average by 3.67% but there was not a statistical difference (p=0.352). Further the frequency

of *gyrB* E501D increased by 1.1%, and was also not statistically significant (p=0.923). Since there was a slight increase in the frequency of these alternative alleles, it is indicated that they are highly competitive with the gWT and likely do not induce a fitness defect. Finally, the additional variant *ppgK* _266S with *gyrA* A90V, did not appear to give the clone a growth advantage over the gWT (p=0.074) or the single A90V mutant harboring clone (p=1.0).

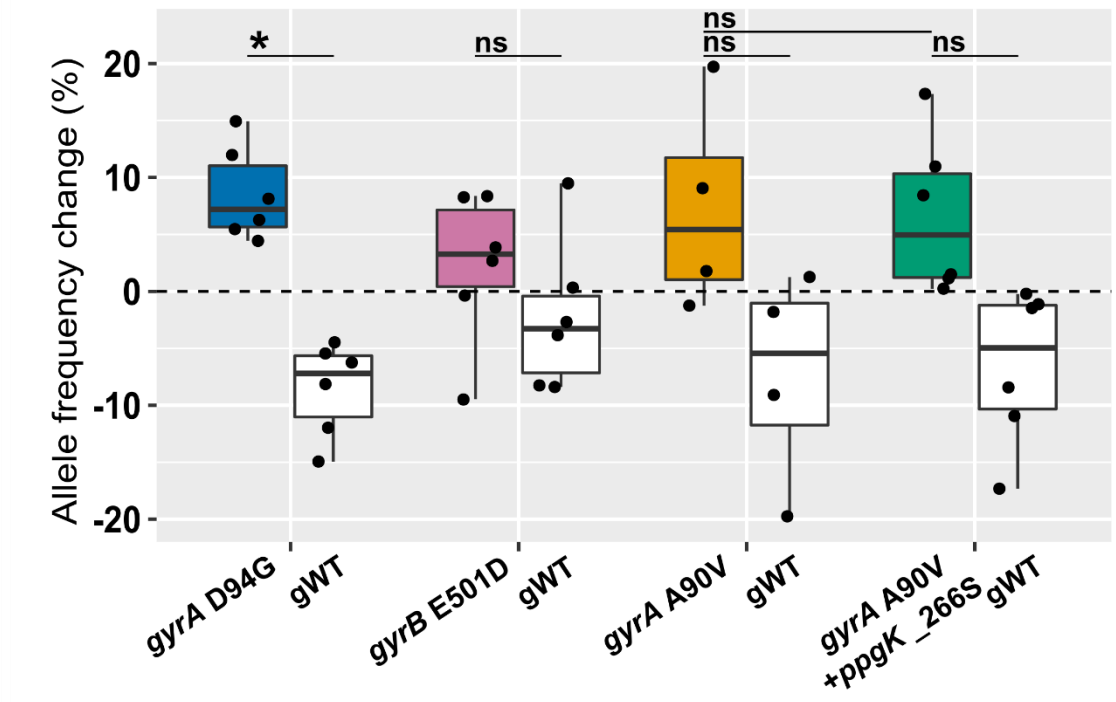

Figure 4.3.3: Allele frequency of moxifloxacin resistance harboring clones. Each mutant clone was co-cultured with the genetically wild-type (gWT) ancestor at a 50:50 ratio. After 14 days (and one culture passage) of growth, the frequency of the resistant variant in the total population was determined by whole genome sequencing. Change in allele frequency was determined by the percent increase or decrease as compared to the starting mutant to gWT ratio.

Statistics: Two independent experiments were conducted, with 4-6 biological replicates total. Statistics was calculated as nonparametric multiple contrast test (Kruskal) with a confidence interval of 95%, p-values between mutant and gWT, Appendix D, Table D.3: *p<0.05, **p<0.01, ***p<0.001

Competition experiments were repeated with the same BDQ resistant mutants evaluated in the previous section (Results 4.3.2). Interesting, 4.7% and 5.5% decrease in allele frequency was observed, for *atpE* mutations A63P (p=0.006) and D28V (p=0.0038) respectively (Figure 4.3.3, Appendix D, Table D.4). The

Rv0678 mutation S68G indicated a 0.75% reduction in allele frequency, which was not statistically significant (p=0.968). The gene disrupting mutation *Rv0678* R156_, presented an average decrease of 4.5% (p=0.053). Finally, the mutant which harbored an additional variant (*Rv0678* S68G plus *mmpL* A423D), did not appear to give a growth advantage over the gWT (p=0.0.999) or the single A90V mutant (p=1.0).

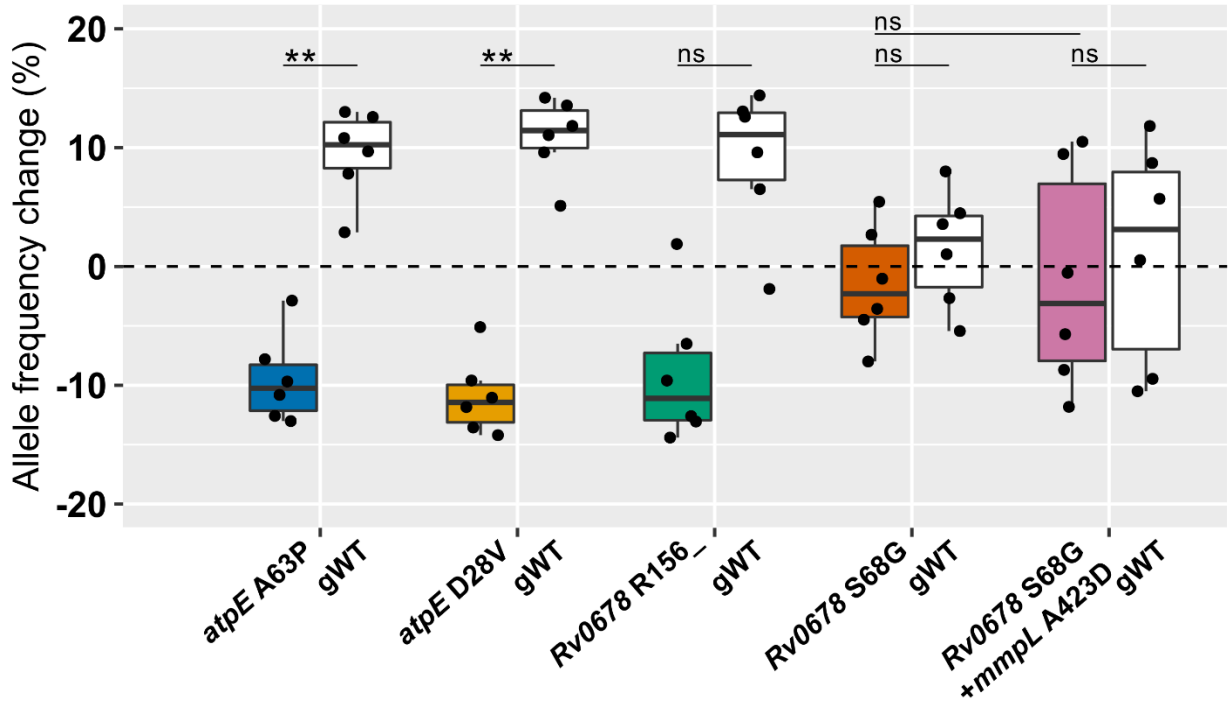

Figure 4.3.4: Competitive relative fitness of bedaquiline resistance harboring clones. Each mutant clone was co-cultured with the genetically wild-type (gWT) ancestor at a 50:50 ratio. After 14 days (and one culture passage) of growth, the frequency of the resistant variant in the total population was determined by whole genome sequencing. Change in allele frequency was determined by the percent increase or decrease as compared to the starting mutant to gWT ratio.

Statistics: Two independent experiments were conducted, with 4-6 biological replicates total. Statistics was calculated as nonparametric multiple contrast test (Kruskal) with a confidence interval of 95%, p-values between mutant and gWT, Appendix D, Table D.4: *p<0.05, **p<0.01, ***p<0.001

4.3.4 Non-canonical mutations potentially implicated in bedaquiline/clofazimine resistance

As previously detailed, WGS performed on the Illumina® platform does not result in a mutation call in all clones derived from single colonies grown on selective media, and although 13 clones presented an elevated MIC to either BDQ or both BDQ and CFZ drugs (Table 4.3.1). Nine clones harbored mutations in

other "off-target" genes, yet four clones were genetically identical to the gWT ancestor based on standard Illumina® WGS data analysis.

Table 4.3.1: Selected mutants with elevated bedaquiline (and clofazimine) minimum inhibitory concentration, with no detectable resistance-associated mutations. Several selected mutants harbored no mutation in *Rv0678, atpE, pepQ* or *Rv1979c*, but presented an elevated minimum inhibitory concentration (MIC) to bedaquiline (BDQ), and mostly clofazimine (CFZ). Three mutants were selected for de novo assembly (*) by single-molecule real-time long-reads on PacBio® Sequel2 platform.

Sequencing ID	Resistance Mutation	Off-target mutation (1)	Off-target mutation (2)	BDQ MIC (mg/L)	CFZ MIC (mg/L)	BDQ or CFZ isolate
LBA-110	None	-	-	2	2	BDQ
LBA-121	None	-	-	1	2	BDQ
LBA-124	None	-	-	1	2	BDQ
LSF-61	None	-	-	2	2	CFZ
LBA-53	None	*Rv0195* 183 del c	-	2	2	BDQ
LBA-58 *	None	*Rv0195* 183 del c	-	2	2	BDQ
LBA-62 *	None	*Rv0195* 183 del c	-	2	2	BDQ
LBA-83 *	None	*Rv0195* 183 del c	-	2	1	BDQ
LBA-138	None	3943382 c>t	3944088 g>a	2	2	BDQ
LBA-143	None	*Rv1330c* R417W	2551370 c>g	4	1	BDQ
LBA-144	None	*Rv3312c* T37I	-	4	4	BDQ
LSF-83	None	*Rv1890c* R119H	-	2	1	CFZ
LSF-115	None	*Rv1860* del †	3941837 c>g	2	2	CFZ

* Selected for long-read sequencing

† *Rv1860* 885 del g, 887 del c, 889 del c, 891 del t, 893 del c, 903 del t

Off-target gene summary:

Gene	Gene Name	Gene Annotation	Functional category
Rv0195	-	Possible two component transcriptional regulatory protein (probably LuxR-family)	Regulatory protein
Rv1890c	-	Hypothetical protein	Conserved hypothetical protein
Rv1330c	*pncB1*	Nicotinic acid phosphoribosyltransferase PncB1	Intermediary metabolism and respiration
Rv3312c	-	hypothetical protein	Conserved hypothetical protein
Rv1860	*apa*	Alanine and proline rich secreted protein Apa (fibronectin attachment protein)	Cell wall and cell processes

To investigate possible resistance mechanisms of these clones, the mutations found in "off-target" genes were examined. These genes were associated with transcriptional regulation (*Rv0195*), nicotinic acid phosphoribosyltransferase metabolism (*Rv1330c*), cell wall processes (*Rv1860*), and conserved

hypothetical proteins (*Rv1890c* and *Rv1860*) (Table 4.3.1). These mutations were not seen in other clones except for *Rv1890c* R119H, which was co-selected with resistance-associated mutations in *gyrB* and *Rv0678* (Appendix D, Table D.1). A search of the >40,000 strain database of the Molecular and Experimental Mycobacteriology Research Group (Research Center Borstel), indicated that none of these mutations were found in clinical isolates, and therefore were most likely not linked with BDQ/CFZ resistance.

Next, the short-read sequencing alignment was explored in detail using IGV software (Broad Institute). In the sequencing alignment, a large break (or scar) in the coding region of *Rv0678* was present (Figure 4.3.5). This break, led to the hypothesis that there was likely a large deletion or insertion, which was not detected by standard short-read sequencing data analysis (one of the limitations of short-read synthesis sequencing). To test this hypothesis, three clones were selected for long-read sequencing on PacBio® Sequel2 system, followed by *de novo* assembly (Table 4.3.1 *). PacBio® Sequel2 sequencing allows for an increase of sequencing read length from 150 base pairs to about 20 kilo-base pairs, thus enabling an efficient detection of large-scale genomic modifications.

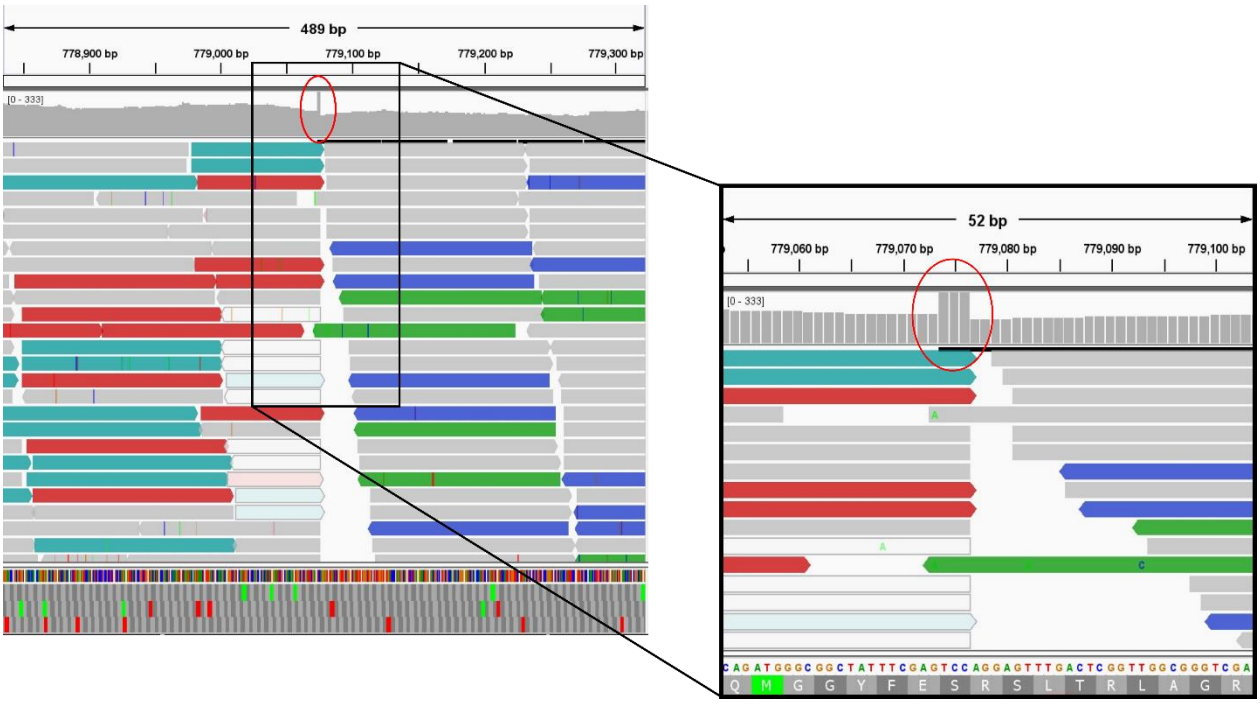

Figure 4.3.5: Short-read sequencing alignment of a genotypically susceptible (but phenotypically resistant) clone. View of the aligned reads of a bedaquiline clone (sequencing ID: LBA-83) which, through Illumina® short-read sequencing, did not appear to harbor a mutation in any known BDQ/CFZ resistance conferring genes. At position 779,061-779,063, a break occurred in the sequencing data reads and alignment.

A *de novo* assembly was produced using PacBio® SMRT® Link software, which generated a closed Mtbc genome with two assemblies, with one and four contiguous sequences (Figure 4.3.6). All assemblies covered more than 99.9% of the reference genome (NC_000962.3). All three clone assemblies showed a large-scale sequence re-arrangement with the borders at position 779,073 (*Rv0678* coding sequence) and 3,552,584 (intergenic region) and flanked by a transposase open reading frame (IS*6110*). A 2.5Mb fragment was inverted and thus split the *Rv0678* gene into halves (Figure 4.3.6).

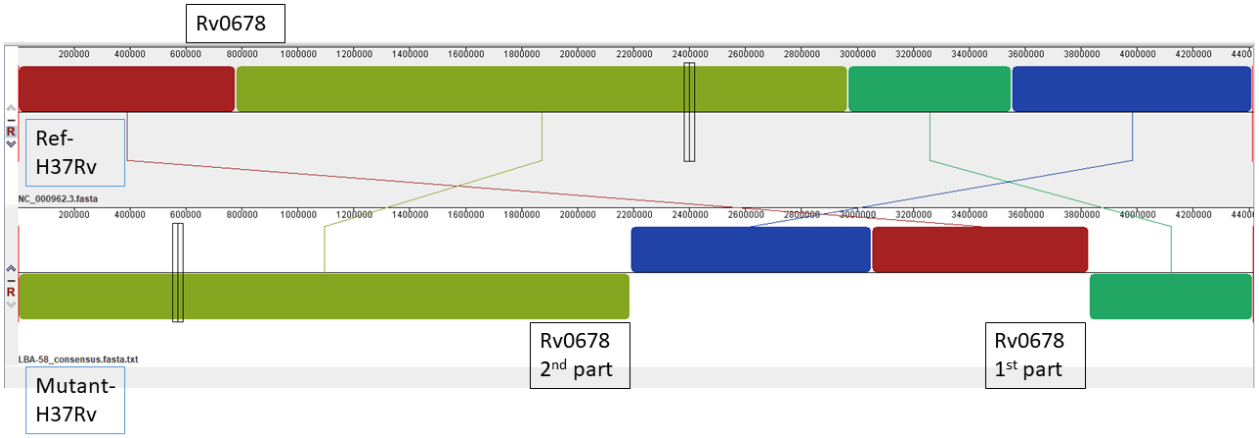

Figure 4.3.6: Large-scale gene rearrangement in *Rv0678* gene. De novo assembly through PacBio® SMRT® Link software indicated large-scale sequence rearrangement in *Rv0678* at positions 779,073 coding sequence and 3,552,584 intergenic regions. Adapted from Sonnenkalb *et al*. 2021 [140].

5. Discussion

Bacteria of the Mtbc are some of the oldest known bacterial pathogens, inflicting humans for the past 40,000-70,000 years [1], [167]. Although there have been major advancements in antibiotic treatments, TB continues to be the most deadly infection over the last decades on a worldwide level, killing over 1.5 million people every year [168]. Despite a steady decrease in TB incidence (Figure 2.1), drug resistant and even MDR-Mtbc strains are rising and spreading world-wide, which could impede global efforts to eradicate this disease (Figure 2.2) [168].

In order to combat these persistent organisms, researchers are putting more focus on understanding evolutionary trajectories which allow Mtbc strains to develop drug resistance and spread. This is accomplished by experimental modeling, intra-patient evolution under treatment, and on global scales through analysis of large strain collections (including transmission chains). In this study, the main aims were to elucidate factors which affected intra-patient resistance evolution, to establish and evaluate a new sub-MIC evolution model for studying resistance development *in vitro*, and to further investigate resistance mechanisms and the MSW to important drugs used in MDR-TB treatment. The main results obtained from this study are discussed in the following sections, as well as final conclusions and outlook.

5.1 Elucidating factors of intra-patient resistance evolution of a *Mycobacterium tuberculosis* complex bacterial infection

As a paramount example for a failing MDR-TB regimen and ongoing resistance acquisition, serial isolates were investigated from a single patient while under longitudinal MDR-TB treatment. This patient suffered from five distinct infectious TB episodes, spanning 56 years of their life, with over 27 years of applied treatment. The final treatment episode lasted 18 years and was the focus of this analysis. This case was retrospectively reviewed, using molecular techniques to evaluate bacterial isolates collected throughout that period, compare with an in-depth patient treatment history and phenotypic testing data (i.e. DST). While several other studies have been conducted evaluating intra-patient strain evolution through analysis of serial isolates [81], [83]–[85], [169], [170], this study is one of the longest treatment histories ever published, in which a single strain acquired resistance to every available drug [87].

This extreme example of a failing treatment with multiple treatment episodes was characterized by three major determinants: inadequate/inefficient drug combinations, co-existing heteroresistant Mtbc

subpopulations, and the acquisition of off-target mutations resulting in strain populations with likely enhanced fitness. To better understand the evolution of this infectious Mtbc strain, selective sweeps linked to phases of ineffective treatment regimens were evaluated, heteroresistant bacterial populations (the adaptive landscape) in different treatment phases were tracked, and the effect of compensatory/tolerance-associated mutations on the selection of particular mutant populations was considered.

5.1.1 Failing treatment regimens foster resistance selection

One of the most important factors in successful TB treatment (for treating any pathogen related illness), is administering an effective treatment regimen. Even susceptible Mtbc infections require a long-term treatment of a four-to-six month regimen, including four antibiotics [171]. The WHO's consolidation guidelines on treating MDR-TB infections includes at least three effective drugs from group A and one from group B (Table 2.2) [172]. As an infectious Mtbc strain gains more resistances, treatment design becomes more complicated and longer. This situation results in a long-term selection pressure, which in combination with weak drug combinations, potentially facilitates further resistance evolution in patients.

The patient investigated here suffered from an exceptionally complex TB infection and course of treatment with frequent changes in drug regimens and final acquisition of seven resistances. The final treatment period analyzed here, started already with an MDR strain, resistant to INH, RIF, EMB, and SM. The first bacterial isolate which was sequenced, harbored resistance-associated variants to INH, RIF, PZA, PTH, SM, PAS, and CS/TRD (Figure 4.1.1, Appendix B, Table B.2). Over thirteen years of treatment, the rise and fixation of mutations conferring FQ, EMB, LZD, CPR, and CRP/AMK/KAN resistances was observed. Considering WGS based resistance predictions, there was only a two month period in which three active drugs were included in the regimen, falling short of WHO treatment guidelines (Figure 4.1.1) [172]. More alarmingly, there were over 85 months in which only one active drug was applied, and 54 months in which no active drugs were administered (Appendix B, Table B.1.). Phenotypic and genotypic resistance predictions were not always congruent in this study, although both indicated over 13-years of suboptimal therapy design. Accordingly, it became clear that poorly designed treatment therapies were responsible for selection of subpopulations with additional resistance mutations in several phases of ineffective treatment regimens.

As a likely consequence of this long-term inefficient therapy, the infecting Mtbc strain went through multiple genetic bottlenecks which facilitated the fixation of additional resistance mediating mutations, in a stepwise manner. For example, nearly 12 months of OFX mono-therapy coincided with the rise and fixation of the FQ resistant variant *gyrA* D94G in the population (Figure 4.1.1, Appendix D, Table D.1). This was followed by LZD then AMK resistance acquisition, after 20 months and 7 months of drug application, respectively. In line with previous studies, even dating back to the development of the first anti-TB drugs [40]–[42], the result obtained here underline the fact that MDR-TB regimens with just one or two effective drugs leads to rapid resistance development, as described in at least three other studies [83], [169], [173]. Furthermore, it has been recently confirmed that 3 to 4 drugs are required to reach high cure rates in patients with MDR-TB infections [174].

Still, it is not evident why ineffective drugs were included in this patient's treatments, even after resistant phenotypic results were provided. Unfortunately, information on the decisions of the treating physicians was not noted, and therefore one can only speculate why the treatments were designed in this way. Even so, there were not many treatment options left for this patient, except for strategies like increasing drug dosage [175]. Finally, it was clear that it took months for these resistance conferring mutations to rise to fixation, therefore a deeper analysis into the sequencing data was performed to understand the adaptive landscape and potential heteroresistant populations.

5.1.2 The adaptive landscape and heterogeneous populations

To define the selection and evolution of the clonal subpopulations in detail, thirteen serial isolates were analyzed for the presence of low- and high-frequency subpopulations. Heteroresistant populations were confirmed if at least two subpopulations with resistant allele(s) with/without the gWT allele, were present in a given sample. The analysis describes a highly heterogeneous intra-patient evolution, with several instances of competing clonal subpopulations and an evolutionary arms race for selection and fixation into the population. Core genome multi locus sequence typing, confirmed that all subpopulations were of the same strain, and that reinfection or a mixed infection with two Mtbc strains could be ruled out (Figure 4.1.2) [176].

The diverse adaptive landscape consisted of several instances of heteroresistant clonal subpopulations, which arose and fluctuated while under antibiotic exposure, even in the absence of the antibiotic in one case. Similar data on the rise and fixation of resistance mutations in patient-derived strains under

longitudinal MDR-TB therapies, have been observed in other studies through the analysis of serial isolates [81], [83]–[85], [169], [170]. However, no other studies have considered a comparable treatment duration. In line with the data obtained here, intra-patient heterogeneity can be clearly associated with poor clinical outcomes when linked with poorly designed treatment regimens [173], [177].

A selection pressure is necessary for the adaptation of Mtbc bacteria, in response to environmental changes such as antibiotic exposure. Over a 14-month period, while under CPR treatment, two subpopulations with different frameshift mutations in the *tlyA* gene arose and competed until one was ultimately selected. One would assume that frameshift mutations in a single gene have a similar (if not equal) effect on the phenotype. This data indicated the effect of a particular mutation on the phenotype, such as resistance level and/or fitness, is not solely accountable for the selection of a mutant subpopulation. In this example, the finally selected frameshift mutation was co-selected with an AMK/CPR/KAN resistance-associated mutation, since the both variants concurrently increased to 100% in the same isolate. Thus, resistance development to a second drug finally facilitated the selection of another resistance associated allele.

The selection of subpopulations with a particular mutation from a heterogenous population was occurring while under antibiotic treatment. Surprisingly, heteroresistant subpopulation competition was also observed with different mutations in the absence of the respective resistance-associated drug. For example, competition between three *Rv0678* mutations over a 37-month period was occurring at low-frequencies (≤70%) ultimately ending in the loss of these variants. This observation is especially interesting as the two drugs most associated with mutations in *Rv0678* are BDQ and CFZ, yet neither was included in any of the treatment regimens (Appendix B, Table B.1) [76], [178]. *Rv0678* is an efflux pump regulator, which has only been associated with BDQ and CFZ, and cross-resistance with other important anti-TB drugs have yet to be explored. However, in a recent study, it was reported that an outbreak strain in Eswatini carried mutation in *Rv0678* even though BDQ and CFZ were not used in the country at the time the strains were isolated [179]. This points to other selection pressures that may select for mutations in *Rv0678,* that later confer resistance to BDQ and CFZ. Here, *in vitro* derived *Rv0678* mutants were evaluated for cross-resistance to DLM and LZD, but no resistance was detected (Table 4.2.6). Thus, further experiments are needed to detect possible unknown mechanisms of *Rv0678*-mediated resistance or virulence, that potentially lead to selection of *Rv0678* variants in Mtbc strains naïve to BDQ and CFZ.

One pitfall of this study is the retrospective nature. These isolates were acquired from sputum and sub-cultured, long before DNA was extracted for WGS. Also, sputum samples are not an optimal method for

detecting heterogeneous populations. A recent study which analyzed lung resections from TB patients found that polyclonal infections were present in 7 out of 18 (39%) individuals, an increase from the 5% of mixed infections determined from sputum samples [180], [181]. For this study all samples were sub-cultured, thus causing another influence on the frequency at which a mutation was detected. Since resistance mutations can reduce bacterial fitness, a resistant allele may have decreased during cultivation if it had not yet reached fixation (nearly 100% population frequency) [165], [182]. The best solution to overcome these potential problems with sub-culturing is to directly sequence sputum, which at present can only be accomplished by amplicon deep sequencing [183], [184]. This methodology was not possible in this study, as sputum samples were not preserved and only bacterial stocks were available.

Despite these technological pitfalls, a diverse adaptive landscape of competing heteroresistant populations was observed, always arising before a single resistance-associated variant researched fixation. Next, this study focused on the analysis of off-target mutations that were co-selected at several time points throughout the complicated treatment duration.

5.2.3 Off-target mutations implementing putative compensatory and tolerance mechanisms

An important topic which has become more prevalent as our scientific knowledge grows, are off-target mutations which potentially ameliorate the fitness of a resistant clone, i.e. compensatory mutations [185], [186]. The compensatory effect of *rpoC* mutations following *rpoB* mutations mediating RIF resistance has been the most well described compensatory mechanism in Mtbc strains in both, *in vitro* studies and molecular epidemiological studies [164], [187]–[190]. Further genes linked to compensatory evolution include: *rpoA* with *rpoB* (RIF), *oxyR'-ahpC* with *katG* (INH), *ubiA* with *embB* (EMB), *pncB2* with *pncA* (PZA), *thyX-hsdS.1* with *thyA*, and *Rv0565c* with *ethA* (ETH/PTH), to name a few [164], [191]–[194].

The gene *Rv0565c* was recently identified as coding for a compensatory enzyme which activates *inhA* when the primary activating enzyme *ethA* is disrupted [193], [194]. Not only are the *ethA* and *Rv0565c* genes coding for enzymes which activate *inhA* in the bacteria, but can also activate PTH/ETH prodrugs (at likely variable degrees) [193], [194]. Mutations in *Rv0565c* have only been detected concurrently with *ethA* mutations in clinical isolates, and *in vitro* experiments have shown that its over expression renders the strain more sensitive to PTH/ETH [194]. Indeed, the mutation *Rv0565c* C298R was detected following the baseline mutation *ethA* 89 del a after intermittent PTH exposure. The fixation of this mutation coincided with a resistant phenotype, so it is probable that this enzyme was compensating for the loss of *ethA*, and

involved still in PTH/ETH activation. Therefore, the compensatory effect of a functional *Rv0565c* may have been ameliorated with this additional mutation, and allowed the bacteria to be more tolerant or resistant to PTH/ETH (Figure 4.1.1).

Drug tolerance is an important survival mechanism, which unlike resistance is not specific to one class of drugs, does not affect the MIC, but extends the necessary time needed for bacterial killing [150], [166], [195]. Although tolerance mechanisms are mainly occurring on the transcriptional level, Hicks *et al*. described mutations in transcription factor *prpR* (*Rv1129c*) as potentially enhancing drug tolerance to a multitude of anti-TB drugs [150]. This hypothesis is in line with this study, as at month 92, the first appearance of the variant *prpR* F334L was observed, which was fixed in the population at month 108 (Appendix B, Table B.2). During that period the strain was exposed to PZA, PTH, CPR, TRD, and LZD, and potentially, the observed *prpR* mutation allowed the strain to tolerate a higher concentration of antibiotics, but this must be further investigated experimentally.

Taken together, the data obtained demonstrated that the evolution of a highly resistant, untreatable infection was a result of poorly designed ineffective treatment regimens in combination with hetero-resistant subpopulations that allowed for selection of the most resistant subpopulations, but is further aided by acquisition of additional compensatory and tolerance mechanism that likely fueled this Mtbc strain’s evolutionary trajectory.

5.2 The impact of sub-inhibitory drug exposure on *Mycobacterium tuberculosis* bacteria

Treatment of TB, especially drug resistant or even MDR-TB, is highly complex and lengthy [171], [172]. This situation further provides a long-term selection pressure which likely fosters the rise of heteroresistant populations in the patient as described above [87]. Another point is that anti-TB drugs are unevenly distributed in infected organs and cellular compartments such as granulomas comprising different cell types such as macrophages, and neutrophils, and can also have a central necrotic zone that is particularly hard to penetrate by several drugs (Figure 2.3)[111], [112], [116], [152], [153], [196]. This may lead to large differences in drug concentrations in different sites of the disease, also resulting in below MIC concentrations, even if the drugs are administered in the right dose [116], [197], [198]. To which extent such situations can lead to the selection of resistant subpopulations has not been well defined for Mtbc bacteria [199].

Most *in vitro* selection experiments which have been utilized to induce spontaneous mutations, i.e. *de novo* evolution, have been carried out at high antibiotic concentrations (at or above the MIC) [127], [136]. Some limitations of these experiments are the tendency to select for variants not commonly found in patients, or entirely miss clinically relevant mutations with low-level resistance profiles [75], [137], [200], [201]. Therefore, this study attempted to develop a new sub-MIC evolution model with Mtbc bacteria. Based on the work of Gullberg, Liu, Andersson, and Hughes, this sub-MIC evolution model was designed, which included long-term, sustained exposure of sub-MIC antibiotic concentrations of the bacteria in liquid culture [132]–[134]. This model was also hypothesized to better reflect the intra-patient situation, by not only providing a drug selection pressure, but also competition with heterogeneous bacterial populations in order to select more fit, clinically relevant mutations.

5.2.1 Sub-inhibitory drug exposure selects resistance conferring clones

First, the sub-MIC evolution model was established for MFX as a proof of concept, since it is a well-studied and superior FQ MDR-TB drug. Then this model was applied to one of the newest drugs on the market, BDQ and the repurposed drug CFZ; drugs which are known to also have a cross-resistance mechanism via mutations in *Rv0678* [73], [163], [202]. To explore a range of antibiotic selection pressures, the bacteria were exposed to the four highest tolerable drug concentrations, with a 2-fold dilution between each concentration, starting at 1:2 the MIC and decreasing (Figure 4.2.3). Minimal growth inhibition was

important and enabled consistent drug dosing, which fostered bacterial sampling that was analyzed throughout the experiment.

For all three drugs, a dose dependent increase of mutant populations was observed, even short-term (four days) exposure of half the MIC resulted in a significant increase in the mutant population, as compared to the antibiotic free control population. This was an important observation, as it is difficult to maintain high levels of antibiotics in patients, and this study showed that reduction of drug concentrations to half of the MIC caused a positive selection of resistant clones [203], [204]. Long-term drug exposure also revealed that drug concentrations as low as 1:16 the MIC can select for resistant populations which significantly increased as compared to drug-free conditions. This data allowed a first insight into the MSW of important MDR-TB treatment drugs and demonstrated that resistant populations could be selected at intra-patient niches, where drug concentrations are low/reduced [152], [196].

5.2.2 Sub-minimum inhibitory concentration evolution model captures a wide diversity of resistance associated mutations

After the positive selection of resistant populations was observed at concentrations far below the MIC, it was investigated if the mutations obtained were diverse, what their impact on resistance levels was, and their potential clinical significance. To address this, single clones were selected by picking mutant colonies from the antibiotic supplemented agar plates. These clones were grown in antibiotic-free culture, and screened for increases in MIC by REMA. All clones which were picked presented an elevated MIC and underwent WGS to determine the resistance associated mutation. In total, 140 MFX mutant clones were selected and characterized, and 215 clones from BDQ/CFZ selection experiments.

Of the clones which were cultivated under MFX exposure, WGS revealed three unique variants in *gyrB* and seven in *gyrA*. All MFX clones presented at least an 8-fold MIC increase, as compared to the gWT. The most common variants selected in *gyrA* were A90V and D94G, which are also most often found in clinical isolates with FQ resistance profiles [142], [156]. Other common variants seen in patient-derived strains recovered were - *gyrA* S91P and four variants affecting codon D94 of *gyrA* [205], [206]. However, many *gyrB* variants were also selected (20% overall), which reflected less the clinical situation, as *gyrB* mutations are less often seen in patient isolates [206], [207]. Even so, all of the mutations selected fell within the QRDR (Figure 4.2.9) [156], [208].

In order to implement a more unbiased approach for variant detection, all mutants growing on MFX-supplemented agar plates were pooled together and WGS deep sequencing was performed (coverage depth average of 595x), to detect all *gyrA* and *gyrB* variants at a frequency ≥1% in a given population (Table 4.2.1). In this approach, five additional mutations in *gyrB* were identified, two of which implemented codons outside of the QRDR (Figure 4.2.9). No additional *gyrA* variants were found. Again, a higher rate of *gyrB* mutations of 20% was observed, whereas mutations in this gene affects only 1-2% of FQ resistant clinical strains [206]. All together, these results confirmed that below MIC concentrations select for relevant resistance mutations and that this *in vitro* design is a good model for selecting mutant clones with clinically relevant mutations, since the majority of the variants selected have been reported also in resistant, patient-derived isolates [142], [156], [206]. Therefore, similar investigations were continued with other important anti-TB drugs.

Next, this sub-MIC evolution model was applied to BDQ and CFZ, drugs of which mechanisms of resistance are not well understood. These drugs are known to have cross-resistance mechanisms through mutations in *Rv0678*, but also likely by mutations in *pepQ* and *Rv1979c* [77], [201], [209], [210]. Resistance to BDQ can also arise due to mutations in the gene coding for its target, *atpE* [75], [160], [201], [211].

BDQ is currently the most important drug for the treatment of MDR/XDR-TB as it has potent bactericidal activity with a novel mode of action - inhibition of ATP synthase [75]. Since BDQ's widespread use in 2014, only three studies have reported BDQ resistance due to an *atpE* mutation in patient-derived isolates [140], [160], [211]. Most resistance in patients is linked to mutations in *Rv0678*, a gene which regulates the expression of the *mmpS-mmpL* efflux pump [76]. CFZ is also an important drug in treating MDR-TB, the precise mode of action remains unknown, but most resistance to CFZ has also been linked to mutations in *Rv0678* [159], [212], [213]. Of the 215 mutant clones selected from either BDQ- or CFZ-supplemented agar plates in this study, 68 unique variants were reported, the largest diversity of mutations reported in a single selection study [74], [136], [212], [214]–[216]. Previous studies selected mutant clones at high BDQ or CFZ concentrations (more than twice the MIC), but did not generate a high quantity or diversity of variants [136], [216], [217]. Here, mutant colonies were selected from both high and low concentration plates, with instances of the same mutant allele growing at both concentrations (the MIC and 2x the MIC) (Appendix C, Table C.9).

In line with studies on patient-derived BDQ/CFZ resistant strains, a minority of mutants (only 18) were obtained that harbored a variant in *atpE*, with five unique mutations selected. As previously mentioned, only three studies have reported BDQ resistance due to an *atpE* mutation in patient-derived isolates [140],

[160], [211], and less than 1% of BDQ resistance seen in patients is attributed to *atpE* mutations [140], [213]. As in previous patient and *in vitro* studies, major increases in the BDQ MIC were observed for clones harboring an *atpE* mutation, which often exceeded the concentrations tested in both REMA (at least 4-fold or higher than the gWT), and MGIT - growing at the highest concentration tested (Tables 4.2.5, 4.2.6). Interestingly, two clones also presented an elevated MIC to CFZ (2-fold above the gWT) in both REMA and MGIT assays. Collateral resistance between BDQ and CFZ has not been established in bacteria with an *atpE* variant, although CFZ testing has been rarely reported in such strains [140], [160], [212].

Furthermore, congruent with BDQ/CFZ resistant patient-derived strains, the majority of variants selected in this study implicated the efflux regulator protein Rv0678. Indeed, more than 99% of *in vitro* and patient-derived isolates harbor variants throughout this gene (Appendix C, Table C.11). The clones selected from single colonies which had a variant in *Rv0678* presented a 2- to 16-fold increase in BDQ MIC and up to a 12-fold increase to CFZ. Of the selected mutant clones, 184 harbored a variant in *Rv0678*, with 25 unique variants selected after BDQ exposure, 31 after CFZ, and eight which were selected in both BDQ and CFZ experiments. Deep sequencing on the total mutant population of a given selection plate was again performed as a less-bias approach to detect additional variants which were not selected as a single colony. From this, no additional *atpE* variants could be identified, but an additional 39 variants in *Rv067*8, and thirteen variants in the gene *pepQ* were determined.

Interestingly, while mutations in *pepQ* or *Rv1979c* could not be detected in clones derived from single colonies, eight non-synonymous and five synonymous SNPs in *pepQ* were detected by the less-biased population (deep) sequencing approach after CFZ exposure (Appendix C, Table C.8, Figure 4.2.10). This may be caused by a competitive growth defect which mirrors the situation in patients, as a clear link between these mutations and failing TB-treatment has not been well established. Based on current knowledge, *pepQ* mediated resistance has only been clearly linked to CFZ resistance from *in vitro/vivo* selection experiments, but not in patients [77]. So far, only one study implicated *Rv1979c* in BDQ/CFZ cross-resistance, and one other study presented CFZ resistance in patients [163], [218]. Accordingly, it appears that the long-term sub-MIC evolution model better reflects the clinical situation leading to the identification of mutations of high clinical relevance.

However, mutations in *Rv1979c* may be more relevant than previously thought, as the large clinical Mtbc strain collection provided by CRyPTIC included four *Rv1979c* variants (in 35 isolates) linked to moderate-to-high BDQ/CFZ resistance (Appendix C, Table C.10). When the CRyPTIC strain collection was searched for

pepQ variants, only susceptible or borderline-resistance phenotypes were consistently reported (Appendix C, Table C.10).

Taken together, the data obtained in this thesis showed that the sub-MIC evolutionary model has high potential for determining resistance variants to TB drugs. Still, this model also involves a potential selection bias and the ratio of selected mutants may not always reflect the situation in the host and in drug resistant clinical strains observed in different parts of the world. However, the data obtained indicate that this sub-MIC evolution model better reflects the clinical situation than other "high MIC selection" models. Taking all evidence together, this model could be applied to less studied anti-TB compounds and new drugs to define resistance mechanisms and enhance our capacity for molecular resistance prediction.

Based on the obtained data on resistance mutations, this study proceeded to further develop an advanced mutation catalogue for the prediction of BDQ/CFZ drug resistance in clinical isolates, e.g. from genome sequencing data.

5.2.3 Developing a mutational catalogue for bedaquiline and clofazimine

As comprehensive molecular approaches to define drug resistances such as WGS, and targeted genome sequencing such as Deeplex®, are becoming more affordable and accessible even in high incidence, low-income settings, valid catalogues for interpretation of WGS data are urgently needed. The detection of high-confidence resistance associated SNPs can predict drug susceptibility to first-line and most secondary drugs, to a degree which can be implemented in the clinic [91]. For the first time, the WHO released a respective mutation catalogue "Catalogue of mutations in *Mycobacterium tuberculosis* complex and their association with drug resistance" with validated resistance mutations to inform genome sequencing based resistance testing [219]. After rigorous screening and quality control steps, 38,215 isolates were included to develop the WHO's catalogue, including 15 different anti-TB drugs. However, no BDQ/CFZ mutations met the criteria to be included in this report, due to the low-frequency of specific mutations in the dataset, MIC values which were too close to the critical concentration, and the phenotypic methodology of the only large study was not sufficiently verified (CRyPTIC).

To tackle this critical need of developing a respective mutation catalogue, the combination of high-quality MIC data from standardized phenotypic DST and WGS data analyzed with a standardized pipeline is needed. As first steps to compile a BDQ/CFZ mutation catalogue, the data generated from the *in vitro* experiments was combined with a large strain collection dataset provided by CRyPTIC and organized into

a user-friendly variant list (Appendix C, Table C.11). In order to get a full spectrum of potential variants implicated in resistance, mutations identified in 25 published studies were also included in this catalogue, although the work of others may not have followed this study's stringent methodology for DST. Altogether this catalogue included 247 unique mutations across four genes. In relation to BDQ, 159 represent a resistant, 30 a borderline, 26 a susceptible, and 15 a variable phenotype. For CFZ phenotypes, 117 were resistant, 25 borderline, 23 susceptible, and 15 were variable.

This first comprehensive catalogue of variants associated with resistance or susceptibility of BDQ/CFZ is a major achievement towards genome sequencing based resistance prediction. Indeed, 94 Mtbc strains in the CRyPTIC collection with mutations in *Rv0678* were classified as susceptible, 39 of which were hypersusceptible (>/= 0.015 mg/L BDQ MIC), warranting further investigation.

5.2.4 Hypersusceptible phenotypes in patient strains with *Rv0678* mutations may be linked to epistasis

It is important to consider that not all mutations in resistance-associated genes lead to resistance and benign mutations can be prevalent in resistance-associated genes [149]. Such mutations do not have an effect on the bacterial resistance phenotype, but may be misclassified as causing resistance, especially in a scenario where no curated mutation catalogue based on robust genotype/phenotype data is available. Another situation, which can affect bacterial sensitivity, is the presence of so-called epistatic mutations, i.e. mutations, often in a separate gene, which affect the phenotype caused by another mutation. These off-target mutations can mitigate the effect of the resistance mutation and can render Mtbc strains hypersusceptible to particular drugs [220], [221]. Vargas *et al.* has proposed that variants in the *mmpS5-mmpL5* efflux pump genes might counteract the resistance associated effect of *Rv0678* mutations by causing a malfunction or inhibition of the efflux pump [220]. Therefore, the genomes of the CRyPTIC strain collection were inspected for co-occurring *Rv0678* and *mmpS5* (*Rv0675c*) or *mmpL5* (*Rv0676c*) mutations.

Overall, 94 strains with a *Rv0678* variant were present in the CRyPTIC strain collection with a susceptible phenotype to BDQ (MIC <0.12 mg/L), 39 of which were hypersusceptible (MIC </=0.015 mg/L). Of the 94 isolates with a low BDQ MIC, 37 (39.4%) harbored a mutation in *mmpS5* or *mmpL5*. In order to ascertain the effect of an additional *mmpS5/mmpL5* variant, one must compare clones with the same *Rv0678* mutation that also harbor a gWT or mutated *mmpS5/mmpL5* gene. The most abundant example for comparison in this dataset included 23 isolates which harbored the mutation *Rv0678* 192 ins g, of which 20 were categorically susceptible to BDQ with a corresponding *mmpL5* mutation. However, one of the

three isolates with no *mmpL5* mutation also had a susceptible phenotype (MIC 0.03 mg/L BDQ), the other two strains were borderline (MIC 0.12 mg/L BDQ) and resistant (MIC 0.25 mg/L BDQ). This sample may be indicative of an epistatic correlation between mutations in these genes in this dataset, but extrapolating a clear connection is too speculative. Although we can assume that the *mmpS5-mmpL5* efflux pump must be active for *Rv0678* mutations to be effective, the functionality of the efflux pump was not verified in these strains.

Taken all evidence together, a clear-cut conclusion on epistatic relationships cannot be made based on the findings obtained. However, considering the wide range of MIC values seen in *in vitro* clones and clinical strains, it became obvious that the establishment of clinical breakpoints for BDQ/CFZ for *Rv0678* mutation harboring strains is very difficult [219]. Although a clear link has been established between *Rv0678* variants and failing BDQ/CFZ treatment regimens, it is not yet fully clear if the moderate increase in the MIC is rendering these drugs fully ineffective or if a change in drug dosing may be possible [159], [163], [222]–[224].

As was presented in this dissertation, Mtbc strains with *Rv0678* mutations on average increased the MIC by 4-fold compared to the gWT ancestor for BDQ and CFZ. Since the WHO and other health authorities have not set efficacy targets for BDQ or CFZ clinical dosing [96], [225],continued treatment with CFZ and/or BDQ at a higher dosage may be a possible treatment option for Mtbc strains harboring a *Rv0678* mutation. There are currently two clinical trials exploring BDQ dosing efficacy and safety [226], [227]. Still, further work is needed to fully elucidate clinical consequences and options for patients infected with Mtbc strains harboring mutations in *Rv0678*. In the following section, this work aimed to elucidate the mechanism and phenotypic effects of these mutations by exploring their effect of bacterial fitness, the interplay with other co-selected variants, the selection of cross-resistant clones, and other potential genomic modifications.

5.3 Deciphering resistance mechanisms and their implications

In the previous section, it was shown that this sub-MIC evolution model selected a large diversity of resistance-associated variants for MFX, BDQ, and CFZ. Further, the potential of this model to predict clinically relevant resistance causing variants was demonstrated, as many of the mutations implicating the drug targets (*gyrA*, *gyrB*, and *atpE*) were described in patient-derived isolates. Indeed, this sub-MIC evolution model also captured the variability of mutations of the off-target gene *Rv0678*, in relation to BDQ and CFZ resistance. Next, several clones were selected which harbored the most important mutations (clinically relevant) and/or types of genetic modifications (missense mutations or indels) for additional analysis. Finally, further investigation was conducted exploring the diversity of resistance mutations throughout target and off-target genes, the rate at which CFZ exposure selected BDQ cross-resistant mutants, and novel resistance mechanisms.

5.3.1 The mutant selection window of resistance-associated mutations in bacteria of the *Mycobacterium tuberculosis* complex

One interesting question that has not been well addressed for major TB drugs is the definition of the MSW. This describes the drug concentration range between the MIC and the minimum selection concentration (the lowest concentration which the mutant outperforms the gWT) (Figure 2.5) [132]. To date, only one study performed in 2007 investigated the MSW with the Mtbc reference strain H37Rv, performed *in vivo* with MFX [228]. There is a major knowledge deficit about the MSW, and better understanding can help optimize treatment regimens by defining the thresholds for potential harmful (non-inhibitory) drug concentrations.

In order to define the MSW, the growth capacity of H37Rv mutant clones with resistance-associated mutations to FQ (MFX) and BDQ were measured in the automated MGIT system, which detects oxygen consumption as an indication of growth. In the case of FQ associated variants, clones were evaluated which harbored the most common *gyrA* mutations observed in clinical isolates - D94G and A90V, also *gyrB* N499D, and the less common *gyrB* E501D. Four clones were evaluated with BDQ resistant phenotypes, two with an *atpE* mutation (E61D or D28V) [160], [211], and two clones with *Rv0678* mutations, the missense S68G and gene disrupting mutation R156_. The minimum selection concentration was extrapolated from the original evolutionary experiments, as resistant populations significantly increased when exposed to concentrations as low as 1:16 the MIC for all antibiotics tested (Figure 4.2.4, 4.2.5, 4.2.6).

These experiments demonstrated that the MSW starts far below the MIC. Indeed, as shown in the sub-MIC evolution model, comparably low drug concentrations of all antibiotics tested, selected mutant clones significantly. Interestingly, the MSW is variable between resistant clones with different mutations, even if mutations occur in the same gene at a different position (Figure 4.3.1, 4.3.2). For example, when analyzing the MSW of four MFX selected mutants, *gyrA* D94G outgrew *gyrA* A90V at antibiotic concentrations of 0.5 and 1.0 mg/L MFX, while D94G had a higher MIC of 2.0 mg/L compared to A90V of 1.0 mg/L MFX. Similarly, *gyrB* E501D exceeded the growth of *gyrB* N499D at 0.5 and 1.0 mg/L MFX, with MICs of 2.0 and 1.0 mg/L MFX respectively (Figure 4.3.1). However, when the same experiments were carried out with BDQ, clones with different variants had similar MSWs, where the MSW was more dependent on which resistance conferring gene was affected (Figure 4.3.2). Therefore, clones harboring different *Rv0678* mutations had the same MSW, and clones with *atpE* mutations had the same MSW. Indeed, the MSW of clones with *atpE* mutations appeared to be much larger than that for clones with a *Rv0678* mutation. However, the precise MSW of the *atpE* mutant clones was unclear, as both clones grew at the highest drug concentrations tested. These findings are especially important when drug combinations are designed and dosages of individual drugs are adjusted, in order to avoid favorable conditions for the selection of these variants. The next topic to explore was the effect of particular mutations on growth of the clones (fitness).

5.3.2 The fitness impact of resistance-associated variants

It has been established that resistance-associated variants can impact the fitness of Mtbc strains [165], [182], [187]. It was hypothesized that the sub-MIC evolution model employed would select more clinically relevant, highly fit variants; since the weak selection pressure applied likely facilitated competition with the highly fit, susceptible gWT population and other resistant subpopulations [132], [165], [185]. This was partially verified as several of the resistance-associated mutations determined in the model were also detected in patient-derived Mtbc isolates, either published or observed in the CRyPTIC strain collection [74], [159], [160], [163], [211]. Although clones with clinically relevant mutations were selected, it was not clear if these variants also impacted the fitness of the bacteria. Therefore, the relative fitness was evaluated through direct competition experiments, between the gWT ancestor and mutant clones, in antibiotic-free conditions.

Fitness experiments which measure the growth of one strain compared to another (typically compared to the gWT ancestor) are the gold standard for decoding fitness effects of unknown mutations [159], [164], [182], [229]. The same clones were investigated as with the MSW experiments (in the previous section).

In the case of FQ associated variants, virtually no fitness loss was linked to *gyrA* A90V and *gyrB* E501D variants. Similar results were also reported by Castro *et al,* which investigated the same variants in different Mtbc strains [182]. However, the clone which harbored *gyrA* D94G, presented a significant fitness defect as compared to the gWT ancestor. This is the most common resistance variant selected in these evolutionary experiments, and also observed in patient isolates. Therefore, it is surprising that a fitness defect was observed, but it could be that during FQ exposure these clones are more competitive.

Next, the competitive fitness was investigated between clones which were selected after BDQ exposure. Both clones with *atpE* mutations revealed a significant fitness loss, which contradicted the work of Huitric *et al.,* who showed Mtbc strains with *atpE* variants do not exhibit a reduction in growth as compared to the gWT ancestor [201]. On the other hand, it was found that clones harboring *Rv0678* variants have various fitness levels, as the clone with the *Rv0678* S68G variant presented no fitness loss, and the clones with the gene disrupting mutation *Rv0678* R156_ had an average reduction in fitness. The fitness effects of *atpE* and *Rv0678* mutations have not been well examined, but these results contradicted Villellas *et al.*, who showed that a gene disrupting *Rv0678* mutation did not confer a loss of fitness in their Mtbc strain [159].

Through direct competition experiments *in vitro*, it was shown that the fitness effects of mutations in resistance associated genes is variable between clones which harbor variants in different genes, but also the same gene at a different locus. Further fitness evaluation should be conducted in primary host cells (macrophages) and *in vivo*; as there may be a fitness effect in more complex biological systems. In the next section, it was questioned whether some clones acquired additional mutations, in genes not associated with resistance, which may affect the phenotype to a measurable degree.

5.3.3 Co-selection of off-target mutations

An important factor which has not been especially approached in *in vitro* selection models, are off-target mutations which might implicate bacterial fitness, tolerance, persistence, or other regulatory mechanisms. Typically, compensatory mutations are identified in large outbreaks of particular MDR-Mtbc strains or genome-wide analysis studies, which comprise of thousands of strains [164], [188], [193], [194]. Although *in vitro* modeling is done to explore the phenotypic effect of these mutations, it is rarely done through *de novo* or stochastic evolution, but by genetic modification [164], [192], [230]. Therefore, it was investigated whether this sub-MIC evolution model also selected additional off-target mutations.

Off-target or "secondary" mutations were determined by comparing all alternative SNPs in non-reparative genes between the mutant and gWT ancestor genome. Of all the selected mutants, 84 harbored an additional mutation in a second gene, previously unrelated to resistance (Appendix D, Table D.1). In total, these included 20 different mutations affecting 20 different genes. The functional associations of these genes included cell wall processes, information pathways, metabolism & respiration, lipid metabolisms, and regulatory proteins; with at least six genes of unknown function. However, it is necessary to consider these may be hitchhiking mutations, which do not implicate the bacterial phenotype, a phenomenon also seen in patient-derived isolates [231]. To further investigate the possible clinical relevance of these variants, an inhouse collection of genome data of over 300,000 strains was screened for these off-target mutations. Unfortunately, there were no direct hits in patient-derived isolates. Since this search only included variants at specific positions in the genome, it is possible that one or more of these genes are clinically relevant, but that a different locus is implicated in patient-derived strains.

Although identical mutations were not detected in clinical Mtbc strains, two clones with different off-target mutations were examined for their phenotypic effect. The first mutation was co-selected with an FQ resistance-associated variant. This mutant clone harbored the combination of the mutations *gyrA* A90V and *ppgK* _266S, the latter was a gene coding for a polyphosphate glucokinase enzyme associated with metabolism and respiration (Appendix D, Table D.1) [232]. When first looking at the MSW of these clones, the mutant with the secondary mutation appeared to have a slight growth advantage in higher drug concentrations compared to the clone lacking the mutation, although this was not significant (Figure 4.3.1). A second clone was investigated, which was resistance to BDQ/CFZ and harbored the mutations *Rv0678* S68G with the second mutation *mmpL5* A423D, a gene which codes for the efflux pump which the Rv0678 protein regulates (Appendix D, Table D.1) [76]. The MSW of the off-target harboring mutant indicated a similar growth capacity as the clone with only the resistance-associated mutation (Figure 4.3.2). Direct competition experiments were also carried out with these clones. For both off-target mutation harboring clones, a statistical difference in their relative fitness (allele frequency) as compared to the pure resistant mutant was not observed (Figure 4.3.3, 4.3.4).

It was shown that this sub-MIC evolution model also selects variants with different off-target, secondary mutations. The two mutations explored through experimentation did not alter resistance, and were determined not to have a fitness effect. These variants could also have been selected by culturing, or simply as hitchhiking mutations. Although seemingly no phenotypic effect was attributed to these mutations, other experiments for a more dynamic evaluation should be conducted. One major pitfall of

the experiments performed here, is that they merely measured growth rate, but other functions should be explored like in-host survival, biological activity, and gene expression.

5.3.4 Cross-resistance between bedaquiline and clofazimine

Cross-resistance or collateral resistance occurs when a pathogen is able to gain resistance to at least two compounds from a single genetic mechanism. There are several instances in which genetic variants are linked with resistance to multiple drugs such as mutations in *rrs* to AMK, CPR, and KAN and in *inhA* to INH, PTH and ETH, to name a few (Table 2.1). Such events are especially concerning, since they can render an Mtbc strain resistant to a drug before exposure, or reduce the effective treatment of combination therapies. Previous data already indicated that BDQ and CFZ have a cross-resistance mechanism via mutations in *Rv0678*, in which mutations can seemingly occur anywhere throughout the gene (Figure 4.2.10) [73], [163], [202]. Interestingly, all of these mutant clones presented an MIC increase to BDQ, regardless of drug exposure (CFZ or BDQ); but some mutants selected after BDQ exposure did not present an elevated MIC to CFZ (Appendix C, Table C.9). Therefore, the magnitude of cross-resistance between these two drugs was explored.

Indeed, most but not all mutations in *Rv0678* result in an elevated MIC to both BDQ and CFZ in the affected clone (Appendix C, Table C.9). As mentioned, all mutant clones selected after CFZ exposure were cross-resistant to both CFZ and BDQ, but some mutants selected after BDQ exposure were still phenotypically susceptible to CFZ. This indicated that cross-resistance with CFZ may be further linked mechanistically. It is hypothesized that SNPs in regions of the *Rv0678* gene affect protein stability and binding more prominently, when the mutations appear in the DNA binding region, protein stability, or dimerization domain [140], [233]. It is of concern that pre-exposure to CFZ fosters resistance to BDQ (the arguably more effective drug) before the strain has come into contact with BDQ. To investigate this experimentally, CFZ exposed cultures were plated on BDQ supplemented agar plates, and the resistant populations were quantified, as compared to BDQ exposed bacteria (Figure 4.2.7). Indeed, CFZ exposure is selected for BDQ resistant populations at a similar rate as BDQ exposure (Figure 4.2.8). Furthermore, the rate at which CFZ pre-selected BDQ resistant populations may be even higher than described, as these experiments were conducted retrospectively, from frozen stocks (stocks which were saved after sub-MIC evolution experiments conducted with CFZ), and likely a significant amount of the overall bacterial population was reduced during the freezing/unfreezing process.

Finally, a number of BDQ-CFZ selected clones were phenotypically resistant, with no genomic modifications in resistance-associated genes. These clones were further analyzed for special mechanisms of resistance.

5.3.5 Large scale gene rearrangement as a novel bedaquiline/clofazimine resistance mechanism

This study validated the important cross-resistance mechanism for BDQ and CFZ by genomic modification of the *Rv0678* gene, which other studies have found to influence *mmpS5-mmpL5* efflux pump expression [73], [140], [202]. For the majority of clones selected after this study's sub-MIC evolution experiments, mutations in *Rv0678* or in *atpE* could be identified as the likely resistance mechanism. Still, 13 clones which were randomly selected from BDQ and CFZ supplemented agar plates, did not harbor a mutation in any of the defined resistance-associated genes (Table 4.3.1). Nine of the thirteen clones had at least one variant in other regions of the chromosome (off-target mutations). To further decipher possible resistance mechanisms in these clones, IGV software was used to look into the genome alignment of BDQ/CFZ resistance-associated genes (Figure 4.3.5). Interestingly there was an unusual coverage signal in the *Rv0678* gene coding region, which indicated a large structural modification (Figure 4.2.11). Large structural modifications, large indels, and duplicated genes are not yet picked up by most short-read sequencing computational pipelines. Therefore, three of these clones were selected for PacBio® long-read sequencing and *de novo* assembly.

After *de novo* assembly, a 2.7 Mb inversion flanked by the transposable element insertion sequence *6110* (IS*6110*) was identified. This inversion is the largest known gene rearrangement in Mtbc to date, and the first to be spontaneously developed *in vitro* and implicated in drug resistance. Due to the special nature of this finding, the sequencing data was sent to colleagues at Cambridge University (by Z. Iqbal, K. Malone, and M. Hunt) for further analysis. The original conclusion was verified, and these external reviewers reported one similar instance in their patient strain collection.

There have been a few studies which demonstrated similar large-scale gene rearrangements in Mtbc clinical isolates. For example, Saw *et al.* observed large and small-scale rearrangement in proline-glutamate/proline-proline-glutamate (PE/PPE), membrane, and transcriptional genes in strains isolated from cerebrospinal fluid [139]. Shitikov *et al.* also presented a large-scale chromosomal rearrangement in a Beijing outbreak, although again it was not linked to resistance [138]. Both of these studies also found flanking of IS*6110*, a sequence used in DNA fingerprinting for Mtbc strain typing [234], [235]. Detection of

structural variations is not routinely integrated in TB genomic research pipelines, likely due to the overwhelming consensus that the Mtbc genome is incredibly stable. Although transposition of these sequences is rare, this and other studies might point at the importance of insertion sequences (or specifically IS*6110*) and repetitive regions (PE/PPE genes) in Mtbc polymorphisms and evolution [138], [139], [235].

In conclusion, the data obtained here showed that large rearrangements in the Mtbc genome can be involved in drug resistance development and thus, represent important genetic information that need to be deciphered for genomic resistance prediction workflows.

5.5 Conclusion

Taken together, this work highlighted the adaptive evolutionary landscape of Mtbc bacteria through intra-patient evolution of a single strain, *in vitro* sub-MIC evolution model, and a large strain collection examination. Indeed, resistance evolution of Mtbc bacteria is highly dynamic, and more diverse than previously thought. By investigating an Mtbc strain evolution throughout a failing MDR-TB therapy, it was shown that resistance evolution is an arms race between heteroresistant subpopulations that is fuelled by inappropriate drug regimens. This study successfully established a sub-MIC long-term evolution model that allowed for effective isolation of resistant mutant clones as a basis for establishing variant catalogues for genomic resistance prediction. Using the sub-MIC evolution model, a large collection of *de novo* mutants with an available gWT ancestor for FQs, BDQ and CFZ was established for future research. This model also demonstrated for the first time that resistant clones can be selected in an environment with a weak selection pressure far below the MIC. The mutant selection window for the main MDR-TB drugs is wider than previously anticipated indicating that sub-inhibitory concentrations, e.g. caused by structural constraints in infected organs, can lead to resistance selection and treatment failure. The data obtained also demonstrated that the majority of mutations in *Rv0678* confer cross-resistance to BDQ and CFZ, and that CFZ exposure selects for mutant populations also resistant to BDQ. Finally, the data obtained was also used to establish a comprehensive mutational catalogue for genotypic, drug resistance prediction for BDQ/CFZ. This study progresses the field of research on resistant TB by introducing an evolution model for antibiotic and resistance screening. By incorporating this information into sequencing-based diagnostic approaches, better treatment therapies can be designed for highly resistant cases, which in the end might help control the spread and evolution of resistant strains.

Still, future questions arose that could not be fully addressed in the current work. Further experiments should be conducted to:

- elucidate functional differences between resistance-associated variants in patient-derived isolates
- additional evaluation of phenotype/fitness of *in vitro* selected mutations - through more competition experiments, measuring growth and infectability of macrophages, and survivability in an *in vivo* model
- understanding of resistance mechanisms observed - like investigating the transcriptional effect of SNPs vs indels in *Rv0678* mutants on the expression of the mmpS-mmpL efflux pump
- analyze the MSW for other drugs currently applied in TB treatment and for new drug candidates that are developed

6. References

[1] T. Wirth *et al.*, "Origin, Spread and Demography of the Mycobacterium tuberculosis Complex," *PLOS Pathogens*, vol. 4, no. 9, p. e1000160, Sep. 2008, doi: 10.1371/journal.ppat.1000160.

[2] I. Comas *et al.*, "Out-of-Africa migration and Neolithic coexpansion of Mycobacterium tuberculosis with modern humans," *Nature Genetics*, vol. 45, no. 10, Art. no. 10, Oct. 2013, doi: 10.1038/ng.2744.

[3] "RKI - Robert Koch." https://www.rki.de/EN/Content/Institute/History/rk_node_en.html (accessed Jan. 06, 2021).

[4] "Global tuberculosis report 2020," Jan. 09, 2021. https://www.who.int/publications-detail-redirect/9789240013131 (accessed Jan. 09, 2021).

[5] N. P. A. S. Johnson and J. Mueller, "Updating the accounts: global mortality of the 1918-1920 'Spanish' influenza pandemic," *Bull Hist Med*, vol. 76, no. 1, pp. 105–115, 2002, doi: 10.1353/bhm.2002.0022.

[6] "WHO Coronavirus (COVID-19) Dashboard." https://covid19.who.int (accessed Nov. 03, 2021).

[7] "Global tuberculosis report 2020." https://www.who.int/publications-detail-redirect/9789240013131 (accessed Jan. 09, 2021).

[8] "Basic TB Facts | TB | CDC," Mar. 27, 2020. https://www.cdc.gov/tb/topic/basics/default.htm (accessed Jan. 09, 2021).

[9] B. J. Marais *et al.*, "Tuberculosis comorbidity with communicable and non-communicable diseases: integrating health services and control efforts," *The Lancet Infectious Diseases*, vol. 13, no. 5, pp. 436–448, May 2013, doi: 10.1016/S1473-3099(13)70015-X.

[10] E. Vynnycky and P. E. Fine, "The natural history of tuberculosis: the implications of age-dependent risks of disease and the role of reinfection," *Epidemiol Infect*, vol. 119, no. 2, pp. 183–201, Oct. 1997, doi: 10.1017/s0950268897007917.

[11] A. van Rie *et al.*, "Exogenous reinfection as a cause of recurrent tuberculosis after curative treatment," *N Engl J Med*, vol. 341, no. 16, pp. 1174–1179, Oct. 1999, doi: 10.1056/NEJM199910143411602.

[12] C.-Y. Chiang and L. W. Riley, “Exogenous reinfection in tuberculosis,” *The Lancet Infectious Diseases*, vol. 5, no. 10, pp. 629–636, Oct. 2005, doi: 10.1016/S1473-3099(05)70240-1.

[13] K. Mallard *et al.*, “Molecular Detection of Mixed Infections of Mycobacterium tuberculosis Strains in Sputum Samples from Patients in Karonga District, Malawi,” *Journal of Clinical Microbiology*, vol. 48, no. 12, pp. 4512–4518, Dec. 2010, doi: 10.1128/JCM.01683-10.

[14] H. Luzze *et al.*, “Relapse more common than reinfection in recurrent tuberculosis 1–2 years post treatment in urban Uganda,” *Int J Tuberc Lung Dis*, vol. 17, no. 3, Art. no. 3, Mar. 2013, doi: 10.5588/ijtld.11.0692.

[15] J. L. Johnson and B. A. Thiel, “Time until Relapse in Tuberculosis Treatment Trials: Implication for Phase 3 Trial Design,” *Am J Respir Crit Care Med*, vol. 186, no. 5, Art. no. 5, Sep. 2012, doi: 10.1164/ajrccm.186.5.464.

[16] P. G. T. Cudahy, D. Wilson, and T. Cohen, “Risk factors for recurrent tuberculosis after successful treatment in a high burden setting: a cohort study,” *BMC Infectious Diseases*, vol. 20, no. 1, p. 789, Oct. 2020, doi: 10.1186/s12879-020-05515-4.

[17] M. Merker *et al.*, “Evolutionary history and global spread of the Mycobacterium tuberculosis Beijing lineage,” *Nat Genet*, vol. 47, no. 3, pp. 242–249, Mar. 2015, doi: 10.1038/ng.3195.

[18] V. Eldholm *et al.*, “Four decades of transmission of a multidrug-resistant Mycobacterium tuberculosis outbreak strain,” *Nature Communications*, vol. 6, no. 1, Art. no. 1, May 2015, doi: 10.1038/ncomms8119.

[19] K. Dheda *et al.*, “The epidemiology, pathogenesis, transmission, diagnosis, and management of multidrug-resistant, extensively drug-resistant, and incurable tuberculosis,” *The Lancet Respiratory Medicine*, vol. 5, no. 4, Art. no. 4, Apr. 2017, doi: 10.1016/S2213-2600(17)30079-6.

[20] W. J. Burman, D. L. Cohn, C. A. Rietmeijer, F. N. Judson, R. R. Reves, and J. A. Sbarbaro, “Noncompliance with directly observed therapy for tuberculosis: Epidemiology and effect on the outcome of treatment,” *Chest*, vol. 111, no. 5, Art. no. 5, May 1997, doi: 10.1378/chest.111.5.1168.

[21] K. S. Babiarz, S. Suen, and J. D. Goldhaber-Fiebert, “Tuberculosis treatment discontinuation and symptom persistence: an observational study of Bihar, India’s public care system covering >100,000,000 inhabitants,” *BMC Public Health*, vol. 14, p. 418, May 2014, doi: 10.1186/1471-2458-14-418.

[22] K. E. Dooley *et al.*, "Risk factors for tuberculosis treatment failure, default, or relapse and outcomes of retreatment in Morocco," *BMC Public Health*, vol. 11, no. 1, p. 140, Feb. 2011, doi: 10.1186/1471-2458-11-140.

[23] S. Srivastava, J. G. Pasipanodya, C. Meek, R. Leff, and T. Gumbo, "Multidrug-Resistant Tuberculosis Not Due to Noncompliance but to Between-Patient Pharmacokinetic Variability," *Journal of Infectious Diseases*, vol. 204, no. 12, Art. no. 12, Dec. 2011, doi: 10.1093/infdis/jir658.

[24] V. Dartois, "The path of anti-tuberculosis drugs: from blood to lesions to mycobacterial cells," *Nature Reviews Microbiology*, vol. 12, no. 3, Art. no. 3, Mar. 2014, doi: 10.1038/nrmicro3200.

[25] P. Miotto, Y. Zhang, D. M. Cirillo, and W. C. Yam, "Drug resistance mechanisms and drug susceptibility testing for tuberculosis," *Respirology*. 2018. doi: 10.1111/resp.13393.

[26] M. I. Gröschel, T. M. Walker, T. S. van der Werf, C. Lange, S. Niemann, and M. Merker, "Pathogen-based precision medicine for drug-resistant tuberculosis," *PLoS Pathogens*, vol. 14, no. 10, 2018, doi: 10.1371/journal.ppat.1007297.

[27] "WHO | What is DOTS?," *WHO*. https://www.who.int/tb/publications/dots-who-guide/en/ (accessed Jan. 22, 2021).

[28] P. E. Fine, "Variation in protection by BCG: implications of and for heterologous immunity," *Lancet*, vol. 346, no. 8986, pp. 1339–1345, Nov. 1995, doi: 10.1016/s0140-6736(95)92348-9.

[29] "Pipeline of vaccines," *TBVI*. https://www.tbvi.eu/what-we-do/pipeline-of-vaccines/ (accessed Jan. 08, 2021).

[30] N. E. Nieuwenhuizen *et al.*, "The Recombinant Bacille Calmette–Guérin Vaccine VPM1002: Ready for Clinical Efficacy Testing," *Front Immunol*, vol. 8, Sep. 2017, doi: 10.3389/fimmu.2017.01147.

[31] L. K. Schrager, J. Vekemens, N. Drager, D. M. Lewinsohn, and O. F. Olesen, "The status of tuberculosis vaccine development," *Lancet Infect Dis*, vol. 20, no. 3, pp. e28–e37, Mar. 2020, doi: 10.1016/S1473-3099(19)30625-5.

[32] S. K. Sharma *et al.*, "Efficacy and Safety of Mycobacterium indicus pranii as an adjunct therapy in Category II pulmonary tuberculosis in a randomized trial," *Sci Rep*, vol. 7, Jun. 2017, doi: 10.1038/s41598-017-03514-1.

[33] A. Schatz, E. Bugle, and S. A. Waksman, “Streptomycin, a Substance Exhibiting Antibiotic Activity Against Gram-Positive and Gram-Negative Bacteria.∗†,” *Proceedings of the Society for Experimental Biology and Medicine*, vol. 55, no. 1, pp. 66–69, Jan. 1944, doi: 10.3181/00379727-55-14461.

[34] C. R. Spotts and R. Y. Stanier, “Mechanism of Streptomycin Action on Bacteria: a Unitary Hypothesis.,” *Nature*, vol. 192, pp. 633–7, 1961, doi: 10.1038/192633a0.

[35] L. Luzzatto, D. Apirion, and D. Schlessinger, “Mechanism of action of streptomycin in E. coli: interruption of the ribosome cycle at the initiation of protein synthesis.,” *Proc Natl Acad Sci U S A*, vol. 60, no. 3, pp. 873–880, Jul. 1968, doi: 10.1073/pnas.60.3.873.

[36] J. F. Murray, D. E. Schraufnagel, and P. C. Hopewell, “Treatment of Tuberculosis. A Historical Perspective,” *Annals ATS*, vol. 12, no. 12, pp. 1749–1759, Dec. 2015, doi: 10.1513/AnnalsATS.201509-632PS.

[37] H. C. Hinshaw, M. M. Pyle, and W. H. Feldman, “Streptomycin in tuberculosis,” *The American Journal of Medicine*, vol. 2, no. 5, pp. 429–435, May 1947, doi: 10.1016/0002-9343(47)90087-9.

[38] J. Lehmann, “PARA-AMINOSALICYLIC ACID IN THE TREATMENT OF TUBERCULOSIS,” *The Lancet*, vol. 247, no. 6384, pp. 15–16, Jan. 1946, doi: 10.1016/S0140-6736(46)91185-3.

[39] J. Crofton and D. A. Mitchison, “Streptomycin Resistance in Pulmonary Tuberculosis,” *Br Med J*, vol. 2, no. 4588, pp. 1009–1015, Dec. 1948, doi: 10.1136/bmj.2.4588.1009.

[40] R. J. W. Rees and J. M. Robson, “Additive Effect of Streptomycin and p-Amino-Salicylic Acid in Experimental Tuberculous Infection,” *Nature*, vol. 164, no. 4165, Art. no. 4165, Aug. 1949, doi: 10.1038/164351a0.

[41] B. M. J. P. Group, “Treatment of Pulmonary Tuberculosis with Streptomycin and Para-Amino-Salicylic Acid: A Medical Research Council Investigation,” *Br Med J*, vol. 2, no. 4688, pp. 1073–1085, Nov. 1950, doi: 10.1136/bmj.2.4688.1073.

[42] S. J. Shane, J. H. Laurie, C. Riley, and M. Boutilier, “Effect of Combined Therapy (Dihydrostreptomycin and PAS) on the Emergence of Streptomycin-Resistant Strains of Tubercle Bacilli,” *New England Journal of Medicine*, vol. 246, no. 4, pp. 132–134, Jan. 1952, doi: 10.1056/NEJM195201242460404.

[43] World Health Organization, *Guidelines for treatment of drug-susceptible tuberculosis and patient care: 2017 update.* 2017.

[44] A. Telenti *et al.*, “Detection of rifampicin-resistance mutations in Mycobacterium tuberculosis,” *The Lancet*, vol. 341, no. 8846, pp. 647–651, Mar. 1993, doi: 10.1016/0140-6736(93)90417-F.

[45] M. R. Farhat *et al.*, “Genomic Analysis Identifies Targets of Convergent Positive Selection in Drug Resistant Mycobacterium tuberculosis,” *Nat Genet*, vol. 45, no. 10, pp. 1183–1189, Oct. 2013, doi: 10.1038/ng.2747.

[46] Y. Zhang, B. Heym, B. Allen, D. Young, and S. Cole, “The catalase-peroxidase gene and isoniazid resistance of Mycobacterium tuberculosis,” *Nature*, vol. 358, no. 6387, pp. 591–593, Aug. 1992, doi: 10.1038/358591a0.

[47] A. Banerjee *et al.*, “inhA, a gene encoding a target for isoniazid and ethionamide in Mycobacterium tuberculosis,” *Science*, vol. 263, no. 5144, pp. 227–230, Jan. 1994, doi: 10.1126/science.8284673.

[48] H. Ando, T. Miyoshi-Akiyama, S. Watanabe, and T. Kirikae, “A silent mutation in mabA confers isoniazid resistance on Mycobacterium tuberculosis,” *Mol Microbiol*, vol. 91, no. 3, pp. 538–547, Feb. 2014, doi: 10.1111/mmi.12476.

[49] H. Safi *et al.*, “Evolution of high-level ethambutol-resistant tuberculosis through interacting mutations in decaprenylphosphoryl-β-d-arabinose biosynthetic and utilization pathway genes,” *Nat Genet*, vol. 45, no. 10, pp. 1190–1197, Oct. 2013, doi: 10.1038/ng.2743.

[50] F. Alcaide, G. E. Pfyffer, and A. Telenti, “Role of embB in natural and acquired resistance to ethambutol in mycobacteria.,” *Antimicrob Agents Chemother*, vol. 41, no. 10, pp. 2270–2273, Oct. 1997, doi: 10.1128/AAC.41.10.2270.

[51] A. Telenti *et al.*, “The emb operon, a gene cluster of Mycobacterium tuberculosis involved in resistance to ethambutol,” *Nat Med*, vol. 3, no. 5, Art. no. 5, May 1997, doi: 10.1038/nm0597-567.

[52] A. Scorpio *et al.*, “Characterization of pncA mutations in pyrazinamide-resistant Mycobacterium tuberculosis.,” *Antimicrob Agents Chemother*, vol. 41, no. 3, pp. 540–543, Mar. 1997, doi: 10.1128/AAC.41.3.540.

[53] W. Shi *et al.*, “Pyrazinamide inhibits trans-translation in Mycobacterium tuberculosis: a potential mechanism for shortening the duration of tuberculosis chemotherapy,” *Science*, vol. 333, no. 6049, pp. 1630–1632, Sep. 2011, doi: 10.1126/science.1208813.

[54] J. Douglass and L. M. Steyn, “A Ribosomal Gene Mutation in Streptomycin-Resistant Mycobacterium tuberculosis Isolates,” *The Journal of Infectious Diseases*, vol. 167, no. 6, pp. 1505–1506, Jun. 1993, doi: 10.1093/infdis/167.6.1505.

[55] M. Finken, P. Kirschner, A. Meier, A. Wrede, and E. C. Böttger, “Molecular basis of streptomycin resistance in Mycobacterium tuberculosis: alterations of the ribosomal protein S12 gene and point mutations within a functional 16S ribosomal RNA pseudoknot,” *Molecular Microbiology*, vol. 9, no. 6, pp. 1239–1246, 1993, doi: 10.1111/j.1365-2958.1993.tb01253.x.

[56] S. Okamoto *et al.*, “Loss of a conserved 7-methylguanosine modification in 16S rRNA confers low-level streptomycin resistance in bacteria,” *Molecular Microbiology*, vol. 63, no. 4, pp. 1096–1106, 2007, doi: 10.1111/j.1365-2958.2006.05585.x.

[57] T. Kocagöz, C. J. Hackbarth, I. Unsal, E. Y. Rosenberg, H. Nikaido, and H. F. Chambers, “Gyrase mutations in laboratory-selected, fluoroquinolone-resistant mutants of Mycobacterium tuberculosis H37Ra.,” *Antimicrobial Agents and Chemotherapy*, vol. 40, no. 8, pp. 1768–1774, Aug. 1996, doi: 10.1128/AAC.40.8.1768.

[58] H. E. Takiff *et al.*, “Cloning and nucleotide sequence of Mycobacterium tuberculosis gyrA and gyrB genes and detection of quinolone resistance mutations.,” *Antimicrob Agents Chemother*, vol. 38, no. 4, pp. 773–780, Apr. 1994, doi: 10.1128/AAC.38.4.773.

[59] L. Jugheli, N. Bzekalava, P. de Rijk, K. Fissette, F. Portaels, and L. Rigouts, “High Level of Cross-Resistance between Kanamycin, Amikacin, and Capreomycin among Mycobacterium tuberculosis Isolates from Georgia and a Close Relation with Mutations in the rrs Gene,” *Antimicrob Agents Chemother*, vol. 53, no. 12, pp. 5064–5068, Dec. 2009, doi: 10.1128/AAC.00851-09.

[60] Y. Suzuki *et al.*, “Detection of Kanamycin-Resistant Mycobacterium tuberculosis by Identifying Mutations in the 16S rRNA Gene,” *J Clin Microbiol*, vol. 36, no. 5, pp. 1220–1225, May 1998, doi: 10.1128/JCM.36.5.1220-1225.1998.

[61] M. A. Zaunbrecher, R. D. Sikes, B. Metchock, T. M. Shinnick, and J. E. Posey, “Overexpression of the chromosomally encoded aminoglycoside acetyltransferase eis confers kanamycin resistance in Mycobacterium tuberculosis,” *Proc Natl Acad Sci U S A*, vol. 106, no. 47, pp. 20004–20009, Nov. 2009, doi: 10.1073/pnas.0907925106.

[62] A. Z. Reeves *et al.*, "Aminoglycoside Cross-Resistance in Mycobacterium tuberculosis Due to Mutations in the 5′ Untranslated Region of whiB7," *Antimicrob Agents Chemother*, vol. 57, no. 4, pp. 1857–1865, Apr. 2013, doi: 10.1128/AAC.02191-12.

[63] C. E. Maus, B. B. Plikaytis, and T. M. Shinnick, "Mutation of tlyA Confers Capreomycin Resistance in Mycobacterium tuberculosis," *AAC*, vol. 49, no. 2, Art. no. 2, Feb. 2005, doi: 10.1128/AAC.49.2.571-577.2005.

[64] A. R. Baulard *et al.*, "Activation of the pro-drug ethionamide is regulated in mycobacteria," *J Biol Chem*, vol. 275, no. 36, pp. 28326–28331, Sep. 2000, doi: 10.1074/jbc.M003744200.

[65] A. E. DeBarber, K. Mdluli, M. Bosman, L. G. Bekker, and C. E. Barry, "Ethionamide activation and sensitivity in multidrug-resistant Mycobacterium tuberculosis," *Proc Natl Acad Sci U S A*, vol. 97, no. 17, pp. 9677–9682, Aug. 2000, doi: 10.1073/pnas.97.17.9677.

[66] J. Zheng *et al.*, "para-Aminosalicylic Acid Is a Prodrug Targeting Dihydrofolate Reductase in Mycobacterium tuberculosis," *J Biol Chem*, vol. 288, no. 32, pp. 23447–23456, Aug. 2013, doi: 10.1074/jbc.M113.475798.

[67] J. Rengarajan, C. M. Sassetti, V. Naroditskaya, A. Sloutsky, B. R. Bloom, and E. J. Rubin, "The folate pathway is a target for resistance to the drug para-aminosalicylic acid (PAS) in mycobacteria," *Mol Microbiol*, vol. 53, no. 1, pp. 275–282, Jul. 2004, doi: 10.1111/j.1365-2958.2004.04120.x.

[68] P. Beckert *et al.*, "rplC T460C Identified as a Dominant Mutation in Linezolid-Resistant Mycobacterium tuberculosis Strains," *Antimicrob. Agents Chemother.*, vol. 56, no. 5, Art. no. 5, May 2012, doi: 10.1128/AAC.06227-11.

[69] D. Hillemann, S. Rüsch-Gerdes, and E. Richter, "In Vitro-Selected Linezolid-Resistant Mycobacterium tuberculosis Mutants," *Antimicrob Agents Chemother*, vol. 52, no. 2, pp. 800–801, Feb. 2008, doi: 10.1128/AAC.01189-07.

[70] D. Awasthy, S. Bharath, V. Subbulakshmi, and U. Sharma, "Alanine racemase mutants of Mycobacterium tuberculosis require D-alanine for growth and are defective for survival in macrophages and mice," *Microbiology (Reading)*, vol. 158, no. Pt 2, pp. 319–327, Feb. 2012, doi: 10.1099/mic.0.054064-0.

[71] J. B. Bruning, A. C. Murillo, O. Chacon, R. G. Barletta, and J. C. Sacchettini, "Structure of the Mycobacterium tuberculosis D-alanine:D-alanine ligase, a target of the antituberculosis drug D-

cycloserine," *Antimicrob Agents Chemother*, vol. 55, no. 1, pp. 291–301, Jan. 2011, doi: 10.1128/AAC.00558-10.

[72] C. A. Desjardins *et al.*, "Genomic and functional analyses of Mycobacterium tuberculosis strains implicate ald in D-cycloserine resistance," *Nat Genet*, vol. 48, no. 5, Art. no. 5, May 2016, doi: 10.1038/ng.3548.

[73] R. C. Hartkoorn, S. Uplekar, and S. T. Cole, "Cross-Resistance between Clofazimine and Bedaquiline through Upregulation of MmpL5 in Mycobacterium tuberculosis," *Antimicrob Agents Chemother*, vol. 58, no. 5, pp. 2979–2981, May 2014, doi: 10.1128/AAC.00037-14.

[74] S. Zhang, J. Chen, P. Cui, W. Shi, W. Zhang, and Y. Zhang, "Identification of novel mutations associated with clofazimine resistance in Mycobacterium tuberculosis," *J Antimicrob Chemother*, vol. 70, no. 9, pp. 2507–2510, Sep. 2015, doi: 10.1093/jac/dkv150.

[75] K. Andries *et al.*, "A Diarylquinoline Drug Active on the ATP Synthase of Mycobacterium tuberculosis," *Science*, vol. 307, no. 5707, pp. 223–227, Jan. 2005, doi: 10.1126/science.1106753.

[76] K. Andries *et al.*, "Acquired Resistance of Mycobacterium tuberculosis to Bedaquiline," *PLoS ONE*, vol. 9, no. 7, Art. no. 7, Jul. 2014, doi: 10.1371/journal.pone.0102135.

[77] D. Almeida *et al.*, "Mutations in pepQ Confer Low-Level Resistance to Bedaquiline and Clofazimine in Mycobacterium tuberculosis," *Antimicrob Agents Chemother*, vol. 60, no. 8, pp. 4590–4599, Jul. 2016, doi: 10.1128/AAC.00753-16.

[78] K.-P. Choi, T. B. Bair, Y.-M. Bae, and L. Daniels, "Use of Transposon Tn5367 Mutagenesis and a Nitroimidazopyran-Based Selection System To Demonstrate a Requirement for fbiA and fbiB in Coenzyme F420 Biosynthesis by Mycobacterium bovis BCG," *J Bacteriol*, vol. 183, no. 24, pp. 7058–7066, Dec. 2001, doi: 10.1128/JB.183.24.7058-7066.2001.

[79] S. Feuerriegel *et al.*, "Impact of Fgd1 and ddn diversity in Mycobacterium tuberculosis complex on in vitro susceptibility to PA-824," *Antimicrob Agents Chemother*, vol. 55, no. 12, pp. 5718–5722, Dec. 2011, doi: 10.1128/AAC.05500-11.

[80] K. Viney *et al.*, "New definitions of pre-extensively and extensively drug-resistant tuberculosis: update from the World Health Organization," *European Respiratory Journal*, vol. 57, no. 4, Apr. 2021, doi: 10.1183/13993003.00361-2021.

[81] G. Sun *et al.*, “Dynamic Population Changes in Mycobacterium tuberculosis During Acquisition and Fixation of Drug Resistance in Patients,” *The Journal of Infectious Diseases*, vol. 206, no. 11, Art. no. 11, Dec. 2012, doi: 10.1093/infdis/jis601.

[82] V. Eldholm *et al.*, “Evolution of extensively drug-resistant Mycobacterium tuberculosisfrom a susceptible ancestor in a single patient,” *Genome Biology*, vol. 15, no. 11, Art. no. 11, Nov. 2014, doi: 10.1186/s13059-014-0490-3.

[83] M. Merker *et al.*, “Whole Genome Sequencing Reveals Complex Evolution Patterns of Multidrug-Resistant Mycobacterium tuberculosis Beijing Strains in Patients,” *PLoS ONE*, vol. 8, no. 12, Art. no. 12, Dec. 2013, doi: 10.1371/journal.pone.0082551.

[84] Q. Liu *et al.*, “Within patient microevolution of Mycobacterium tuberculosis correlates with heterogeneous responses to treatment,” *Sci Rep*, vol. 5, no. 1, Art. no. 1, Dec. 2015, doi: 10.1038/srep17507.

[85] B. Müller, S. Borrell, G. Rose, and S. Gagneux, “The heterogeneous evolution of multidrug-resistant Mycobacterium tuberculosis,” *Trends in Genetics*, vol. 29, no. 3, Art. no. 3, Mar. 2013, doi: 10.1016/j.tig.2012.11.005.

[86] R. E. Colman *et al.*, “Detection of Low-Level Mixed-Population Drug Resistance in Mycobacterium tuberculosis Using High Fidelity Amplicon Sequencing,” *PLoS ONE*, vol. 10, no. 5, Art. no. 5, May 2015, doi: 10.1371/journal.pone.0126626.

[87] L. Sonnenkalb *et al.*, “Microevolution of Mycobacterium tuberculosis hetero-resistance subpopulations in a patient receiving 27 years of tuberculosis treatment in Germany,” *Antimicrob Agents Chemother*, Jun. 2021, doi: 10.1128/AAC.02520-20.

[88] “WHO | Systematic screening for active tuberculosis: principles and recommendations,” *WHO*. https://www.who.int/tb/tbscreening/en/ (accessed Feb. 08, 2021).

[89] “WHO consolidated guidelines on tuberculosis Module 3: Diagnosis - Rapid diagnostics for tuberculosis detection.” https://www.who.int/publications-detail-redirect/who-consolidated-guidelines-on-tuberculosis-module-3-diagnosis---rapid-diagnostics-for-tuberculosis-detection (accessed Feb. 08, 2021).

[90] “Technical manual for drug susceptibility testing of medicines used in the treatment of tuberculosis.” https://www.who.int/publications-detail-redirect/9789241514842 (accessed Jul. 12, 2021).

[91] CRyPTIC Consortium and the 100,000 Genomes Project *et al.*, "Prediction of Susceptibility to First-Line Tuberculosis Drugs by DNA Sequencing," *N. Engl. J. Med.*, vol. 379, no. 15, Art. no. 15, 11 2018, doi: 10.1056/NEJMoa1800474.

[92] V. Dreyer *et al.*, "Detection of low-frequency resistance-mediating SNPs in next-generation sequencing data of Mycobacterium tuberculosis complex strains with binoSNP," *Scientific Reports*, vol. 10, no. 1, Art. no. 1, May 2020, doi: 10.1038/s41598-020-64708-8.

[93] Z. Zhang, Y. Wang, Y. Pang, and C. Liu, "Comparison of Different Drug Susceptibility Test Methods To Detect Rifampin Heteroresistance in Mycobacterium tuberculosis," *Antimicrobial Agents and Chemotherapy*, vol. 58, no. 9, pp. 5632–5635, Sep. 2014, doi: 10.1128/AAC.02778-14.

[94] A. M. Cabibbe, T. M. Walker, S. Niemann, and D. M. Cirillo, "Whole genome sequencing of Mycobacterium tuberculosis," *European Respiratory Journal*, vol. 52, no. 5, Nov. 2018, doi: 10.1183/13993003.01163-2018.

[95] S. Feuerriegel *et al.*, "PhyResSE: a Web Tool Delineating Mycobacterium tuberculosis Antibiotic Resistance and Lineage from Whole-Genome Sequencing Data," *Journal of Clinical Microbiology*, vol. 53, no. 6, pp. 1908–1914, Jun. 2015, doi: 10.1128/JCM.00025-15.

[96] "WHO | Technical report on critical concentrations for TB drug susceptibility testing of medicines used in the treatment of drug-resistant TB," *WHO*. http://www.who.int/tb/publications/2018/WHO_technical_report_concentrations_TB_drug_susceptibility/en/ (accessed Feb. 09, 2021).

[97] D. Sivakumaran *et al.*, "Combining host-derived biomarkers with patient characteristics improves signature performance in predicting tuberculosis treatment outcomes," *Communications Biology*, vol. 3, no. 1, Art. no. 1, Jul. 2020, doi: 10.1038/s42003-020-1087-x.

[98] J. L. Izquierdo-Garcia *et al.*, "Discovery and validation of an NMR-based metabolomic profile in urine as TB biomarker," *Scientific Reports*, vol. 10, no. 1, Art. no. 1, Dec. 2020, doi: 10.1038/s41598-020-78999-4.

[99] V. Nikolayevskyy *et al.*, "Biomarkers of treatment success in fully sensitive pulmonary tuberculosis patients: a multicenter longitudinal study," *Biomarkers in Medicine*, vol. 14, no. 15, pp. 1439–1452, Oct. 2020, doi: 10.2217/bmm-2020-0246.

[100] "Home," *FIND*. https://www.finddx.org/ (accessed Feb. 09, 2021).

[101] J. Barrios-Payán *et al.*, "Extrapulmonary Locations of Mycobacterium tuberculosis DNA During Latent Infection," *The Journal of Infectious Diseases*, vol. 206, no. 8, pp. 1194–1205, Oct. 2012, doi: 10.1093/infdis/jis381.

[102] M. Pai *et al.*, "Tuberculosis," *Nat Rev Dis Primers*, vol. 2, no. 1, pp. 1–23, Oct. 2016, doi: 10.1038/nrdp.2016.76.

[103] J. Furin, H. Cox, and M. Pai, "Tuberculosis," *The Lancet*, vol. 393, no. 10181, pp. 1642–1656, Apr. 2019, doi: 10.1016/S0140-6736(19)30308-3.

[104] N. van der Wel *et al.*, "M. tuberculosis and M. leprae Translocate from the Phagolysosome to the Cytosol in Myeloid Cells," *Cell*, vol. 129, no. 7, pp. 1287–1298, Jun. 2007, doi: 10.1016/j.cell.2007.05.059.

[105] L. Ramakrishnan, "Revisiting the role of the granuloma in tuberculosis," *Nature Reviews Immunology*, vol. 12, no. 5, Art. no. 5, May 2012, doi: 10.1038/nri3211.

[106] S. Ehlers and U. E. Schaible, "The Granuloma in Tuberculosis: Dynamics of a Host–Pathogen Collusion," *Front. Immunol.*, vol. 3, 2013, doi: 10.3389/fimmu.2012.00411.

[107] G. González-Avila *et al.*, "Mycobacterium tuberculosis Effects on Fibroblast Collagen Metabolism," *RES*, vol. 77, no. 2, pp. 195–202, 2009, doi: 10.1159/000163064.

[108] J. Roman, Y.-J. Jeon, A. Gal, and R. L. Perez, "Distribution of Extracellular Matrices, Matrix Receptors, and Transforming Growth Factor-β1 in Human and Experimental Lung Granulomatous Inflammation," *The American Journal of the Medical Sciences*, vol. 309, no. 3, pp. 124–133, Mar. 1995, doi: 10.1097/00000441-199503000-00002.

[109] A. J. Lenaerts *et al.*, "Location of Persisting Mycobacteria in a Guinea Pig Model of Tuberculosis Revealed by R207910," *Antimicrobial Agents and Chemotherapy*, vol. 51, no. 9, pp. 3338–3345, Sep. 2007, doi: 10.1128/AAC.00276-07.

[110] S. Ehlers and U. E. Schaible, "The Granuloma in Tuberculosis: Dynamics of a Host–Pathogen Collusion," *Front. Immunol.*, vol. 3, 2013, doi: 10.3389/fimmu.2012.00411.

[111] J. M. Cicchese, V. Dartois, D. E. Kirschner, and J. J. Linderman, "Both Pharmacokinetic Variability and Granuloma Heterogeneity Impact the Ability of the First-Line Antibiotics to Sterilize Tuberculosis Granulomas," *Front. Pharmacol.*, vol. 11, 2020, doi: 10.3389/fphar.2020.00333.

[112] B. Prideaux *et al.*, "The association between sterilizing activity and drug distribution into tuberculosis lesions," *Nat Med*, vol. 21, no. 10, pp. 1223–1227, Oct. 2015, doi: 10.1038/nm.3937.

[113] R. R. Kempker *et al.*, "Lung Tissue Concentrations of Pyrazinamide among Patients with Drug-Resistant Pulmonary Tuberculosis," *Antimicrob Agents Chemother*, vol. 61, no. 6, Jun. 2017, doi: 10.1128/AAC.00226-17.

[114] J. P. Sarathy *et al.*, "Prediction of Drug Penetration in Tuberculosis Lesions," *ACS Infect Dis*, vol. 2, no. 8, pp. 552–563, Aug. 2016, doi: 10.1021/acsinfecdis.6b00051.

[115] M. E. Urbanowski, A. A. Ordonez, C. A. Ruiz-Bedoya, S. K. Jain, and W. R. Bishai, "Cavitary tuberculosis: the gateway of disease transmission," *The Lancet Infectious Diseases*, vol. 20, no. 6, pp. e117–e128, Jun. 2020, doi: 10.1016/S1473-3099(20)30148-1.

[116] K. Dheda *et al.*, "Drug-Penetration Gradients Associated with Acquired Drug Resistance in Patients with Tuberculosis," *Am J Respir Crit Care Med*, vol. 198, no. 9, pp. 1208–1219, Jun. 2018, doi: 10.1164/rccm.201711-2333OC.

[117] D. Rifat *et al.*, "Pharmacokinetics of rifapentine and rifampin in a rabbit model of tuberculosis and correlation with clinical trial data," *Sci Transl Med*, vol. 10, no. 435, p. eaai7786, Apr. 2018, doi: 10.1126/scitranslmed.aai7786.

[118] M. Zimmerman *et al.*, "Ethambutol Partitioning in Tuberculous Pulmonary Lesions Explains Its Clinical Efficacy," *Antimicrobial Agents and Chemotherapy*, vol. 61, no. 9, pp. e00924-17, doi: 10.1128/AAC.00924-17.

[119] C. D. Hamilton *et al.*, "The value of end-of-treatment chest radiograph in predicting pulmonary tuberculosis relapse," *Int J Tuberc Lung Dis*, vol. 12, no. 9, pp. 1059–1064, Sep. 2008., doi: not applicable.

[120] V. Dartois, "Tuberculosis: the impact of lesion diversity on drug penetration and sterilization," European Society of Mycobacteriology Congress, Jun. 26, 2017, doi: not applicable.

[121] A. Fleming, "Penicillin - Nobel Lecture," *The Nobel Prize*, Dec. 11, 1945. https://www.nobelprize.org/prizes/medicine/1945/fleming/lecture/ (accessed Jan. 11, 2021).

[122] J. E. Davies, "Origins, acquisition and dissemination of antibiotic resistance determinants," *Ciba Found Symp*, vol. 207, pp. 15–27; discussion 27-35, 1997, PMID: 9189632.

[123] M. McGrath, N. C. Gey van Pittius, P. D. van Helden, R. M. Warren, and D. F. Warner, “Mutation rate and the emergence of drug resistance in Mycobacterium tuberculosis,” *Journal of Antimicrobial Chemotherapy*, vol. 69, no. 2, pp. 292–302, Feb. 2014, doi: 10.1093/jac/dkt364.

[124] P. L. Foster, “Stress-Induced Mutagenesis in Bacteria,” *Crit Rev Biochem Mol Biol*, vol. 42, no. 5, pp. 373–397, 2007, doi: 10.1080/10409230701648494.

[125] R. Sergeev, C. Colijn, M. Murray, and T. Cohen, “Modeling the Dynamic Relationship Between HIV and the Risk of Drug-Resistant Tuberculosis,” *Science Translational Medicine*, vol. 4, no. 135, pp. 135ra67-135ra67, May 2012, doi: 10.1126/scitranslmed.3003815.

[126] S. M. Rosenberg, C. Shee, R. L. Frisch, and P. J. Hastings, “Stress-induced mutation via DNA breaks in Escherichia coli: a molecular mechanism with implications for evolution and medicine,” *Bioessays*, vol. 34, no. 10, pp. 885–892, Oct. 2012, doi: 10.1002/bies.201200050.

[127] S. E. Luria and M. Delbrück, “Mutations of Bacteria from Virus Sensitivity to Virus Resistance,” *Genetics*, vol. 28, no. 6, pp. 491–511, Nov. 1943.

[128] W. A. Rosche and P. L. Foster, “Determining Mutation Rates in Bacterial Populations,” *Methods*, vol. 20, no. 1, pp. 4–17, Jan. 2000, doi: 10.1006/meth.1999.0901.

[129] Q. Zheng, “Toward a Unique Definition of the Mutation Rate,” *Bull Math Biol*, vol. 79, no. 4, pp. 683–692, Apr. 2017, doi: 10.1007/s11538-017-0247-8.

[130] A. Gutierrez *et al.*, “β-Lactam antibiotics promote bacterial mutagenesis via an RpoS-mediated reduction in replication fidelity,” *Nat Commun*, vol. 4, p. 1610, 2013, doi: 10.1038/ncomms2607.

[131] J. A. Imlay and S. Linn, “Mutagenesis and stress responses induced in Escherichia coli by hydrogen peroxide.,” *J Bacteriol*, vol. 169, no. 7, pp. 2967–2976, Jul. 1987, doi: 10.1128/jb.169.7.2967-2976.1987.

[132] D. I. Andersson and D. Hughes, “Evolution of antibiotic resistance at non-lethal drug concentrations,” *Drug Resistance Updates*, vol. 15, no. 3, Art. no. 3, Jun. 2012, doi: 10.1016/j.drup.2012.03.005.

[133] E. Gullberg *et al.*, “Selection of Resistant Bacteria at Very Low Antibiotic Concentrations,” *PLoS Pathogens*, vol. 7, no. 7, Art. no. 7, Jul. 2011, doi: 10.1371/journal.ppat.1002158.

[134] A. Liu *et al.*, “Selective Advantage of Resistant Strains at Trace Levels of Antibiotics: a Simple and Ultrasensitive Color Test for Detection of Antibiotics and Genotoxic Agents,” *Antimicrob. Agents Chemother.*, vol. 55, no. 3, pp. 1204–1210, Mar. 2011, doi: 10.1128/AAC.01182-10.

[135] E. Huitric, J. Werngren, P. Juréen, and S. Hoffner, “Resistance Levels and rpoB Gene Mutations among In Vitro-Selected Rifampin-Resistant Mycobacterium tuberculosis Mutants,” *Antimicrob Agents Chemother*, vol. 50, no. 8, pp. 2860–2862, Aug. 2006, doi: 10.1128/AAC.00303-06.

[136] N. Ismail, S. V. Omar, N. A. Ismail, and R. P. H. Peters, “In vitro approaches for generation of Mycobacterium tuberculosis mutants resistant to bedaquiline, clofazimine or linezolid and identification of associated genetic variants,” *J Microbiol Methods*, vol. 153, pp. 1–9, Oct. 2018, doi: 10.1016/j.mimet.2018.08.011.

[137] I. L. Bergval, A. R. J. Schuitema, P. R. Klatser, and R. M. Anthony, “Resistant mutants of Mycobacterium tuberculosis selected in vitro do not reflect the in vivo mechanism of isoniazid resistance,” *J Antimicrob Chemother*, vol. 64, no. 3, pp. 515–523, Sep. 2009, doi: 10.1093/jac/dkp237.

[138] E. A. Shitikov *et al.*, “Unusual Large-Scale Chromosomal Rearrangements in Mycobacterium tuberculosis Beijing B0/W148 Cluster Isolates,” *PLoS One*, vol. 9, no. 1, Jan. 2014, doi: 10.1371/journal.pone.0084971.

[139] S. H. Saw, J. L. Tan, X. Y. Chan, K. G. Chan, and Y. F. Ngeow, “Chromosomal rearrangements and protein globularity changes in Mycobacterium tuberculosis isolates from cerebrospinal fluid,” *PeerJ*, vol. 4, Sep. 2016, doi: 10.7717/peerj.2484.

[140] L. Sonnenkalb *et al.*, “Deciphering Bedaquiline and Clofazimine Resistance in Tuberculosis: An Evolutionary Medicine Approach,” *bioRxiv*, p. 2021.03.19.436148, Mar. 2021, doi: 10.1101/2021.03.19.436148.

[141] R. Medzhitov and S. Stearns, *Evolutionary Medicine*, 1st ed. Sinauer Associates, 2015.

[142] T. M. Walker *et al.*, “Whole-genome sequencing for prediction of Mycobacterium tuberculosis drug susceptibility and resistance: a retrospective cohort study,” *The Lancet Infectious Diseases*, vol. 15, no. 10, Art. no. 10, Oct. 2015, doi: 10.1016/S1473-3099(15)00062-6.

[143] P. Miotto *et al.*, “A standardised method for interpreting the association between mutations and phenotypic drug resistance in Mycobacterium tuberculosis,” *European Respiratory Journal*, vol. 50, no. 6, Dec. 2017, doi: 10.1183/13993003.01354-2017.

[144] P. W. Fowler *et al.*, "Automated detection of bacterial growth on 96-well plates for high-throughput drug susceptibility testing of Mycobacterium tuberculosis," *Microbiology*, vol. 164, no. 12, Art. no. 12, Dec. 2018, doi: 10.1099/mic.0.000733.

[145] "Minos: variant adjudication and joint genotyping of cohorts of bacterial genomes | bioRxiv." https://www.biorxiv.org/content/10.1101/2021.09.15.460475v2 (accessed Nov. 23, 2021).

[146] T. A. Kohl *et al.*, "MTBseq: a comprehensive pipeline for whole genome sequence analysis of Mycobacterium tuberculosis complex isolates," *PeerJ*, vol. 6, p. e5895, Nov. 2018, doi: 10.7717/peerj.5895.

[147] P. M. V. Rancoita *et al.*, "Validating a 14-Drug Microtiter Plate Containing Bedaquiline and Delamanid for Large-Scale Research Susceptibility Testing of Mycobacterium tuberculosis," *Antimicrob Agents Chemother*, vol. 62, no. 9, Art. no. 9, Jun. 2018, doi: 10.1128/AAC.00344-18.

[148] T. A. Kohl *et al.*, "Whole-genome-based Mycobacterium tuberculosis surveillance: A standardized, portable, and expandable approach," *Journal of Clinical Microbiology*, vol. 52, no. 7, pp. 2479–2486, 2014, doi: 10.1128/JCM.00567-14.

[149] M. Merker *et al.*, "Phylogenetically informative mutations in genes implicated in antibiotic resistance in Mycobacterium tuberculosis complex," *Genome Med*, vol. 12, no. 1, Art. no. 1, Dec. 2020, doi: 10.1186/s13073-020-00726-5.

[150] N. D. Hicks *et al.*, "Clinically prevalent mutations in Mycobacterium tuberculosis alter propionate metabolism and mediate multidrug tolerance," *Nat Microbiol*, vol. 3, no. 9, Art. no. 9, Sep. 2018, doi: 10.1038/s41564-018-0218-3.

[151] N. D. Hicks, A. F. Carey, J. Yang, Y. Zhao, and S. M. Fortunea, "Bacterial genome-wide association identifies novel factors that contribute to ethionamide and prothionamide susceptibility in mycobacterium tuberculosis," *mBio*, vol. 10, no. 2, 2019, doi: 10.1128/mBio.00616-19.

[152] V. Dartois, "The path of anti-tuberculosis drugs: from blood to lesions to mycobacterial cells," *Nat Rev Micro*, vol. 12, no. 3, Art. no. 3, März 2014, doi: 10.1038/nrmicro3200.

[153] N. Strydom *et al.*, "Tuberculosis drugs' distribution and emergence of resistance in patient's lung lesions: A mechanistic model and tool for regimen and dose optimization," *PLOS Medicine*, vol. 16, no. 4, p. e1002773, Apr. 2019, doi: 10.1371/journal.pmed.1002773.

[154] D. Rifat *et al.*, "Pharmacokinetics of rifapentine and rifampin in a rabbit model of tuberculosis and correlation with clinical trial data," *Sci Transl Med*, vol. 10, no. 435, Art. no. 435, Apr. 2018, doi: 10.1126/scitranslmed.aai7786.

[155] M. Zimmerman *et al.*, "Ethambutol Partitioning in Tuberculous Pulmonary Lesions Explains Its Clinical Efficacy," *Antimicrobial Agents and Chemotherapy*, vol. 61, no. 9, Art. no. 9, Jul. 2021, doi: 10.1128/AAC.00924-17.

[156] F. Maruri *et al.*, "A systematic review of gyrase mutations associated with fluoroquinolone-resistant Mycobacterium tuberculosis and a proposed gyrase numbering system," *Journal of Antimicrobial Chemotherapy*, vol. 67, no. 4, pp. 819–831, Apr. 2012, doi: 10.1093/jac/dkr566.

[157] S. Malik, M. Willby, D. Sikes, O. V. Tsodikov, and J. E. Posey, "New insights into fluoroquinolone resistance in Mycobacterium tuberculosis: functional genetic analysis of gyrA and gyrB mutations," *PLoS One*, vol. 7, no. 6, p. e39754, 2012, doi: 10.1371/journal.pone.0039754.

[158] S. Battaglia *et al.*, "Characterization of genomic variants associated with resistance to bedaquiline and delamanid in naïve Mycobacterium tuberculosis clinical strains," Microbiology, preprint, May 2020. doi: 10.1101/2020.05.27.120451.

[159] C. Villellas *et al.*, "Unexpected high prevalence of resistance-associated Rv0678 variants in MDR-TB patients without documented prior use of clofazimine or bedaquiline," *J. Antimicrob. Chemother.*, p. dkw502, Dec. 2016, doi: 10.1093/jac/dkw502.

[160] S. Andres *et al.*, "Bedaquiline-Resistant Tuberculosis: Dark Clouds on the Horizon," *Am J Respir Crit Care Med*, vol. 201, no. 12, Art. no. 12, Jun. 2020, doi: 10.1164/rccm.201909-1819LE.

[161] C. Nimmo *et al.*, "Population-level emergence of bedaquiline and clofazimine resistance-associated variants among patients with drug-resistant tuberculosis in southern Africa: a phenotypic and phylogenetic analysis," *The Lancet Microbe*, vol. 1, no. 4, pp. e165–e174, Aug. 2020, doi: 10.1016/S2666-5247(20)30031-8.

[162] N. Veziris *et al.*, "Rapid emergence of Mycobacterium tuberculosis bedaquiline resistance: lessons to avoid repeating past errors," *Eur Respir J*, vol. 49, no. 3, Art. no. 3, Mar. 2017, doi: 10.1183/13993003.01719-2016.

[163] A. Ghodousi *et al.*, "Acquisition of Cross-Resistance to Bedaquiline and Clofazimine following Treatment for Tuberculosis in Pakistan," *Antimicrob Agents Chemother*, vol. 63, no. 9, Art. no. 9, Jul. 2019, doi: 10.1128/AAC.00915-19.

[164] I. Comas *et al.*, "Whole-genome sequencing of rifampicin-resistant Mycobacterium tuberculosis strains identifies compensatory mutations in RNA polymerase genes," *Nat Genet*, vol. 44, no. 1, pp. 106–110, Jan. 2012, doi: 10.1038/ng.1038.

[165] S. Gagneux, "Fitness cost of drug resistance inMycobacterium tuberculosis," *Clinical Microbiology and Infection*, vol. 15, pp. 66–68, Jan. 2009, doi: 10.1111/j.1469-0691.2008.02685.x.

[166] S. N. Goossens, S. L. Sampson, and A. Van Rie, "Mechanisms of Drug-Induced Tolerance in Mycobacterium tuberculosis," *Clinical Microbiology Reviews*, vol. 34, no. 1, pp. e00141-20, doi: 10.1128/CMR.00141-20.

[167] I. Comas *et al.*, "Out-of-Africa migration and Neolithic co-expansion of Mycobacterium tuberculosis with modern humans," *Nat Genet*, vol. 45, no. 10, pp. 1176–1182, Oct. 2013, doi: 10.1038/ng.2744.

[168] "WHO | Global tuberculosis report 2019," World Health Organization, Oct. 2019. Accessed: Sep. 09, 2020. [Online]. Available: http://www.who.int/tb/publications/global_report/en/

[169] G. V. Bloemberg *et al.*, "Acquired Resistance to Bedaquiline and Delamanid in Therapy for Tuberculosis," *N Engl J Med*, vol. 373, no. 20, Art. no. 20, Nov. 2015, doi: 10.1056/NEJMc1505196.

[170] V. Eldholm *et al.*, "Evolution of extensively drug-resistant Mycobacterium tuberculosisfrom a susceptible ancestor in a single patient," *Genome Biol*, vol. 15, no. 11, Art. no. 11, Nov. 2014, doi: 10.1186/s13059-014-0490-3.

[171] "WHO | Guidelines for treatment of drug-susceptible tuberculosis and patient care (2017 update)," *WHO*. http://www.who.int/tb/publications/2017/dstb_guidance_2017/en/ (accessed Feb. 08, 2021).

[172] "WHO Consolidated Guidelines on Tuberculosis, Module 4: Treatment - Drug-Resistant Tuberculosis Treatment." https://www.who.int/publications-detail-redirect/9789240007048 (accessed Jan. 11, 2021).

[173] E. M. Meumann *et al.*, "Genome sequence comparisons of serial multi-drug-resistant Mycobacterium tuberculosis isolates over 21 years of infection in a single patient," *Microb Genom*, vol. 1, no. 5, p. e000037, Nov. 2015, doi: 10.1099/mgen.0.000037.

[174] N. Ahmad *et al.*, "Treatment correlates of successful outcomes in pulmonary multidrug-resistant tuberculosis: an individual patient data meta-analysis," *Lancet*, vol. 392, no. 10150, pp. 821–834, Sep. 2018, doi: 10.1016/S0140-6736(18)31644-1.

[175] Y. Xu, J. Wu, S. Liao, and Z. Sun, "Treating tuberculosis with high doses of anti-TB drugs: mechanisms and outcomes," *Ann Clin Microbiol Antimicrob*, vol. 16, p. 67, Oct. 2017, doi: 10.1186/s12941-017-0239-4.

[176] T. A. Kohl *et al.*, "Whole-Genome-Based Mycobacterium tuberculosis Surveillance: a Standardized, Portable, and Expandable Approach," *Journal of Clinical Microbiology*, vol. 52, no. 7, Art. no. 7, Jul. 2014, doi: 10.1128/JCM.00567-14.

[177] N. M. Zetola *et al.*, "Clinical outcomes among persons with pulmonary tuberculosis caused by Mycobacterium tuberculosis isolates with phenotypic heterogeneity in results of drug-susceptibility tests," *J Infect Dis*, vol. 209, no. 11, pp. 1754–1763, Jun. 2014, doi: 10.1093/infdis/jiu040.

[178] N. A. Ismail *et al.*, "Defining Bedaquiline Susceptibility, Resistance, Cross-Resistance and Associated Genetic Determinants: A Retrospective Cohort Study," *EBioMedicine*, vol. 28, pp. 136–142, Feb. 2018, doi: 10.1016/j.ebiom.2018.01.005.

[179] P. Beckert *et al.*, "MDR M. tuberculosis outbreak clone in Eswatini missed by Xpert has elevated bedaquiline resistance dated to the pre-treatment era," *Genome Medicine*, vol. 12, no. 1, p. 104, Nov. 2020, doi: 10.1186/s13073-020-00793-8.

[180] M. Moreno-Molina *et al.*, "Genomic analyses of Mycobacterium tuberculosis from human lung resections reveal a high frequency of polyclonal infections," *Nat Commun*, vol. 12, no. 1, Art. no. 1, May 2021, doi: 10.1038/s41467-021-22705-z.

[181] S. Tarashi, A. Fateh, M. Mirsaeidi, S. D. Siadat, and F. Vaziri, "Mixed infections in tuberculosis: The missing part in a puzzle," *Tuberculosis (Edinb)*, vol. 107, pp. 168–174, Dec. 2017, doi: 10.1016/j.tube.2017.09.004.

[182] R. A. D. Castro *et al.*, "The Genetic Background Modulates the Evolution of Fluoroquinolone-Resistance in Mycobacterium tuberculosis," *Molecular Biology and Evolution*, vol. 37, no. 1, Art. no. 1, Jan. 2020, doi: 10.1093/molbev/msz214.

[183] A. Jouet *et al.*, "Deep amplicon sequencing for culture-free prediction of susceptibility or resistance to 13 anti-tuberculous drugs," *European Respiratory Journal*, Jan. 2020, doi: 10.1183/13993003.02338-2020.

[184] A. M. Cabibbe *et al.*, "Application of Targeted Next-Generation Sequencing Assay on a Portable Sequencing Platform for Culture-Free Detection of Drug-Resistant Tuberculosis from Clinical Samples," *Journal of Clinical Microbiology*, vol. 58, no. 10, Sep. 2020, doi: 10.1128/JCM.00632-20.

[185] D. I. Andersson and B. R. Levin, "The biological cost of antibiotic resistance," *Curr Opin Microbiol*, vol. 2, no. 5, pp. 489–493, Oct. 1999, doi: 10.1016/s1369-5274(99)00005-3.

[186] J. Björkman, I. Nagaev, O. G. Berg, D. Hughes, and D. I. Andersson, "Effects of environment on compensatory mutations to ameliorate costs of antibiotic resistance," *Science*, vol. 287, no. 5457, pp. 1479–1482, Feb. 2000, doi: 10.1126/science.287.5457.1479.

[187] T. Song *et al.*, "Fitness costs of rifampicin resistance in Mycobacterium tuberculosis are amplified under conditions of nutrient starvation and compensated by mutation in the β′ subunit of RNA polymerase," *Molecular Microbiology*, vol. 91, no. 6, pp. 1106–1119, 2014, doi: 10.1111/mmi.12520.

[188] M. Merker *et al.*, "Compensatory evolution drives multidrug-resistant tuberculosis in Central Asia," *eLife*, vol. 7, p. e38200, Oct. 2018, doi: 10.7554/eLife.38200.

[189] M. de Vos *et al.*, "Putative Compensatory Mutations in the rpoC Gene of Rifampin-Resistant Mycobacterium tuberculosis Are Associated with Ongoing Transmission," *Antimicrob Agents Chemother*, vol. 57, no. 2, pp. 827–832, Feb. 2013, doi: 10.1128/AAC.01541-12.

[190] S. Wang *et al.*, "Characteristics of compensatory mutations in the rpoC gene and their association with compensated transmission of Mycobacterium tuberculosis," *Front. Med.*, vol. 14, no. 1, pp. 51–59, Feb. 2020, doi: 10.1007/s11684-019-0720-x.

[191] J.-H. Lee *et al.*, "Isoniazid resistance without a loss of fitness in Mycobacterium tuberculosis," *Nat Commun*, vol. 3, no. 1, p. 753, Mar. 2012, doi: 10.1038/ncomms1724.

[192] D. R. Sherman *et al.*, "Compensatory ahpC Gene Expression in Isoniazid-Resistant Mycobacterium tuberculosis," *Science*, vol. 272, no. 5268, pp. 1641–1643, Jun. 1996, doi: 10.1126/science.272.5268.1641.

[193] F. Coll *et al.*, “Genome-wide analysis of multi- and extensively drug-resistant Mycobacterium tuberculosis,” *Nat Genet*, vol. 50, no. 2, pp. 307–316, Feb. 2018, doi: 10.1038/s41588-017-0029-0.

[194] N. D. Hicks, A. F. Carey, J. Yang, Y. Zhao, and S. M. Fortune, “Bacterial Genome-Wide Association Identifies Novel Factors That Contribute to Ethionamide and Prothionamide Susceptibility in Mycobacterium tuberculosis,” *mBio*, vol. 10, no. 2, pp. e00616-19, /mbio/10/2/mBio.00616-19.atom, Apr. 2019, doi: 10.1128/mBio.00616-19.

[195] N. Q. Balaban *et al.*, “Definitions and guidelines for research on antibiotic persistence,” *Nat Rev Microbiol*, vol. 17, no. 7, pp. 441–448, 2019, doi: 10.1038/s41579-019-0196-3.

[196] M. C. Kjellsson *et al.*, “Pharmacokinetic Evaluation of the Penetration of Antituberculosis Agents in Rabbit Pulmonary Lesions,” *Antimicrobial Agents and Chemotherapy*, vol. 56, no. 1, Art. no. 1, Jan. 2012, doi: 10.1128/AAC.05208-11.

[197] A. Fearns, D. J. Greenwood, A. Rodgers, H. Jiang, and M. G. Gutierrez, “Correlative light electron ion microscopy reveals in vivo localisation of bedaquiline in Mycobacterium tuberculosis–infected lungs,” *PLOS Biology*, vol. 18, no. 12, p. e3000879, Dec. 2020, doi: 10.1371/journal.pbio.3000879.

[198] D. J. Greenwood *et al.*, “Subcellular antibiotic visualization reveals a dynamic drug reservoir in infected macrophages,” *Science*, vol. 364, no. 6447, pp. 1279–1282, Jun. 2019, doi: 10.1126/science.aat9689.

[199] R. A. D. Castro, S. Borrell, and S. Gagneux, “The within-host evolution of antimicrobial resistance in Mycobacterium tuberculosis,” *FEMS Microbiology Reviews*, vol. 45, no. 4, Jul. 2021, doi: 10.1093/femsre/fuaa071.

[200] G. P. Morlock, B. B. Plikaytis, and J. T. Crawford, “Characterization of Spontaneous, In Vitro-Selected, Rifampin-Resistant Mutants of Mycobacterium tuberculosisStrain H37Rv,” *Antimicrobial Agents and Chemotherapy*, vol. 44, no. 12, pp. 3298–3301, Dec. 2000, doi: 10.1128/AAC.44.12.3298-3301.2000.

[201] E. Huitric, P. Verhasselt, A. Koul, K. Andries, S. Hoffner, and D. I. Andersson, “Rates and mechanisms of resistance development in Mycobacterium tuberculosis to a novel diarylquinoline ATP synthase inhibitor,” *Antimicrob Agents Chemother*, vol. 54, no. 3, pp. 1022–1028, Mar. 2010, doi: 10.1128/AAC.01611-09.

[202] N. A. Ismail *et al.*, “Defining Bedaquiline Susceptibility, Resistance, Cross-Resistance and Associated Genetic Determinants: A Retrospective Cohort Study,” *EBioMedicine*, vol. 28, pp. 136–142, Feb. 2018, doi: 10.1016/j.ebiom.2018.01.005.

[203] S. K. Heysell *et al.*, “Plasma Drug Activity Assay for Treatment Optimization in Tuberculosis Patients ▿,” *Antimicrob Agents Chemother*, vol. 55, no. 12, pp. 5819–5825, Dec. 2011, doi: 10.1128/AAC.05561-11.

[204] J. B. Prahl, I. S. Johansen, A. S. Cohen, N. Frimodt-Møller, and Å. B. Andersen, “Clinical significance of 2 h plasma concentrations of first-line anti-tuberculosis drugs: a prospective observational study,” *Journal of Antimicrobial Chemotherapy*, vol. 69, no. 10, pp. 2841–2847, Oct. 2014, doi: 10.1093/jac/dku210.

[205] A. S. Ginsburg *et al.*, “Fluoroquinolone resistance in patients with newly diagnosed tuberculosis,” *Clin Infect Dis*, vol. 37, no. 11, pp. 1448–1452, Dec. 2003, doi: 10.1086/379328.

[206] E. Avalos *et al.*, “Frequency and geographic distribution of gyrA and gyrB mutations associated with fluoroquinolone resistance in clinical Mycobacterium tuberculosis isolates: a systematic review,” *PLoS One*, vol. 10, no. 3, p. e0120470, 2015, doi: 10.1371/journal.pone.0120470.

[207] J.-Y. Chien, W.-Y. Chiu, S.-T. Chien, C.-J. Chiang, C.-J. Yu, and P.-R. Hsueh, “Mutations in gyrA and gyrB among Fluoroquinolone- and Multidrug-Resistant Mycobacterium tuberculosis Isolates,” *Antimicrob Agents Chemother*, vol. 60, no. 4, pp. 2090–2096, Apr. 2016, doi: 10.1128/AAC.01049-15.

[208] A. Pantel *et al.*, “Extending the Definition of the GyrB Quinolone Resistance-Determining Region in Mycobacterium tuberculosis DNA Gyrase for Assessing Fluoroquinolone Resistance in M. tuberculosis,” *Antimicrobial Agents and Chemotherapy*, vol. 56, no. 4, pp. 1990–1996, Apr. 2012, doi: 10.1128/AAC.06272-11.

[209] S. Zhang *et al.*, “Mycobacterium tuberculosis Mutations Associated with Reduced Susceptibility to Linezolid,” *Antimicrob. Agents Chemother.*, vol. 60, no. 4, Art. no. 4, Apr. 2016, doi: 10.1128/AAC.02941-15.

[210] Y. Liu *et al.*, “Acquisition of clofazimine resistance following bedaquiline treatment for multidrug-resistant tuberculosis,” *International Journal of Infectious Diseases*, vol. 102, pp. 392–396, Jan. 2021, doi: 10.1016/j.ijid.2020.10.081.

[211] D. V. Zimenkov *et al.*, “Examination of bedaquiline- and linezolid-resistant Mycobacterium tuberculosis isolates from the Moscow region,” *Journal of Antimicrobial Chemotherapy*, vol. 72, no. 7, Art. no. 7, Jul. 2017, doi: 10.1093/jac/dkx094.

[212] N. Ismail, R. P. H. Peters, N. A. Ismail, and S. V. Omar, “Clofazimine Exposure In Vitro Selects Efflux Pump Mutants and Bedaquiline Resistance,” *Antimicrob Agents Chemother*, vol. 63, no. 3, Feb. 2019, doi: 10.1128/AAC.02141-18.

[213] S. Kadura *et al.*, “Systematic review of mutations associated with resistance to the new and repurposed Mycobacterium tuberculosis drugs bedaquiline, clofazimine, linezolid, delamanid and pretomanid,” *Journal of Antimicrobial Chemotherapy*, vol. 75, no. 8, pp. 2031–2043, Aug. 2020, doi: 10.1093/jac/dkaa136.

[214] J. Xu *et al.*, “Verapamil Increases the Bioavailability and Efficacy of Bedaquiline but Not Clofazimine in a Murine Model of Tuberculosis,” *Antimicrobial Agents and Chemotherapy*, vol. 62, no. 1, pp. e01692-17, doi: 10.1128/AAC.01692-17.

[215] G. Wang *et al.*, “Prevalence and molecular characterizations of seven additional drug resistance among multidrug-resistant tuberculosis in China: A subsequent study of a national survey,” *J Infect*, vol. 82, no. 3, pp. 371–377, Mar. 2021, doi: 10.1016/j.jinf.2021.02.004.

[216] N. Ismail, N. A. Ismail, S. V. Omar, and R. P. H. Peters, “In Vitro Study of Stepwise Acquisition of rv0678 and atpE Mutations Conferring Bedaquiline Resistance,” *Antimicrobial Agents and Chemotherapy*, vol. 63, no. 8, pp. e00292-19, doi: 10.1128/AAC.00292-19.

[217] G. Degiacomi, J. C. Sammartino, V. Sinigiani, P. Marra, A. Urbani, and M. R. Pasca, “In vitro Study of Bedaquiline Resistance in Mycobacterium tuberculosis Multi-Drug Resistant Clinical Isolates,” *Front. Microbiol.*, vol. 0, 2020, doi: 10.3389/fmicb.2020.559469.

[218] J. Xu *et al.*, “Primary Clofazimine and Bedaquiline Resistance among Isolates from Patients with Multidrug-Resistant Tuberculosis,” *Antimicrob Agents Chemother*, vol. 61, no. 6, pp. e00239-17, e00239-17, Jun. 2017, doi: 10.1128/AAC.00239-17.

[219] “Catalogue of mutations in Mycobacterium tuberculosis complex and their association with drug resistance.” https://www.who.int/publications-detail-redirect/9789240028173 (accessed Jun. 27, 2021).

[220] R. Vargas *et al.*, "The role of epistasis in amikacin, kanamycin, bedaquiline, and clofazimine resistance in Mycobacterium tuberculosis complex," *bioRxiv*, p. 2021.05.07.443178, May 2021, doi: 10.1101/2021.05.07.443178.

[221] M. R. Farhat *et al.*, "Genetic Determinants of Drug Resistance in Mycobacterium tuberculosis and Their Diagnostic Value," *Am J Respir Crit Care Med*, vol. 194, no. 5, pp. 621–630, Sep. 2016, doi: 10.1164/rccm.201510-2091OC.

[222] C. Nimmo *et al.*, "Bedaquiline resistance in drug-resistant tuberculosis HIV co-infected patients," *Eur Respir J*, vol. 55, no. 6, p. 1902383, Jun. 2020, doi: 10.1183/13993003.02383-2019.

[223] M. de Vos *et al.*, "Bedaquiline Microheteroresistance after Cessation of Tuberculosis Treatment," *N Engl J Med*, vol. 380, no. 22, pp. 2178–2180, May 2019, doi: 10.1056/NEJMc1815121.

[224] S. Polsfuss *et al.*, "Emergence of Low-level Delamanid and Bedaquiline Resistance During Extremely Drug-resistant Tuberculosis Treatment," *Clinical Infectious Diseases*, vol. 69, no. 7, pp. 1229–1231, Sep. 2019, doi: 10.1093/cid/ciz074.

[225] C. U. Köser, F. P. Maurer, and K. Kranzer, "'Those who cannot remember the past are condemned to repeat it': Drug-susceptibility testing for bedaquiline and delamanid," *Int J Infect Dis*, vol. 80S, pp. S32–S35, Mar. 2019, doi: 10.1016/j.ijid.2019.02.027.

[226] Global Alliance for TB Drug Development, "A Phase 3 Partially-blinded, Randomized Trial Assessing the Safety and Efficacy of Various Doses and Treatment Durations of Linezolid Plus Bedaquiline and Pretomanid in Participants With Pulmonary Infection of Either Extensively Drug-resistant Tuberculosis (XDR-TB), Pre-XDR-TB or Treatment Intolerant or Non-responsive Multi-drug Resistant Tuberculosis (MDR-TB)," clinicaltrials.gov, Clinical trial registration NCT03086486, Feb. 2021. Accessed: Nov. 14, 2021. [Online]. Available: https://clinicaltrials.gov/ct2/show/NCT03086486

[227] Global Alliance for TB Drug Development, "An Open-Label, Partially Randomized Trial to Evaluate the Efficacy, Safety and Tolerability of a 4-month Treatment of Bedaquiline Plus Pretomanid Plus Moxifloxacin Plus Pyrazinamide (BPaMZ) Compared to a 6-month Treatment of HRZE/HR (Control) in Adult Participants With Drug-Sensitive Smear-Positive Pulmonary Tuberculosis (DS-TB) and a 6-month Treatment of BPaMZ in Adult Participants With Drug Resistant, Smear-Positive Pulmonary Tuberculosis (DR-TB)," clinicaltrials.gov, Clinical trial registration NCT03338621, Apr. 2021. Accessed: Nov. 14, 2021. [Online]. Available: https://clinicaltrials.gov/ct2/show/NCT03338621

[228] D. Almeida, E. Nuermberger, S. Tyagi, W. R. Bishai, and J. Grosset, “In vivo validation of the mutant selection window hypothesis with moxifloxacin in a murine model of tuberculosis,” *Antimicrob Agents Chemother*, vol. 51, no. 12, pp. 4261–4266, Dec. 2007, doi: 10.1128/AAC.01123-07.

[229] S. Gagneux, “The Competitive Cost of Antibiotic Resistance in Mycobacterium tuberculosis,” *Science*, vol. 312, no. 5782, Art. no. 5782, Jun. 2006, doi: 10.1126/science.1124410.

[230] D. Shcherbakov, R. Akbergenov, T. Matt, P. Sander, D. I. Andersson, and E. C. Böttger, “Directed mutagenesis of Mycobacterium smegmatis 16S rRNA to reconstruct the in vivo evolution of aminoglycoside resistance in Mycobacterium tuberculosis,” *Mol Microbiol*, vol. 77, no. 4, pp. 830–840, Aug. 2010, doi: 10.1111/j.1365-2958.2010.07218.x.

[231] I. Bergval *et al.*, “A proportion of mutations fixed in the genomes of in vitro selected isogenic drug-resistant Mycobacterium tuberculosis mutants can be detected as minority variants in the parent culture,” *FEMS Microbiology Letters*, vol. 362, no. 2, pp. 1–7, Jan. 2015, doi: 10.1093/femsle/fnu037.

[232] P. C. Hsieh, B. C. Shenoy, D. Samols, and N. F. Phillips, “Cloning, expression, and characterization of polyphosphate glucokinase from Mycobacterium tuberculosis,” *J Biol Chem*, vol. 271, no. 9, pp. 4909–4915, Mar. 1996, doi: 10.1074/jbc.271.9.4909.

[233] A. Radhakrishnan *et al.*, “Crystal Structure of the Transcriptional Regulator Rv0678 of Mycobacterium tuberculosis,” *J Biol Chem*, vol. 289, no. 23, pp. 16526–16540, Jun. 2014, doi: 10.1074/jbc.M113.538959.

[234] J. D. van Embden *et al.*, “Strain identification of Mycobacterium tuberculosis by DNA fingerprinting: recommendations for a standardized methodology.,” *J Clin Microbiol*, vol. 31, no. 2, pp. 406–409, Feb. 1993, doi: 10.1128/jcm.31.2.406-409.1993.

[235] D. van Soolingen, P. W. Hermans, P. E. de Haas, D. R. Soll, and J. D. van Embden, “Occurrence and stability of insertion sequences in Mycobacterium tuberculosis complex strains: evaluation of an insertion sequence-dependent DNA polymorphism as a tool in the epidemiology of tuberculosis.,” *Journal of Clinical Microbiology*, vol. 29, no. 11, Art. no. 11, 1991, doi: 10.1128/JCM.29.11.2578-2586.1991.

[236] World Health Organization, “The use of next-generation sequencing technologies for the detection of mutations associated with drug resistance in Mycobacterium tuberculosis complex: technical guide,” World Health Organization, WHO/CDS/TB/2018.19, 2018. Accessed: Sep. 09, 2020. [Online]. Available: https://apps.who.int/iris/handle/10665/274443

[237] X. Zhang, L. Liu, Y. Zhang, G. Dai, H. Huang, and Q. Jin, “Genetic Determinants Involved in p-Aminosalicylic Acid Resistance in Clinical Isolates from Tuberculosis Patients in Northern China from 2006 to 2012,” *Antimicrob. Agents Chemother.*, vol. 59, no. 2, Art. no. 2, Feb. 2015, doi: 10.1128/AAC.03695-14.

[238] P. W. Fowler *et al.*, “Automated detection of bacterial growth on 96-well plates for high-throughput drug susceptibility testing of mycobacterium tuberculosis,” *Microbiology (United Kingdom)*, 2018, doi: 10.1099/mic.0.000733.

[239] K. Kaniga *et al.*, “A Multilaboratory, Multicountry Study To Determine Bedaquiline MIC Quality Control Ranges for Phenotypic Drug Susceptibility Testing,” *J Clin Microbiol*, vol. 54, no. 12, pp. 2956–2962, Dec. 2016, doi: 10.1128/JCM.01123-16.

[240] T. Schön *et al.*, “Wild-type distributions of seven oral second-line drugs against Mycobacterium tuberculosis,” *Int J Tuberc Lung Dis*, vol. 15, no. 4, pp. 502–509, Apr. 2011, doi: 10.5588/ijtld.10.0238.

[241] H. Hoffmann *et al.*, “Delamanid and Bedaquiline Resistance in Mycobacterium tuberculosis Ancestral Beijing Genotype Causing Extensively Drug-Resistant Tuberculosis in a Tibetan Refugee,” *Am J Respir Crit Care Med*, vol. 193, no. 3, pp. 337–340, Feb. 2016, doi: 10.1164/rccm.201502-0372LE.

[242] J. S. Yang, K. J. Kim, H. Choi, and S. H. Lee, “Delamanid, Bedaquiline, and Linezolid Minimum Inhibitory Concentration Distributions and Resistance-related Gene Mutations in Multidrug-resistant and Extensively Drug-resistant Tuberculosis in Korea,” *Ann Lab Med*, vol. 38, no. 6, pp. 563–568, Nov. 2018, doi: 10.3343/alm.2018.38.6.563.

[243] E. Martinez, D. Hennessy, P. Jelfs, T. Crighton, S. C.-A. Chen, and V. Sintchenko, “Mutations associated with in vitro resistance to bedaquiline in Mycobacterium tuberculosis isolates in Australia,” *Tuberculosis (Edinb)*, vol. 111, pp. 31–34, Jul. 2018, doi: 10.1016/j.tube.2018.04.007.

[244] Y. Pang *et al.*, “In Vitro Drug Susceptibility of Bedaquiline, Delamanid, Linezolid, Clofazimine, Moxifloxacin, and Gatifloxacin against Extensively Drug-Resistant Tuberculosis in Beijing, China,” *Antimicrob Agents Chemother*, vol. 61, no. 10, pp. e00900-17, e00900-17, Oct. 2017, doi: 10.1128/AAC.00900-17.

[245] E. Segala, W. Sougakoff, A. Nevejans-Chauffour, V. Jarlier, and S. Petrella, “New mutations in the mycobacterial ATP synthase: new insights into the binding of the diarylquinoline TMC207 to the ATP synthase C-ring structure,” *Antimicrob Agents Chemother*, vol. 56, no. 5, pp. 2326–2334, May 2012, doi: 10.1128/AAC.06154-11.

7. List of Figures

Figure 2.1: Estimated tuberculosis incidence rates per 100,000 in 2020. 8

Figure 2.2: Percentage of rifampicin or multi-drug resistant tuberculosis among newly-reported tuberculosis cases worldwide..... 9

Figure 2.3: Capacity of anti-tuberculosis drugs to accumulate throughout the granuloma and lung cavitation. 16

Figure 2.4 Mutation rate calculations based on mutability of resistance-associated genes. 18

Figure 2.5 The mutant selection window and fitness/resistance level selection. 19

Figure 3.1 Resazurin emission microtiter assay set-up. 36

Figure 4.1.1: Final treatment episode: treatment history, phenotypic drug susceptibility results, and genetic diversity of resistance-associated mutations. 43

Figure 4.1.2: Minimum spanning tree based on a core genome multi locus sequence type analysis of thirteen serial isolates. 45

Figure 4.2.1: Experimental flow chart. 49

Figure 4.2.2: Sub-minimum inhibitory drug exposure of moxifloxacin, bedaquiline, and clofazimine over two culture passages. 50

Figure 4.2.3: Sub-minimum inhibitory concentration evolution model experimental design for resistant variant selection, detection and analysis. 52

Figure 4.2.4: Sub-inhibitory exposure of moxifloxacin affects bacterial growth and mutant enrichment in a dose-dependent manner. 55

Figure 4.2.5: Sub-inhibitory exposure of bedaquiline affects bacterial growth and mutant enrichment in a dose-dependent manner. 57

Figure 4.2.6: Sub-inhibitory exposure of clofazimine affects bacterial growth and mutant enrichment in a dose-dependent manner. 59

Figure 4.2.7: Experimental flow chart: bedaquiline/clofazimine cross-resistance. 60

Figure 4.2.8: Cross-resistance comparison of bedaquiline and clofazimine exposure. 61

Figure 4.2.9: Characterization of mutations throughout *gyrA* and *gyrB* genes. 65

Figure 4.2.10: Mutations detected after *in vitro* experiments, mapped to *atpE*, *Rv0678*, and *pepQ* genes. 72

Figure 4.2.11: Patient-derived resistance-associated variant mapping throughout *Rv0678*, *atpE*, *Rv1979c*, and *pepQ*. 75

Figure 4.2.12: Resistance association by codon position in *Rv0678* gene. 77

Figure 4.3.1: Mutant selection window of moxifloxacin resistant clones. 80

Figure 4.3.2: Mutant selection window of bedaquiline resistant clones. 82

Figure 4.3.3: Allele frequency of moxifloxacin resistance harboring clones. 83

Figure 4.3.4: Competitive relative fitness of bedaquiline resistance harboring clones. 84

Figure 4.3.5: Short-read sequencing alignment of a genotypically susceptible (but phenotypically resistant) clone. 86

Figure 4.3.6: Large-scale gene rearrangement in *Rv0678* gene. 87

Figure C.1: Mutant enrichment after sub-inhibitory drug exposure; mutants per total colony forming units. 155

Figure D.1: Mutant selection window of bedaquiline resistance mutations. 195

8. List of Tables

Table 2.1 Overview of the most important anti-tuberculosis drugs 12

Table 2.2 World Health Organization drug grouping and treatment recommendation for multi-drug resistant tuberculosis regimens 13

Table 3.1: Antibiotic concentrations examined in evolutionary experiments. 34

Table 4.2.1: Summary of variant diversity in *gyrA* and *gyrB* genes of mutant population after moxifloxacin evolutionary experiments. 63

Table 4.2.2: Genotypic and phenotypic characterization of resistant variants isolated after moxifloxacin exposure. 64

Table 4.2.3: Summary of variant diversity in *Rv0678* and *atpE* genes of mutant population after bedaquiline evolutionary experiment. 66

Table 4.2.4: Summary of variant diversity in *Rv0678* and *pepQ* (Rv2535c) genes of mutant population after clofazimine evolutionary experiment..... 68

Table 4.2.5: Genotypic and phenotypic characterization of resistant variants isolated after bedaquiline or clofazimine evolutionary experiments. 69

Table 4.2.6: Mycobacterium growth indicator tube testing of *Rv0678* and *atpE* mutants. 71

Table 4.2.7 Patient cohort dataset summary. 73

Table 4.3.1: Selected mutants with elevated bedaquiline (and clofazimine) minimum inhibitory concentration, with no detectable resistance-associated mutations. 85

Table A.1 Distribution of tuberculosis drugs throughout the granuloma and lung cavitation. 142

Table B.1: Patient treatment history, including phenotypic drug resistance testing, over five TB treatment episodes..... 143

Table B.2: Population frequency of resistance, compensatory, and tolerance associated mutations. 149

Table B.3: Statistical analysis of low-frequency variants. 151

Table C.1 Generation time of H37Rv lab strain. 153

Table C.2: P-values of evolutionary experiments, colony forming units, and mutant enrichment. 156

Table C.3: P-values of cross-resistance comparison between bedaquiline and clofazimine selection of bedaquiline mutants. 157

Table C.4: Next generation sequencing statistics of deep sequencing run with moxifloxacin exposed bacterial populations. 157

Table C.5: Next generation sequencing statistics of deep sequencing run with bedaquiline exposed bacterial populations. 158

Table C.6: Variant diversity in *Rv0678* and *atpE* genes of mutant population after bedaquiline evolutionary experiment. 160

Table C.7: Next generation sequencing statistics of deep sequencing run with clofazimine exposed bacterial populations. 161

Table C.8: Variant diversity in *Rv0678* and *pepQ (Rv2535c)* genes of mutant population after clofazimine evolutionary experiment. 162

Table C.9: Genotypic and phenotypic characterization of resistant variants isolated after bedaquiline or clofazimine evolutionary experiments. 165

Table C.10 Genomic summary of CRyPTIC strains with variants in bedaquiline/clofazimine resistance-associated genes 168

Table C.11 Catalogue of mutations in bedaquiline and clofazimine resistance-associated gene in bacteria of the *Mycobacterium tuberculosis* complex. 175

Table D.1 Off-target mutations co-selected with resistance-associated mutations after *in vitro* evolutionary experiments. 190

Table D.2: P-values of mutant selection window of moxifloxacin resistant mutants. 193

Table D.3: P-values of fitness experiments of MFX resistant mutants. 194

Table D.4: P-values of fitness experiments of BDQ resistant mutants. 194

9. Abbreviations

_	stop codon
a	adenine
AA	amino acid
alt.	alternative
AMC	amoxicillin + clavulanic acid
AMK	amikacin
BCG	bacillus Calmette-Guerin
BDQ	bedaquiline
bp	base pair
c	cytosine
CFU	colony forming unit
CFZ	clofazimine
CLR	clarithromycin
conc.	concentration
CPR	capreomycin
CRyPTIC	Comprehensive Resistance Prediction for Tuberculosis: an International Consortium
CS	cycloserine
CTAB	hexadecyltrimethylammonium bromide
del	deletion
DLM	delamanid
DNA	deoxyribonucleic acid
DOTS	directly observed treatment, short-course
DST	drug susceptibility testing
EMB	ethambutol
et al	"and others"
ETH	ethionamide
FQ	fluoroquinolone
fs	frameshift
g	guanine

GFX	gatifloxacin
gWT	genetically wild-type
i.e.	id est "in other word"
indel	insertion or deletion
INH	isoniazid
ins	insertion
IS6110	insertion sequence 6110
KAN	kanamycin
LFX	levofloxacin
LZD	linezolid
MDR	multidrug resistant
MFX	moxifloxacin
MGIT	mycobacterium growth indicator tube
MIC	minimum inhibitory concentration
MSC	minimum selection concentration
MSW	mutant selection window
Mtbc	*Mycobacterium tuberculosis* complex
NA	not applicable
NGS	next generation sequencing
ns	not significant
NT	nucleotide
OD	optical density
OFX	ofloxacin
OP	out-patient
PAS	para-aminosalicylic Acid
PCR	polymerase-chain reaction
PE/PPE	proline-glutamate/proline-proline-glutamate
PRT	pretomanid
PTH	prothionamide
PZA	pyrazinamide
QRDR	quinolone resistance determining regions
RBT	rifabutin

rcf	relative centrifugal force
ref.	reference
REMA	resazurin emission microtiter assay
RIF	rifampicin
RNA	ribonucleic acid
RR	rifampicin-resistant
rRNA	ribosomal RNA
RT	room temperature
Subs	substitutions
SDS	sodium dodecyl sulphate
SFX	sparfloxacin
SM	streptomycin
SNP	single nucleotide polymorphisms
t	thymine
TB	tuberculosis
TRD	terizidone
WGS	whole genome sequencing
WHO	World Health Organization
XDR	extensively-drug resistant

Appendix A

Introduction supplementary materials and extended data

Table A.1 Distribution of tuberculosis drugs throughout the granuloma and lung cavitation. Drug concentrations below (low), less than (med), or at or above (high) the critical concentration.

Granuloma

Drug	Plasma/ blood	Fibrous cuff	Cellular layer	Caseum	Intra-macrophage
INH	high†[114]	low*[112]	med*[112]	high†[114]	low*[112]
RIF	low†[114]	high*[112]	med*[112], high†[114]	none*[112], low†[114]	low*[112]
EMB	high†[114]				
PZA	high†[114]	med/high*[112]	med*[112], high*[113]	med*[112], high*[113]	none*[112]
PTH/ETH	med†[114]				
PAS	med†[114]				
FQ (MFX)	high†[114]	high*[112]	high*[112]	none*[112]	low*[112]
CFZ	none†[114]	high*[112], high†[114]	med/high*[112], high†[114]	none*[112]	high*[112]
BDQ	none†[114]	low†[114]	high/med†[114]	none†[114]	

Lung Cavitation

Drug	Blood(serum)	NALT	Cavity Wall	Cavity Center	Airway surface
INH	high*[116] +[111]	high*[116]	high*[116]	high*[116]	high*[116]
RIF	High †[154] +[111]	High †[154]	High †[154]	low †[154]	low †[154]
EMB	high*[116] +[111]	high*[116] †[155]	low*[116] †[155]	low*[116] †[155]	med-low*[116] †[155]
PZA	high*[116] +[111]	low*[116], high*[113] +[111]	low*[116], +[111], high*[113]	high*[116] +[111]	high*[116]
PTH/ETH	high*[116]	low*[116]	low*[116]	low*[116]	low*[116]
PAS	high*[116]	low*[116]	low*[116]	low*[116]	low*[116]
FQ (MFX)	high*[116]	high*[116]	high*[116]	low*[116]	low*[116]
CFZ	med-low*[116]	low*[116]	low*[116]	low*[116]	low*[116]

NALT - nasal associated lymphoid tissue, *human, †rabbit model, +computer simulations

Appendix B

Supplementary Material and extended tables of Results 4.1

Table B.1: Patient treatment history, including phenotypic drug resistance testing, over five TB treatment episodes. Phenotypic resistance/susceptibility was reported by several diagnostic labs throughout Germany, including Research Centre Borstel. Once a resistant phenotype was reported regular testing may not have been repeated, thus the phenotypic results at given intervals are not completely comprehensive. Emerging genotypic resistances were predicted for 13 available patient-derived isolates; date of collection indicated by months since the start of therapy "Therapy (month)".

Therapy (month)	Hospital	Treatment Regimen	Clinical notes	Phenotypic Resistance	Phenotypic Susceptibility	Genotypic Resistance	Active drugs in treatment by genotype	Active drugs in treatment by phenotype
1st TB Episode								
1-4	1	INH, PAS, SM†, tyloxapol‡						
No TB symptoms - 17 years								
2nd TB Episode								
1	2	INH, EMB, SM						
2-4	3	INH, RIF, EMB	Culture negative					
No TB symptoms - 1 year								
3rd TB Episode								
1-6	4	INH, RIF, SM	Cavities in left and right upper lobes					
7-41	OP	INH, RIF, SM	No bacilli detected					
No TB symptoms - 8 years								
4th TB Episode								
1	-	PZA, SM, TRD	Bacilli detected and lung cavitation observed					
1-3	5	INH, RIF, EMB, PZA, CPR						

Therapy (month)	Hospital	Treatment Regimen	Clinical notes	Phenotypic Resistance	Phenotypic Susceptibility	Genotypic Resistance	Active drugs in treatment by genotype	Active drugs in treatment by phenotype
4	5	INH, RIF, EMB, PAS	Culture positive	(month 4) INH, EMB, PZA, PTH, SM	(month 4) RIF, PAS			
5-12	6	PZA, SM, TRD	Sputum negative	(month 9) INH, RIF	(month 9) EMB, PZA, PTH, SM, CPR, CS, KAN			
13-15	-	RIF, PZA, SM, TRD	Sputum positive	(month 15) INH, RIF	(month 15) EMB, SM			
16	-	EMB, PZA, SM						
16-20	OP	PZA, SM, TRD						
21-22	OP	RIF, PZA, SM, TRD						
23-35	OP	RIF, PZA, SM, TRD	Culture positive	(month 24/26/35) INH, RIF	(month 24/26/35) EMB, SM			
36-64	-	RIF, PZA, SM, TRD	Culture positive	(month 39) INH, RIF, PTH	(month 39) EMB, PZA, SM			
65-88	OP	RIF, CLR, PTH	Alternating between positive and negative culture and microscopy					
No TB symptoms - ~6 months								
5th TB Episode								
1	7	RBT, PAS, CLR, OFX	Culture positive					
2-10	7, OP	RBT, SM, PAS, CLR, OFX	Culture positive, new infiltration in left and right lungs	INH, RIF, EMB, PZA, SM			1 (CLR*)	1 (CLR*)

Therapy (month)	Hospital	Treatment Regimen	Clinical notes	Phenotypic Resistance	Phenotypic Susceptibility	Genotypic Resistance	Active drugs in treatment by genotype	Active drugs in treatment by phenotype
10-12	7, OP	RBT, SM, PAS, CLR, OFX		INH, RIF/RBT, PZA, SM, PAS, OFX, CFZ, PZA, TRD/CS	(month 10) EMB[b], CPR[b]	(Month 10) Baseline resistance: INH, RIF/RBT, PZA, SM, PAS, PTH, CS/TRD, FQ(OFX)		
13-14	8,9	INH, EMB, PTH, AMK, AMC					3 (EMB/ AMK/ AMC)	4 (EMB, PTH, AMK, AMC)
15-21	OP	INH, EMB, PTH, AMC	AMK discontinued due to hearing loss				2 (AMC*/ EMB)	3 (EMB, PTH, AMC)
22-25	OP,9	INH, EMB, PTH, OFX, AMC	Culture positive	(month 22) INH, RIF, EMB, PZA, OFX, PAS, CFZ, CS, AMC	(month 22) PTH, AMK, CPR, SM[b]		2(AMC*/ EMB)	1 (PTH)
26-34	OP	INH, EMB, OFX					1 (EMB)	0
35-39	OP	EMB, PTH, OFX, AMC					2 (AMC*/ EMB)	1 (PTH)
40-42	10	INH, EMB, PTH, OFX, AMC					2 (AMC*/ EMB)	1 (PTH)
43-44	10	INH, EMB, PZA, PTH, OFX, AMC	Culture positive		(month 43) PZA, PTH, PAS, CPR, CFX (FQ)		2 (AMC*/ EMB)	3 (PZA, PTH, OFX)
45-51	OP	INH, EMB, PTH, OFX, AMC	Culture & microscopy positive	(month 48) INH, RIF, EMB, PZA, SM, CLR, OFX, MFX, LFX, CFZ, PZA, CS/TRD	(month 48) PTH, CPR, AMK	(month 47) baseline + EMB	1 (AMC*)	2 (PTH, AMC)

Therapy (month)	Hospital	Treatment Regimen	Clinical notes	Phenotypic Resistance	Phenotypic Susceptibility	Genotypic Resistance	Active drugs in treatment by genotype	Active drugs in treatment by phenotype
52-80	OP	EMB, PZA, OFX, AMC	Culture & microscopy positive	(month 71/79) INH, RIF, EMB, SM, OFX	(month 71) PTH, CPR, AMK, LZD, PZA[b], CS/TRD[b]	(month 71) baseline + EMB	1 (AMC*)	2 (PZA, AMC)
81	OP	EMB, PZA, OFX, AMC					1 (AMC*)	2 (PZA, AMC)
82-87	9, 11, OP	PZA, CPR, PTH, LZD	Culture positive, microscopy negative				2 (CPR/ LZD)	4
88-91	OP	PZA, LZD	Culture positive		(month 89/91) PTH, CPR, AMK, CS/TRD, LZD, PZA[b]	(month 89) baseline + EMB	1 (LZD)	2
92-93	-	PZA, LZD				(month 92) baseline + EMB	1 (LZD)	2
94	-	PZA, LZD	Culture positive	(month 94) PZA, PTH	(month 94) CPR, AMK, LZD, CS/TRD		1 (LZD)	1 (LZD)
95-101	OP	PZA, CPR, PTH, LZD					2 (CPR/ LZD)	2 (CPR/ LZD)
102	OP	LZD, TRD					1 (LZD)	2
103-104	OP	LZD, TRD	Culture positive	(month 104) PTH	(month 104) PZA, CPR, AMK LZD	(month 104) Baseline + EMB, LZD/CPR/CLR	0	2

Therapy (month)	Hospital	Treatment Regimen	Clinical notes	Phenotypic Resistance	Phenotypic Susceptibility	Genotypic Resistance	Active drugs in treatment by genotype	Active drugs in treatment by phenotype
105-110	OP	LZD, TRD	Culture positive		(month 108) PZA, CPR, AMK, CS/TRD	(Month 108) baseline + EMB, LZD	0	2
111	OP	LZD, TRD					0	2
112-129	7, OP	PZA, CPR, TRD	Culture positive,	(month 112) LZD	(month 112) PZA, CPR, AMK, CS/TRD		1 (CPR)	3
			Patient quit drinking alcohol	(month 122) PTH	(month 114) PZA, CPR, AMK			
					(month 122) CPR, AMK CS/TRD, PZA[b]			
130-132	OP	PZA, CPR, TRD	Culture positive		(month 132) AMK, PZA[b]	(Month 130) baseline + EMB, LZD, CPR	0	
133	7	PZA, PAS, AMK, TRD					1 (AMK)	4
134-139	OP	PZA, PAS, AMK, TRD	Patient quit smoking	(month 134) RIF, PZA, CPR	(month 134) PAS, AMK, CS/TRD	(Month 135) baseline + EMB, LZD, CPR	1 (AMK)	3 (PAS, AMK, TRD)
140	-	PZA, PAS, AMK, TRD	Culture positive	(month 140) PZA, AMK	(month 140) PTH, PAS, CS		1 (AMK)	2 (PAS, TRD)
141-153	7	PAS, PTH, TRD	Culture positive	(month 147) PTH	(month 147) PAS, CS/TRD	(Month 144) baseline + EMB, LZD, CPR, KAN, AMK	0	2 (PAS, TRD)
154-169	OP	NONE	Culture positive	(month 156) R (month 163) PAS	(month 163) CS/TRD	(Month 160) baseline + EMB, LZD, CPR, KAN, AMK		

Therapy (month)	Hospital	Treatment Regimen	Clinical notes	Phenotypic Resistance	Phenotypic Susceptibility	Genotypic Resistance	Active drugs in treatment by genotype	Active drugs in treatment by phenotype
170-200	7, OP	TRD	Microscopy positive, radiology indicated progression (month 189)		(month 170) CS/TRD (month 178) CS/TRD	(Month 172) baseline + EMB, LZD, CPR, KAN, AMK	0	1
201	7	MFX, TRD					0	1
202-214	OP	-						
215	7	TRD	Microscopy positive				0	1
216	12							

*Phenotypic test was considered for "Active drugs in treatment" as no genotypic markers are available for these drugs (CLR and AMC)

[†]Treated with dihydrothenat, a SM derivative

[‡]tyloxapol is an anti-mucosal

[b] border-line resistance (often viewed as some bacterial growth but below or on the border of the resistance threshold)

AMK - amikacin, AMC - amoxicillin+clavulanic acid, CFX - ciprofloxacin, CFZ - clofazimine, CLR - clarithromycin, CPR - capreomycin, CS - cycloserine, EMB - ethambutol, FQ - fluoroquinolone, INH - isoniazid, KAN - kanamycin, LZD - linezolid, MFX - moxifloxacin, OP - out-patient, PAS - para-aminosalicylic acid, PTH - prothionamide, RIF - rifampicin, RBT - rifabutin, SM - streptomycin, SFX - sparfloxacin, TRD - terizidone, Z - pyrazinamid

Table B.2: Population frequency of resistance, compensatory, and tolerance associated mutations. Thirteen serial isolates were collected in the final treatment episode of an MDR turned XDR-TB infection. Frequency was calculated from whole genome sequencing data, as the percentage of alternative allele reads. High-confidence mutations, indicated in bold font, were predicted to have an effect on phenotype.

				Frequency of mutation in isolate												
Isolate identification number				**1060-97**	**4177-97**	**2698-00**	**1633-02**	**9512-03**	**31-04**	**10202-04**	**3444-05**	**1126-07**	**5257-07**	**3082-08**	**6974-09**	**7686-10**
Average genome wide coverage				178x	154x	153x	181x	136x	168x	122x	135x	119x	149x	129x	172x	148x
Month isolate was collected				10	13	47	71	89	92	104	108	130	135	144	160	172
Drug	**Gene Name**	**Variant**	**Literature Reference**													
INH	*katG*	S315T	[236]	100%	100%	100%	99%	100%	99%	100%	100%	100%	99%	100%	100%	100%
	fabG1	-17 g>t	[91]	-	-	-	-	-	-	-	-	-	-	-	-	99%
RIF/RBT	*rpoB*	F424V		5%	29.5%	96%	100%	100%	100%	100%	100%	100%	100%	100%	100%	99%
	rpoB	L430P	[236]	100%	100%	100%	100%	100%	100%	100%	99%	100%	99%	100%	100%	100%
	rpoB	D435G	[236]	99%	100%	100%	99%	99%	99%	100%	100%	100%	100%	99%	100%	99%
EMB	*embA*	-43 g>c	[91]	99%	99%	99%	100%	100%	99%	100%	100%	99%	99%	99%	99%	100%
	embB	G406A	[142]	-	-	93%	99%	100%	100%	100%	100%	100%	100%	99%	100%	99%
PZA	*pncA*	T76P	[236]	100%	100%	100%	99%	100%	100%	99%	100%	100%	100%	99%	100%	100%
PAS	*ribD*	-12 g>a	[237]	99%	99%	100%	99%	100%	100%	99%	100%	100%	99%	100%	100%	100%
SM	*gid*	102 del g	*[142]	96%	97%	97%	97%	95%	95%	98%	96%	94%	96%	95%	95%	98%
PTH, ETH	*ethA*	89 del a		100%	99%	100%	100%	100%	100%	99%	100%	100%	100%	100%	100%	100%
INH, PTH, ETH	*Rv3083*	C258F		-	-	-	-	-	-	100%	-	-	-	-	-	-
PTH / compen-satory	*Rv0565c*	1312 ins g		-	-	-	-	-	-	97%	-	-	-	-	-	-
	Rv0565c	C298R	[151]	-	-	-	-	-	-	-	99%	100%	100%	100%	100%	100%

Table B.2 continued

				Frequency of mutation in isolate												
Isolate identification number				**1060-97**	**4177-97**	**2698-00**	**1633-02**	**9512-03**	**31-04**	**10202-04**	**3444-05**	**1126-07**	**5257-07**	**3082-08**	**6974-09**	**7686-10**
Month isolate was collected				10	13	47	71	89	92	104	108	130	135	144	160	172
Drug	**Gene Name**	**Variant**	**Literature Reference**													
FQ	*gyrA*	D94G	[236]	20.6%	93%	93%	100%	100%	99%	100%	100%	100%	100%	100%	100%	100%
CPR	*tlyA*	350 ins g	*[63]	-	-	-	-	-	-	-	-	78.9%	71.4%	97%	96%	99%
	tlyA	584 ins t	[63]	-	-	-	-	-	-	-	-	-	27.5%	-	-	-
AMK, KAN, CPR	*rrs*	1401 a>g	[236]	-	-	-	-	-	-	-	-	-	-	100%	29.5%	99%
LZD, CPR, CLR	*rrl*	2746 g>a	[209]	-	-	-	-	-	-	100%	-	-	-	-	-	-
LZD	*rplC*	C154R	[68]	-	-	-	-	-	-	-	100%	100%	100%	100%	100%	99%
CFZ, BDQ	*Rv0678*	I67S	[140]	-	36.4%	-	-	-	-	-	-	-	-	-	-	-
	Rv0678	R96Q	*10	-	10%	-	-	-	-	-	-	-	-	-	-	-
	Rv0678	132 ins gt	*[140]	22.4%	-	3.6%	-	-	-	-	-	-	-	-	-	-
CS, TRD	*ald*	L343V		-	96%	-	-	-	-	-	-	-	-	-	-	-
	ald	77 ins a	*[72]	99%	99%	96%	97%	96%	96%	99%	97%	97%	98%	99%	98%	96%
tolerance associated	*prpR*	F334L	*[150]	-	-	-	-	-	100%	-	100%	100%	100%	100%	100%	100%

*not exact mutation described in publication

AMK - amikacin, BDQ - bedaquiline, CFZ - clofazimine, CLR - clarithromycin, CPR - capreomycin, CS - cycloserine, EMB - ethambutol, ETH - ethionamide, FQ - fluoroquinolone, INH - isoniazid, KAN - kanamycin, LZD - linezolid, PAS - para-aminosalicylic acid, PTH - prothionamide, RIF - rifampicin, RBT - rifabutin, SM - streptomycin, TRD - terizidone, PZA - pyrazinamide

Table B.3: Statistical analysis of low-frequency variants. Variants detected at a frequency below 70% were verified using low-frequency SNP detection tool binoSNP. Only high-quality calls (minimum base quality: phred = 20) were considered at each position. Variant was included in final dataset if statistically significant ($p \leq 0.05$).

Isolate	Variant position	Gene	Variant	Ref	Alt	DP	#ALT	Freq (ALT)	p-value	Antibiotic
1060-97	7582	*gyrA*	D94G	a	g	155	32	20.6%	7.16E-70	FQ
1060-97	761076	*rpoB*	F424V	t	g	154	7	4.5%	8.29E-12	RIF
1060-97	779121	*Rv0678*	132 ins gt	g	gt	210	47	22.4%	1.45E-44	BDQ/CFZ
1060-97	3087846	*ald*	L343V	C	g	114	1	0.877%	0.75	CS/TRD
4177-97	761076	*rpoB*	F424V	t	g	139	41	29.5%	2.68E-94	RIF
4177-97	779121	*Rv0678*	132 ins gt	g	gt	160	2	1.3%	0.5726	BDQ/CFZ
4177-97	779189	*Rv0678*	I67S	t	g	132	48	36.4%	1.48E-117	BDQ/CFZ
4177-97	779276	*Rv0678*	R96Q	g	a	120	12	10.0%	1.68E-23	BDQ/CFZ
2698-00	779121	*Rv0678*	132 ins gt	g	gt	193	7	3.63%	0.00915	BDQ/CFZ
1126-07	1918523	*tlyA*	584 ins t	-	t	106	2	1.9%	0.363	CPR
5257-07	1918289	*tlyA*	350 ins g	a	g	154	110	71.4%	1.85E-173	CPR
5257-07	1918523	*tlyA*	584 ins t	-	t	131	36	27.5%	4.83E-38	CPR
6974-09	1473246	*rrs*	1401 a>g	a	g	254	75	29.5%	1.28E-178	AMK, KAN, CPR

Alt: alternative allele, #ALT: number of alternative alleles at position, DP: filtered coverage depth at position, Freq (ALT): frequency of alternative allele, Pos: position, Ref: reference allele

AMK - amikacin, BDQ - bedaquiline, CFZ - clofazimine, CPR - capreomycin, CS - cycloserine, FQ - fluoroquinolone, KAN - kanamycin, RIF - rifampicin, TRD - terizidone

Appendix C

Supplementary Material and extended tables of Results 4.2

Table C.1 Generation time of H37Rv lab strain. Generation time was calculated for each evolutionary experiment, from the first culture passage of the antibiotic free control.

$$Generation\ time\ =\ Total\ hours\ \div\ (\frac{\log\ (CFU_{final})}{\log\ (CFU_{start})} \div \log(2))$$

Experiment	CFU inoculum	Growth time (hours)	Final CFU	Generations	Generation time (hours)
1	1.16×10^7	95	1.45×10^8	3.6	26.1
2	1.11×10^7	95	1.22×10^8	3.3	28.6
3	8.59×10^6	96	1.31×10^8	3.9	24.4
4	6.16×10^6	98	2.25×10^8	5.2	18.9
5	2.50×10^7	97	1.18×10^8	2.2	43.4
6	1.58×10^7	97	1.43×10^8	3.2	30.6
7	3.17×10^7	96	2.41×10^8	2.9	32.8
8	2.65×10^7	96	2.13×10^8	3.0	32.0
9	2.09×10^7	96	1.74×10^8	3.1	31.4
Average:				3.4	29.8
Standard deviation:				0.8	6.7

CFU - colony forming unit

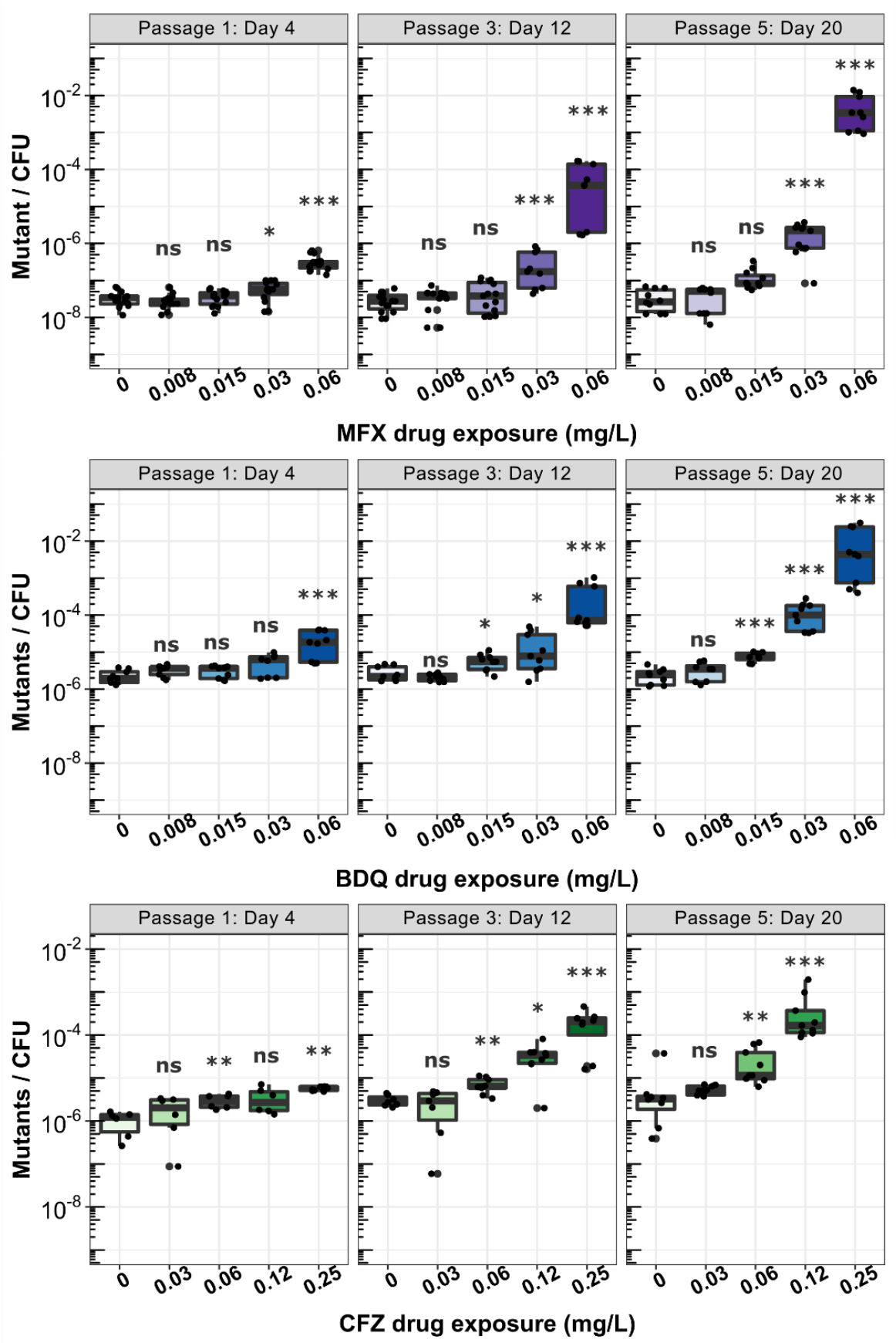
Passage 1: Day 4
Passage 3: Day 12
Passage 5: Day 20
Mutant / CFU
10^{-2}
10^{-4}
10^{-6}
10^{-8}
ns
ns
*
***
ns
ns
***
***
ns
ns
***
***
0
0.008
0.015
0.03
0.06
MFX drug exposure (mg/L)
Mutants / CFU
ns
ns
ns
***
ns
*
*
***
ns
***
***
***
BDQ drug exposure (mg/L)
ns
**
ns
**
ns
**
*
***
ns
**
***
0
0.03
0.06
0.12
0.25
CFZ drug exposure (mg/L)

Figure C.1: Mutant enrichment after sub-inhibitory drug exposure; mutants per total colony forming units. The *Mycobacterium tuberculosis* complex lab strain H37Rv was exposed sub-inhibitory concentrations of either (A) moxifloxacin (MFX), (B) bedaquiline (BDQ), or (C) clofazimine (CFZ); concentrations between 1:2 to 1:16 below the strain minimum inhibitory concentration (MIC). The bacteria were exposed to the antibiotic for 20 days, consisting of five culture passages. Bacterial samples were evaluated at three time points during the experiment, after day 4 or "passage: 1", day 12 "passage: 3", and day 20 "passage: 5". The cultures were plated on 7H10 agar plates for CFU counting for bacterial quantification, additionally cultures were plated on 7H10 (for MFX) or 7H11 (for BDQ or CFZ) plates supplemented with antibiotic at the critical concentration (0.25 mg/L MFX), or the strain MIC (0.12 mg/L BDQ, 0.5 mg/L CFZ). Mutant enrichment was calculated as the number of colonies / mL counted on antibiotic supplemented media divided by the total CFU per mL (number of colonies on selected media divided by colonies counted on antibiotic free media).

Statistics: Three independent experiments were conducted with 1 biological replicate per experimental condition, with 3 to 5 technical replicates each. Statistics were calculated as nonparametric multiple contrast test (Kruskal) with a confidence interval of 95%, p-values between drug exposed and the antibiotic free control (0 mg/L of antibiotic): *$p<0.05$, **$p<0.01$, ***$p<0.001$

Table C.2: P-values of evolutionary experiments, colony forming units, and mutant enrichment. Colony forming units (CFU) of each experimental condition were compared to the antibiotic free control in the corresponding experiment. Each statistical test was conducted using R studio, see Appendix E.

MFX - CFU

Passage	Cont. - 0.008mg/L	Cont. - 0.015mg/L	Cont. - 0.03mg/L	Cont. - 0.06mg/L
1	0.577	0.884	0.132	2.87×10^{-4}
3	0.861	0.999	0.064	0.024
5	0.821	0.448	2.9×10^{-4}	2.7×10^{-6}

MFX - Mutant Enrichment

Passage	Cont. - 0.008mg/L	Cont. - 0.015mg/L	Cont. - 0.03mg/L	Cont. - 0.06mg/L
1	0.685	0.976	0.112	1.57×10^{-9}
3	0.745	0.722	7.9×10^{-5}	9.5×10^{-7}
5	0.995	2.4×10^{-4}	1.7×10^{-7}	9.5×10^{-8}

BDQ - CFU

Passage	Cont. - 0.008mg/L	Cont. - 0.015mg/L	Cont. - 0.03mg/L	Cont. - 0.06mg/L
1	0.269	0.046	0.191	3.4×10^{-5}
3	0.804	0.227	0.029	4.9×10^{-3}
5	0.12	9.8×10^{-3}	2.8×10^{-4}	2.4×10^{-7}

BDQ - Mutant Enrichment

Passage	Cont. - 0.008mg/L	Cont. - 0.015mg/L	Cont. - 0.03mg/L	Cont. - 0.06mg/L
1	0.174	0.45	0.104	7.3×10^{-5}
3	0.755	0.018	0.076	1.04×10^{-6}
5	0.39	2.8×10^{-10}	6.4×10^{-14}	1.4×10^{-13}

CFZ - CFU

Passage	Cont. - 0.03mg/L	Cont. - 0.06mg/L	Cont. - 0.12mg/L	Cont. - 0.25mg/L
1	0.825	0.372	0.113	7.5×10^{-4}
3	0.926	0.778	0.072	4.9×10^{-4}
5	0.999	0.981	0.95	-

CFZ - Mutant Enrichment

Passage	Cont. - 0.03mg/L	Cont. - 0.06mg/L	Cont. - 0.12mg/L	Cont. - 0.25mg/L
1	0.599	5.5×10^{-3}	0.053	1.1×10^{-3}
3	1.0	1.9×10^{-3}	0.016	2.2×10^{-5}
5	0.22	2.4×10^{-3}	3.5×10^{-5}	-

BDQ - bedaquiline, CFU - colony forming unit, CFZ - clofazimine, Cont. - control, MFX - moxifloxacin

Table C.3: P-values of cross-resistance comparison between bedaquiline and clofazimine selection of bedaquiline mutants. Comparison of bedaquiline (BDQ) resistant mutant populations (mutants/million colony forming units; CFU), recovered after BDQ or clofazimine (CFZ) exposure. Populations were compared between concentrations relative to the MIC (1:16, 1:8, 1:4, 1:2, and no antibiotic), and corresponding exposure time (passage 1, 3, or 5). Each statistical test was conducted using R studio, see Appendix E.

Passage	BDQ control vs. CFZ control	1:16 MIC BDQ vs. 1:16 MIC CFZ	1:8 MIC BDQ vs. 1:8 MIC CFZ	1:4 MIC BDQ vs. 1:4 MIC CFZ	1:2 MIC BDQ vs. 1:2 MIC CFZ
1	9.55×10^{-2}	0.002	0.010	0.116	8.85×10^{-2}
3	0.32	0.57	0.042	0.999	0.336
5	0.94	0.999	0.999	0.877	6.18×10^{-10}

Table C.4: Next generation sequencing statistics of deep sequencing run with moxifloxacin exposed bacterial populations.

Sample ID	Exp.	MFX exposure (mg/L)	Time Point (passage)	Read Length	Cov Any Bases	Cov Unam Bases	Cov Unam Mean	SNPs	Dels	Ins	Unc	Subs
LT22100	1	0	1	151bp	4411304	4407147	385	81	14	14	228	44
LT221015	1	0.015	1	151bp	4411457	4410692	590	87	22	19	75	46
LT22103	1	0.03	1	151bp	4411450	4409354	635	86	18	20	82	45
LT22106	1	0.06	1	151bp	4411417	4409583	639	86	21	19	115	46
LT22112	1	0.12	1	151bp	4411328	4408222	712	86	23	19	204	46
LT22300	1	0	3	151bp	4411453	4411153	1087	86	20	19	79	49
LT223015	1	0.015	3	151bp	4411356	4408429	516	83	23	18	176	44
LT22303	1	0.03	3	151bp	4411448	4410706	670	87	20	22	84	46
LT22306	1	0.06	3	151bp	4411453	4410781	837	87	18	19	79	46
LT22312	1	0.12	3	151bp	4411386	4408492	485	84	23	12	146	45
LT22500	1	0	5	151bp	4411274	4407071	461	84	19	20	258	44
LT225015	1	0.015	5	151bp	4411328	4407178	582	85	21	18	204	46
LT22503	1	0.03	5	151bp	4411456	4410483	626	86	19	18	76	46
LT22506	1	0.06	5	151bp	4411401	4408701	477	84	16	13	131	44
LT23100	2	0	1	151bp	4411437	4405360	461	84	19	14	95	44
LT231015	2	0.015	1	151bp	4411449	4408216	669	85	21	22	83	45
LT23103	2	0.03	1	151bp	4411451	4411193	743	87	21	19	81	46
LT23106	2	0.06	1	151bp	4411407	4409605	556	85	25	13	125	45
LT23112	2	0.12	1	151bp	4411446	4410781	690	87	21	20	86	46
LT23300	2	0	3	151bp	4411453	4410485	632	87	18	21	79	46
LT233015	2	0.015	3	151bp	4411453	4410128	699	85	22	13	79	45
LT23303	2	0.03	3	151bp	4411456	4411251	884	87	19	19	76	46

Table C.4 continued

Sample ID	Exp.	MFX exposure (mg/L)	Time Point (passage)	Read Length	Cov Any Bases	Cov Unam Bases	Cov Unam Mean	SNPs	Dels	Ins	Unc	Subs
LT23306	2	0.06	3	151bp	4411452	4409136	577	88	20	19	80	47
LT23500	2	0	5	151bp	4411450	4409418	438	86	21	18	82	46
LT235015	2	0.015	5	151bp	4411453	4409622	489	86	19	19	79	45
LT23503	2	0.03	5	151bp	4411463	4411290	670	86	18	22	69	47
LT23512	2	0.12	5	151bp	4410990	4409315	491	87	22	19	542	46
LT24100	3	0	1	151bp	4411453	4410361	508	87	22	22	79	46
LT241015	3	0.015	1	151bp	4411461	4410966	668	87	23	23	71	46
LT24103	3	0.03	1	151bp	4411453	4411088	448	87	18	19	79	46
LT24106	3	0.06	1	151bp	4411458	4411310	927	89	23	22	74	48
LT24112	3	0.12	1	151bp	4411453	4410926	806	87	19	19	79	46
LT24300	3	0	3	151bp	4411242	4410562	721	87	21	22	290	46
LT243015	3	0.015	3	151bp	4411447	4410863	627	88	28	21	85	47
LT24306	3	0.06	3	151bp	4411453	4410809	552	89	19	23	79	48
LT24312	3	0.12	3	151bp	4411456	4410217	277	86	21	21	76	46
LT24500	3	0	5	151bp	4411446	4409959	519	87	19	20	86	46
LT245015	3	0.015	5	151bp	4411054	4410717	381	90	18	22	478	50
LT24503	3	0.03	5	151bp	4411457	4411243	462	89	18	20	75	48
LT24506	3	0.06	5	151bp	4411463	4411329	424	89	22	21	69	51
LT24512	3	0.12	5	151bp	4411464	4411220	381	92	15	20	68	51

Cov - coverage, Dels - deletions, Exp. - experiment, Ins - incretions, MFX - moxifloxacin, SNPs - single nucleotide polymorphisms, Subs - substitutions, Unam - unambiguous, Unc - uncovered

Table C.5: Next generation sequencing statistics of deep sequencing run with bedaquiline exposed bacterial populations.

Sample ID	Exp.	BDQ exposure (mg/L)	Time Point (passage)	Read Length	Cov Any Bases	Cov Unam Bases	Cov Unam Mean	SNPs	Dels	Ins	Unc	Subs
LS01100	1	0	1	151bp	4411457	4408984	383	84	21	18	75	45
LS01108	1	0.008	1	151bp	4411476	4407978	320	84	23	17	56	45
LS011015	1	0.015	1	151bp	4411313	4405120	291	80	26	17	219	42
LS01103	1	0.03	1	151bp	4411365	4406850	363	81	22	17	167	42
LS01106	1	0.06	1	151bp	4411068	4402627	292	80	23	15	464	41
LS01300	1	0	3	151bp	4411366	4405268	328	81	21	17	166	42
LS01308	1	0.008	3	151bp	4411259	4405123	271	81	21	17	273	42
LS013015	1	0.015	3	151bp	4411451	4405955	293	83	23	20	81	45
LS01303	1	0.03	3	151bp	4411427	4405156	252	81	21	15	105	42

Table C.5 continued

Sample ID	Exp.	BDQ exposure (mg/L)	Time Point (passage)	Read Length	Cov Any Bases	Cov Unam Bases	Cov Unam Mean	SNPs	Dels	Ins	Unc	Subs
LS01306	1	0.06	3	151bp	4411447	4406617	258	86	21	17	85	45
LS01500	1	0	5	151bp	4411451	4409631	314	87	21	19	81	46
LS01508	1	0.008	5	151bp	4411457	4409732	356	86	21	19	75	46
LS015015	1	0.015	5	151bp	4411421	4406337	316	83	21	16	111	43
LS01503	1	0.03	5	151bp	4411447	4405740	245	82	21	15	85	43
LS01506	1	0.06	5	151bp	4411294	4405644	291	83	21	17	238	44
LS02100	2	0	1	151bp	4411415	4403541	274	83	21	17	117	44
LS02108	2	0.008	1	151bp	4411346	4403480	273	82	20	17	186	43
LS021015	2	0.015	1	151bp	4411200	4402273	232	84	18	15	332	45
LS02103	2	0.03	1	151bp	4411442	4403073	276	82	20	15	90	43
LS02106	2	0.06	1	151bp	4411294	4404426	282	82	22	15	238	44
LS02300	2	0	3	151bp	4411354	4404674	221	81	25	17	178	43
LS02308	2	0.008	3	151bp	4411319	4402280	260	81	20	17	213	43
LS023015	2	0.015	3	151bp	4411411	4406268	324	82	20	18	121	44
LS02303	2	0.03	3	151bp	4411215	4405097	271	85	20	16	317	46
LS02500	2	0	5	151bp	4411221	4400979	220	81	16	15	311	43
LS02508	2	0.008	5	151bp	4411289	4402852	234	82	22	10	243	43
LS025015	2	0.015	5	151bp	4411328	4400793	259	81	23	15	204	43
LS02503	2	0.03	5	151bp	4411328	4404131	275	82	18	17	204	43
LS03100	3	0	1	151bp	4411183	4398216	205	81	23	16	349	42
LS03108	3	0.008	1	151bp	4411226	4404412	290	81	19	10	306	42
LS031015	3	0.015	1	151bp	4411436	4404239	262	84	19	17	96	45
LS03103	3	0.03	1	151bp	4411291	4403608	273	82	17	18	241	42
LS03106	3	0.06	1	151bp	4411405	4405975	281	83	20	18	127	43
LS03300	3	0	3	151bp	4411354	4403786	317	81	19	17	178	42
LS03308	3	0.008	3	151bp	4411241	4401271	284	83	18	18	291	44
LS033015	3	0.015	3	151bp	4411128	4401103	355	83	18	17	404	44
LS03303	3	0.03	3	151bp	4411300	4407249	372	83	22	18	232	44
LS03306	3	0.06	3	151bp	4411159	4400497	288	79	17	15	373	42
LS03500	3	0	5	151bp	4411411	4404351	295	82	18	18	121	42
LS03508	3	0.008	5	151bp	4411390	4405381	222	83	18	15	142	44
LS035015	3	0.015	5	151bp	4411372	4402585	293	81	20	18	160	42
LS03503	3	0.03	5	151bp	4411179	4400499	256	81	19	17	353	42
LS03506	3	0.06	5	151bp	4411238	4398933	229	74	11	8	294	39

Cov - coverage, Dels - deletions, Exp - experiment, Ins - incretions, MFX - moxifloxacin, SNPs - single nucleotide polymorphisms, Subs - substitutions, Unam - unambiguous, Unc - uncovered

Table C.6: Variant diversity in *Rv0678* and *atpE* genes of mutant population after bedaquiline evolutionary experiment. Mutant populations were individually collected and pooled by experiment, time point, and drug exposure. Highest frequency representative of one collected mutant population.

Gene name	Variant position	Variant	Type	Reference allele	Alternative allele	Appearance in n-populations
Rv0678	779015	26 del ag	Del	a	-	8
Rv0678	779024	35 del c	Del	c	-	13
Rv0678	779099	G37D	SNP	g	a	7
Rv0678	779117	L43P	SNP	t	c	33
Rv0678	779117	L43R	SNP	t	g	9
Rv0678	779126	C46Y	SNP	g	a	15
Rv0678	779137	R50W	SNP	c	t	30
Rv0678	779181	192 ins g	Ins	c	g	28
Rv0678	779182	193 del g	Del	g	-	34
Rv0678	779183	G65V	SNP	g	t	9
Rv0678	779183	G65E	SNP	g	a	1
Rv0678	779191	S68G	SNP	a	g	30
Rv0678	779204	R72L	SNP	g	t	13
Rv0678	779210	L74P	SNP	t	c	20
Rv0678	779217	228 ins t	Ins	a	t	2
Rv0678	779224	235 del t	Del	t	-	7
Rv0678	779224	F79L	SNP	t	c	1
Rv0678	779225	F79C	SNP	t	g	20
Rv0678	779281	292 del a	Del	a	-	19
Rv0678	779285	A99V	SNP	c	t	32
Rv0678	779285	A99G	SNP	c	g	1
Rv0678	779293	A102T	SNP	g	a	14
Rv0678	779296	G103R	SNP	g	c	4
Rv0678	779330	L114P	SNP	t	c	22
Rv0678	779339	L117Q	SNP	t	a	8
Rv0678	779349	360 del g	Del	g	-	19
Rv0678	779351	G121E	SNP	g	a	16
Rv0678	779384	R132P	SNP	g	c	9
Rv0678	779392	R135W	SNP	c	t	12
Rv0678	779393	R135L	SNP	g	t	16
Rv0678	779396	L136P	SNP	t	c	8
Rv0678	779413	L142V	SNP	c	g	13
Rv0678	779440	S151P	SNP	t	c	16
Rv0678	779450	L154P	SNP	t	c	11
Rv0678	779450	461 del t	Del	t	-	1
Rv0678	779455	R156_	SNP	c	t	7

Table C.6 continued

Gene name	Variant position	Variant	Type	Reference allele	Alternative allele	Appearance in n-populations
Rv0678	779455	466 del c	Del	c	-	2
Rv1305	1461127	D28G	SNP	a	g	1
Rv1305	1461231	A63P	SNP	g	c	3

Del - deletion, Ins - insertion, n - number, SNP - single nucleotide polymorphism, _ - stop codon insertion

Table C.7: Next generation sequencing statistics of deep sequencing run with clofazimine exposed bacterial populations.

Sample ID	Exp.	CFZ exposure (mg/L)	Time point (passage)	Read length	Cov any bases	Cov unam bases	Cov unam mean	SNPs	Dels	Ins	Unc	Subs
LS07100	1	0	1	151bp	4411374	4401881	340	81	21	15	158	42
LS07103	1	0.03	1	151bp	4411441	4408394	393	86	23	19	91	46
LS07106	1	0.06	1	151bp	4411441	4407747	382	84	22	19	91	44
LS07112	1	0.12	1	151bp	4411225	4402383	373	81	23	17	307	42
LS07125	1	0.25	1	151bp	4411342	4402817	323	82	26	16	190	43
LS07100	1	0	3	151bp	4411444	4407551	400	83	21	17	88	44
LS07103	1	0.03	3	151bp	4411298	4402523	335	82	23	19	234	43
LS07106	1	0.06	3	151bp	4411241	4400492	331	80	19	19	291	42
LS07112	1	0.12	3	151bp	4411414	4403238	422	82	18	15	118	43
LS07325	1	0.25	3	151bp	4411051	4396690	334	80	21	17	481	41
LS07100	1	0	5	151bp	4411284	4402147	414	81	21	17	248	42
LS07103	1	0.03	5	151bp	4411178	4400526	379	82	21	15	354	42
LS07106	1	0.06	5	151bp	4411245	4399603	330	83	25	10	287	44
LS07112	1	0.12	5	151bp	4411434	4409091	358	86	18	18	98	45
LS07525	1	0.25	5	151bp	4411180	4401760	389	84	20	17	352	44
LS08100	2	0	1	151bp	4411439	4407017	296	84	21	15	93	45
LS08103	2	0.03	1	151bp	4411291	4401796	280	81	22	15	241	42
LS08112	2	0.12	1	151bp	4411442	4407553	302	84	18	17	90	45
LS08125	2	0.25	1	151bp	4411304	4405145	350	82	21	17	228	43
LS08300	2	0	3	151bp	4411379	4407616	310	84	21	11	153	45
LS08306	2	0.06	3	151bp	4411453	4409823	290	86	19	15	79	46
LS08312	2	0.12	3	151bp	4411396	4405414	301	82	23	15	136	43
LS08325	2	0.25	3	151bp	4411282	4399407	344	80	24	15	250	42
LS08500	2	0	5	151bp	4411441	4408277	306	86	22	15	91	46
LS08506	2	0.06	5	151bp	4411360	4405405	318	82	18	15	172	43
LS08525	2	0.25	5	151bp	4411071	4399137	310	74	13	12	461	40
LS09100	3	0	1	151bp	4411354	4402922	318	81	23	8	178	42

Table C.7 continued

Sample ID	Exp.	CFZ exposure (mg/L)	Time point (passage)	Read length	Cov any bases	Cov unam bases	Cov unam mean	SNPs	Dels	Ins	Unc	Subs
LS09103	3	0.03	1	151bp	4411275	4400398	312	80	21	15	257	42
LS09112	3	0.12	1	151bp	4411413	4407692	277	85	21	18	119	46
LS09125	3	0.25	1	151bp	4411422	4407656	404	85	22	18	110	45
LS09103	3	0.03	3	151bp	4411440	4407542	257	85	20	18	92	45
LS09106	3	0.06	3	151bp	4411051	4399253	299	80	25	17	481	42
LS09112	3	0.12	3	151bp	4411346	4402116	291	81	20	17	186	42
LS09325	3	0.25	3	151bp	4411193	4403366	381	83	21	17	339	44
LS09103	3	0.03	5	151bp	4411301	4403208	321	81	19	17	231	42
LS09106	3	0.06	5	151bp	4410934	4396651	298	77	21	10	598	39
LS09112	3	0.12	5	151bp	4411268	4403498	322	80	18	20	264	42
LS09525	3	0.25	5	151bp	4411217	4401313	388	82	20	20	315	42

Cov - coverage, Dels - deletions, Exp. - experiment, Ins - incretions, MFX - moxifloxacin, SNPs - single nucleotide polymorphisms, Subs - substitutions, Unam - unambiguous, Unc - uncovered

Table C.8: Variant diversity in *Rv0678* and *pepQ (Rv2535c)* genes of mutant population after clofazimine evolutionary experiment. Mutant populations were individually collected and pooled by experiment, time point, and drug exposure.

Gene	Gene name	Variant position	Variant	Type	Reference allele	alternative allele	Appearance in n-populations
Rv0678	-	778991	V1A	SNP	t	c	14
Rv0678	-	779005	16 del g	Del	g	-	7
Rv0678	-	779038	49 del a	Del	a	-	6
Rv0678	-	779060	G24V	SNP	g	t	8
Rv0678	-	779063	G25D	SNP	g	a	2
Rv0678	-	779101	R38_	SNP	c	t	10
Rv0678	-	779109	120 del g	Del	g	-	1
Rv0678	-	779109	L40L	SNP	g	a	1
Rv0678	-	779115	W42_	SNP	g	a	6
Rv0678	-	779117	128 del t	Del	t	-	1
Rv0678	-	779117	L43P	SNP	t	c	7
Rv0678	-	779117	L43Q	SNP	t	a	1
Rv0678	-	779119	130 del c	Del	c	-	1
Rv0678	-	779120	L44P	SNP	t	c	15
Rv0678	-	779121	132 ins g	Ins	g	g	11
Rv0678	-	779121	132 ins t	Ins	g	t	11
Rv0678	-	779126	C46Y	SNP	g	a	15

Table C.8 continued

Gene	Gene name	Variant position	Variant	Type	Reference allele	alternative allele	Appearance in n-populations
Rv0678	-	779137	R50W	SNP	c	t	22
Rv0678	-	779141	152 del a	Del	a	-	1
Rv0678	-	779159	A57E	SNP	c	a	1
Rv0678	-	779171	182 ins g	Ins	c	g	1
Rv0678	-	779176	S63G	SNP	a	g	11
Rv0678	-	779181	192 ins g	Ins	c	g	15
Rv0678	-	779182	193 del g	Del	g	-	21
Rv0678	-	779182	G65R	SNP	g	a	1
Rv0678	-	779183	G65E	SNP	g	a	8
Rv0678	-	779183	G65V	SNP	g	t	2
Rv0678	-	779185	G66R	SNP	g	c	1
Rv0678	-	779185	G66W	SNP	g	t	1
Rv0678	-	779191	S68G	SNP	a	g	15
Rv0678	-	779203	R72G	SNP	c	g	1
Rv0678	-	779203	R72W	SNP	c	t	4
Rv0678	-	779210	L74P	SNP	t	c	14
Rv0678	-	779215	Q76_	SNP	c	t	2
Rv0678	-	779224	235 del t	Del	t	-	1
Rv0678	-	779224	F79I	SNP	t	a	1
Rv0678	-	779224	F79V	SNP	t	g	14
Rv0678	-	779225	F79C	SNP	t	g	8
Rv0678	-	779226	F79L	SNP	c	g	1
Rv0678	-	779236	L83F	SNP	c	t	1
Rv0678	-	779263	274 ins a	Ins	t	a	6
Rv0678	-	779280	291 ins a	Ins	c	a	8
Rv0678	-	779285	A99V	SNP	c	t	33
Rv0678	-	779293	A102S	SNP	g	t	2
Rv0678	-	779330	L114P	SNP	t	c	2
Rv0678	-	779349	360 del g	Del	g	-	11
Rv0678	-	779351	G121E	SNP	g	a	25
Rv0678	-	779354	365 del t	Del	t	-	14
Rv0678	-	779354	L122P	SNP	t	c	6
Rv0678	-	779355	366 del g	Del	g	-	15
Rv0678	-	779370	381 ins g	Ins	c	g	1
Rv0678	-	779396	407 del t	Del	t	-	1
Rv0678	-	779396	L136P	SNP	t	c	2
Rv0678	-	779414	L142P	SNP	t	c	7
Rv0678	-	779424	Y145_	SNP	t	a	3

Table C.8 continued

Gene	Gene name	Variant position	Variant	Type	Reference allele	alternative allele	Appearance in n-populations
Rv0678	-	779447	458 del c	Del	c	-	3
Rv0678	-	779447	A153D	SNP	c	a	1
Rv0678	-	779450	L154P	SNP	t	c	7
Rv0678	-	779454	465 ins c	Ins	g	c	7
Rv0678	-	779455	R156_	SNP	c	t	10
Rv2535c	*pepQ*	2860078	L114R	SNP	a	c	4
Rv2535c	*pepQ*	2860087	A111G	SNP	g	c	1
Rv2535c	*pepQ*	2860099	L107R	SNP	a	c	1
Rv2535c	*pepQ*	2860113	V102V	SNP	g	c	3
Rv2535c	*pepQ*	2860114	V102G	SNP	a	c	2
Rv2535c	*pepQ*	2860130	F97V	SNP	a	c	2
Rv2535c	*pepQ*	2860131	G96G	SNP	g	c	2
Rv2535c	*pepQ*	2860140	G93G	SNP	t	c	2
Rv2535c	*pepQ*	2860144	V92G	SNP	a	c	1
Rv2535c	*pepQ*	2860146	G91G	SNP	g	c	1
Rv2535c	*pepQ*	2860150	A90G	SNP	g	c	2
Rv2535c	*pepQ*	2860155	G88G	SNP	g	c	1
Rv2535c	*pepQ*	2860159	A87G	SNP	g	c	9

Del - deletion, Ins - insertion, n - number, SNP - single nucleotide polymorphism, _ - stop codon insertion

Table C.9: Genotypic and phenotypic characterization of resistant variants isolated after bedaquiline or clofazimine evolutionary experiments. Whole genome sequencing of mutation under selection, including minimum inhibitory concentration values measured by resazurin microtiter assay and compared to the genetically wild-type ancestor H37Rv strain.

Gene	Variant position	Variant	BDQ MIC (mg/L)	CFZ MIC (mg/L)	Type	Ref. allele	Alt. allele	Number of isolates	BDQ or CFZ isolate	Selection media drug conc. (mg/L)
Susceptible ancestor (gWT)			0.25-0.5	0.5-1.0						
Rv0678	778980	-9 ins g	2	1	Ins	a	g	1	BDQ	0.12
Rv0678	779005	16 del g	1	2	Del	g	-	1	BDQ	0.12
Rv0678	779015	26 del ag	2	NA	Del	a	-	1	BDQ	0.12
Rv0678	779029	40 del c	2	2	Del	c	-	1	BDQ	0.12
Rv0678	779038	49 del a	2	2	Del	a	-	1	CFZ	0.25
Rv0678	779051	62 del a	2	1	Del	a	-	1	BDQ	0.12
Rv0678	779060	G24V	2	2	SNP	g	t	3	CFZ	0.25
Rv0678	779062	G25S	2	NA	SNP	g	a	1	BDQ	0.25
Rv0678	779078	89 del g	2	2	Del	g	-	1	CFZ	0.25
Rv0678	779101	R38_	2	2	SNP	c	t	4	CFZ	0.25
Rv0678	779102	R38P	1	2	SNP	g	c	1	CFZ	0.25
Rv0678	779108	L40S	1	2	SNP	t	c	1	CFZ	0.25
Rv0678	779109	120 del g	1	2	Del	g	-	1	CFZ	0.25
Rv0678	779117	L43P	1-2	2	SNP	t	c	5	BDQ/ CFZ	0.12 / 0.25
Rv0678	779117	L43R	1	2	SNP	t	g	1	BDQ	0.12
Rv0678	779120	L44P	1	2	SNP	t	c	4	CFZ	0.25
Rv0678	779137	R50W	1-2	2	SNP	c	t	16	CFZ	0.25
Rv0678	779141	Q51R	2	4	SNP	a	g	2	CFZ	0.25
Rv0678	779149	E54_	2	2	SNP	g	t	1	CFZ	0.25
Rv0678	779152	E55_	1	2	SNP	g	t	1	CFZ	0.25
Rv0678	779159	A57E	2	2	SNP	c	a	1	CFZ	0.25
Rv0678	779174	A62D	2	2	SNP	c	a	1	CFZ	0.25
Rv0678	779176	S63G	2	2	SNP	a	g	3	CFZ	0.25
Rv0678	779181	192 ins g	1-4	2-4	Ins	c	g	18	BDQ/ CFZ	0.12 / 0.25
Rv0678	779182	193 del g	1-2	2-4	Del	g	-	13	BDQ/ CFZ	0.12 & 0.25 / 0.25
Rv0678	779186	G66E	2	1	SNP	g	a	1	BDQ	0.12

Table C.9 continued

Gene	Variant position	Variant	BDQ MIC (mg/L)	CFZ MIC (mg/L)	Type	Ref. allele	Alt. allele	Number of isolates	BDQ or CFZ isolate	Selection media drug conc. (mg/L)
Rv0678	779191	S68G	1-2	2	SNP	a	g	9	BDQ/ CFZ	0.12 / 0.25
Rv0678	779203	R72W	1-2	2	SNP	c	t	2	CFZ	0.25
Rv0678	779204	R72L	2-4	2-6	SNP	g	t	3	BDQ	0.12
Rv0678	779210	L74P	1-2	2-4	SNP	t	c	8	BDQ/ CFZ	0.12 / 0.25
Rv0678	779217	228 ins t	2	NA	Ins	a	t	1	BDQ	0.12
Rv0678	779224	F79V	1	2	SNP	t	g	1	CFZ	0.25
Rv0678	779225	F79C	1	2	SNP	t	g	2	BDQ	0.12
Rv0678	779240	A84V	1-2	1-2	SNP	c	t	2	BDQ	0.12
Rv0678	779252	263 ins t	2	1	Ins	a	t	1	BDQ	0.12
Rv0678	779263	274 ins a	1	2	Ins	t	a	3	CFZ	0.25
Rv0678	779270	281 del g	2	2	Del	g	-	1	CFZ	0.25
Rv0678	779280	291 ins a	2	2	Ins	c	a	2	CFZ	0.25
Rv0678	779281	292 del a	2	2	Del	a	-	1	BDQ	0.12
Rv0678	779285	A99V	1-2	1-2	SNP	c	t	17	BDQ/ CFZ	0.12 / 0.25
Rv0678	779293	A102T	1-4	2-4	SNP	g	a	4	BDQ	0.12
Rv0678	779296	G103R	1	2	SNP	g	c	1	BDQ	0.12
Rv0678	779330	L114P	2	2	SNP	t	c	1	CFZ	0.25
Rv0678	779332	Q115_	2	2	SNP	c	t	1	BDQ	0.12
Rv0678	779342	A118D	1	2	SNP	c	a	1	CFZ	0.25
Rv0678	779349	360 del g	1-4	2-4	Del	g	-	8	BDQ/ CFZ	0.12 / 0.25
Rv0678	779351	G121E	2	2-4	SNP	g	a	3	CFZ	0.25
Rv0678	779354	L122P	2	2	SNP	t	c	1	CFZ	0.25
Rv0678	779363	374 del t	2	2	Del	t	-	1	BDQ	0.12
Rv0678	779363	L125P	2	2	SNP	t	c	1	CFZ	0.25
Rv0678	779384	R132P	2	2	SNP	g	c	1	CFZ	0.25
Rv0678	779392	R135W	2	2	SNP	c	t	1	BDQ	0.12
Rv0678	779396	L136P	2	2-4	SNP	t	c	2	BDQ	0.12
Rv0678	779406	417 ins 20bp	1-2	2	Ins	g	ins cgggatctgttggcatatat	3	BDQ	0.12

Table C.9 continued

Gene	Variant position	Variant	BDQ MIC (mg/L)	CFZ MIC (mg/L)	Type	Ref. allele	Alt. allele	Number of isolates	BDQ or CFZ isolate	Selection media drug conc. (mg/L)
Rv0678	779414	425 del t	2	2	Del	t	-	1	CFZ	0.25
Rv0678	779415	426 ins 8bp	2	NA	Ins	g	ins ttgg cata	1	BDQ	0.12
Rv0678	779424	Y145_	1-2	NA	SNP	t	g	5	BDQ	0.12 & 0.25
Rv0678	779424	Y145_	2	2	SNP	t	a	1	CFZ	0.25
Rv0678	779440	S151P	2	2	SNP	t	c	1	BDQ	0.12
Rv0678	779450	L154P	2	2	SNP	t	c	2	CFZ	0.25
Rv0678	779450	L154R	NA	NA	SNP	t	g	1	CFZ	0.25
Rv0678	779454	465 ins c	2	2	Ins	g	c	2	CFZ	0.25
Rv0678	779455	R156_	2	NA	SNP	c	t	3	BDQ/ CFZ	0.12 & 0.25 / 0.25
Rv1305	1461127	D28G	≥10	NA	SNP	a	g	1	BDQ	0.25
Rv1305	1461127	D28V	≥4	NA	SNP	a	t	3	BDQ	0.25
Rv1305	1461227	E61D	≥4	1	SNP	g	c	4	BDQ	0.25
Rv1305	1461227	E61D	2-≥10	2	SNP	g	t	3	BDQ	0.12 & 0.25
Rv1305	1461231	A63P	≥8	1-2	SNP	g	c	7	BDQ	0.25
NA	NA	NA	2	1-2	-	-	-	13	BDQ/ CFZ	0.12

AA - amino acid, Alt. - alternative, BDQ - bedaquiline, CFZ - clofazimine, Del - deletion, gWT - genetically wild-type, Ins - insertion, MIC - minimum inhibitory concentration, NA - not available, NT - nucleotide, Ref. - reference, _ - stop codon

Table C.10 Genomic summary of CRyPTIC strains with variants in bedaquiline/clofazimine resistance-associated genes. Patient isolates collected by Comprehensive Resistance Prediction for Tuberculosis: An International Consortium partners (CRyPTIC) and interpreted by Joshua Carter (Yale University, CRyPTIC member). List includes only minimum inhibitory concentration verified isolates (to at least bedaquiline; BDQ) in UKMYC5/6 broth microtiter plates.

Gene	Variant	Alternative allele	Type	BDQ MIC	CFZ MIC	*mmpL5* variant	*mmpS5* variant	Strain ID
Rv0678	S2R	aga	SNP	0.03	≤0.06	-	-	CR1
Rv0678	S2R	aga	SNP	0.06	0.12	-	-	CR2
Rv0678	S2R	aga	SNP	0.06	0.12	-	-	CR3
Rv0678	N4T	acc	SNP	0.12	NA	-	-	CR4
Rv0678	N4T	acc	SNP	0.06	NA	-	-	CR5
Rv0678	N4T	acc	SNP	0.06	0.12	-	-	CR6
Rv0678	N4T	acc	SNP	0.12	NA	-	-	CR7
Rv0678	15 del c	NA	indel	0.5	0.25	-	-	CR8
Rv0678	D8G	ggt	SNP	0.06	NA	R946R	-	CR9
Rv0678	28 ins t	NA	indel	0.12	≤0.06	-	-	CR12
Rv0678	29 del t	NA	indel	0.25	0.12	-	-	CR10
Rv0678	M10I	atc	SNP	0.12	NA	-	-	CR11
Rv0678	A12A	gct	SNP	0.03	≤0.06	-	-	CR13
Rv0678	P14L	ctc	SNP	0.12	≤0.06	-	-	CR15
Rv0678	P14S	tcc	SNP	0.25	0.5	-	-	CR14
Rv0678	D15G	ggc	SNP	0.25	NA	-	-	CR16
Rv0678	F19S	tcc	SNP	0.5	0.5	A298A	-	CR17
Rv0678	V20A	gcc	SNP	0.12	0.12	-	-	CR18
Rv0678	E21K	aaa	SNP	0.06	0.12	-	-	CR19
Rv0678	M23V	gtg	SNP	≤0.015	≤0.06	-	-	CR20
Rv0678	F27F	ttt	SNP	0.03	≤0.06	-	-	CR21
Rv0678	S29S	tct	SNP	0.12	0.12	-	-	CR22
Rv0678	L32S	tcg	SNP	0.12	0.12	-	-	CR23
Rv0678	107 ins g	NA	indel	0.5	0.25	V123I	-	CR27
Rv0678	A36A	gct	SNP	0.06	NA	-	-	CR24
Rv0678	A36A	gct	SNP	0.06	NA	-	-	CR25
Rv0678	A36A	gct	SNP	0.06	0.06	-	-	CR26
Rv0678	R38_	tga	SNP	0.03	≤0.06	-	-	CR28
Rv0678	R38_	tga	SNP	0.03	≤0.06	-	-	CR29
Rv0678	L40F	ttc	SNP	0.5	NA	-	-	CR38
Rv0678	L40M	atg	SNP	0.5	0.25	-	-	CR30
Rv0678	L40S	tcg	SNP	0.06	0.12	-	-	CR39
Rv0678	L40V	gtg	SNP	≤0.008	≤0.03	-	-	CR31

Table C.10 continued

Gene	Variant	Alternative allele	Type	BDQ MIC	CFZ MIC	*mmpL5* variant	*mmpS5* variant	Strain ID
Rv0678	L40V	gtg	SNP	≤0.015	≤0.06	-	-	CR32
Rv0678	L40V	gtg	SNP	≤0.015	≤0.06	-	-	CR33
Rv0678	L40V	gtg	SNP	≤0.015	≤0.06	-	-	CR34
Rv0678	L40V	gtg	SNP	≤0.015	≤0.06	-	-	CR35
Rv0678	L40V	gtg	SNP	≤0.015	≤0.06	-	-	CR36
Rv0678	L40V	gtg	SNP	≤0.015	0.12	-	-	CR37
Rv0678	W42R	cgg	SNP	0.25	0.25	-	-	CR40
Rv0678	L43L	ttg	SNP	0.06	0.12	-	-	CR41
Rv0678	137 ins g	NA	indel	0.25	1	-	-	CR43
Rv0678	137 ins g	NA	indel	0.25	1	-	-	CR44
Rv0678	137 ins g	NA	indel	0.25	0.25	-	-	CR46
Rv0678	138 ins g	NA	indel	0.25	0.25	-	-	CR45
Rv0678	C46R	cgt	SNP	0.25	1	P355P	-	CR42
Rv0678	141 ins c	NA	indel	0.12	0.12	-	-	CR47
Rv0678	141 ins c	NA	indel	0.25	0.12	-	-	CR48
Rv0678	141 ins c	NA	indel	0.06	0.12	-	-	CR49
Rv0678	141 ins c	NA	indel	0.12	0.06	-	-	CR50
Rv0678	141 ins c	NA	indel	0.06	NA	-	-	CR51
Rv0678	141 ins c	NA	indel	0.25	NA	-	-	CR52
Rv0678	P48L	ctc	SNP	0.25	0.12	-	-	CR53
Rv0678	P48L	ctc	SNP	0.5	NA	-	-	CR54
Rv0678	R50Q	cag	SNP	0.25	0.5	-	-	CR55
Rv0678	Q51K	aag	SNP	0.25	1	-	-	CR59
Rv0678	Q51R	cgg	SNP	0.5	1	-	-	CR56
Rv0678	Q51R	cgg	SNP	0.25	1	-	-	CR57
Rv0678	Q51R	cgg	SNP	0.25	0.5	-	-	CR58
Rv0678	S52P	ccc	SNP	0.06	0.12	-	-	CR60
Rv0678	E55D	gac	SNP	0.06	0.25	-	-	CR61
Rv0678	E55D	gac	SNP	0.03	≤0.06	-	-	CR62
Rv0678	E55D	gac	SNP	0.06	≤0.06	-	-	CR63
Rv0678	E55D	gac	SNP	0.06	0.5	-	-	CR64
Rv0678	L56L	cta	SNP	0.12	≤0.06	-	-	CR65
Rv0678	A62T	acc	SNP	0.12	0.5	-	-	CR66
Rv0678	192 ins g	NA	indel	0.25	0.12	-	-	CR67
Rv0678	192 ins g	NA	indel	0.03	0.12	-	-	CR68
Rv0678	192 ins g	NA	indel	0.12	0.12	-	-	CR69
Rv0678	192 ins g	NA	indel	≤0.008	NA	606 del a	-	CR70
Rv0678	192 ins g	NA	indel	≤0.008	≤0.03	606 del a	-	CR71

Table C.10 continued

Gene	Variant	Alternative allele	Type	BDQ MIC	CFZ MIC	*mmpL5* variant	*mmpS5* variant	Strain ID
Rv0678	192 ins g	NA	indel	≤0.015	≤0.06	606 del a	-	CR72
Rv0678	192 ins g	NA	indel	≤0.015	≤0.06	606 del a	-	CR73
Rv0678	192 ins g	NA	indel	≤0.015	≤0.06	606 del a	-	CR74
Rv0678	192 ins g	NA	indel	≤0.015	≤0.06	606 del a	-	CR75
Rv0678	192 ins g	NA	indel	≤0.015	≤0.06	606 del a	-	CR76
Rv0678	192 ins g	NA	indel	≤0.015	≤0.06	D128H	-	CR77
Rv0678	192 ins g	NA	indel	0.03	≤0.06	606 del a	-	CR78
Rv0678	192 ins g	NA	indel	≤0.015	≤0.06	606 del a	-	CR79
Rv0678	192 ins g	NA	indel	≤0.015	≤0.06	606 del a	-	CR80
Rv0678	192 ins g	NA	indel	≤0.015	≤0.06	606 del a	-	CR81
Rv0678	192 ins g	NA	indel	≤0.015	≤0.06	606 del a	-	CR82
Rv0678	192 ins g	NA	indel	≤0.015	≤0.06	606 del a	-	CR83
Rv0678	192 ins g	NA	indel	≤0.015	≤0.06	606 del a	-	CR84
Rv0678	192 ins g	NA	indel	≤0.015	≤0.06	606 del a	-	CR85
Rv0678	192 ins g	NA	indel	≤0.015	≤0.06	606 del a	-	CR86
Rv0678	192 ins g	NA	indel	≤0.015	≤0.06	606 del a	-	CR87
Rv0678	192 ins g	NA	indel	≤0.015	≤0.06	606 del a	-	CR88
Rv0678	192 ins g	NA	indel	≤0.015	≤0.06	606 del a	-	CR89
Rv0678	G65G	gga	SNP	0.03	NA	-	-	CR90
Rv0678	G65G	gga	SNP	0.03	≤0.06	-	-	CR91
Rv0678	I67L	ctc	SNP	0.5	0.12	-	-	CR92
Rv0678	I67S	agc	SNP	0.5	0.25	-	-	CR93
Rv0678	S68N	aac	SNP	0.5	2	-	-	CR94
Rv0678	N70D	gat	SNP	0.25	NA	-	-	CR95
Rv0678	211 del g	NA	indel	0.03	≤0.06	-	-	CR96
Rv0678	R72W	tgg	SNP	0.25	>4	-	-	CR97
Rv0678	R72W	tgg	SNP	0.06	≤0.06	-	-	CR98
Rv0678	L74V	gtg	SNP	0.25	0.12	-	-	CR99
Rv0678	I75V	gtc	SNP	≤0.015	≤0.06	-	-	CR100
Rv0678	F79L	tta	SNP	0.12	0.12	-	-	CR101
Rv0678	I80S	agt	SNP	0.03	≤0.06	-	-	CR102
Rv0678	L83F	ttc	SNP	0.5	NA	-	-	CR103
Rv0678	L83P	ccc	SNP	0.25	1	-	-	CR104
Rv0678	A84V	gtg	SNP	0.06	≤0.06	-	-	CR105
Rv0678	A84T	acg	SNP	0.06	0.12	-	-	CR106
Rv0678	A84T	acg	SNP	0.06	NA	-	-	CR107
Rv0678	V85A	gcc	SNP	0.25	0.25	A298A	-	CR108
Rv0678	G87R	cgg	SNP	≤0.015	≤0.06	-	-	CR109

Table C.10 continued

Gene	Variant	Alternative allele	Type	BDQ MIC	CFZ MIC	*mmpL5* variant	*mmpS5* variant	Strain ID
Rv0678	G87R	cgg	SNP	0.06	NA	-	-	CR110
Rv0678	R89L	ctg	SNP	0.12	0.12	-	-	CR111
Rv0678	R90C	tgc	SNP	0.06	NA	-	-	CR112
Rv0678	R90C	tgc	SNP	0.12	0.12	-	-	CR113
Rv0678	R90C	tgc	SNP	0.12	0.12	A667S	-	CR114
Rv0678	R90C	tgc	SNP	0.25	0.12	-	-	CR115
Rv0678	R90C	tgc	SNP	0.25	≤0.06	-	-	CR116
Rv0678	R90C	tgc	SNP	0.5	0.25	-	-	CR117
Rv0678	R90C	tgc	SNP	0.06	≤0.06	-	-	CR118
Rv0678	R90C	tgc	SNP	0.25	0.12	-	-	CR119
Rv0678	274 ins a	NA	indel	0.25	0.5	-	-	CR120
Rv0678	R96G	ggg	SNP	0.25	0.25	-	-	CR121
Rv0678	R96L	ctg	SNP	0.25	NA	-	-	CR122
Rv0678	291 del t	NA	indel	0.03	≤0.06	-	-	CR123
Rv0678	N98D	gac	SNP	0.06	0.06	-	-	CR124
Rv0678	N98D	gac	SNP	0.12	≤0.06	-	-	CR125
Rv0678	N98D	gac	SNP	0.03	0.12	-	-	CR126
Rv0678	N98D	gac	SNP	0.03	0.06	P355P	-	CR127
Rv0678	A99A	gcg	SNP	≤0.015	≤0.06	-	-	CR128
Rv0678	A101E	gag	SNP	0.25	0.12	Y586Y	-	CR129
Rv0678	G103G	ggt	SNP	0.06	NA	-	-	CR132
Rv0678	G103S	agc	SNP	0.12	0.5	-	-	CR130
Rv0678	G103S	agc	SNP	0.03	NA	-	-	CR131
Rv0678	E106E	gag	SNP	0.03	≤0.06	-	-	CR133
Rv0678	R107C	tgc	SNP	0.25	NA	-	-	CR134
Rv0678	I108T	acc	SNP	0.25	0.12	-	-	CR136
Rv0678	I108V	gtc	SNP	0.12	0.25	-	-	CR135
Rv0678	325 ins g	NA	indel	1	NA	-	-	CR137
Rv0678	R109Q	cag	SNP	≤0.015	0.25	-	38 ins t	CR138
Rv0678	329 del c	NA	indel	0.12	≤0.06	-	-	CR139
Rv0678	E113K	aaa	SNP	0.25	0.25	-	-	CR140
Rv0678	Q115_	tag	SNP	0.12	0.25	-	-	CR141
Rv0678	L117R	cgg	SNP	0.06	0.12	-	-	CR142
Rv0678	L117R	cgg	SNP	0.25	0.12	-	-	CR143
Rv0678	L117R	cgg	SNP	0.015	0.06	-	-	CR144
Rv0678	G121G	gga	SNP	0.25	0.12	-	-	CR145
Rv0678	G121R	agg	SNP	0.5	NA	-	-	CR146
Rv0678	382 del g	NA	indel	≤0.015	≤0.06	-	-	CR147

Table C.10 continued

Gene	Variant	Alternative allele	Type	BDQ MIC	CFZ MIC	*mmpL5* variant	*mmpS5* variant	Strain ID
Rv0678	A128A	gca	SNP	0.06	≤0.06	-	-	CR148
Rv0678	P130P	ccc	SNP	0.015	≤0.03	-	-	CR149
Rv0678	400 del cgacggctg cgg	NA	indel	≤0.015	≤0.06	-	-	CR150
Rv0678	L136L	cta	SNP	0.12	NA	-	-	CR151
Rv0678	M139I	ata	SNP	0.25	0.25	-	-	CR152
Rv0678	Y145Y	tac	SNP	0.015	0.06	P355P	-	CR153
Rv0678	M146T	acg	SNP	0.12	0.12	P355P	-	CR155
Rv0678	M146T	acg	SNP	0.12	0.12	P355P	-	CR156
Rv0678	M146T	acg	SNP	0.06	0.06	P355P	-	CR157
Rv0678	M146T	acg	SNP	0.12	NA	P355P	-	CR158
Rv0678	M146T	acg	SNP	0.06	0.06	P355P	-	CR159
Rv0678	M146T	acg	SNP	0.03	0.06	P355P	-	CR160
Rv0678	M146T	acg	SNP	0.12	NA	P355P	-	CR161
Rv0678	M146T	acg	SNP	0.25	NA	P355P	-	CR162
Rv0678	M146T	acg	SNP	0.12	NA	-	-	CR163
Rv0678	M146T	acg	SNP	0.12	NA	P355P	-	CR164
Rv0678	M146T	acg	SNP	0.12	0.12	P355P	-	CR165
Rv0678	E147E	gaa	SNP	0.06	≤0.06	-	-	CR166
Rv0678	N148H	cac	SNP	0.03	≤0.06	-	-	CR167
Rv0678	V149V	gtt	SNP	0.06	≤0.06	-	-	CR168
Rv0678	V149V	gtt	SNP	0.06	≤0.06	-	-	CR169
Rv0678	461 del t	NA	indel	0.12	0.5	-	-	CR170
Rv0678	L154L	ttg	SNP	0.06	0.12	-	-	CR171
Rv0678	464 ins gc	NA	indel	0.5	1	-	-	CR173
Rv0678	465 ins c	NA	indel	0.12	0.25	-	-	CR172
Rv0678	R156Q	caa	SNP	0.03	≤0.06	G246G	-	CR174
Rv0678	S158R	aga	SNP	0.015	≤0.03	-	-	CR175
Rv0678	G162E	gaa	SNP	0.06	≤0.06	V149I	-	CR176
Rv0678	G162E	gaa	SNP	≤0.015	≤0.06	F696L	-	CR177
Rv0678	G162E	gaa	SNP	≤0.015	≤0.06	-	-	CR178
Rv0678	492 ins ga	NA	indel	0.25	NA	-	-	CR179
Rv1305	A18A	gca	SNP	0.5	0.25	-	-	CR180
Rv1305	E61D	gac	SNP	2	0.12	-	-	CR181
Rv1305	E61D	gac	SNP	0.25	0.06	-	-	CR182
Rv1979c	E38D	gac	SNP	0.25	0.12	-	-	CR183
Rv1979c	Y51N	aat	SNP	0.25	0	-	-	CR184

Table C.10 continued

Gene	Variant	Alternative allele	Type	BDQ MIC	CFZ MIC	*mmpL5* variant	*mmpS5* variant	Strain ID
Rv1979c	D249E	gag	SNP	0.5	0	-	-	CR185
Rv1979c	D249E	gag	SNP	0.5	0.12	-	-	CR186
Rv1979c	D249E	gag	SNP	0.5	0	-	-	CR187
Rv1979c	R409Q	caa	SNP	0.25	0.25	-	-	CR188
Rv1979c	R409Q	caa	SNP	0.25	0.25	-	-	CR189
Rv1979c	R409Q	caa	SNP	0.5	0.5	-	-	CR190
Rv1979c	R409Q	caa	SNP	0.5	0	-	-	CR191
Rv1979c	R409Q	caa	SNP	0.25	0	-	-	CR192
Rv1979c	R409Q	caa	SNP	0.25	0.12	-	-	CR193
Rv1979c	R409Q	caa	SNP	0.5	0.5	-	-	CR194
Rv1979c	R409Q	caa	SNP	0.5	0	-	-	CR195
Rv1979c	R409Q	caa	SNP	0.25	1	-	-	CR196
Rv1979c	R409Q	caa	SNP	0.5	1	-	-	CR197
Rv1979c	R409Q	caa	SNP	0.25	0.12	-	-	CR198
Rv1979c	R409Q	caa	SNP	0.25	0.06	-	-	CR199
Rv1979c	R409Q	caa	SNP	0.25	0.25	-	-	CR200
Rv1979c	R409Q	caa	SNP	0.25	0	-	-	CR201
Rv1979c	R409Q	caa	SNP	0.25	0.5	-	-	CR202
Rv1979c	R409Q	caa	SNP	0.25	0.25	-	-	CR203
Rv1979c	R409Q	caa	SNP	0.25	0.25	-	-	CR204
Rv1979c	R409Q	caa	SNP	0.25	1	-	-	CR205
Rv1979c	R409Q	caa	SNP	0.25	0.5	-	-	CR206
Rv1979c	R409Q	caa	SNP	0.25	0	-	-	CR207
Rv1979c	R409Q	caa	SNP	0.25	0.5	-	-	CR208
Rv1979c	R409Q	caa	SNP	0.25	0.5	-	-	CR209
Rv1979c	R409Q	caa	SNP	0.25	0.5	-	-	CR210
Rv1979c	R409Q	caa	SNP	0.25	0	-	-	CR211
Rv1979c	R409Q	caa	SNP	0.25	0	-	-	CR212
Rv1979c	R409Q	caa	SNP	0.25	0	-	-	CR213
Rv1979c	R409Q	caa	SNP	0.25	0	-	-	CR214
Rv1979c	R409Q	caa	SNP	0.25	0	-	-	CR215
Rv1979c	R409Q	caa	SNP	0.25	0	-	-	CR216
Rv1979c	R409Q	caa	SNP	0.25	1	-	-	CR217
Rv2535c	V45L	ctg	SNP	0.12	0.12	-	-	CR218
Rv2535c	V45L	ctg	SNP	0.12	≤0.06	-	-	CR219
Rv2535c	V45L	ctg	SNP	0.12	0	-	-	CR220
Rv2535c	V45L	ctg	SNP	0.12	0.25	-	-	CR221
Rv2535c	F46L	ctc	SNP	0.12	0	-	-	CR222

Table C.10 continued

Gene	Variant	Alternative allele	Type	BDQ MIC	CFZ MIC	*mmpL5* variant	*mmpS5* variant	Strain ID
Rv2535c	F46L	ctc	SNP	0.12	0	-	-	CR223
Rv2535c	I193T	acc	SNP	0.12	0.25	-	-	CR224
Rv2535c	I193T	acc	SNP	0.12	0.12	-	-	CR225
Rv2535c	I193T	acc	SNP	0.12	0	-	-	CR226
Rv2535c	G197R	agg	SNP	0.12	0.06	-	-	CR227
Rv2535c	G197R	agg	SNP	0.12	0	-	-	CR228
Rv2535c	G197R	agg	SNP	0.12	0	-	-	CR229
Rv2535c	G197R	agg	SNP	0.12	0	-	-	CR230
Rv2535c	G197R	agg	SNP	0.12	0	-	-	CR231
Rv2535c	G197R	agg	SNP	0.12	0	-	-	CR232
Rv2535c	A268A	gcg	SNP	0.12	0.12	-	-	CR233
Rv2535c	G291G	ggg	SNP	0.12	0	-	-	CR234
Rv2535c	V328F	ttc	SNP	0.12	≤0.06	-	-	CR235
Rv2535c	V328F	ttc	SNP	0.12	0	-	-	CR236

BDQ - bedaquiline, CFZ - clofazimine, CRyPTIC - Comprehensive Resistance Prediction for Tuberculosis: An International Consortium, DST - drug susceptibility testing, ID - identification, MIC - minimum inhibitory concentration, SNP - single nucleotide polymorphism

Table C.11 Catalogue of mutations in bedaquiline and clofazimine resistance-associated gene in bacteria of the *Mycobacterium tuberculosis* complex. Resistant, borderline and susceptible variants found in bedaquiline (BDQ) and clofazimine (CFZ) resistance-associated genes. Table includes mutations defined in the *in vitro* and patient isolate datasets, plus a literature review of all resistance-associated variants detected in clinical isolates, *in vitro* and *in vivo* isolates. Adapted from Sonnenkalb *et al.* 2021 [140].

Minimum inhibitory concentration was determined by: [A] BD-MGIT™, [B] UKMYC5/UKMYC6 plates, [C] Alamar blue/resazurin assay, [D] 7H10 plates, [E] 7H11 plates

Resistant I, borderline (B), and susceptible (S) phenotype was defined by test of study as: [A] 1mg/L BDQ/CFZ [96]; [B] 0.12-0.25mg/L BDQ/CFZ [238], [C] defined by study authors, [D] 0.5mg/L BDQ [239]/CFZ [240], [E] 0.25 mg/L BDQ [96] -CFZ determined by study authors

Gene	Variant position	Variant	Alt. allele	Type	BDQ MIC (mg/L)	CFZ MIC (mg/L)	Phenotype interpreta-tion BDQ-R, B, S	Phenotype interpreta-tion CFZ- R, B, S	DST method	Isolate source	Ref.
Rv0678	778980	-	-9 ins g	indel	2	1	R	S	[C]	*in vitro*	this study
Rv0678	778991	V1A	c	SNP	NA/ 6.4/ >2/ 0.5	1/ >4/ NA/ NA	R	R	[E]/ [A]/ [D]/ [A]	*in vitro*/ patient/ *in vitro*/ patient	[74]/ [169] / [216]/ [241]
Rv0678	778994	S2I	t	SNP	0.73	4	R	R	[C]	patient	[218]
Rv0678	778995	S2R	a	SNP	0.06	0.12	S	B	[B]	patient	CRyPTIC
Rv0678	779000	N4T	c	SNP	0.06-0.12	0.12	S-B	B	[B]	patient	CRyPTIC
Rv0678	779004	5fs	15 del c	indel	0.5	0.25	R	R	[B]	patient	CRyPTIC
Rv0678	779005	6fs	16 del g	indel	1	2	R	R	[C]	*in vitro*	this study
Rv0678	779018	6fs	18 del gg	indel	0.5	NA	R	NA	[E]	patient	[162]
Rv0678	779016	6fs	16 del gg	indel	0.5	NA	B	NA		patient	[158]
Rv0678	779012	D8G	g	SNP	0.06	NA	S	NA	[B]	patient	CRyPTIC
Rv0678	779015	9fs	26 del ag	indel	2	NA	R	NA	[C]	*in vitro*	this study
Rv0678	779018	10fs	29 ins t	indel	NA	1	NA	R	[E]	*in vitro*	[74]
Rv0678	779018	10fs	29 del t	indel	0.25	0.12	R	B	[B]	patient	CRyPTIC

Table C.11 continued

Gene	Variant position	Variant	Alt. allele	Type	BDQ MIC (mg/L)	CFZ MIC (mg/L)	Phenotype interpretation BDQ- R, B, S	Phenotype interpretation CFZ- R, B, S	DST method	Isolate source	References
Rv0678	779017	10fs	28 ins t	indel	0.12	≤0.06	B	S	[B]	patient	CRyPTIC
Rv0678	779019	M10I	c	SNP	0.12	NA	B	NA	[B]	patient	CRyPTIC
Rv0678	779021	11fs	32 del g	indel	0.06-0.25	NA	R	NA	[E]	patient	[211]
Rv0678	779022	G11G	t	SNP	0.5-2.0	NA	R	NA	[C]	patient	[242]
Rv0678	779029	14fs	40 del c	indel	2	2	R	R	[C]	*in vitro*	this study
Rv0678	779030	P14L	t	SNP	0.12	≤0.06	B	S	[B]	patient	CRyPTIC
Rv0678	779029	P14S	t	SNP	0.25	0.5	R	R	[B]	patient	CRyPTIC
Rv0678	NA	D15G	NA	SNP	0.25	NA	R	NA	[B]	patient	CRyPTIC
Rv0678	779038	17fs	49 del a	indel	2	2	R	R	[C]	*in vitro*	this study
Rv0678	779045	F19S	c	SNP	0.5	NA	R	NA	[B]	patient	CRyPTIC
Rv0678	779047	V20F	t	SNP	NA	1	NA	NA	[E]	*in vitro*	[74]
Rv0678	779048	V20G	NA	SNP	0.25/ 2/ 0.25/ 0.25	NA/ 2/ NA/ 4	R/ B	R	[E]/ [A]/ [A]/ [E]	patient	[163]/ [163]/ [222]/ [161]
Rv0678	779048	V20A	c	SNP	0.12	0.12	B	B	[B]	patient	CRyPTIC
Rv0678	779051	21fs	62 del a	indel	2	1	R	S	[C]	*in vitro*	this study
Rv0678	779050	E21K	a	SNP	0.06	0.12	S	B	[B]	patient	CRyPTIC
Rv0678	779052	E21D	c	SNP	0.5-1.0	NA	R	NA	[C]	patient	[242]
Rv0678	779052	E21D	t	SNP	>8	NA	R	NA	[A]	*in vitro*	[136]
Rv0678	779054	Q22L	t	SNP	8	4	R	R	[A]	*in vitro*	[212]
Rv0678	779056	M23V	g	SNP	<=0.015	≤0.06	S	S	[B]	patient	CRyPTIC
Rv0678	779060	G24V	t	SNP	2	2	R	R	[C]	*in vitro*	this study
Rv0678	779063	G25D	a	SNP	NA	≥4	NA	R	[A]	*in vitro*	[136]
Rv0678	779062	G25S	a	SNP	2	NA	R	NA	[C]	*in vitro*	this study
Rv0678	779076	S29S	t	SNP	0.12	0.12	B	B	[B]	patient	CRyPTIC

Table C.11 continued

Gene	Variant position	Variant	Alt. allele	Type	BDQ MIC (mg/L)	CFZ MIC (mg/L)	Phenotype interpretation BDQ- R, B, S	Phenotype interpretation CFZ- R, B, S	DST method	Isolate source	References
Rv0678	779078	30fs	89 del g	indel	2	2	R	R	[C]	*in vitro*	this study
Rv0678	779080	S31R	c	SNP	0.5	NA	R	NA	[C]	patient	[242]
Rv0678	779084	L32S	c	SNP	0.12	0.12	B	B	[B]	patient	CRyPTIC
Rv0678	779086	T33A	g	SNP	4-8/ 0.5/ >2	4/ 2/ NA	R	R	[A]/ [C]/ [D]	*in vitro*/ patient/ *in vitro*	[212]/ [76]/ [216]
Rv0678	779087	T33N	a	SNP	NA	1	NA	R	[E]	*in vitro*	[74]
Rv0678	779087	T33S	g	SNP	2	NA	R	NA	[C]	patient	[242]
Rv0678	779096	A36V	t	SNP	NA/ 0.5	4-Jan	R	R	[E]/ [C]	*in vitro*/ patient	[74]/ [76]
Rv0678	779096	36fs	107 ins g	indel	0.25	0.25	R	R	[B]	patient	CRyPTIC
Rv0678	779097	A36A	t	SNP	0.06	NA	S	NA	[B]	patient	CRyPTIC
Rv0678	NA	A36T	NA	SNP	1	NA	R	NA	[D]	*in vitro*	[216]
Rv0678	779101	R38_	t	SNP	2/ 0.03	2/ ≤0.06	R/ S	R/ S	[C]/ [B]	*in vitro*/ patient	this study/ CRyPTIC
Rv0678	779102	R38P	c	SNP	1	2	R	R	[C]	*in vitro*	this study
Rv0678	779108	L40S	c	SNP	1/ 0.06	2/ 0.12	R/ S	R	[C]/ [B]	*in vitro*/ patient	this study/ CRyPTIC
Rv0678	779109	40fs	120 del g	indel	1	2	R	R	[C]	*in vitro*	this study
Rv0678	779109	L40F	c	SNP	0.5	NA	R	NA	[B]	patient	CRyPTIC
Rv0678	779107	L40M	a	SNP	0.5	NA	R	NA	[B]	patient	CRyPTIC
Rv0678	779107	L40V	g	SNP	≤0.015	0.12	S	B	[B]	patient	CRyPTIC
Rv0678	779113	W42R	c	SNP	0.25/ 0.12	0.25/ 2	R	R	[B]/ [D]	patient	CRyPTIC/ [159]
Rv0678	NA	W42_	NA	SNP	>2	NA	R	NA	[D]	*in vitro*	[216]

Table C.11 continued

Gene	Variant position	Variant	Alt. allele	Type	BDQ MIC (mg/L)	CFZ MIC (mg/L)	Phenotype interpretation BDQ- R, B, S	Phenotype interpretation CFZ- R, B, S	DST method	Isolate source	References
Rv0678	779117	L43R	g	SNP	NA/ 1	2-Jan	R	R	[E]/ [C]	*in vitro*	[74]/ this study
Rv0678	779117	L43P	c	SNP	1-2	2	R	R	[C]	*in vitro*	this study
Rv0678	779116	L43L	t	SNP	0.06	0.12	S	B	[B]	patient	CRyPTIC
Rv0678	779120	L44P	c	SNP	1/ NA	2/ ≥4	R	R	[C]/ [A]	*in vitro*	this study/ [136]
Rv0678	779126	C46Y	a	SNP	NA	1	NA	R	[E]	*in vitro*	[74]
Rv0678	NA	46fs	136 ins g	indel	1	NA	R	NA	[E]	patient	[222]
Rv0678	779126	46fs	137 ins g	indel	0.25	1	R	R	[B]	patient	CRyPTIC
Rv0678	779125	C46R	c	SNP	0.25-1	NA	R	NA	[B]/ [D]	patient/ *in vitro*	CRyPTIC/ [216]
Rv0678	779127	46fs	138 ing g	indel	0.5/ 0.125-0.25/ 2/ >1/ 1	0.25/ NA/ 4/ NA/ NA	R	R	[B]/ [E]/ [A]/ [E]/ [E]	patient	CRyPTIC/ [163]/ [163]/ [223]/ [222]
Rv0678	779127	46fs	138 ins ga	indel	>1	NA	R	NA	[E]	patient	[223]
Rv0678	NA	47fs	139 ins g	indel	0.25	NA	R	NA	[E]	patient	[211]
Rv0678	NA	47fs	140 ins g	indel	0.25	NA	R	NA	[E]	patient	[162]
Rv0678	NA	47fs	NA	indel	0.5	2/ NA	R	R	[E]/ [A]	patient	[161]/ [243]
Rv0678	779130	47fs	141 ins c	indel	0.06-0.25/ 0.5/ 4/ 0.5	0.06-1/ NA/ 4/ NA	S-R	S-R	[B]/ [E]/ [A]/ [E]	patient	CRyPTIC/ [163]/ [163]/ [222]

Table C.11 continued

Gene	Variant position	Variant	Alt. allele	Type	BDQ MIC (mg/L)	CFZ MIC (mg/L)	Phenotype interpretation BDQ- R, B, S	Phenotype interpretation CFZ- R, B, S	DST method	Isolate source	References
Rv0678	NA	48fs	144 ins c	indel	0.25	NA	R	NA	[E]	patient	[211]
Rv0678	779132	P48L	t	SNP	0.25-0.5	0.12	R	B	[B]	patient	CRyPTIC
Rv0678	NA	49fs	NA	indel	0.03-0.25	0.25-2	S-R	R	[E]	patient	[161]
Rv0678	779137	R50W	t	SNP	1/ 3.658	2/ 7.48	R	R	[C]	*in vitro*	this study/ [214]
Rv0678	779138	R50Q	a	SNP	0.25	NA	R	NA	[B]	patient	CRyPTIC
Rv0678	779141	Q51R	g	SNP	0.25-0.5/ 2/ NA	0.5-1/ 4/ 1	R	R	[B]/ [C]/ [E]	patient/ *in vitro*/ *in vitro*	CRyPTIC/ this study/ [74]
Rv0678	779140	Q51K	a	SNP	0.25	1	R	R	[B]	patient	CRyPTIC
Rv0678	NA	S52F	NA	SNP	0.48	NA	R	NA	[D]	patient	[159]
Rv0678	779143	S52P	c	SNP	0.06	0.12	S	B	[B]	patient	CRyPTIC
Rv0678	779147	S53L	t	SNP	0.39/ 0.25-0.4/ 0.25/ NA	2.09/ 2/ 2/ 1	R	R	[C]/ [C]/ [C]/ [E]	Patient/ patient/ patient/ *in vitro*	[214]/ [218]/ [244]/ [74]
Rv0678	NA	S53P	NA	SNP	0.5/ 0.5/ 1	2-4/ 2-4/ NA	R	R	[C]/ [C]/ [D]	patient/ patient/ *in vitro*	[218]/ [244]/ [216]
Rv0678	779149	E54_	t	SNP	2	2	R	R	[C]	*in vitro*	this study
Rv0678	779152	E55_	t	SNP	1	2	R	R	[C]	*in vitro*	this study
Rv0678	779154	E55D	c	SNP	0.06	≤0.06-0.5	S	S-R	[B]	patient	CRyPTIC
Rv0678	779159	A57E	a	SNP	2	2	R	R	[C]	*in vitro*	this study
Rv0678	NA	58fs	172 ins IS*6110*	indel	0.5	1	R	R	[C]	patient	[76]

Table C.11 continued

Gene	Variant position	Variant	Alt. allele	Type	BDQ MIC (mg/L)	CFZ MIC (mg/L)	Phenotype interpretation BDQ- R, B, S	Phenotype interpretation CFZ- R, B, S	DST method	Isolate source	References
Rv0678	779165	A59V	t	SNP	0.48/ NA	NA/ 1	R	R	[D]/ [E]	patient/ *in vitro*	[159]/ [74]
Rv0678	779174	A62D	a	SNP	2	2	R	R	[C]	*in vitro*	this study
Rv0678	NA	A62V	NA	SNP	0.48	NA	R	NA	[D]	patient	[159]
Rv0678	779173	A62T	a	SNP	0.12	0.5	B	R	[B]	patient	CRyPTIC
Rv0678	779177	S63N	a	SNP	NA/ 0.25	0.5/ NA	NA	R	[E]/ [A]	*in vitro*	[74]/ [215]
Rv0678	779176	S63G	g	SNP	2	2	R	R	[C]	*in vitro*	this study
Rv0678	779178	S63R	a	SNP	0.5-4	1.25/ 4	R	R	[C]/ [A]	patient/ *in vitro*	[73]/ [212]
Rv0678	779181	64fs	192 ins g	indel	0.03-0.25/ 1-4/ 0.5/ 4	0.12/ 2-4/ NA/ 4	R	R	[B]/ [C]/ [E]/ [A]	patient/ *in vitro*/ patient	CRyPTIC/ this study/ [163]/ [163]
Rv0678	779181	64fs	192 ins g	indel	≤0.008-0.03	≤0.03-≤0.06	S	S	[B]	patient	CRyPTIC
Rv0678	779181	64fs	192 ins c	indel	>1	NA	R	NA	[E]	patient	[223]
Rv0678	779182	65fs	193 ins a	indel	NA	1	NA	R	[E]	*in vitro*	[74]
Rv0678	779182	65fs	193 del g	indel	1-2/ NA/ 8	2-4/ 1/ 2-4	R	R	[C]/ [E]/ [A]	*in vitro*	this study/ [74]/ [212]
Rv0678	779183	G65E	a	SNP	NA	0.5-1.0	NA	R	[E]	*in vitro*	[74]
Rv0678	779184	G65G	a	SNP	0.03	≤0.06	S	S	[B]	patient	CRyPTIC
Rv0678	779186	G66V	t	SNP	NA	0.5	NA	R	[E]	*in vitro*	[74]
Rv0678	779186	G66E	a	SNP	2	1	R	S	[C]	*in vitro*	this study

Table C.11 continued

Gene	Variant position	Variant	Alt. allele	Type	BDQ MIC (mg/L)	CFZ MIC (mg/L)	Phenotype interpretation BDQ- R, B, S	Phenotype interpretation CFZ- R, B, S	DST method	Isolate source	References
Rv0678	NA	66fs	198 ins g	indel	0.24-1	NA	R	NA	[D]	patient	[159]
Rv0678	NA	67fs	NA	indel	0.25-0.5/ 1-2	2/ NA	R	R	[E]/ [D]	patient/ *in vitro*	[161]/ [216]
Rv0678	779188	I67L	c	SNP	0.5	0.12	R	B	[B]	patient	CRyPTIC
Rv0678	779189	I67S	g	SNP	0.5	0.25	R	R	[B]	patient	CRyPTIC
Rv0678	779190	67fs	201 del t	indel	>8	NA	R	NA	[A]	*in vitro*	[136]
Rv0678	779191	S68G	g	SNP	1-2/ NA	2/ ≥1	R	R	[C]/ [E]	*in vitro*	this study/ [74]
Rv0678	779192	S68N	a	SNP	0.5	2	R	R	[B]	patient	CRyPTIC
Rv0678	779193	S68R	a	SNP	NA	≥4	NA	R	[A]	*in vitro*	[136]
Rv0678	779197	N70D	g	SNP	0.25	NA	R	NA	[B]	patient	CRyPTIC
Rv0678	779200	71fs	211 del t	indel	0.03	≤0.06	S	S	[B]	patient	CRyPTIC
Rv0678	NA	71fs	212 del c	indel	0.5	1	R	R	[C]	patient	[76]
Rv0678	779203	R72W	t	SNP	0.06-0.25/ 1-2/ 8/ 1	≤0.06->4/ 2/ 2/ NA	S-R	S-R	[B]/ [C]/ [A]/ [D]	patient/ *in vitro*/ *in vitro*/ *in vitro*	CRyPTIC/ this study/ [212]/ [216]
Rv0678	779204	R72L	t	SNP	2-4	4-6	R	R	[C]	*in vitro*	this study
Rv0678	779204	R72Q	a	SNP	0.757	2.77	R	R	[C]	patient	[214]
Rv0678	779210	L74P	c	SNP	½/2001	2-4/ NA	R	R	[C]/ [D]	*in vitro*	this study/ [216]
Rv0678	779209	L74V	g	SNP	0.25	0.12	R	B	[B]	patient	CRyPTIC
Rv0678	NA	75fs	224 ins a	indel	0.24	NA	R	NA	[D]	patient	[159]
Rv0678	779211	I75V	c	SNP	≤0.015	≤0.06	S	S	[B]	patient	CRyPTIC
Rv0678	779215	Q76_	t	SNP	NA	0.5	NA	R	[E]	*in vitro*	[74]

Table C.11 continued

Gene	Variant position	Variant	Alt. allele	Type	BDQ MIC (mg/L)	CFZ MIC (mg/L)	Phenotype interpretation BDQ- R, B, S	Phenotype interpretation CFZ- R, B, S	DST method	Isolate source	References
Rv0678	779217	76fs	228 ins t	indel	2	NA	R	NA	[C]	*in vitro*	this study
Rv0678	779224	F79V	g	SNP	1	2	R	R	[C]	*in vitro*	this study
Rv0678	779225	F79C	g	SNP	1	2	R	R	[C]	*in vitro*	this study
Rv0678	779225	F79L	t	SNP	0.12	0.12	B	B	[B]	patient	CRyPTIC
Rv0678	779228	I80S	g	SNP	0.03	≤0.06	S	S	[B]	patient	CRyPTIC
Rv0678	NA	L83F	NA	SNP	0.5	NA	R	NA	[B]	patient	CRyPTIC
Rv0678	779237	L83P	c	SNP	0.25/ >2	1/ NA	R	R	[B]/ [D]	patient/ *in vitro*	CRyPTIC/ [216]
Rv0678	779240	A84E	a	SNP	NA	1	NA	R	[E]	*in vitro*	[74]
Rv0678	779240	A84V	t	SNP	0.06/ 1-2	≤0.06/ 1-2	S/ R	S/ R	[B]/ [C]	patient/ *in vitro*	CRyPTIC/ this study
Rv0678	NA	A84T	g	SNP	0.06	0.12	S	B	[B]	patient	CRyPTIC
Rv0678	779243	V85A	c	SNP	0.25/ 0.12	0.25	R	R	[B]/ [E]	patient	CRyPTIC/ [211]
Rv0678	779248	G87R	c	SNP	0.06	NA	S	NA	[B]	patient	CRyPTIC
Rv0678	779252	88fs	263 ins t	indel	2	1	R	S	[C]	*in vitro*	this study
Rv0678	779254	R89L	t	SNP	0.12/ NA	0.12/ 1	B	B/ S	[B]/ [E]	patient/ *in vitro*	CRyPTIC/ [74]
Rv0678	779258	R90P	c	SNP	NA	0.5	NA	R	[E]	*in vitro*	[74]
Rv0678	779257	R90C	t	SNP	0.06-0.5/ 1	≤0.06-0.25/ NA	S-/ R	S-R	[B]/ [C]	patient	CRyPTIC/ [242]
Rv0678	779263	92fs	274 ins a	indel	0.25/ 1/ 1	0.5/ 2/ NA	R	R	[B]/ [C]/ [D]	patient/ *in vitro*/ patient	CRyPTIC/ this study/ [159]
Rv0678	NA	F93D	NA	SNP	0.25	NA	R	NA	[E]	patient	[222]

Table C.11 continued

Gene	Variant position	Variant	Alt. allele	Type	BDQ MIC (mg/L)	CFZ MIC (mg/L)	Phenotype interpretation BDQ- R, B, S	Phenotype interpretation CFZ- R, B, S	DST method	Isolate source	References
Rv0678	NA	F93S	NA	SNP	0.25	1	R	R	[E]	patient	[161]
Rv0678	779270	94fs	281 del g	indel	2	2	R	R	[C]	*in vitro*	this study
Rv0678	NA	R94W	NA	SNP	2	4	R	R	[A]	patient	[160]
Rv0678	NA	R94Q	NA	SNP	0.25	NA	S	NA	[A]	patient	[243]
Rv0678	NA	R96W	NA	SNP	0.25	NA	R	NA		patient	[158]
Rv0678	779275	R96G	g	SNP	0.25	0.25	R	R	[B]	patient	CRyPTIC
Rv0678	779276	R96L	t	SNP	0.25	NA	R	NA	[B]	patient	CRyPTIC
Rv0678	779280	97fs	291 ins a	indel	2	2	R	R	[C]	*in vitro*	this study
Rv0678	779280	97fs	291 del t	indel	0.03/ 0.25	≤0.06/ NA	S/ R	S/ R	[B]/ [E]	patient	CRyPTIC/ [211]
Rv0678	779281	98fs	292 del g	indel	2/ NA	1-Feb	R	R	[C]/ [B]	*in vitro*/ patient	this study/ [74]
Rv0678	779281	N98D	g	SNP	0.25	≤0.06-0.12/ NA/ 0.75-1/ NA	R	S-R	[B]/ [C]/ [A]/ [C]	patient	CRyPTIC/ [242]/ [179]/ [215]
Rv0678	NA	N98fs	NA	indel	>2	NA	R	NA	[D]	*in vitro*	[216]
Rv0678	779285	A99V	t	SNP	1-2/ 0.25	1-2/ NA	R	B	[C]/ [E]	*in vitro*/ patient	this study/ [211]
Rv0678	779291	A101E	a	SNP	0.25	0.12	R	B	[B]	patient	CRyPTIC
Rv0678	779293	A102T	a	SNP	1-4/ NA	2/4/2001	R	R	[C]/ [E]	*in vitro*	this study/ [74]
Rv0678	779294	A102V	t	SNP	NA	1	NA	R	[E]	*in vitro*	[74]
Rv0678	NA	A102P	NA	SNP	>2	NA	R	NA	[D]	*in vitro*	[216]
Rv0678	779296	G103R	c	SNP	1	2	R	R	[C]	*in vitro*	this study

Table C.11 continued

Gene	Variant position	Variant	Alt. allele	Type	BDQ MIC (mg/L)	CFZ MIC (mg/L)	Phenotype interpreta-tion BDQ- R, B, S	Phenotype interpreta-tion CFZ- R, B, S	DST method	Isolate source	References
Rv0678	779298	G103G	t	SNP	0.06	NA	S	NA	[B]	patient	CRyPTIC
Rv0678	779296	G103S	a	SNP	0.03-0.12	0.5	S-B	R	[B]	patient	CRyPTIC
Rv0678	779308	R107C	t	SNP	0.25	NA	R	NA	[B]	patient	CRyPTIC
Rv0678	779312	I108T	c	SNP	0.25	0.12	R	B	[B]	patient	CRyPTIC
Rv0678	779311	I108V	g	SNP	0.12	0.25	B	R	[B]	patient	CRyPTIC
Rv0678	779314	109fs	325 ing g	indel	1	NA	R	NA	[B]	patient	CRyPTIC
Rv0678	779315	R109Q	a	SNP	<=0.015	0.25	S	R	[B]	patient	CRyPTIC
Rv0678	779318	110fs	329 del t	indel	0.12	≤0.06	B	S	[B]	patient	CRyPTIC
Rv0678	NA	A110V	NA	SNP	0.5	0.5	B	R	[A]	patient	[179]
Rv0678	NA	M111K	NA	SNP	0.25	NA	R	NA		patient	[158]
Rv0678	779326	E113K	a	SNP	0.25	0.25	R	R	[B]	patient	CRyPTIC
Rv0678	779330	L114P	c	SNP	2/ NA	1-Feb	R	R	[C]/ [E]	*in vitro*	this study/ [74]
Rv0678	779332	Q115_	t	SNP	0.12/ 2	0.25/ 2	B/ R	R	[B]/ [C]	patient/ *in vitro*	CRyPTIC/ this study
Rv0678	779339	L117R	g	SNP	0.015-0.25/ 1.54	0.06-0.12/ 4.16	R	S-R	[B]/ [C]	patient	CRyPTIC/ [218]
Rv0678	779342	A118D	c	SNP	1	2	R	R	[C]	*in vitro*	this study
Rv0678	779349	120fs	360 del g	indel	1-4	2-4	R	R	[C]	*in vitro*	this study
Rv0678	779351	G121E	a	SNP	2/ 0.25	2-4/ NA	R	R	[C]/ [E]	*in vitro*/ patient	this study/ [211]
Rv0678	779352	G121G	a	SNP	0.03-0.12	≤0.06	S-B	B	[B]	patient	CRyPTIC
Rv0678	779350	G121R	a	SNP	0.5/ 0.75	NA/ 2	B	R	[B]/ [A]	patient	CRyPTIC/ [179]

Table C.11 continued

Gene	Variant position	Variant	Alt. allele	Type	BDQ MIC (mg/L)	CFZ MIC (mg/L)	Phenotype interpretation BDQ- R, B, S	Phenotype interpretation CFZ- R, B, S	DST method	Isolate source	References
Rv0678	779353	122fs	364 ins	indel	NA	≥1	NA	R	[E]	*in vitro*	[74]
Rv0678	779354	L122P	c	SNP	2/ NA	1-Feb	R	R	[C]/ [E]	*in vitro*	this study/ [74]
Rv0678	779357	R123K	a	SNP	1	NA	R	NA	[C]	patient	[242]
Rv0678	779360	124fs	371 del cgctgggc	indel	NA	1	NA	R	[E]	*in vitro*	[74]
Rv0678	779363	125fs	374 del t	indel	2	2	R	R	[C]	*in vitro*	this study
Rv0678	779363	L125P	c	SNP	2	2	R	R	[C]	*in vitro*	this study
Rv0678	779371	128fs	382 del t	indel	≤0.015	≤0.06	B	S	[B]	patient	CRyPTIC
Rv0678	779384	R132P	c	SNP	2	2	R	R	[C]	*in vitro*	this study
Rv0678	779389	134fs	400 del cgacggctg cgg	indel	≤0.015	≤0.06	S	S	[B]	patient	CRyPTIC
Rv0678	779389	R134_	t	SNP	0.5	1.25	R	R	[C]	patient	[73]
Rv0678	779392	R135G	g	SNP	4	≥4	R	R	[A]	*in vitro*	[212]
Rv0678	779392	R135W	t	SNP	2	2	R	R	[C]	*in vitro*	this study
Rv0678	779396	L136P	c	SNP	2/ NA/ 4-8	2-4/ ≥4/ 1	R	R	[C]/ [A]/ [A]	*in vitro*	this study/ [136]/ [212]
Rv0678	779397	L136L	a	SNP	0.12	NA	B	NA	[B]	patient	CRyPTIC
Rv0678	NA	138fs	NA	indel	>2	NA	R	NA	[D]	*in vitro*	[216]
Rv0678	779406	139fs	417 ins cgggatctgt tggcatatat	indel	1-2	2	R	R	[C]	*in vitro*	this study

Table C.11 continued

Gene	Variant position	Variant	Alt. allele	Type	BDQ MIC (mg/L)	CFZ MIC (mg/L)	Phenotype interpretation BDQ- R, B, S	Phenotype interpretation CFZ- R, B, S	DST method	Isolate source	References
Rv0678	NA	M139T	NA	SNP	0.25	NA	R	NA	[E]	patient	[162]
Rv0678	779406	M139I	a	SNP	0.25	0.25	R	R	[B]	patient	CRyPTIC
Rv0678	NA	141fs	421 ins g	indel	0.25	NA	R	NA	[E]	patient	[211]
Rv0678	779414	142fs	425 del t	indel	2	2	R	R	[C]	*in vitro*	this study
Rv0678	779415	142fs	426 ins ttggcata	indel	2	NA	R	NA	[C]	*in vitro*	this study
Rv0678	NA	L142R	NA	SNP	0.25-1.0	NA	R	NA	[E]	patient	[211]
Rv0678	779424	Y145_	g	SNP	1-2	2	R	R	[C]	*in vitro*	this study
Rv0678	NA	145fs	435 del t	indel	0.25	NA	R	NA	[E]	patient	[211]
Rv0678	779426	M146T	t	SNP	0.78	1.2	R	R	[C]	patient	[214]
Rv0678	NA	146fs	438 ins t	indel	0.25	0.5	R	R	[E]	patient	[222], [161]
Rv0678	779426	M146T	c	SNP	0.03-0.25/ 0.78/ 0.25-1	0.06-0.12/ 0.78/ 0.5-1	S-R	S-R	[B]/ [C]/ [A]	patient	CRyPTIC/ [218]/ [179]
Rv0678	779431	N148H	c	SNP	0.03	≤0.06	S	S	[B]	patient	CRyPTIC
Rv0678	779433	148fs	444 del cg	indel	NA	1	NA	R	[E]	*in vitro*	[74]
Rv0678	779440	S151P	c	SNP	2	2	R	R	[C]	*in vitro*	this study
Rv0678	779450	L154P	c	SNP	2/ >8	2/ NA	R	R	[C]/ [A]	*in vitro*	this study/ [136]
Rv0678	779450	154fs	461 del t	indel	0.12	0.5	B	R	[B]	patient	CRyPTIC
Rv0678	779449	L154L	t	SNP	0.06	0.12	S	B	[B]	patient	CRyPTIC
Rv0678	779454	155fs	465 ins c	indel	0.12/ 1-2	0.25/ 2	B/ R	R	[B]/ [C]	patient	CRyPTIC/ this study
Rv0678	779453	155fs	464 ins gc	indel	0.5	1	R	R	[B]	patient	CRyPTIC

Table C.11 continued

Gene	Variant position	Variant	Alt. allele	Type	BDQ MIC (mg/L)	CFZ MIC (mg/L)	Phenotype interpretation BDQ- R, B, S	Phenotype interpretation CFZ- R, B, S	DST method	Isolate source	References
Rv0678	779455	R156_	t	SNP	2/ NA	2/ 0.5-≥1	R	R	[C]/ [E]	*in vitro*	this study/ [74]
Rv0678	779456	R156Q	a	SNP	0.03	≤0.06	S	S	[B]	patient	CRyPTIC
Rv0678	NA	156fs	NA	indel	>2	NA	R	NA	[D]	*in vitro*	[216]
Rv0678	NA	Y157A	NA	SNP	0.125	2	B	R	[C]	patient	[244]
Rv0678	779463	S158R	g	SNP	0.015	≤0.03	S	S	[B]	patient	CRyPTIC
Rv0678	779474	G162E	a	SNP	≤0.015-0.06	≤0.06	S	S	[B]	patient	CRyPTIC
Rv0678	779481	164fs	492 ins ga	indel	0.25	NA	R	NA	[B]	patient	CRyPTIC
Rv0678	-	-	-	inversion	2	2	R	R	[C]	*in vitro*	this study
Rv1305	1461098	A18A	a	SNP	0.5	0.25	R	R	[B]	patient	CRyPTIC
Rv1305	NA	E21P	t	SNP	>8	NA	R	NA	[A]	*in vitro*	[136]
Rv1305	NA	D28A	c	SNP	>8	NA	R	NA	[A]	*in vitro*	[136]
Rv1305	1461127	D28G	g	SNP	≥10/ >8/ 4/ 0.5/ >2	NA/ NA/ 0.25-0.5/ NA/ NA	R	S	[C]/ [A]/ [A]/ [E]/ [D]	*in vitro*	this study/ [136]/ [212]/ [245]/ [216]
Rv1305	NA	D28N	NA	SNP	0.12	NA	B	NA	[E]	patient	[211]
Rv1305	NA	D28P	ggc	SNP	0.3	NA	R	NA	[D]	*in vitro*	[201]
Rv1305	1461127	D28V	t	SNP	>8/ ≥4-≥8/ 0.48	NA/ 0.25-0.5/ NA	R	S	[C]/ [A]/ [D]	*in vitro*	this study/ [212]/ [201]
Rv1305	NA	L59V	NA	SNP	0.25	NA	R	NA	[E]	*in vitro*	[245]

Table C.11 continued

Gene	Variant position	Variant	Alt. allele	Type	BDQ MIC (mg/L)	CFZ MIC (mg/L)	Phenotype interpretation BDQ- R, B, S	Phenotype interpretation CFZ- R, B, S	DST method	Isolate source	References
Rv1305	1461227	E61D	t	SNP	≥8/ >8/ 0.5-1/ ≥2	1-2/ NA/ NA/ NA	R	B	[C]/ [A]/ [E]/ [D]	*in vitro*	this study/ [136]/ [245]/ [216]
Rv1305	1461227	E61D	c	SNP	0.25-2/ 2-≥10/ 0.25-0.96	0.06-0.12/ 1/ NA	R	S/ B	[B]/ [C]/ [D]	patient/ *in vitro*/ *in vitro*	CRyPTIC/ this study/ [201]
Rv1305	1461231	A63P	c	SNP	>8/ >8/ ≥10-≥20/ >8/ 1.92-3.84/ 4	NA/ 0.5/ NA/ 1-2/ 2/ NA/ NA	R	B	[A]/ [A]/ [C]/ [A]/ [D]/ [E]	*in vitro*/ *in vitro*/ *in vitro*/ patient/ *in vitro*/ *in vitro*/ *in vitro*	[136]/ [212]/ this study/ [160]/ [201]/ [245]
Rv1305	NA	A63V	NA	SNP	1	NA	R	NA	[E]	patient	[211]
Rv1305	NA	I66M	atg	SNP	0.48/ 1	NA	R	NA	[D]/ [E]	*in vitro*	[201]/ [245]
Rv1979c	2223051	E38D	c	SNP	0.25	0.12	R	B	[B]	patient	CRyPTIC
Rv1979c	2223014	Y51N	a	SNP	0.25	NA	R	NA	[B]	patient	CRyPTIC
Rv1979c	NA	V52G	c	SNP	0.08	1.2	S	R	[C]	patient	[218]
Rv1979c	2222418	D249E	g	SNP	0.5	0.12	R	B	[B]	patient	CRyPTIC
Rv1979c	2221939	R409Q	a	SNP	0.25-0.5	0.06-0.5	R	S/ B	[B]	patient	CRyPTIC
Rv1979c	2221732	P478G	NA	SNP	0.03/ 0.5	NA/ 0.5	B	R	[E]/ [A]	patient	[163]/ [163]

Table C.11 continued

Gene	Variant position	Variant	Alt. allele	Type	BDQ MIC (mg/L)	CFZ MIC (mg/L)	Phenotype interpretation BDQ- R, B, S	Phenotype interpretation CFZ- R, B, S	DST method	Isolate source	References
Rv2535c	NA	14fs	40 ins c	indel	0.12	0.5-1.0	B	R	[D]	*in vitro*/ *in vivo*	[77]
Rv2535c	NA	L44P	NA	SNP	0.12	0.5-1.0	B	R	[D]	*in vitro*/ *in vivo*	[77]
Rv2535c	2860286	V45L	c	SNP	0.12	≤0.06-0.25	B	S/ B	[B]	patient	CRyPTIC
Rv2535c	2860283	F46L	c	SNP	0.12	NA	B	NA	[B]	patient	CRyPTIC
Rv2535c	2859841	I193T	c	SNP	0.12	0.12-0.25	B	B/ S	[B]	patient	CRyPTIC
Rv2535c	2859830	G197R	a	SNP	0.12	0.06	B	S	[B]	patient	CRyPTIC
Rv2535c	2859615	A268A	g	SNP	0.12	0.12	B	B	[B]	patient	CRyPTIC
Rv2535c	NA	271fs	811 ins c	indel	0.12	0.5-1.0	B	R	[D]	*in vitro*/ *in vivo*	[77]
Rv2535c	2859546	G291G	g	SNP	0.12	NA	B	NA	[B]	patient	CRyPTIC
Rv2535c	2859437	V328F	t	SNP	0.12	≤0.06	B	S	[B]	patient	CRyPTIC

Alt. - alternative, B - borderline, BDQ - bedaquiline, CFZ - clofazimine, del – deletion, DST - drug susceptibility testing, fs – frameshift, ins – insertion, IS*6110* - insertion sequence *6110*, NA – not available, R - resistant, Ref. - reference, S - susceptible, SNP – single nucleotide polymorphism, _ – stop codon insertion

Appendix D

Supplementary Material and extended tables of Results 4.3

Table D.1 Off-target mutations co-selected with resistance-associated mutations after *in vitro* evolutionary experiments. All mutations were present in clones at a frequency >98%, with no additional mutations detected, as compared to the wild-type ancestor strain. Clones with more than one off-target mutation were not included.

2° Mutation							Accompanied FQ resistant mutation			
Variant position	**Gene**	**Gene name**	**Variant**	**Gene annotation**	**Functional category**	**# of clones**	**Variant position**	**Gene**	**Variant**	**MFX MIC**
3017654	*Rv2702*	*ppgK*	_266S	Polyphosphate glucokinase PpgK	Intermediary metabolism and respiration	3	7570	*Rv0006*	A90V	1
2879238	*Rv2559c*	-	A231V	Conserved hypothetical alanine leucine valine rich protein	Conserved hypotheticals	6	7582	*Rv0006*	D94G	2
3372353	*Rv3013*	-	A180D	hypothetical protein	Conserved hypotheticals	1	7582	*Rv0006*	D94G	1
4069527	*Rv3630*	-	G118D	Probable conserved integral membrane protein	Cell wall and cell processes	1	7570	*Rv0006*	A90V	0.5
2139332	*Rv1890c*	-	R119H	Hypothetical protein	Conserved hypotheticals	22	6734	*Rv0005*	N499D	1
1400160	*Rv1253*	*deaD*	T64M	Probable cold-shock DeaD-box protein A homolog DeaD	Information pathways	1	7570	*Rv0006*	A90V	1
3420207	*Rv3059*	*cyp136*	V239A	Probable cytochrome P450 136	Intermediary metabolism and respiration	13	7570	*Rv0006*	A90V	1-2

Table D.1 continued

2° Mutation							Accompanied BDQ resistant mutation			
Variant position	**Gene**	**Gene name**	**Variant**	**Gene annotation**	**Functional category**	**# of clones**	**Variant position**	**Gene**	**Variant**	**BDQ MIC**
523446	*Rv0435c*	-	D363G	Putative conserved ATPase	Cell wall and cell processes	1	1461227	*atpE*	E61D	≥8
578094	*Rv0488*	-	V144G	Probable conserved integral membrane protein	Cell wall and cell processes	1	779182	*Rv0678*	193 del G	2
761364	*Rv0667*	*rpoB*	D520N	DNA-directed RNA polymerase (beta chain)	Information pathways	2	779349	*Rv0678*	360 del G	1-4
777213	*Rv0676c*	*mmpL5*	A423D	Probable conserved transmembrane transport protein MmpL5	Cell wall and cell processes	1	779191	*Rv0678*	S68G	2
783925	*Rv0684*	*fusA1*	G481C	Probable elongation factor G FusA1 (EF-G)	Information pathways	5	779424	*Rv0678*	Y145_	1-4
894086	*Rv0800*	*pepC*	V257M	Probable aminopeptidase PepC	Intermediary metabolism and respiration	2	779210	*Rv0678*	L74P	2
2121497	*Rv1871c*	-	_130R	hypothetical protein	Conserved hypotheticals	1	779029	*Rv0678*	40 del C	2
						1	779293	*Rv0678*	A102T	1-4
						4	779005	*Rv0678*	16 del G	1
						1	1461231	*atpE*	A63P	≥8
2139332	*Rv1890c*	-	R119H	hypothetical protein	Conserved hypotheticals	1	779182	*Rv0678*	193 del G	2
						1	779217	*Rv0678*	228 ins T	2

Table D.1 continued

Variant position	Gene	Gene name	Variant	Gene annotation	Functional category	# of clones	Variant position	Gene	Variant	BDQ MIC
2809621	*Rv2160c*	-	T106A	hypothetical protein	Regulatory protein	1	779181	*Rv0678*	192 ins G	2
2818576	*Rv2503c*	*scoB*	C184_	Probable succinyl-CoA:3-ketoacid-coenzyme A transferase (beta subunit) ScoB	Lipid metabolism	1	1461231	*atpE*	A63P	≥20
2° Mutation							**Accompanied CFZ resistant mutation**			
Variant position	**Gene**	**Gene name**	**Variant**	**Gene annotation**	**Functional category**	**# of clones**	**Variant position**	**Gene**	**Variant**	**CFZ MIC**
51622	*Rv0047c*	-	Y36H	hypothetical protein	Conserved hypotheticals	1	779120	*Rv0678*	L44P	2
858327	*Rv0765c*	-	T180A	Probable oxidoreductase	Intermediary metabolism and respiration	1	779152	*Rv0678*	E55_	2
1676070	*Rv1486c*	-	S272P	hypothetical protein	Conserved hypotheticals	1	779285	*Rv0678*	A99V	2
2139332	*Rv1890c*	-	R119H	Hypothetical protein	Conserved hypotheticals	3	779342	*Rv0678*	A118D	1
						3	779060	*Rv0678*	G24V	2
						1	779174	*Rv0678*	A62D	2
						1	779182	*Rv0678*	193 del G	2
3214725	*Rv2905*	*lppW*	S33I	Probable conserved alanine rich lipoprotein LppW	Cell wall and cell processes	3	779191	*Rv0678*	S68G	2

BDQ - bedaquiline, CFZ - clofazimine, del - deletion, FQ- fluoroquinolone, ins - insertion, MFX - moxifloxacin, MIC - minimum inhibitory concentration, _ - stop codon insertion, # - number

Table D.2: P-values of mutant selection window of moxifloxacin resistant mutants. Each statistical test was conducted using R studio, see Appendix E.

Drug concentration (mg/L)	gWT - *gyrA* A90V	gWT - *gyrA* D94G	gWT - *gyrB* N499D	gWT - *gyrB* E501D	gWT - *gyrA* A90V+ *ppgK* _266S
0.0	0.601	0.018	0.972	0.0066	0.66
0.03	0.0041	0.00276	0.0053	5.3×10^{-6}	0.00266
0.06	0.003	0.0038	0.0092	0.046	0.0058
0.12	0.0044	0.0003	0.0048	0.0003	0.0009
0.25	0.022	2.9 x 10-4	0.033	0.0051	1.0×10^{-4}
0.5	0.514	0.515	8.3×10^{-5}	0.513	5.86×10^{-5}
1.0	1.0	0.879	0.556	1.0	0.548
2.0	1.0	0.879	0.556	1.0	0.548
4.0	1.0	0.879	0.556	1.0	0.548

Drug concentration (mg/L)	*gyrA* A90V - *gyrA* D94G	*gyrA* A90V - *gyrB* N499D	*gyrA* A90V - *gyrB* E501D	*gyrA* A90V - *gyrA* A90V+ *ppgK* _266S	*gyrB* E501D - *gyrA* A90V+ *ppgK* _266S
0.0	0.998	0.012	0.617	0.255	0.0486
0.03	0.965	0.115	0.879	0.074	0.006
0.06	0.999	0.007	0.604	0.968	0.60
0.12	0.83	0.076	0.991	0.32	0.156
0.25	0.005	0.993	0.0118	0.667	0.496
0.5	0.0048	0.988	0.0017	0.999	0.0038
1.0	0.548	0.879	0.556	1.0	0.555
2.0	0.548	0.879	0.556	1.0	0.555
4.0	0.548	0.879	0.556	1.0	0.555

Drug concentration (mg/L)	*gyrA* D94G - *gyrB* N499D	*gyrA* D94G - *gyrB* E501D	*gyrA* D94G - *gyrA* A90V+ *ppgK* _266S	*gyrB* N499D - *gyrB* E501D	*gyrB* N499D - *gyrA* A90V+ *ppgK* _266S
0.0	0.0453	0.571	0.228	0.522	0.00045
0.03	0.0188	0.547	0.356	0.384	9.8×10^{-5}
0.06	0.014	0.642	0.981	0.137	0.146
0.12	0.0033	0.558	0.868	0.122	5.1×10^{-4}
0.25	0.026	0.72	0.21	0.062	0.926
0.5	0.03	0.0	0.012	0.0092	0.999
1.0	0.964	0.999	0.549	0.94	0.88
2.0	0.964	0.999	0.549	0.94	0.88
4.0	0.964	0.999	0.549	0.94	0.88

Table D.3: P-values of fitness experiments of MFX resistant mutants. Each statistical test was conducted using R studio, see Appendix E.

Comparison	gWT - *gyrA* D94G	gWT - *gyrA* A90V	gWT - *gyrB* E501D	gWT - gyrA A90V + *ppgK* _266S	*gyrA* A90V+ *ppgK* _266S
p-value	0.015	0.352	0.923	0.074	1

Table D.4: P-values of fitness experiments of BDQ resistant mutants. Each statistical test was conducted using R studio, see Appendix E.

Comparison	gWT - *atpE* A63P	gWT - *atpE* D28V	gWT - *Rv0678* R156_	gWT - *Rv0678* S68G	gWT - *Rv0678* S68G +mmpL A423D	*Rv0678* S68G - *Rv0678* S68G +mmpL A423D
p-value	0.006	0.0038	0.053	0.968	0.999	1.0

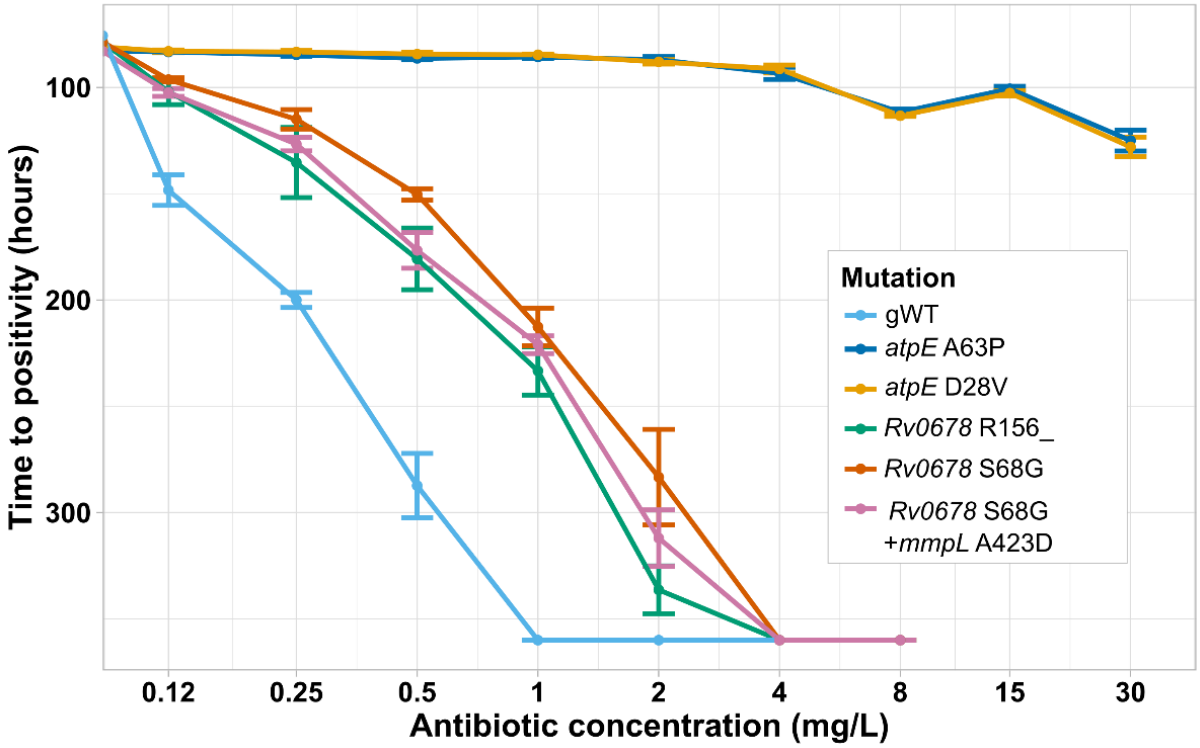

Figure D.1: Mutant selection window of bedaquiline resistance mutations. Resistance-associated mutations *atpE* A63P, *atpE* D28V, *Rv0678* R156_, and *Rv0678* S68G were isolated from BDQ evolutionary experiments. Each mutant clone was separately cultured in Mycobacterium growth indicator tubes (MGIT) and growth was measured hourly, until time to positivity (fluorescence signal measured greater than or equal to 400 units) was achieved. Data is representative of two independent experiments, with a total of five biological replicates.

Appendix E

Statistics

All statistical tests were performed as non-parametric Kruskal-Wallis test, computed in R statistical program. R-script as follows:

```
##Statistical Test##

head(mfxfit)

# Show the group levels

levels(mfxfit$mutation)



# Compute summary statistics by groups

library(dplyr)

group_by(mfxfit, mutation) %>%

 summarise(

   count = n(),

   mean = mean(freq_change, na.rm = TRUE),

   sd = sd(freq_change, na.rm = TRUE),

   median = median(freq_change, na.rm = TRUE),

   IQR = IQR(freq_change, na.rm = TRUE)

 )



kruskal.test(freq_change ~ mutation, data = mfxfit)
```

```
##########################

##Kruskal Rank Sum Test ##

##########################

a <- mfxfit$freq_change[which(mfxfit$mutation=="D94G")]

b <- mfxfit$freq_change[which(mfxfit$mutation=="gWT1")]

c <- mfxfit$freq_change[which(mfxfit$mutation=="A90V")]

d <- mfxfit$freq_change[which(mfxfit$mutation=="gWT2")]

e <- mfxfit$freq_change[which(mfxfit$mutation=="E501D")]

f <- mfxfit$freq_change[which(mfxfit$mutation=="gWT3")]


Value <- c(a, b, c, d, e, f)

Treatment <- c(rep(1,length(a)),rep(2,length(b)),rep(3,length(c)),rep(4,length(d)),
rep(5,length(e)),rep(6,length(f)))


kruskal.test(Value, Treatment)

#Save data for p-value calculations#

library(nparcomp)


analysisDf <- data.frame(Value, Treatment)


comp <- mctp(Value ~ Treatment, data = analysisDf, asy.method = "fisher",

        type = "Tukey", alternative = "two.sided")

summary(comp)
```

Acknowledgments

Without the help and dedication of many colleagues, family, friends, and people; this dissertation would not have been possible.

First, I would like to thank my supervisor **Prof. Dr. Stefan Niemann**. Stefan is truly an amazing researcher and scientist, who has an uncanny ability to develop projects and collaborations which I did not know was possible. I am very lucky that I had the ability to work with and learn from such a person. More so, I am so grateful that Stefan is easy to talk to, get along with, drink a beer with, and someone who loves people and wants to help the world. Most of all Stefan has been an incredible mentor to me, and provided me with so many opportunities and support in my career that I am forever grateful. I hope that I can emulate his style of supervision one day.

I would next like to thank my junior supervisor **Prof. Dr. Matthias Merker**, for his dedication to my project, especially the endless, invaluable intellectual and creative advice. Matthias really put countless hours into helping me succeed – from experimental designs, correcting my writing/presentations/reports, teaching me how to use different computational programs, helping with figure design, and the list goes on. But Matthias was also a kind person who provided me with an optimistic and realistic view of the scientific profession (and especially the world of publishing), and just a decent person to everyone. I hope that I can also emulate his style of supervision one day.

Also, a special thank you to **Prof. Dr. Torsten Goldman**, who as a co-supervisor offered me additional mentoring support and was also a kind person to sit with and enjoy a coffee. Torsten gave me really wonderful advice and reassurance which I really appreciated.

A number of my colleagues I would also like to acknowledge for their additional technical support such as **Ivan Barilar** who helped me with various analyses in this study, **Dr. Patrick Beckert** who was the most welcoming person and a great lunch time companion. To **Dr. Viola Dreyer**, an amazing mathematician who not only helped me analyze my data with the binoSNP tool she developed, but made time to help me with my statistical and various analyses. Also, **Dr. Christian Utpatel** who especially helped me with the PacBio® analysis. Finally, to **Dr. Susanne Homolka**, **Dr. Sven Malm** and **Dr. Silke Feuerriegel**, who gave me valuable input when designing my experiments, especially in the beginning of my thesis work.

I want to thank **Dr. Christiane Gerlach**, not only was she the project manager for EvoLUNG, but also an amazing group member who was always kind and patient with me. She is a person who really listens when you are talking and has a love for science which I find very inspiring.

Next, I want to give a special thank you to my dear friend and EvoLUNG colleague **Jessica Ojong**, for her help and kindness. Jessica has been an inspiration to always do my best, and she provided me with stimulating scientific conversation and helpful advice related to my work.

I want to thank all of the **EvoLUNG team**, but especially for the help and input from **Prof. Dr. Heinrich Schulenburg** and **Dr. Leif Tüffers**, who were wonderful to talk with and share ideas, but also gave me important mentoring for my project and future scientific career.

A number of post-doctoral researches in the Molecular and Experimental Mycobacteriology group have been also wonderful and helpful throughout my work including **Dr. Thomas Kohl**, **Dr. Judith Petersen**, **Dr. Meriem Belheouane**, and **Dr. Margo Diricks**.

I had further help from colleagues at the National Reference Center for Mycobacterium in Borstel, such as performing diagnostic tests, selecting strains, and collaborating on my first paper. Thank you so much **Dr. Sönke Andres**, **Dr. Doris Hillemann**, and **Dr. Florian Maurer**. Also, thank you to the technical support from **Ilse Radzio** and **Anne-Katrin Witt**.

I want to give a huge appreciation and thank you to the technicians in my group, especially **Doreen Beyer** and **Silvia Maaß** who gave me all my initial laboratory training and helped me with large experiments. To **Carina Hahn**, **Ménie Wiemer**, and **Larissa Mohr** for their help in the biosafety level 3 laboratory. Also, to **Anja Lüdemann** and **Tanja Struve-Sonnenschein** for their help in the molecular lab and training me in DNA isolation. Last but not least, a big big thank you to **Fenja Boysen**, **Vanessa Mohr**, and **Tanja Niemann** for their help and training in library preparation and next generation sequencing.

To the doctoral students in my group, a big thank you for your help, support, and ideas. But an even bigger thank you for just being an awesome group of people who were wonderful to share an office with and spend time with outside of work: **Harriet Blankson**, **Johanna Perez-Llanos**, **Emilie Rousseau**, **Jana Schönfeld**, **Dr. Yassir Shuaib**, and **Teresa Waltz**. With an extra special thank you to **Dr. Matthias Gröschel** who is an amazing scientist and gave me invaluable tips to improve my experiments.

Further help from people outside of Research Center Borstel included **Dr. Claudio Kösner** who gave intellectual contributions and project collaborations, to **Dr. Gerald Strohe** for collecting and sharing data for my first publication.

To my colleagues in the CRyPTIC consortium for their help with analysis, writing of our collaborative paper and sharing strains for my second publication – **Dr Andrea Spitaleri** and **Prof. Dr. Daniela Cirillo** from IRCCS San Raffaele Scientific Institute; **Prof. Dr. Zamin Iqbal**, **Dr. Kerri Malone**, and **Dr. Martin Hunt** from the

European Bioinformatic Institute in Cambridge; and especially **Joshua Carter** and **Prof. Dr. Philip Fowler** for their extensive work on our collaboration. Further I want to thank all **CRyPTIC** partners for their hard work on an amazing project and advancements in molecular and phenotypic diagnostics for detecting drug resistant TB.

I want to thank my friends. Some of whom contributed intellectually to my work, but mostly for helping keep me sane - **Sarah Thom-Carter**, **Clint Carter**, **Sandra Júkic**, **Ombretta Colasanti, Laura Lollman, Joshua Lollman, Nicole Moreno**, **Dr. Christina Rau**, **Jason Rau**, **Antonio Rivera, Aracelli Rivera, Chelsea Rivera, Simone Tazoll**, and **Jacqueline Wax**. But especially to **Iretiolu Ogunsulire** and **Denise Ohnezeit** who even read my thesis and gave me awesome input.

I want to also give a special thanks to the funding entities for whom none of this work would have been possible, thank you for taking the risk on these projects – Evolutionary Medicine of the lung (EvoLUNG), Research Center Borstel Leibniz Lung Center, Christian-Albrechts-Universität Kiel, Max Planck Institute for Evolutionary Biology, Leibniz Gemeinschaft, and Schleswig-Holstein.

Finally, I would like to thank my family **Jim Tucker**, **Carla Tucker**, **James Tucker** and **John Tucker** for their encouragement, love, and financial/emotional support. And a big thank you to my German family **Elisabeth Sonnenkalb, Jürgen Sonnenkalb**, **Nikolas Sonnenkalb**, and **Mari Hase** for their love and support. Thank you to my little angle **Klaus**, without any formal training he is an outstanding emotional support animal.

Last but not least, I want to thank my husband **Roman Sonnenkalb**, without him I would not have had the strength to attempt such an endeavor. Thank you so much for your love and understanding, for keeping me sane and well fed. I love you forever and always.

List of Publications

M. Merker, L. Tueffers, M. Vallier, E. Groth, **L. Sonnenkalb**, D. Unterweger, J. Baines, S. Niemann, H. Schulenburg "Evolutionary Approaches to Combat Antibiotic Resistance: Opportunities and Challenges for Precision Medicine," *Frontiers in Immunology*, vol. 11, p. 1938, 2020, doi: 10.3389/fimmu.2020.01938.

Status: published

L. Sonnenkalb, G. Strohe, V. Dreyer, S. Andres, D. Hillemann, F. Maurer, S. Niemann, M. Merker "Microevolution of *Mycobacterium tuberculosis* hetero-resistance subpopulations in a patient receiving 27 years of tuberculosis treatment in Germany," *Antimicrob Agents Chemother*, Jun. 2021, doi: 10.1128/AAC.02520-20.

Status: published

L. Sonnenkalb, JJ. Carter, A. Spitaleri, Z. Iqbal, M. Hunt, K. Malone, C. Utpatel, DM. Cirillo, C. Rodrigues, KS. Nilgiriwala, CRyPTIC, PW. Fowler, M. Merker, S. Niemann "Deciphering Bedaquiline and Clofazimine Resistance in Tuberculosis: An Evolutionary Medicine Approach," *bioRxiv*, p. 2021.03.19.436148, Mar. 2021, doi: 10.1101/2021.03.19.436148.

Status: in review

List of Presentations

Keystone Conference: Tuberculosis – April 2018 – Whistler, CA

Poster: Intra-patient *Mycobacterium tuberculosis* strain dynamics – A 12-year M/XDR- TB treatment history

European Society of Mycobacteriology – June 2018 – Dresden, DE

Oral: Antibiotic resistance evolution of *Mycobacterium tuberculosis* – A 57-year M/XDR- TB treatment history

2nd Joint Congress of Evolutionary Biology – August 2018 – Montpellier, FR

Poster: Intra-patient *Mycobacterium tuberculosi*s strain dynamics – A 18-year M/XDR- TB treatment history

International Society of Evolutionary: Medicine and Public Health - August 2019 – Zurich, CH

Oral: Antibiotic resistance evolution of *Mycobacterium tuberculosis* complex bacteria, during sub-lethal drug exposure

Join annual meeting DGI-DZIF – November 2019 – Bad Nauheim, DE

Poster: Antibiotic resistance evolution of *Mycobacterium tuberculosis* complex bacteria during sub-lethal moxifloxacin and bedaquiline exposure

International Symposium: Precision Medicine in Chronic Inflammation –

February 2020 – Hamburg, DE

Poster: Sub-lethal exposure drives resistance evolution in *Mycobacterium tuberculosis* complex bacteria